

Polycyclic compounds as carriers for neuroactive non-steroidal anti-inflammatory drugs

Modupe K. Abaniwonda, B.Pharm

Student number: 2832025

Dissertation submitted in fulfilment of the requirement for
the degree



Supervisor: Prof Jacques Joubert

Co-supervisor: Prof Sarel Malan

July 2017



DEPARTMENT OF PHARMACEUTICAL CHEMISTRY, SCHOOL OF PHARMACY,
UNIVERSITY OF THE WESTERN CAPE, PRIVATE BAG X17, BELLVILLE 7353

DECLARATION

I declare that *Novel Polycyclic compounds as carriers for neuroactive non-steroidal anti-inflammatory drugs* is my own work and that it has not been submitted for any other degree or examination at any other university, and that all the sources I have used or quoted have been indicated and acknowledged by complete reference.

Modupe K Abaniwonda



July, 2017.

A handwritten signature in blue ink, appearing to read "Modupe K Abaniwonda".

Signature

ACKNOWLEDGEMENTS

I will like to appreciate the support of my supervisors, Prof Joubert and Prof Malan. Your kindness, patience and guidance gave me the motivation needed to complete this project.

This journey was full of challenges and I will like to acknowledge the unsung heroes, my “cheer leaders” and support base who cheered on until I crossed the finish line. Through this experience I have discovered myself in more ways than words can express and I will be forever grateful to the following people:

My parents “my pillars”, I say thank you for the sacrifices, the love shown and always believing in me. I owe you the world mom and daddy. You are my greatest assets.

To my siblings, Kola, Kunle, Demo and Iya B, you guys are an incredible bunch. Thanks for the encouragement, kind words and sometimes sarcasm. You all make my life colourful. I love you.

Ms Ramplin, Mr Sharma, Ms Shireen Mentor and Mr Kippie, Thank you for the assistance in the laboratory and outside. I lack words to fully express my gratitude.

Ayoola Osinowo, my “trouble maker”, my life partner I thank you for bearing all my excesses and being so understanding. Ademi you are simply amazing.

Elton Fortuin my “partner in crime”, thank you for the late night talks, you are a blessing to me. Richo, I embraced my emotions, my weaknesses and my environment for me and by me. I love you. Thank you for introducing me to the part of me that I never knew existed.

Adeyemi and Ayodeji, thank you for being such wonderful big brothers to me. I am so grateful for your support financially and otherwise.

My friends, Sibongile, Tshenolo, Nokuthula, Blessing Abu, Thata, Germaine, Osaro and Alvine. Thank you for lending me your shoulders when I needed it most.

To the entire staff of UWC School of pharmacy, I am so grateful for providing a welcoming environment.

I will like to specially thank Pastor Baldwin Nwachukwu, Pastor Meg Nwachukwu and the entire workforce of GRA Parklands. My story changed the moment I encountered this Grace.

Lastly but not least my appreciation goes to bro Obi, Funi and Rena as well as my landlord uncle Leon. I could count on you at the oddest hours of the night during the process of writing this dissertation and never got turned back. Thank you.

To God be the glory



KEYWORDS

Neurodegenerative disorders

Oxidative stress

Excitotoxicity

Inflammation

Non-steroidal anti-inflammatory drugs

Polycyclic cage compounds

Prodrugs

Blood-brain barrier



ABSTRACT

Recent scientific findings have highlighted the beneficial roles of polycyclic cage compounds in neurodegenerative disorders such as Alzheimer's and Parkinson's diseases. Further interest into the chemistry of these compounds is stimulated by their remarkable ability to improve the pharmacokinetics profile of known neuroprotective agents. As potent lipophilic scaffolds, they can be employed to target the brain delivery of desired compounds.

Inflammation is a key mediator of neuronal cell's degeneration as activated microglia and other inflammatory mediators propagate oxidative damage and neuronal loss. Epidemiological and clinical evidence suggests that non-steroidal anti-inflammatory drugs (NSAIDs) slow down the progression and onset of neurodegenerative diseases. The beneficial effects of NSAIDs in ND can be attributed to their ability to inhibit cyclooxygenase enzymes thereby halting the biosynthesis of prostaglandins (PG) which are powerful mediators of inflammation. NSAIDs also inhibit the expression of pro-inflammatory genes. Despite their potential neuroprotective activity, NSAIDs are poorly lipophilic due to the presence of polar carboxylic acid groups and will therefore ionise at physiological pH, deterring them from reaching the desired site of action in the central nervous system (CNS).

A series of amide and ester prodrugs comprising of polycyclic compounds such as amantadine or pentacycloundecanes and carboxylic acid containing NSAIDs were selected for synthesis. The carboxylic acids were conjugated to the polycyclic structures *via* amination using activation chemistry with CDI. The prodrugs of ibuprofen, ketoprofen, naproxen and aspirin were selected based on availability of parent NSAID, physicochemical property of desired compound, feasibility and ease of synthesis.

Eleven polycyclic NSAID prodrugs were successfully synthesised and were demonstrated to possess significant antioxidant properties through the deactivation of ABTS and/or DPPH free radicals using the standard antioxidant agent, trolox as a reference. Using a BBB endothelial cell model, the permeability coefficient of the ibuprofen series was determined and the results indicate a favourable BBB permeation of the polycyclic ibuprofen prodrugs in comparison to the parent NSAID.

Seven of the synthesised compounds produced inhibition of ABTS and DPPH radicals by up to 50% between 1000 μM and 1 μM . The results from the antioxidant study shows the conjugation of the polycyclic moieties to NSAIDs enhanced the antioxidant properties with IC_{50} values of up to 61.1 μM which is significantly comparable to that of the known potent antioxidant, trolox ($\text{IC}_{50} = 27 \mu\text{M}$). The apparent permeability coefficient (P_{app}) for the ibuprofen polycyclic conjugates was increased by 86.72% with a mean average value of $2.8083 \times 10^{-6} \text{ cms}^{-1}$ of the ibuprofen conjugates compared with P_{app} of $1.504 \times 10^{-6} \text{ cms}^{-1}$ of the parent ibuprofen. The result of this study suggests that polycyclic structures can serve as lipophilic scaffolds to improve the pharmacokinetic profile of NSAIDs to improve the CNS permeation in the management and treatment of neurodegenerative diseases.



TABLE OF CONTENTS

ACKNOWLEDGEMENTS	ii
ABSTRACT	v
TABLE OF CONTENTS	vi-xi
ABBREVIATIONS	xii-xiv
LIST OF FIGURES	ix
LIST OF TABLES	x
LIST OF SCHEMES	xi
CHAPTER ONE (INTRODUCTION)	1-8
1.1 Background	1
1.2 Rationale	2
1.2.1 Uncontrolled inflammation in neurodegenerative disorders	2
1.2.2 Polycyclic structures	4
1.3 Aim of study	5
1.4 Conclusion	8
CHAPTER TWO (LITERATURE REVIEW)	9-45
2.1 Neurodegenerative disorders	9
2.1.1 Apoptosis	12
2.1.2 Necrosis	13
2.1.3 Autophageal cell death	14
2.2 Calcium homeostasis	15
2.3 Mechanism of neurodegeneration	16

2.3.1	Excitotoxicity	17
2.3.2	Oxidative stress	21
2.3.3	Mitochondrial dysfunction	23
2.4	Inflammation	25
2.5	The blood brain barrier	28
2.5.1	Physicochemical properties necessary for BBB permeation	29
2.5.2	Strategies employed for CNS drug delivery	32
2.6	Non-steroidal anti-inflammatory therapy in neurodegenerative diseases	39
2.7	Polycyclic amines as lipophilic scaffolds	43
2.8	Conclusion	45
CHAPTER THREE (SYNTHESIS)		46-67
3.1	Pre-synthesis study	46
3.2	Standard synthesis procedures	46
3.2.1	Chemicals	46
3.2.2	Instrumentation	47
3.2.3	Chromatographic methods	49
3.2.4	General synthetic design	49
3.2.4.1	Synthesis of 3-(1-adamantylamino)propanenitrile (6)	51
3.2.4.2	Synthesis of pentacyclo[5.4.0 ^{2,6} .0 ^{3,10} .0 ^{5,9}]undecane-8,11-dione	52
3.2.4.3	Synthesis of 8-(2-aminoethanol)-8,11-oxapentacyclo[5.4.0 ^{2,6} .0 ^{3,10} .0 ^{5,9}]undecane (8)	53



3.2.4.4 Synthesis of 8-(3-aminopropanol)-8,11-oxapentacyclo ^{2 6 3 10 5,9} [5.4.0'.0'.0]undecane (9)	54
3.2.4.5 Synthesis of 3-hydroxy-4-aza-8-oxoheptacyclo[9.4.1.0 ^{2,10} .0 ^{3,14} .0 ^{4,9} .0 ^{9,13} .0 ^{12,15}]tetradecane (10)	55
3.2.4.6 Synthesis of 2-(6-methoxy-2-naphthyl)-N-(adamantyl)propanamide (5.1)	56
3.2.4.7 Synthesis of 2-N-[3-(1-adamantylamino)propyl]-2-(6-methoxy-2-naphthyl)propanamide (6.1)	56
3.2.4.8 Synthesis of 3-(4-aza-8-oxo-heptacyclo-[0.4.1.0 ²¹⁰ .0 ^{3,14} .0 ^{4,909,13} .0 ^{12,15}]-tetradecyl)- (6-methoxy-naphthyl)propanoate (10.1)	57
3.2.4.9 Synthesis of 2-(3-benzoylphenyl)-N-(adamantyl)propanamide (5.2)	58
3.2.4.10 Synthesis of (2R)-N-[3-(1-adamantylamino)propyl]-2-(3-benzoylphenyl)propanamide (6.2)	59
3.2.4.11 Synthesis of 3-(4-aza-8-oxo-heptacyclo[0.4.1.0 ²¹⁰ .0 ^{3,14} .0 ^{4,9 09,13} .0 ^{12,15}]-tetradecyl)-(3-benzoylphenyl)propanoate (10.2)	60
3.2.4.12 Synthesis of 2-(4-Isobutylphenyl)-N-(adamantyl)propanamide (5.3)	61
3.2.4.13 Synthesis of (2S)-N-[3-(1-adamantylamino)propyl]-2-(4-isobutylphenyl)propanamide (6.3)	62
3.2.4.14 Synthesis of 8,11-Oxapentacyclo ^{2 6 3 10 5,9} [5.4.0'.0'.0]undecane-8-(2-aminoethyl)-(4-isobutylphenyl)-propanoate (8.3)	63
3.2.4.15 Synthesis of 8,11-Oxapentacyclo ^{2 6 3 10 5,9} [5.4.0'.0'.0]undecane-8-(3-aminopropyl)-(4-isobutylphenyl)-propanoate (9.3)	64
3.2.4.16 Synthesis of 3-(4-aza-8-oxo-heptacyclo-[9.4.1.0 ^{2,10} .0 ^{3,14} .0 ^{4,9} .0 ^{9,13} .0 ^{12,15}]-tetradecyl)-(4-isobutylphenyl)propanoate (10.3)	65
3.3 Discussion	65

3.4	Conclusion	67
CHAPTER FOUR (BIOLOGICAL EVALUATION)		68-77
4.1	Materials and method for the antioxidant assays	68
4.1.1	2,2-Diphenyl-1-picrylhydrazyl (DPPH) assay	69
4.1.2	2,2-Azinobis (3-ethyl-benzothiazoline-6-sulfonic acid) (ABTS) assay	69
4.1.3	Materials and method for BBB permeability assay	70
4.2	<i>In vitro</i> blood-brain barrier permeability study	70
4.3	Result and discussion	71-76
4.3.1	Antioxidant evaluation	71
4.3.2	Permeability Coefficient (Papp)	75
4.4	Conclusion	77
CHAPTER FIVE (SUMMARY AND CONCLUSION)		78-80
5.1	Introduction	78
5.2	Synthesis	79
5.3	Biological Evaluation	79
5.4	Conclusion	80



LIST OF FIGURES

Fig 1.1	Blood-brain barrier, transport mechanisms	2
Fig 1.2	Representative non-steroidal anti-inflammatory drugs	3
Fig 1.3	Structural similarities between polycyclic amines	4
Fig 1.4	Synthesis of pentacyclo[5.4.0 ^{2,6} .0 ^{3,10} .0 ^{5,9}]undecane-8,11-dione	5
Fig 1.5	Polycyclic amines selected for conjugation with NSAIDs	6
Fig 1.6	Polycyclic NSAIDs designed for synthesis	7
Fig 1.7	Structural activity relationship of polycyclic NSAID prodrugs	8
Fig 2.1	Cellular defence mechanisms against protein aggregation	10
Fig 2.2	Selective neuronal nitric oxide synthase inhibitors	22
Fig 2.3	Role of inflammation in Neurodegenerative diseases	27
Fig 2.4	Physiological barriers of the central nervous system	29
Fig 2.5	Movement of molecules across the BBB	30
Fig 2.6	Representative active efflux transporter	34
Fig 2.7	Hydrolysis of the cyclic prodrugs of DADLE	35
Fig 2.8	Bioconversion of dopamine-CDS	39
Fig 3.1	Structures selected for conjugation (1-4) to the polycyclic cage scaffolds (5-10)	47
Fig 3.2	Synthesis of Cookson's diketone cage compound	49
Fig 4.1	Polycyclic-NSAID conjugates evaluated	68
Fig 4.2	Blood-brain barrier model using rat brain endothelial cells	70
Fig 4.3	ABTS ⁺ scavenging assay of parent NSAIDs and	

	synthesised compounds showing average % inhibition	73
Fig 4.4	DPPH radical scavenging assay of parent NSAIDs and synthesised showing % inhibition	74
Fig 5.1	Polycyclic NSAIDs synthesised	80



LIST OF TABLES

Table 2.1: Pathological hallmarks in neurodegenerative diseases	11
Table 3.1: <i>In Silico</i> analysis of potential prodrugs for blood-brain barrier Permeation	48
Table 4.1: Result of antioxidant evaluation of test compounds showing level of statistical significance	72
Table 4.2: Absorbance reading of test compounds after incubation with ABTS ⁺ solution	73
Table 4.3: Absorbance reading of test compounds after incubation with DPPH solution	73
Table 4.4: % recovery of test compounds from rat endothelial BBB model	76
SCHEMES	
Scheme 1: Synthetic route for direct conjugation of amantadine to NSAIDs	50
Scheme 2: Synthesis of amantadine-NSAIDs conjugates	50
Scheme 3: Synthesis of pentacycloundecane-NSAID conjugates	51
REFERENCES	82-105
APPENDIX	
Annexure A: Infrared, mass and nuclear magnetic resonance spectra	106-130

ABBREVIATIONS

6-OHDA	6-hydroxydopamine
AD	alzheimer's disease
AET	active efflux transport
AIDS	acquired immune deficiency syndrome
ALIS	aggresome-like inducible structure
ALP	autophagosome-lysosome system
ALS	amyotrophic Lateral Sclerosis
AMPA	α -amino-3-hydroxy-5-methyl-4-isoxasoleprionic acid
AMT	adsorptive-mediated transport
ATP	adenosine triphosphate
BBB	blood-brain barrier
BZAs	benzodiazepines
Ca ²⁺	calcium ion
CDI	N,N'-Carbonyldiimidazole
CDS	chemical delivery systems
CMT	carrier-mediated transport
CNS	central nervous system
COMT	catechol-O-methyltransferase
COX	cyclooxygenase
CSF	cerebrospinal fluid
DA	dopamine
DCM	dichloromethane
DHPs	1,4-dihydropyridines
DNA	deoxyribonucleic acid
ER	endoplasmic reticulum
H ₂ O ₂	hydrogen peroxide



HD	huntington's disease
Hsp	heat shock proteins
IL	interleukin
IP ₃ Rs	inositol-1,4,5-trisphosphate receptors
K ⁺	potassium ion
KA	kainic acid
MAO	monoamine oxidase
MDR	multidrug-resistant
MPTP	1-methyl-4-phenyl-1,2,3,6-tetrahydropyridine
Na ⁺	sodium ion
NADH	nicotinamide adenine dinucleotide
NCX	sodium-calcium exchanger
ND	neurodegenerative diseases
NMDA	<i>N</i> -methyl- <i>D</i> -aspartate
NO	nitric oxide
NOS	nitric oxide synthase
NSAIDs	non-steroidal anti-inflammatory drugs
ONOO ⁻	peroxynitrites
PAAs	phenylalkylamines
PCC	polycyclic cage compounds
PCD	programmed cell death
PCM	polycyclic cage moieties
PCP	phencyclidine
PD	parkinson's disease
PG	prostaglandins
P-gp	p-glycoprotein
PMCA	plasma membrane calcium pump



PPAR γ	peroxisome proliferator-activated receptor gamma
RMT	receptor-mediated transcytosis
RNS	reactive nitrogen species
ROS	reactive oxygen species
RyRs	ryanodine receptors
THF	tetrahydrofuran
TNF	tumour necrosis factor
UPR	unfolded-protein response
UPS	ubiquitin-proteasome system.
UV	ultraviolet



CHAPTER ONE

INTRODUCTION

1.1 Background

Neurodegenerative disorders (ND) are a class of detrimental brain disorders involving atrophy of central nervous system (CNS) cells, leading to loss of motor and/or cognitive functions and consequently severe economic burden as they encroach on the lifestyle of sufferers thereby resulting in low productivity (Gustavsson *et al.*, 2011; Fratiglioni and Qiu, 2009). The past decade has witnessed a surge in the prevalence of these disorders with Alzheimer's disease (AD), Parkinson's disease (PD), Huntington's disease (HD) and Amyotrophic lateral sclerosis (ALS) being the most common especially amongst the older population (Farooqui and Farooqui, 2009).

The term neurodegeneration is used to describe processes leading to the loss of neuronal cell function or the death thereof. These disorders have been the focus of scientific research for decades and are observed to be propagated by similar complex processes encompassing the activation of a cascade of neurotoxic events involving protein aggregation, inflammation, oxidative stress and excitotoxicity which will eventually result in neuronal death (Shachar *et al.*, 2004; Zádori *et al.*, 2012). Using the 1-methyl-4-phenyl-1,2,3,6-tetrahydropyridine (MPTP) and 6-hydroxydopamine (6-OHDA) animal models of PD, the neuroprotective potential of iron chelators, free radical scavengers, calcium channel blockers, glutamate receptor antagonists, trophic factors and antioxidants have been demonstrated (Mandel *et al.*, 2003).

Despite the vast advancements made in understanding the pathogenesis and diagnosis of neurodegenerative diseases, current drug therapies only offer palliative relief of symptoms for a short period of time and no effect in halting disease progression (Obeso *et al.*, 2010). Many drugs designed have poor pharmacokinetic profile and fail to reach the market. A major challenge in developing CNS active drugs is the constraint posed by the Blood-Brain Barrier (BBB). The vascular endothelium is responsible for homeostatic control of the brain by regulating the extracellular fluid's composition. The presence of a monolayer endothelial cell, high-resistance tight junctions, astrocyte's foot process and specialised transport systems (**Fig 1.1**) ensure the selective movement of compounds into the brain (Krueger and Bechmann,

2009). The design of compounds with favourable physicochemical properties for BBB permeation is of paramount importance in the treatment of diseases of the CNS.

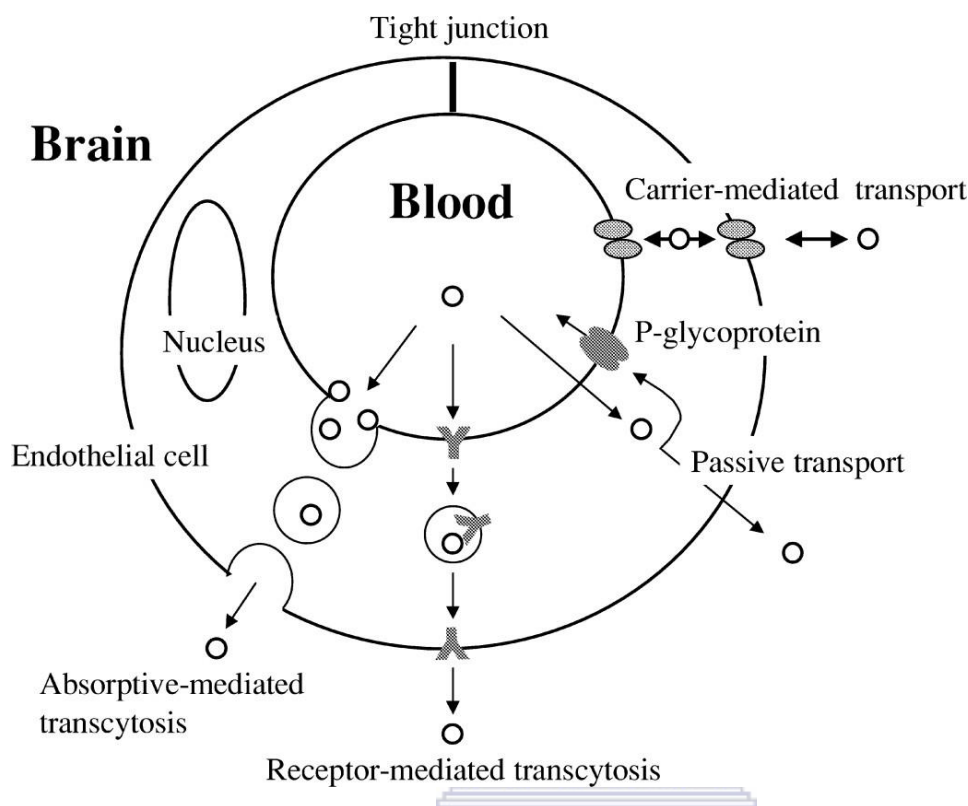


Fig 1.1: Blood-brain barrier, transport mechanisms (Norinder & Haerberlein, 2002)

Good BBB permeation, reasonable metabolic stability and a desirable toxicity profile are the cornerstone of designing CNS-active compounds (Varma *et al.*, 2010). Drug development can be time and money consuming hence the Lipinski's 'rule of 5' is widely accepted as a simple tool for predicting the oral bioavailability of potential therapeutic agents (Franc *et al.*, 1997).

1.2 Rationale

1.2.1 Uncontrolled inflammation in neurodegenerative disorders

Inflammation is a crucial component of the innate immune system which is essential for cell survival as it offers protection against infections and injuries. Acute inflammation is of utmost importance for tissue survival and cell maintenance. Conversely, inappropriate activation of the inflammatory response during chronic inflammation induces focal damage to neighbouring healthy tissues. This is a major hallmark in ND progression as a continuous surge in the expression of inflammatory mediators cause continuous damage to neurons

(Balistreri *et al.*, 2009; Amor *et al.*, 2010; Glass *et al.*, 2010). Inflammatory response in neurons involve activation of microglia, astrocytes, macrophages and lymphocytes accompanied by the release of pro-inflammatory cytokines, chemokines, neurotransmitters and reactive oxygen species (ROS).

Epidemiological studies, clinical data as well as animal-model studies of ND suggests that anti-inflammatory mediators such as NSAIDs; naproxen, ketoprofen, ibuprofen and aspirin (1-4) (Fig 1.2), steroidal anti-inflammatory drugs, antibiotics, stimulators of the peroxisome proliferator-activated receptor-c (PPARc) and inhibitors of pro-inflammatory transcription factors offer some neuroprotective effects (Vlad *et al.*, 2008; Choi *et al.*, 2013). The NSAID-ibuprofen for example, produced a decrease in adjusted odds ratio for AD from 1.03 for less than one year of use to 0.56 for more than five years of use. Genetic studies have also provided strong evidence that polymorphism of pro-inflammatory factors has profound effects on the risk of developing ND (Candore *et al.*, 2007). ND progression may therefore be significantly reduced if not completely halted by modulating the inflammatory process occurring in the brain.

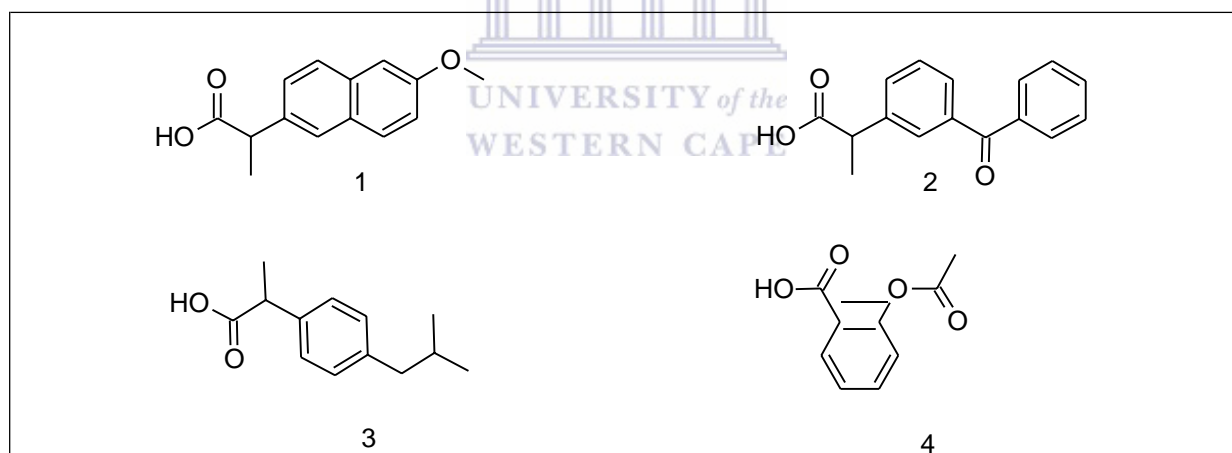


Fig 1.2: Representative non-steroidal anti-inflammatory drugs

Several mechanisms have been proposed for the neuroprotective activity of NSAIDs, notably through the inhibition of cyclooxygenases resulting in decreased biosynthesis of pro-inflammatory prostaglandin (PG) (Vlad *et al.*, 2008; McGeer and McGeer, 2007). NSAIDs produced a dose-dependent reduction of behavioural deficits in transgenic animal models of AD. At therapeutically significant doses for ND, the side effect profile of NSAIDs is greatly increased as they cause irritation and ulceration of the gastro-intestinal tract (GIT) thus limiting their clinical use.

NSAIDs are highly lipophilic and should easily cross the BBB by passive diffusion (Habgood *et al.*, 2000). However, most NSAIDs are weakly acidic, over 99% ionised at physiological pH due to their carboxylic acid functional group and therefore exhibit poor distribution into the CNS (Eriksen *et al.*, 2003).

1.2.2 Polycyclic structures

The chemistry and activity of polycyclic cage compounds has been extensively investigated following the discovery that amantadine (1-adamantylamine) (**5**) has potent antiviral properties and can therefore be used in treatment of Influenza A infections. Clinical observations later showed that patients experienced decreased tremor and dyskinesia typical in PD when treated for flu with amantadine (Schwab *et al.*, 1972).

The discovery of the neuroprotective effects of the adamantanes stimulated further interest into the chemistry of similar cage structures. The structural relationship between the pentacycloundecane amines (**7** and **7.1**) and adamantane amines is widely reported (**Fig 1.3**), in addition to their successful utilization in the development of lead compounds for ND (Grobler *et al.*, 2006; Van der Schyf *et al.*, 2009; Joubert *et al.*, 2011). Polycyclic cage compounds (PCC) can be employed as scaffolds for side chain attachment to modify drugs, increase lipophilicity and improve their pharmacological profile.

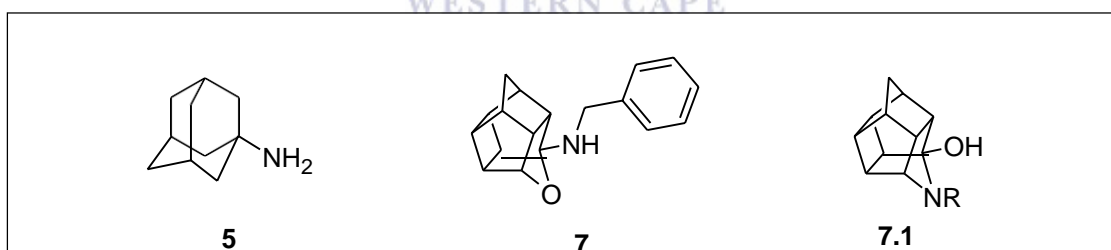


Fig 1.3: Structural similarities between polycyclic amines

Amantadine has an amino group which will ionize at physiological pH and should expectedly hinder BBB permeation. However, the bulky hydrocarbon backbone confers high lipid-solubility and good CNS distribution. Polycyclic cage moieties (PCM) can therefore improve the lipophilicity and BBB permeation of privileged pharmaceutical agents (Zah *et al.*, 2003).

Pentacycloundecylamines are saturated hydrocarbon ‘cage’ compounds derived from the reductive amination of the Cookson’s diketone known as pentacyclo[5.4.0^{2,6}.0^{3,10}.0^{5,9}]undecane-8,11-dione. This ‘bird cage’ compound is obtained from the intramolecular {2+2} photocyclization of the Diels-Alder adduct obtained from the

reaction between *p*-benzoquinone and cyclopentadiene (Fig 1.4) (Cooksen *et al.*, 1958; Sasaki *et al.*, 1974; Marhand and Allen, 1991).

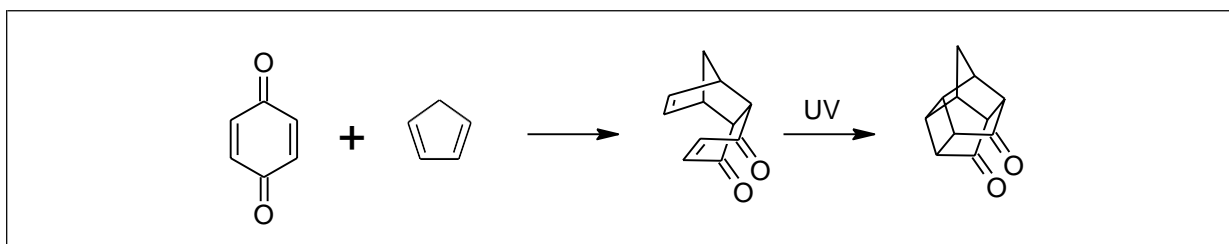


Fig 1.4: Synthesis of pentacyclo[5.4.0^{2,6}.0^{3,10}.0^{5,9}]undecane-8,11-dione

A carbinolamine is formed when a ketone group of the diketone cage molecule is reacted with an amine. The product can be subsequently reduced under different conditions to either oxa- or aza- polycyclic cage imines for further derivatization.

1.3 Aim of study

The purpose of this study was to evaluate novel conjugates of NSAIDs and polycyclic moieties for enhanced BBB permeability of the parent drug. The NSAIDs; naproxen, ketoprofen, ibuprofen and aspirin were selected for this study based on clinical data which suggest their potential neuroprotective properties once modified to reach the CNS at significant concentrations due to their intrinsic anti-inflammatory properties. The availability of parent drug was also a criterion for selecting these NSAIDs.

The design of polycyclic NSAIDs prodrug required the selection of suitable polycyclic cage structures to improve the pharmacokinetic properties of the parent NSAIDs. The carboxylic end of the NSAID can undergo esterification and amidation reactions with corresponding carbinolamine or amide derivatives. The presence of a large polycyclic framework will also reduce steric interactions and increase the stability of conjugated compounds (Brookes *et al.*, 1992). This is an added advantage as the parent compound is protected from metabolic degradation and lower therapeutic doses required with less side effects. These prodrugs have the ability to modulate voltage gated calcium channels (Van der Schyf *et al.*, 1986 Malan *et al.*, 2000; Joubert *et al.*, 2011) which is important for the stimulation of efflux pumps that actively preclude drugs out of the CNS. This may be of benefit in increasing the CNS concentration of parent NSAIDs after successful BBB permeation.

Four series of compounds were planned for synthesis with each series consisting of an NSAID: naproxen (1), ketoprofen (2), Ibuprofen (3) or aspirin (4) conjugated to amantadine

(5), N-(1-adamantyl)-1,3-propanediamine (6), 8-(2-aminoethanol)-8,11-oxapentacyclo[5.4.0^{2,6}.0^{3,10}.0^{5,9}]undecane (8),
 oxapentacyclo[5.4.0^{2,6}.0^{3,10}.0^{5,9}]undecane (9) or 3-hydroxy-4-aza-8-oxoheptacyclo[9.4.1.0^{2,10}.0^{3,14}.0^{4,9}.0^{9,13}.0^{12,15}]tetradecane (10).

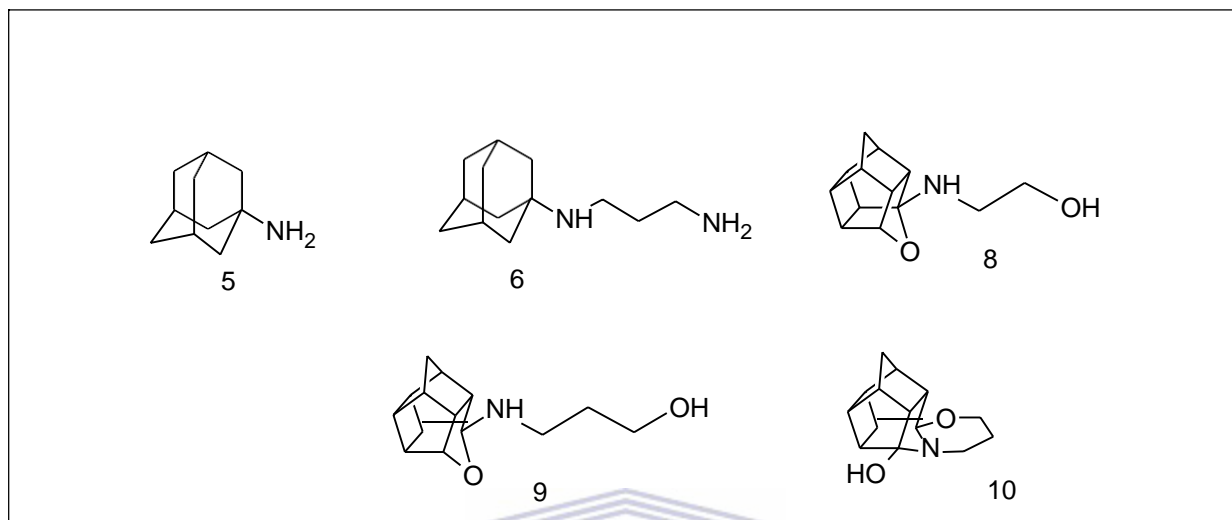


Fig 1.5: Polycyclic amines selected for conjugation with NSAIDs

The following objectives were set as a guide towards achieving this aim:

- Perform *In silico* studies to evaluate prodrugs for oral bioavailability and BBB permeability;
- Synthesise the selected compounds (**Fig 1.6**) by conjugating the polycyclic compounds to the selected NSAIDs *via* amidation and esterification reactions;
- Perform structure elucidation of the novel compounds by means of ¹H-NMR, ¹³C-NMR, MS and IR;
- *In vitro* antioxidant evaluation of synthesised prodrugs for free-radical scavenging activity;
- Perform *in vitro* BBB permeability studies on a series of the polycyclic NSAIDs conjugates.

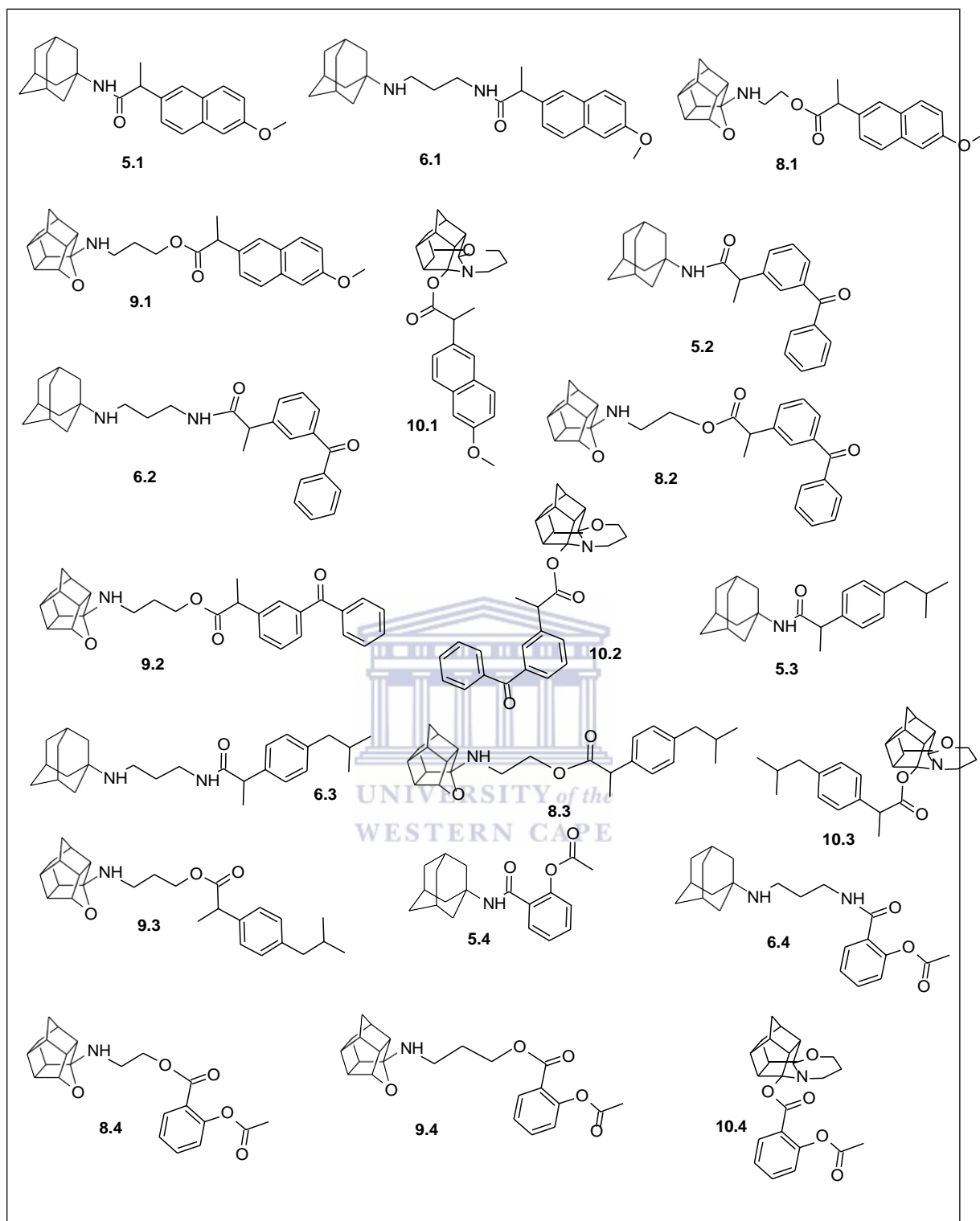


Fig 1.6: Polycyclic NSAIDs designed for synthesis

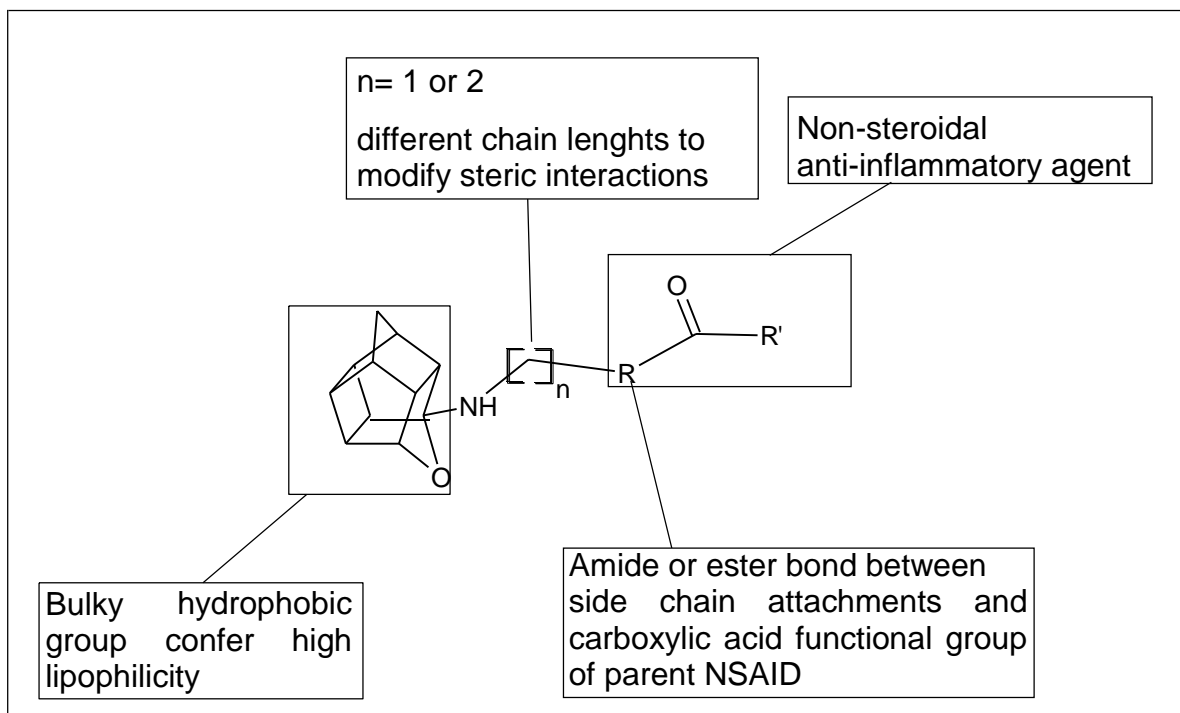


Fig 1.7: Structural activity relationship of polycyclic NSAID prodrugs

1.4 Conclusion

Neurodegenerative disorders are disorders of the brain and therefore pharmacologically active drugs targeting these disorders should readily transverse the BBB. Unregulated inflammation is a major driver of neurodegenerative disease progression however the beneficial effects of NSAIDs as potent anti-inflammatory mediators in the brain is not fully utilised as these agents will not reach the site of action in the CNS. The cage-like structure of adamantanes and pentacycloundecylamines confers high lipophilicity (**Fig 1.7**) and will diffuse across the BBB at pharmacologically significant concentrations. These moieties can therefore be employed as lipophilic scaffolds to improve the BBB permeability of NSAIDs. This study postulates that the novel compounds will possess good BBB permeability to produce significant anti-inflammatory effects in the CNS.

CHAPTER TWO

LITERATURE REVIEW

This chapter describes the neurodegenerative processes, cellular mechanisms involved and therapeutic strategies aimed at reversing and/or halting disease progression. The blood brain barrier's role in central nervous system disorders and strategies to improve drug delivery to the brain is also explored.

2.1 Neurodegenerative disorders

Neurodegenerative diseases (ND) is an umbrella term for over 600 diseases involving progressive dysfunction and loss of neuronal cells coupled with the accumulation of misfolded disease-specific proteins hence, they are sometimes referred to as conformational diseases or proteopathies (Golde & Miller 2009; Frost & Diamond 2010). The abnormal protein causes synaptic dysfunction in the nervous system and organelle damage on aggregating in nuclear, extracellular and cytoplasmic inclusions.

About 30 % of newly synthesised proteins are misfolded and prone to aggregation (Schubert *et al.*, 2000). Under normal physiological conditions, chaperones of the protein quality control system such as heat shock proteins (Hsp) reprocess and repair the damaged proteins (Hartl *et al.*, 2011). As depicted in **Fig 2.1**, the chaperones may also degrade abnormal proteins *via* the autophagosome-lysosome pathway (ALP) for long-lived proteins and organelles in the cytoplasm (d) or the ubiquitin-proteasome system (UPS) which digests short-lived proteins in the nucleus and cytoplasm (c) (Dikic *et al.*, 2009). Proteins that cannot be reprocessed or eliminated are sequestered within cells *via* their interaction with the cytoplasmic microtubule dynein (e) (Brundin *et al.*, 2010). In neurodegenerative conditions, these systems are dysfunctional and aggregated proteins accumulate.

A myriad of evidence suggests that activators of heat shock proteins can prevent neurotoxic cascades in neurodegenerative diseases by monitoring disease-specific misfolded proteins and preventing the aggregation thereof (Arawaka *et al.*, 2010; Klaic *et al.*, 2011). Protein misfolding may occur due to the damaging effects of reactive oxygen species (ROS) or less commonly due to mutation (Wang *et al.*, 2012). Inhibition of kinases and other proteolytic enzymes involved in the conformational change that leads to misfolding of proteins have

been explored as potential therapeutic strategies to halt protein misfolding and aggregation in ND (Meijer *et al.*, 2000; Lin *et al.*, 2009; Panza *et al.*, 2009; Palomo *et al.*, 2011).

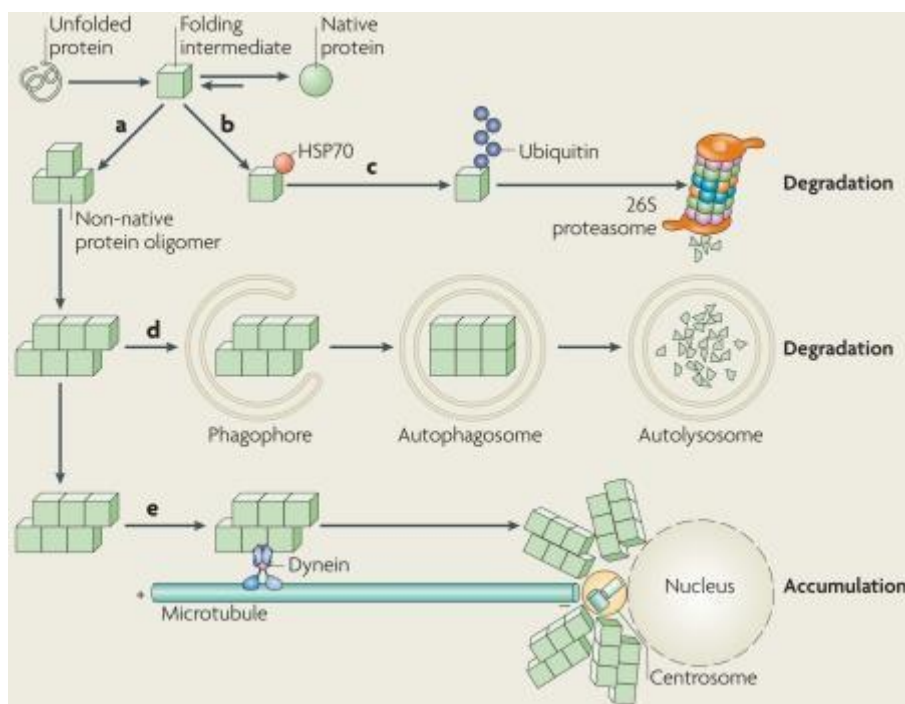


Fig 2.1: Cellular defence mechanisms against protein aggregation (Brundin *et al.*, 2010)

The most common neurodegenerative diseases are Alzheimer's disease (AD), Parkinson's disease (PD), Amyotrophic Lateral Sclerosis (ALS) and Huntington's disease (HD) (Forman *et al.*, 2004). AD is the fourth leading cause of death in developed countries, characterised by progressive loss of memory and cognitive functions leading to dementia. There are about 28 million people worldwide diagnosed with AD and the prevalence is expected to triple by the year 2050 with immense economic and social implications (Mount & Downton 2006; Minati *et al.*, 2009).

To circumvent the negative effect of the expected increase in the prevalence of ND, there has been an accelerated research effort in the field of drug design in neuroscience. Therapeutic options are still very limited as current drugs are merely palliative in managing symptoms as known drugs do not halt or prevent disease progression (Cowan & Kandel 2001; Melnikova 2007; Habibi *et al.*, 2011). The clinical manifestations of these diseases are dependent on the neuronal subtype affected (**Table 2.1**), resulting in motor coordination and/or cognitive difficulties. Consequently, the patient's intellect, economic productivity, personality and social interactions are impaired (Ivanhoe *et al.*, 2005).

The increase in the prevalence of ND amongst the older population can be attributed to changes in the processes of protein synthesis, folding and degradation due to age (greatest risk factor for ND), environmental factors, genetic predisposition and mutation (Glass *et al.*, 2010; Kalaria *et al.*, 2008). The result of disturbances in the processing of proteins is a transformation in the protein structure into a beta sheath rich conformation (Lee & Trojanowski 2006; Bucciantini *et al.*, 2002). This new irreversible conformation is very adhesive as it exposes the buried hydrophobic regions within the natively folded conformation of proteins thereby promoting protein oligomerization, aggregation and fibril formation (Ross & Poirier 2004; Bolognesi *et al.*, 2010). Aggregated proteins may also migrate to neighbouring cells to cause misfolding of other proteins (Walker & Levine 2012; Calignon *et al.*, 2012). This continuous migration may account for the gradual progression of most neurodegenerative diseases over time as aggregated proteins accumulate and spread to initiate neuronal death.

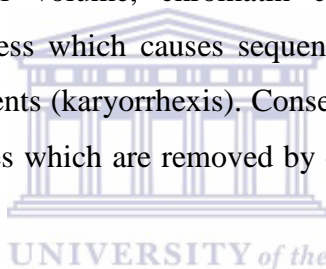
Table 2.1: Pathological hallmarks in neurodegenerative diseases (Bruijn *et al.*, 1998; Jankovic 2008; Farooqui & Farooqui 2009; Grosskreutz *et al.*, 2010)

ND	Neuron subtype implicated	Aggregated proteins	Symptoms
AD	Hippocampal and cortical neurons	β -amyloid (A β) peptide, Hyperphosphorylated tau protein	Cognitive impairment, depression and sleep disorders
PD	Dopaminergic midbrain neurons	Alpha--synuclein	Tremor, rigidity, bradykinesia
HD	Striatum and cerebral cortex	Huntingtin	Chorea, dystonia, cognitive impairment and behavioural difficulties
ALS	Lower motor neurons in brainstem and spinal cord	Superoxide dismutase-1 (SOD-1)	Progressive muscle weakness, atrophy, spasticity and paralysis

The cumulative effect of concurrent pathological pathways involving protein aggregation, mitochondrial dysfunction, oxidative stress, phosphorylation impairment and metal dyshomeostasis causes irreversible damage to neurons but the exact mechanism is poorly understood (Zecca *et al.*, 2004; Arrasate *et al.*, 2004; Savitt *et al.*, 2006). Homeostatic control of neuronal population is coordinated by a balance between cell mitosis and cell death. Morphologically, neuronal cell death can occur, depending on the extent of neuronal damage *via* three processes namely apoptosis, necrosis and autophagy.

2.1.1 Apoptosis

Cells undergo suicide as a mechanism to control the process of mitosis (cell division) and enable proper functioning and development of cells. Apoptosis is a distinct form of programmed cell death (PCD) that maintains tissue homeostasis without harming adjacent cells (Hellwig *et al.*, 2011). The apoptotic process is characterized by the rounding up of damaged cells, reduced cellular volume, chromatin condensation (pyknosis) and the activation of endonucleotic process which causes sequential cleavage of deoxyribonucleic acid (DNA) to oligosomal fragments (karyorrhexis). Consequently, cells condense into small membrane-bound apoptotic bodies which are removed by circulating phagocytes (Los *et al.*, 1999; Rashedi *et al.*, 2007).



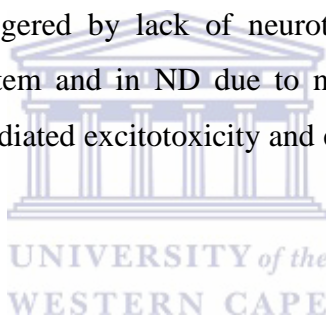
A classic example of the importance of apoptosis is seen in cancer pathology where the process of apoptosis is halted. In cervical cancer, the genetic material of the human papilloma virus is integrated into the host's DNA and expresses anti-apoptotic proteins. Misfolded proteins are not processed and eventually accumulate to trigger unfolded-protein response (UPR) which if prolonged, may activate toxic pathways (Sherman & Goldberg 2001; Taylor *et al.*, 2002).

Apoptosis is an active metabolic process that occurs under physiological and pathological conditions, brought about by a family of intracellular cysteine proteases which cleave with a remarkably high specificity at a small subset of aspartic acid residue of proteins. Caspases are activated through two major pathways involving signalling by tumour necrosis factor (TNF) receptors and the release of pro-apoptotic proteins from damaged mitochondria. In the fast extrinsic pathway, cell-surface death receptors such as TNF receptors are stimulated to activate caspase-8 and subsequently caspase-3 and -7 (Rashedi *et al.*, 2007). The intrinsic pathway involves the release of cytochrome c from the mitochondria and the subsequent activation of caspase-9 due to a shift in the balance of apoptotic Bcl2 members towards the

anti-apoptotic proteins which accumulate in the outer membrane of the mitochondria (Wallach *et al.*, 1999; Green *et al.*, 1998; Fuchs & Steller 2011).

The nucleus, endoplasmic reticulum (ER) and Golgi apparatus are also linked to apoptotic pathways. The activation of caspases is highly regulated by inhibitor of apoptosis proteins which are controlled by the mitochondria (Ghavami *et al.*, 2008; Fuchs & Steller 2011). Following apoptotic stimulation, the mitochondria releases Apoptosis-Inducing Factor, a flavoprotein-oxidoreductase capable of inducing caspase-independent apoptosis (Cande *et al.*, 2002).

Despite the positive contribution of apoptosis in preventing autoimmune disorders, cancers and repeated viral infections amongst other diseases, it also plays a crucial role in acquired immune deficiency syndrome (AIDS) and ND progression (Hellwig *et al.*, 2011). Apoptosis ensures proper neuronal development and function (Miura 2011) however, detrimental apoptotic processes may be triggered by lack of neurotrophic factor support during the development of the nervous system and in ND due to neuronal damage by free radicals, misfolded proteins, glutamate-mediated excitotoxicity and environmental toxins (Tendi *et al.*, 2010).



2.1.2 Necrosis

Necrotic cell death occurs in hypoxic or ischaemic conditions in the presence of pathological factors such as injury, toxins, oxidative stress, high temperature, ultraviolet (UV) radiation, ionising radiation, nutrient deprivation, hypoglycaemia and anti-tumour drugs. Both necrosis and apoptosis play a major role in most ND (Martin *et al.*, 1999) however, very few studies have been done to investigate the mechanism of necrotic cell death. The use of genetic models suggests that necrotic cell death during neurodegeneration occurs through endocytosis and disturbed intracellular trafficking (Lee *et al.*, 2012). This supports previous studies implicating disrupted intracellular trafficking in neurodegenerative diseases (De Vos *et al.*, 2007).

Mediators of necrotic cell death include increased intracellular calcium ion (Ca^{2+}) concentration, ROS, immune response and DNA damage. Studies done on *C.elegans* have shown that proteases play a major role in necrotic cell death. During the early stage of necrotic accidental cell death, cytoplasmic calpain proteases are activated due to increased intracellular calcium concentration. This result in cleavage of the $\text{Na}^+/\text{Ca}^{2+}$ exchanger to

cause a further increase in intracellular Ca^{2+} concentration and cell death. Calpain also attack the membrane proteins of lysosomes to release lysosomal content including hydrolytic cathepsin proteases and acidify the cytoplasm (Artal-Sanz *et al.*, 2006; Syntichaki *et al.*, 2002).

The cathepsin released further propagates necrotic cell death by breaking down molecules in the cytoplasm that were not exposed to proteases prior to lysosomal leakage. This result in swelling of the mitochondria, rupture of the plasma membrane to disperse chromatin and eventually cell destruction *via* the activation of endonucleolytic processes involving the sequential cleavage of chromosomal DNA to oligosomal DNA fragments coupled with the activation of an inflammatory response. Breakdown products of the cell including phospholipids such as arachidonic acid are released into the extracellular space. Arachidonic acid is a free fatty acid that acts as a substrate for cyclooxygenases to synthesise eicosanoids including prostaglandins which mediate inflammatory responses. Unlike apoptosis, necrosis is a passive, catabolic process and only occurs under pathological conditions (Samara & Tavernarakis, 2008).

2.1.3 Autophageal cell death

This is a protective form of cell death that occurs during starvation to degrade protein aggregates and damaged organelles. The misfolded protein or targeted organelle is encircled *via* initiation, elongation and maturation into a vesicle to form an amphisome which then fuses with a lysosome for degradation (Alavian *et al.*, 2011; Glick *et al.*, 2010). This results in the production of energy and amino acids for protein synthesis in the starving cell. Autophagy occurs at a very low level in cells and is only upregulated during nutrient starvation (Levine & Yuan 2005). The mammalian target of rapamycin is the main regulator of autophagy related genes under normal physiological conditions (Glick *et al.*, 2010).

The cell body of neurons is highly polarized due to the presence of trophic factors such as nerve growth factor and membrane transport systems that connect cell bodies with axons and dendrites. This polarization coupled with the post-mitotic nature and small size of neurons enables them to easily accumulate damaged cytoplasmic components and membranes. Neuronal cells uses autophagy as a means to eliminate toxins (Tooze & Schiavo 2008). PD, AD, HD and transmissible spongiform encephalopathy (prion disease) have been linked to a dysfunctional autophageal process (Anglade *et al.*, 1997; Cataldo *et al.*, 1996; Kegel *et al.*, 2000; Liberski *et al.*, 2004).

The role of autophagy in ND is very controversial as increasing evidence suggests that autophagy is required for some form of cell death to occur. Interestingly, cells deficient in pro-apoptotic proteins on exposure to etoposide and staurosporine, both classical inducers of apoptosis, undergo cell death with characteristics typical in autophagy (Shimizu *et al.*, 2004). Inhibition of apoptotic cell death by administration of the general caspase inhibitor zVAD initiated autophageal cell death (Yu *et al.*, 2004). These studies suggest that anti-apoptotic therapies may induce cell death *via* non-apoptotic pathways therefore different cell death pathways should be investigated when designing therapies for proteopathies (Sureda *et al.*, 2011). Using mice model of ND, Komatsu's group observed that inclusion bodies accumulate and cause neuronal death within 28 days in mice deficient in the ATG7 gene. This infers that autophagy plays a crucial role in the survival of neuronal cells and insufficient autophagy may be involved in the pathophysiology of ND (Komatsu *et al.* 2006).

2.2 Calcium homeostasis

Calcium and phosphate ions are capable of altering protein conformation by occupying four to twelve oxygen atoms (Strynadka & James 1989). The high concentration gradient between extracellular calcium ion (Ca^{2+}) concentration (1.2 mM) and the intracellular concentration (100 nM) under physiological conditions makes calcium the main determinant of intracellular ionic concentration since the more abundant potassium ion (K^+) and sodium ion (Na^+) are relatively balanced after depolarisation. Various Ca^{2+} binding proteins and Ca^{2+} -dependent biochemical pathways coordinate many physiological functions of cells. In neurons, calcium functions as a second messenger in coordinating the conduction of signals and neurotransmitter release from post synaptic cells depending on the membrane potential of pre-synaptic neuron (Hausser 2000). This coordination prevents unnecessary synaptic connections and over-excitation.

Calcium dysregulation and overload is implicated in the pathophysiology of a number of ND (Gleichmann & Mattson 2010; Prahlad & Morimoto 2009). Ca^{2+} influx into neurons activate a variety of proteins including neuronal NOS which catalyses the synthesis of nitric oxide (NO), a highly reactive molecule that produces ROS such as superoxide and peroxynitrites (ONOO^-) which are mediators of oxidative stress, causing damage to lipids, proteins and DNA. Local changes in Ca^{2+} concentration are responsible for regulation of blood flow to neurons as well as signal transduction between neurons and glia cells. Homeostatic regulation of Ca^{2+} is maintained at a narrow range through voltage- and ligand-gated channels in

neurons and calcium release from the ER (Zamponi 2005). The sodium-calcium exchanger (NCX) is the main pathway for calcium efflux however, reverse mode exchange during hyper depolarisation and increased Na^+ concentration can induce Ca^{2+} influx and overload (Rizzuto & Pozzan 2006).

The ER is physiologically in close proximity to the mitochondria and plays a vital role in the calcium signalling pathway as it is the main storage site for Ca^{2+} . Using the ER proteins, the movement of calcium ions is controlled to maintain a higher concentration in the ER lumen (10-100 μM) compared to that in the cytoplasm (100-300 nM). This concentration gradient is maintained by the sequestration of Ca^{2+} into the ER by sarco-endoplasmic reticulum Ca^{2+} -ATPase (SERCA) and its release into the cytoplasm from the ER on activation of inositol-1,4,5-trisphosphate receptors (IP_3Rs) and ryanodine receptors (RyRs) where it can be taken up by the mitochondria (Rizzuto & Pozzan 2006).

Neuronal energy supply is primarily dependent on adenosine triphosphate (ATP) generation in the mitochondria through oxidative phosphorylation (Herrero-Mendez et al., 2009). The mitochondria functions as a buffer for Ca^{2+} (Rizzuto *et al.*, 2000). In the electron transport chain, oxygen is reduced to water while hydrogen and ATP is pumped to the mitochondrial intermembrane space from the matrix. This creates a negative membrane potential in the matrix and Ca^{2+} being highly electropositive will accumulate in the mitochondrial matrix through the Ca^{2+} /uniporter and plasma membrane calcium pump (PMCA) especially when energy demand is low. This influx is balanced by Ca^{2+} efflux *via* the mitochondrial NCX and open mitochondrial pores during mitochondrial permeability transition (Kapu` s *et al.*, 1991; Rizzuto *et al.*, 2000).

Calcium signalling is therefore closely linked to mitochondrial function. An increase in matrix calcium concentration coordinates increased energy demand signals to the mitochondria by increasing the activity of pyruvate dehydrogenase, isocitrate dehydrogenase and α -ketoglutarate dehydrogenase from the kerb cycle as well as F_1F_0 -ATPase to increase the production of ATP and nicotinamide adenine dinucleotide (Denton 2009).

2.3 Mechanism of neurodegeneration

The degree of accumulation of specific proteins is observed to be related to oxidative stress, loss of mitochondrial function, calcium dysregulation and membrane depolarization observed in neurodegeneration. Despite the differences in the clinical manifestations of ND, they have

been found to be propagated by similar complex and integrated mechanisms encompassing calcium dysregulation, oxidative stress and mitochondria dysfunction (Panov *et al.*, 2002; Firdaus *et al.*, 2006).

2.3.1 Excitotoxicity

Aspartate and glutamate are the major excitatory amino acid neurotransmitters in the central nervous system (CNS) with about 40 % of synapses being glutamatergic, predominantly in the cerebral cortex and limbic regions of the brain (Fairman & Amara 1999). On release of glutamate from nerve endings of glutamatergic neurons, different glutamate receptors are activated to partake in neuronal signalling. Under physiological conditions, glutamate released from the presynaptic neuron activates ionotropic glutamatergic receptors on post-synaptic neurons. This causes membrane depolarisation and the generation of an action potential due to influx of Na⁺ and Ca²⁺ into the cell (Kanai & Hediger 2003). Homeostatic control of glutamate concentration in the synaptic cleft is therefore of paramount importance in preventing neuronal death.

Hypoglycaemia, hypoxia and aggregated proteins induce increased glutamate release followed by the over-excitation of postsynaptic neurons *via* activation of excitatory glutamate metabotropic and ionotropic receptors. *N*-methyl-*D*-aspartate (NMDA), α -amino-3-hydroxy-5-methyl-4-isoxasolepropionic acid (AMPA) and kainic acid (KA) ionotropic receptors are activated to stimulate increased Ca²⁺ influx and subsequent calcium overload in neuronal cells, leading to activation of series of enzymes including phospholipases, neuronal NOS, and xanthine oxidase that catalyse reactions that produce reactive free radicals in association with the disruption of calcium homeostasis and loss of mitochondrial membrane potential with subsequent mitochondrial damage thereof (Emerit *et al.*, 2004; Abramov & Duchon 2008). The products of such reactions coupled with the reactive species further stimulate the release of glutamate, thereby sustaining a vicious circle of excitotoxicity and free-radical induced neuronal damage. Under severe pathological conditions, irreversible loss of mitochondrial membrane potential elicits the opening of the mitochondrial permeability transition pore to induce cell death.

High-affinity sodium-dependent transporter systems are the primary mechanisms for uptake of glutamate and maintenance of glutamate concentration in the brain (Kanai & Hediger 2003). All CNS cells express these transport systems, however astrocytes are prominently responsible for the rapid removal of glutamate from the extracellular space (Fairman &

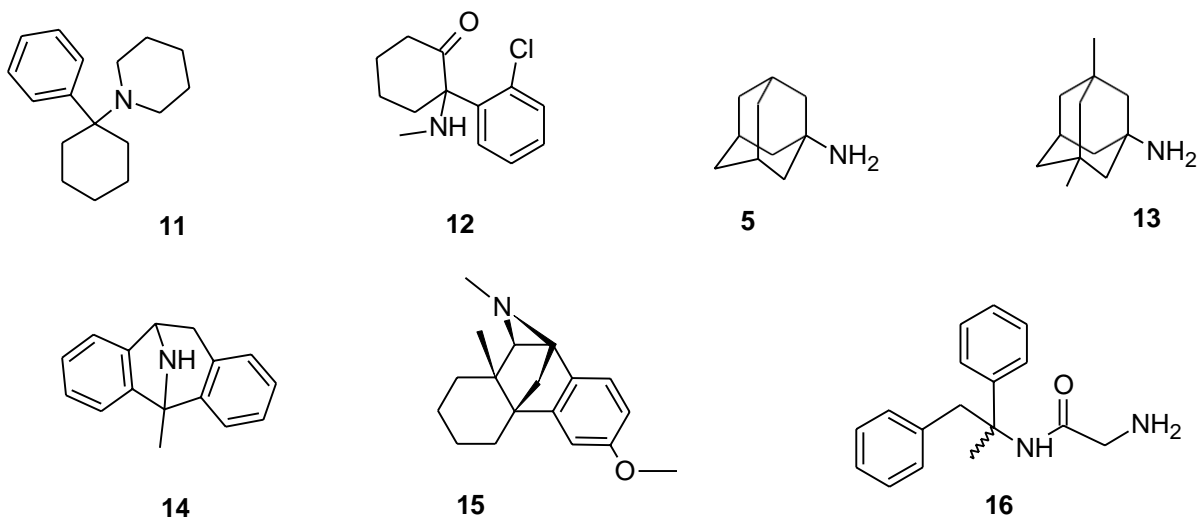
Amara 1999; Kanai & Hediger 2003; Bunch *et al.*, 2009). Several studies have established that mutation in astrocytes play a propagatory role in neurodegenerative diseases (Di Giorgio *et al.*, 2008; Marchetto *et al.*, 2008; Van Damme *et al.*, 2007). The inability of astrocytes to modulate increased glutamate levels predisposes nearby neurons to neuronal injury and may account for the accelerated neuronal degeneration (Rossi & Volterra 2009). Several strategies have been explored to prevent glutamate-mediated excitotoxicity in neurodegenerative disorders and are discussed below.

a. NMDA Antagonists

NMDA receptors are ligand-gated receptors that are activated by glutamate and NMDA. On activation of the NMDA receptor, Ca^{2+} moves into postsynaptic cells and activates neuronal signalling pathways. Overstimulation of NMDA receptors has been implicated in neurodegenerative processes. The NMDA receptor channel pore is widely investigated as a drug target in preventing excitotoxicity induced neuronal death (Paoletti & Neyton 2007).

Uncompetitive NMDA antagonists such as phencyclidine (PCP) (**11**), ketamine (**12**) and dizocilpine (**14**) also known as MK-801, are associated with severe side effects and exacerbation of PD symptomology due to their high affinity for the NMDA receptor's binding site and non-selectivity for NMDA receptor subtypes (Crossman *et al.*, 1989; Chen & Lipton 2006). Amantadine (**5**) which is approved by the Food and Drugs Administration (FDA) for the symptomatic management of PD blocks the NMDA channel pore (Luginger *et al.*, 2000). The ability of amantadine to stimulate dopamine release and inhibit its re-uptake is also beneficial in increasing dopamine level in PD. Amantadine however has limited clinical use due to its undesirable side effect profile as it causes cognitive impairment (Macchio *et al.*, 1993). Moreover, the duration of efficacy is highly varied and unpredictable (Wolf *et al.*, 2010).

Interests in adamantanes was further stimulated when the 1-amino-3,5-dimethyl derivative of amantadine, memantine (**13**) was discovered to antagonise the NMDA receptor with low affinity resulting in good clinical tolerance (Lipton 2006). Other low-affinity uncompetitive antagonists of the NMDA receptor such as dextromethorphan (**15**) and remacemide (**16**) possess good safety profiles although with less potency than the high-affinity antagonists (Monaghan *et al.*, 2012).



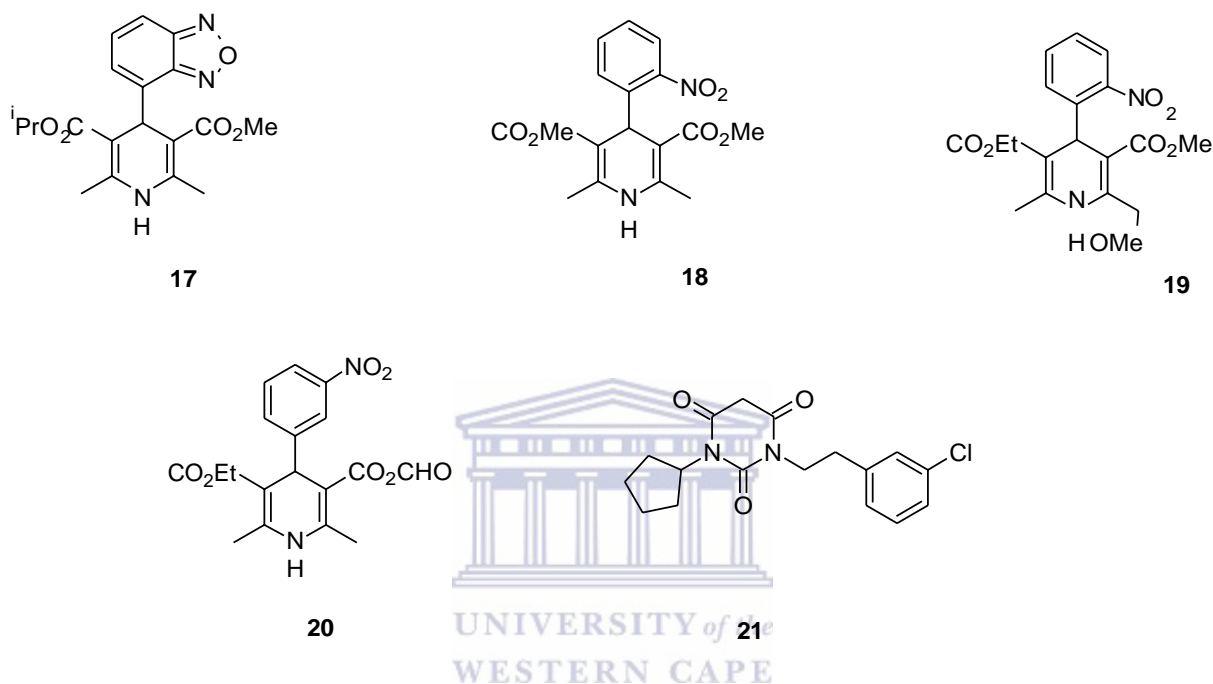
b. Calcium channel blockers

Voltage gated calcium channels expressed on plasma membranes also play a significant role in modulating neuronal Ca^{2+} concentration (Zamponi 2005). Calcium ions (Ca^{2+}) are conducted from the extracellular space into neuronal cell through various α_1 -subunits of the channel on arrival of an action potential (Catterall *et al.*, 2003). The $\text{Ca}_v1.2$ and $\text{Ca}_v1.3$ L-type α_1 - subunits are involved in neuronal calcium signalling in the cardiovascular system and CNS (Striggow & Ehrlich 1996; Striessnig *et al.*, 2006). L-type calcium channel antagonists commonly used in the management of cardiovascular and/or CNS diseases include benzodiazepines (BZAs), phenylalkylamines (PAAs) and 1,4-dihydropyridines (DHPs) (Helton *et al.*, 2005).

In animal models of PD, antagonism of $\text{Ca}_v1.3$ L-type calcium channels protected against calcium overload and oxidative stress in dopaminergic neurons. The dihydropyridine isradipine (**17**) is a potent L-type calcium channel antagonist that has been demonstrated to reduce oxidative stress in animal models of PD (Chan *et al.*, 2007), its non-selectivity for $\text{Ca}_v1.2$ and $\text{Ca}_v1.3$ L-type voltage gated calcium channels however limits its clinical safety as hypotension occurs due to prolonged antagonism of $\text{Ca}_v1.2$ calcium channels (Sinnegger-Brauns *et al.*, 2009). Chemical modification of the DHP nifedipine (**18**) produced several 4-substituted 1,4-dihydropyridines with little selectivity for $\text{Ca}_v1.3$. The most selective of these agents (**19**) and (**20**) only possess two fold selectivity for $\text{Ca}_v1.3$ over $\text{Ca}_v1.2$ with very low activity (Chang *et al.*, 2010).

Using a calcium-sensing fluorescent assay, the laboratory of Silverman screened over 60 000 molecules for selective $\text{Ca}_v1.3$ channel inhibition, however the results were disappointing due

to poor pharmacokinetic profile and $Ca_v1.2$ activity (Chang *et al.*, 2010). The group of Xia augmented this study by investigating the calcium inhibition of a series of pyrimidine-2,4,6-triones (PYT) and some compounds in Silverman's series that possessed anti-aggregation properties as well as good pharmacokinetic profiles (Xia *et al.*, 2011). These studies generated the lead compound for the first potent selective antagonist of the $Ca_v1.3$ channel (**21**) (Kang *et al.*, 2012).

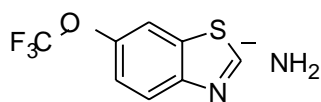


c. Other agents that halt glutamate mediated excitotoxicity

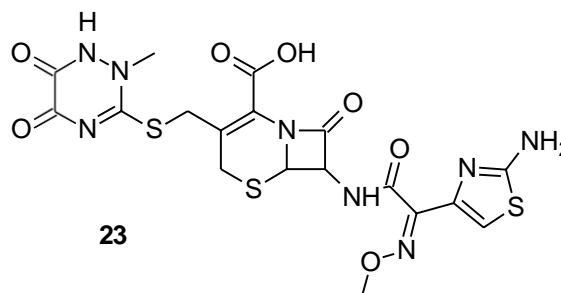
The beneficial neuroprotective effect from NMDA inhibition will be reduced in the presence of *L*-type voltage-gated calcium channels as the later can also cause excitotoxicity due to Ca^{2+} overload (Surmeier *et al.*, 2011). Dual antagonism is therefore desired in preventing glutamate mediated antagonism. The polycyclic cage amine, NGP1-01 provides neuronal protection by blocking both channels (Youdim *et al.*, 2007; Geldenhuys *et al.*, 2011). The glutamate release inhibitor riluzole (**22**) protects against NMDA-induced neuronal excitotoxicity however it produced sub-minimal efficacy in treating ALS and PD symptoms (Jankovic & Hunter 2002). The third-generation cephalosporin ceftriaxone (**23**) modulates glutamate uptake transporters *via* excitatory amino acid transporter-2 (EAAT2) in astrocytes (Lee *et al.*, 2008).

Inhibition of metabotropic glutamate receptors is also a viable strategy in preventing glutamate mediated excitotoxicity. This strategy provides the added advantage of modulating

voltage-gated calcium channels and has been shown in animal models of ND to reduce neuronal death (Nicoletti *et al.*, 1996; Caraci *et al.*, 2012).



22



23

2.3.2 Oxidative stress

Physiologically, neuronal cells are susceptible to the damaging effects of oxidative stress due to the high concentration of fatty acids capable of being peroxidised to neurotoxic products (equation 2.1 and 2.2). In normal neurons, redox homeostasis maintains a balance between antioxidant pathways and generation of minimal levels of oxidative species such as superoxide and peroxynitrite from nitric oxide (equation 2.4). Nitric oxide is produced from *L*-arginine, oxygen and NADPH in a reaction catalysed by NOS. The three isoforms of NOS: neuronal NOS, endothelial NOS and inducible NOS are responsible for the synthesis of nitric oxide in neurons as a neurotransmitter, in blood vessels to cause relaxation of smooth muscles and the induction of immune response respectively. Overstimulation of the NMDA receptor plays a central role in activating neuronal NOS due to increased influx of calcium ions and subsequent generation of reactive species (Garthwaite *et al.*, 1988). Selective neuronal NOS inhibitors (24-28) (Fig 2.2) have been synthesised and explored as potential therapeutic agents in neurodegenerative disorders, however this approach has been widely unsuccessful with a few exceptions due to the homologous nature of the NOS isoforms especially at the active site (Annedi *et al.*, 2012).

Reactive species are important for signalling processes including the modulation of the activities of protein kinases and transcription factors (Chen *et al.*, 2011). Unfortunately in ND, enzymes such as catalase, glutathione peroxidase and superoxide dismutase which catalyses antioxidant reactions are limited and the generation of ROS will trigger neuronal death (Fridovich 1997; Adibhatla & Hatcher 2010). Molecules that mimic these enzymes or stimulate their biosynthesis have demonstrated neuroprotective properties *via* the prevention of neuronal oxidative damage (Peng *et al.*, 2005; Garcia-Garcia *et al.*, 2012). Oxidative damage is further worsened by the high concentration of transition metals in the brain

catalysing the generation of free radicals from the 20% of the body's oxygen consumed by the brain (Fridovich 1997).

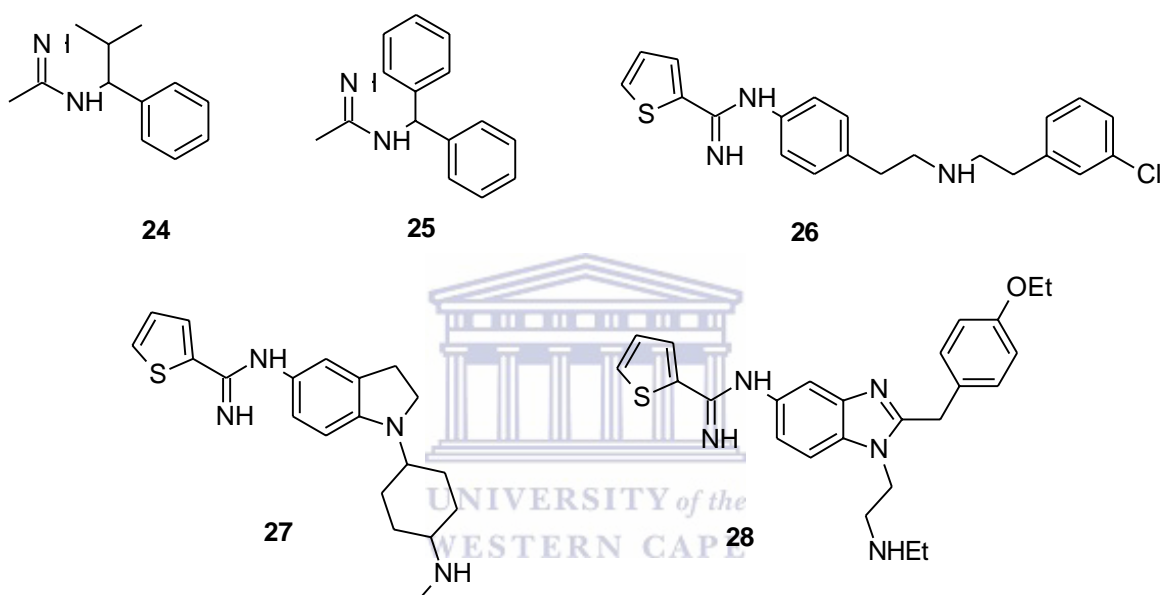
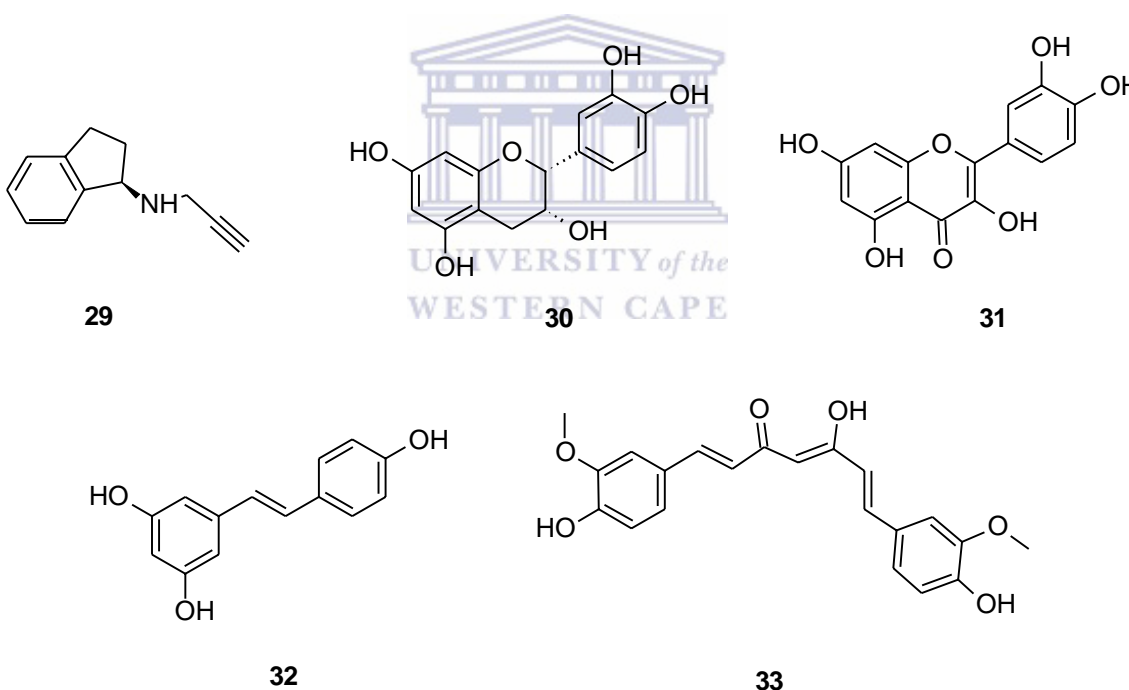


Fig 2.2: Selective neuronal nitric oxide synthase inhibitors

The generation of ROS activates disease-specific proteins which interact with the mitochondria and alter mitochondrial calcium homeostasis thereby further stimulating calcium overload. Nitric oxide is a good leaving group, reacting with cysteine residues to cause nitration of proteins which will propagate protein aggregation, as seen in Parkinson's disease (Giasson *et al.*, 2000). Further protein aggregation occurs due to NO inhibiting the activity of the ubiquitin system as mentioned earlier, thereby inhibiting beneficial apoptotic removal of misfolded proteins (Nakamura & Lipton 2009). S-Nitrosylation of pro-apoptotic proteins and parkin, an ubiquitin protein is associated with PD advancement (Chung *et al.*, 2004; Tsang & Chung 2009). Overexpression of NO is also implicated in ND progression (Chung & David 2010).

Several studies suggest that compounds with potent antioxidant properties may decrease the progression of neurodegenerative disorders. The double-blinded study by Olanow's group suggests that the benefits of early use of rasagiline (**29**), a monoamine oxidase (MAO)-B inhibitor therapy at 1 mg/day, could be related to some neurodegenerative disease-modifying effects (Olanow *et al.*, 2009). Antioxidants such as flavonoids; quercetin (**30**) and epicatechin (**31**), as well as polyphenols; resveratrol (**32**) and curcumin (**33**) have been extensively evaluated for neuroprotective properties and observed to prevent neuronal damage by deactivating free radicals (Aggarwal & Harikumar 2009; Richard *et al.*, 2011; Pietta 2000). In addition, polyphenols modulate neuronal inflammatory responses by inhibiting the expression of inflammatory genes (Aquilano *et al.*, 2008). The neuroprotective properties of antioxidants may also be accomplished by removal of oxygen molecules, inhibition of ROS production *via* inhibition of enzymes that catalyse oxidation reactions and up-regulation of endogenous antioxidation reactions (Fahn & Cohen 1992).



2.3.3 Mitochondrial dysfunction

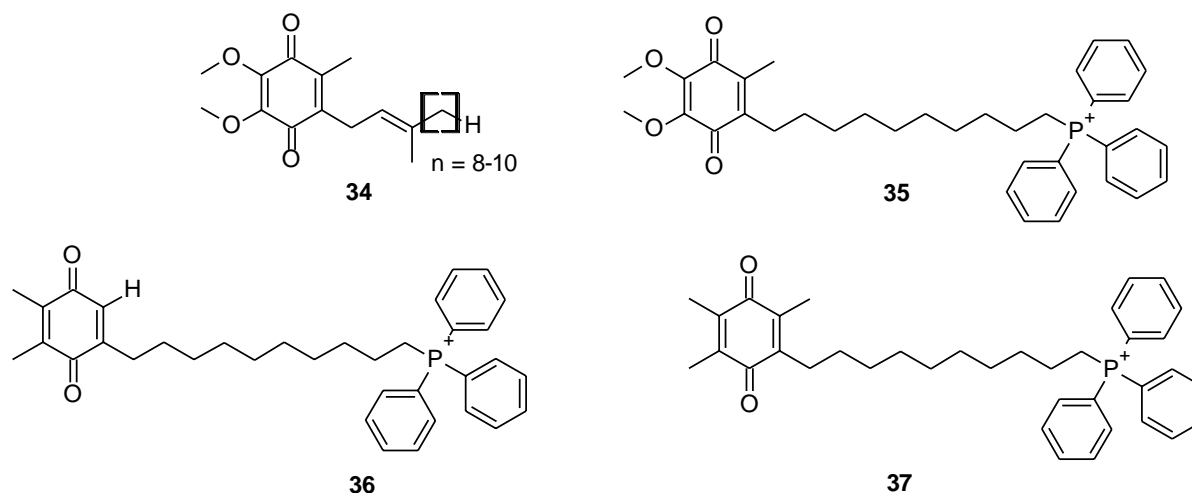
The main function of the mitochondrial electron transport chain is the synthesis of ATP which is vital for normal brain functions. In the mitochondrial respiratory chain, oxygen in the ground state (having two unpaired electrons in its outermost shell) is reduced by cytochrome c oxidase which ensures complete electron transfer to form water. About 2% of the oxygen molecules are converted to superoxide radical anion (O_2^-) in the Complex I (NADH dehydrogenase) and Complex III (ubisemiquinone) sites of the respiratory chain. The

superoxide radical anion undergoes dismutation to hydrogen peroxide (H₂O₂) peroxide either spontaneously or by magnesium or copper/zinc SOD in the mitochondrial matrix and cytosol respectively to generate hydroxyl radicals in a reaction catalysed by transition metals (Turrens *et al.*, 1985). Production of reactive oxygen and nitrogen species is increased when complex I is deficient as in the case of the *substantia nigra* in PD (Vila *et al.*, 2008).

Mitochondrial damage causes diminished energy metabolism related to defects in complex I (PD), complex II (HD) or complex IV (AD) (Damiano *et al.*, 2010; Alleyne *et al.*, 2011). Neurons have a high energy demand and energy deficiency due to mitochondrial inefficiency predisposes them to cell death. In PD, the metabolism of dopamine (DA) creates a favourable environment for the generation of ROS as 3,4-dihydroxyphenylacetaldehyde and H₂O₂ are produced in the reaction catalysed by MAO with subsequent auto-oxidation into DA-semiquinone which binds to complex I, thereby halting complex I's activity with the generation of oxygen radicals (O₂⁻). Ubiquinone (**34**) also known as coenzyme Q₁₀, the essential cofactor in the electron transport chain has demonstrated neuroprotective effects in ND (Bhat & Weiner 2005; Yang *et al.*, 2010).

Blood platelets of PD sufferers have decreased level of coenzyme Q₁₀ in the mitochondria hence a decline in complex-I activity. A study by Krantic's group demonstrated that MPP⁺ decreases ATP synthesis in the mitochondria by inhibiting complex I, thereby resulting in excessive glutamate release and apoptotic cell death (Krantic *et al.*, 2005). The anti-apoptotic (Szeto-Schiller) mitochondrial proteins SS-31 and SS-20 may offer protection against MPTP-induced neurotoxicity (Yang *et al.*, 2008).

These findings led to the synthesis of the antioxidant MitoQ (**35**), which is coenzyme Q₁₀ linked to triphenylphosphonium to protect the mitochondrion after glutathione depletion in neurodegenerative disorders (Bolognesi *et al.*, 2009). Other analogues of ubiquinone (**36** and **37**) have also demonstrated promising neuroprotective potentials and are already in clinical trials (Szeto & Schiller 2011; Skulachev 2012). The cationic triphenylphosphonium group in ubiquinone analogues fosters targeted delivery to the mitochondria as a result of the negative potential gradient in the inner membrane of the mitochondria.



2.4 Inflammation

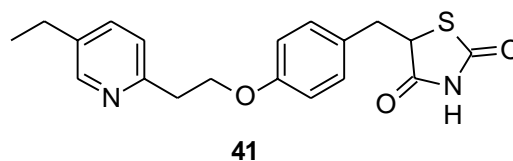
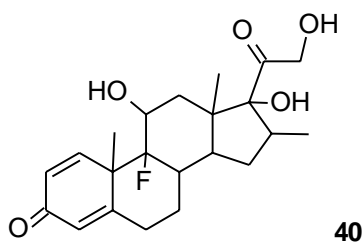
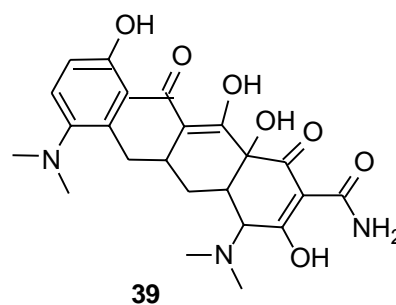
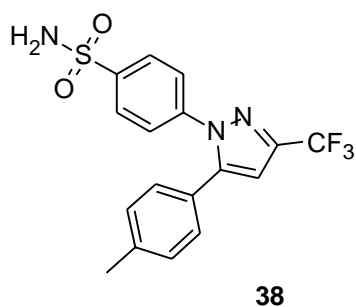
Expanding research has highlighted the dual role of inflammation and the immune response in neurodegeneration; beneficial in tissue repair and neuroprotection yet contributing to tissue damage (**Fig 2.3**) (Amor *et al.*, 2009; Glass *et al.*, 2010). Mediators of the immune response originate in the brain and systemic inflammatory response has a profound effect on neuronal function (Czirr *et al.*, 2012). Chronic activation of the innate immune response is reported in ND. An injury to a neuron results in the production of cell fragments that stimulate microglia activation. Toll-like receptors expressed largely in CNS cells are responsible for microglia activation, hence playing a vital role in mediating inflammatory responses and neuroprotection (Hanisch *et al.*, 2008; Drouin-Ouellet *et al.*, 2012).

Once activated in response to infection or injury, the microglia cells become highly motile in readiness for phagocytosis and release various inflammatory factors including chemokines, cytokines and neurotoxic substances such as interleukin-1 β (IL-1 β), TNF- α coupled with the expression of inducible NOS and ROS generation. The immunological response results in the release of cytotoxic agents and activation of the complement cascade. Microglia activation is necessary as a defence mechanism against invading pathogens as well as the clearance of apoptotic bodies and misfolded proteins thereby maintaining tissue regeneration and homeostasis. Exaggerated innate immune response can however induce focal damage to neighbouring neurons by activating not only microglia but also astrocytes, natural killer cells, mast cells and granulocytes to produce a vicious cycle of chronic inflammatory response and neuronal cell death (**Fig 2.3**) (Kierdorf & Prinz 2013; Skaper *et al.*, 2013). The dysregulation of synaptic remodelling roles of microglia during CNS injury is peculiar in ND (Salter & Beggs 2014).

The adaptive immune response also plays a role in neurodegeneration. Mice deficient in CD4 T-cells showed more resistance to MPTP-induced dopaminergic neuronal loss in PD mouse models however, ALS mouse models demonstrated a protective role of T-cells (Czirr & Wyss-Coray 2012). While animal models of neurodegenerative disorders suggests that anti-inflammatory therapies have beneficial effects in ND, clinical trials have not provided conclusive evidence for their efficacy in ND. In AD mouse models, celecoxib (**38**), an inhibitor of cyclooxygenase 2 (COX-2), prevented cognitive decline however it failed to produce similar results in AD patients (Gilgun-Sherki *et al.*, 2006; Group *et al.*, 2008). Genetic factors and extent of disease progression may account for the inconsistency in the results of clinical trials and will require further investigation.

The production of ROS including peroxynitrate contributes to the initiation and maintenance of the inflammatory auto-toxic loop in neurodegeneration. Peroxynitrate is an oxidising as well as nitrating agent which can attack and denature proteins as well as induce lipid peroxidation (Squadrito & Pryor 1998). These events contribute to a decline in autoimmune anti-inflammatory ability of the cell and consequently predisposing it to further damages and resulting in neuronal cell death by altering the biosynthesis of proteins, lipids, and nucleic acids. Inappropriate inflammatory responses also trigger reactive astrocytes which can form scar tissue on cells or generate neurotoxic species and prevent tissue repair and demyelination resulting in neuronal death (Brambilla & Abbracchio 2001). Acute inflammatory responses and high baseline levels of TNF- α in AD sufferers have been reported to be associated with a 2- fold and 4-fold increase in the rate of cognitive decline respectively within six months (Holmes *et al.*, 2009) .

Increased levels of cytokines and pro-inflammatory markers are implicated in neurodegenerative conditions (Monson *et al.*, 2014; Collins *et al.*, 2012; Kwan *et al.*, 2012). In AD for example, inflammatory mediators are activated in the presence of A β plaques (Doens & Fernández 2014). The immune system also coordinates the kynurenine enzymatic pathway which converts tryptophan to several neuroactive compounds including serotonin that partake in neurodegenerative disease progression (Schwarcz *et al.*, 2012). Kynurenic acid has displayed significant antioxidant properties as well as potent competitive inhibition of ionotropic glutamate receptors (Lugo-Huitron *et al.*, 2011). This reinforces the role of the immune response in preventing glutamate mediated excitotoxicity and neuronal death.



2.5 The blood brain barrier

The BBB is an endothelial barrier which restricts the passage of leucocytes, plasma components and red blood cells into the brain (Abbott *et al.*, 2006). Due to the increasing prevalence of CNS disorders, the drug delivery market for these disorders is expected to reach a staggering 26 billion dollars in 2017 (Jain 2008). The BBB is very thin and has a large surface area for a large volume of capillary endothelium providing a highly dense capillary network so that the distance between a neuron and a capillary is less than 20 μm . Through the transvascular route, compounds are delivered directly to the brain based on the close proximity of virtually all neurons to the capillary network (Pardridge 2001). However, over 90% of potential CNS active drugs are excluded by the resistance posed by the BBB aided by tightly joined brain capillaries' endothelial cells, astrocytes and pericytes (Neuwelt 2004).

The CNS is composed of the spinal cord and brain inside the meninges, the spinal cord lacking choroid plexus and circumventricular organs (CVOs) and uses nerve entries to transport compounds to the periphery (**Fig 2.4**). Other barriers that regulate the free movement of matter to the brain includes the arachnoid membrane which restricts the movement of molecules to the brain from the cerebrospinal fluid (CSF) and the blood–cerebrospinal fluid barrier composed of the choroid plexus in ventricles (Neuwelt *et al.*, 2008). Small hydrophilic molecules transverse the BBB epithelium by simple diffusion through the paracellular pathway, the movement is however very limited due to the presence of tight junctions. Conversely, small lipophilic molecules transverse the BBB epithelium *via*

passive diffusion (transcellular route) (Fig 2.5), which is highly dependent on the drug properties (Hammarlund-Udenaes *et al.*, 2008). The Lipinski's rule-of-five is used as a guide to predict the ability of drugs to cross physiological barriers however most CNS drug candidates do not conform to this rule (Pardridge 2003; Ghose *et al.*, 1999).

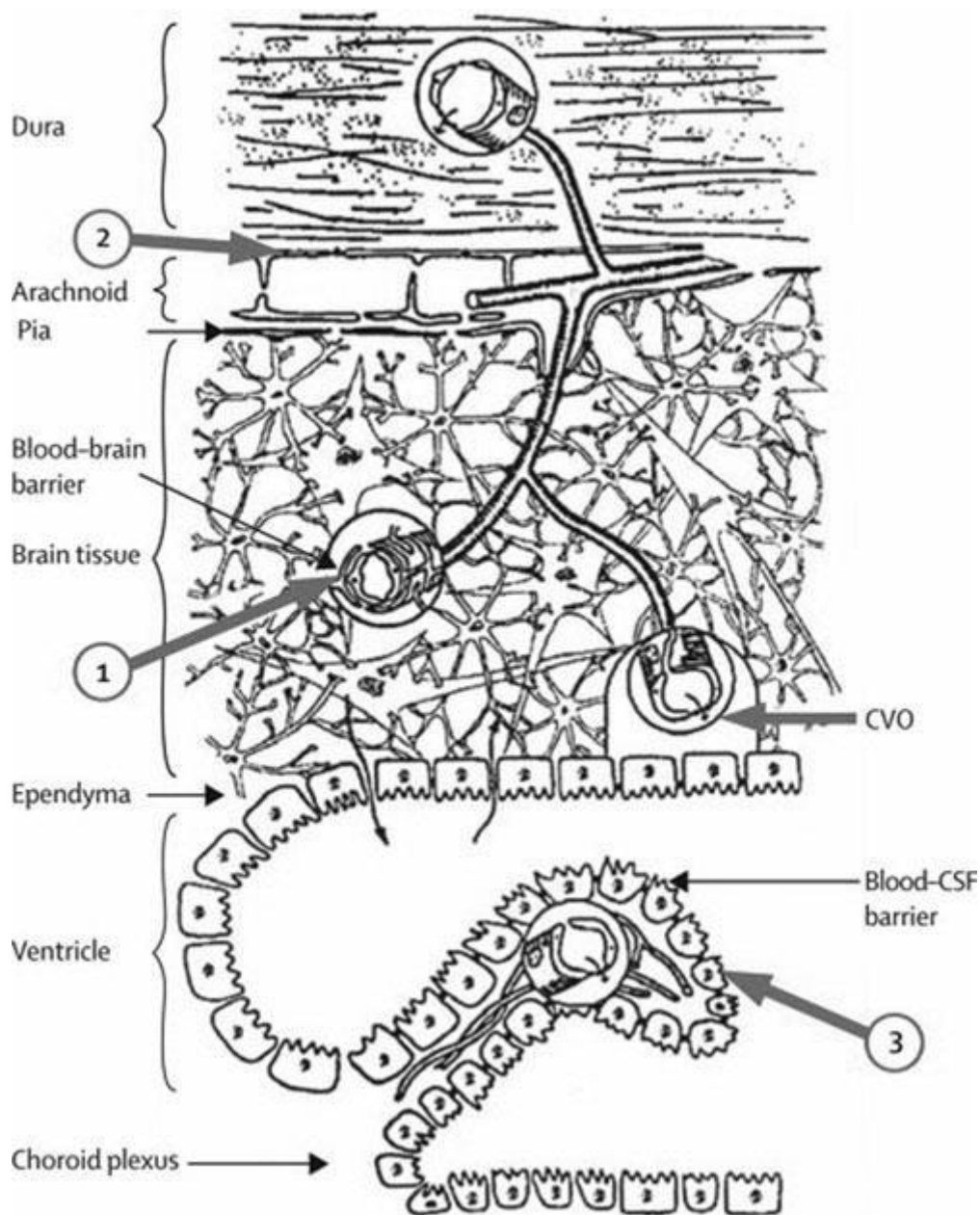


Fig 2.4: Physiological barriers of the central nervous system (Abbott 2004)

2.5.1 Physicochemical properties necessary for BBB permeation

In vitro and *in silico* BBB models are generally used to select potential CNS active drugs in the pre-development stage to minimize waste of time and resources during drug development.

While *in vitro* models assess drug permeability on brain cell endothelial cells of various cell lines, *in silico* prediction is based on various intrinsic physicochemical properties of drug molecules discussed below.

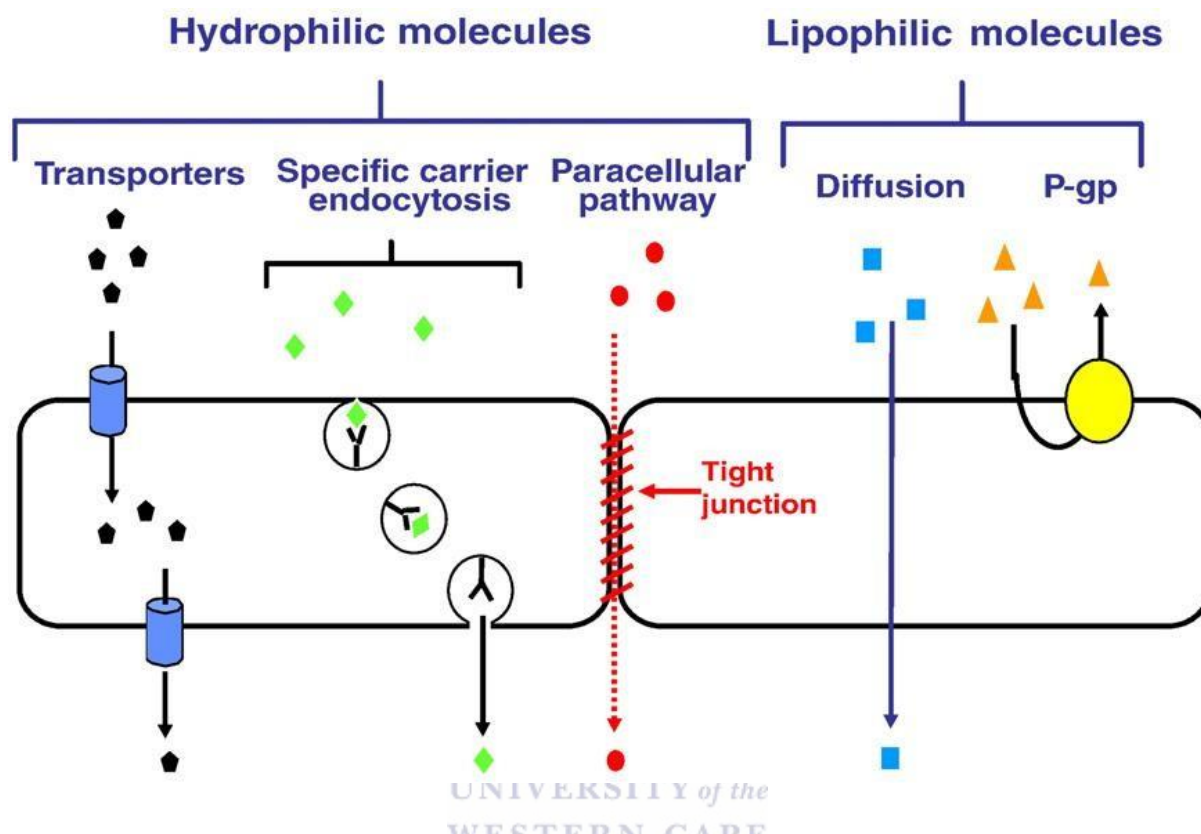


Fig 2.5: Movement of molecules across the BBB (Gabathuler 2010)

a. Lipophilicity:

Increased lipid solubility often correlates with increased potency of a drug however, this is also accompanied by poor oral solubility, metabolic instability and a high toxicity profile (Leeson & Springthorpe 2007). This may be accounted for by the effect of lipophilicity on rate and extent of distribution across biological membranes including the BBB. The octanol–water partition coefficient (LogP) is a valuable measure of permeation and cLogP values of 2 were suggested as optimal to minimize metabolism and toxicity problems. The octanol–water distribution coefficient (LogD) is pH dependent and provides a more reliable indication of a drug’s lipophilicity, with cLogD values of 1-4 suggested to be optimal for brain permeation (Leo et al., 1971; Van de Waterbeemd *et al.*, 1998; Wager *et al.*, 2010). Log_{BBB} is the brain to blood concentration of a drug at a defined time point after administration. This gives an estimation of drug distribution into the brain (Mehdipour & Hamidi 2009).

$$\log_{BBB} = \log C_{\text{brain}}/C_{\text{blood}}$$

equation 2.5

The equilibrium partition coefficient ($K_{p \text{ brain}}$) is a reliable *in vivo* method to determine the extent of brain permeation of a drug. It is a measure of the ratio of the drug concentration in the brain to the steady state plasma concentration. It can also be obtained from the area under time curves of the brain and blood total blood concentrations (Mehdipour & Hamidi 2009).

$$K_{p, \text{brain}} = C_{ss, \text{brain}} / C_{ss, \text{blood}} = \text{AUC}_{\text{brain}} / \text{AUC}_{\text{blood}} \quad \text{equation 2.6}$$

The simplicity of brain permeation prediction models makes them a generally accessible and useful tool in the development of CNS active drugs, however they do not provide an indication of the pharmacodynamic properties of drug molecules. Drug binding to plasma proteins and distribution into various brain compartments affects the concentration at the site of action and hence efficacy (Reichel 2009). Pharmacokinetic parameters such as the rate of transport across the BBB, unbound drug partition coefficient ratio of interstitial fluid to plasma and volume of distribution in brain of unbound drug provide a more accurate measure of the rate and extent of drug delivery to the brain (Reichel 2009; Hammarlund-Udenaes *et al.*, 2008).

b. Hydrogen Bond capacity:

Desolvation of water molecules affects lipid solubility and passive membrane permeability. Increased H-bonding potential reduces membrane permeability and increases affinity of compounds for P-gp (Veber *et al.*, 2002; Hitchcock 2012). CNS active drugs have a lower number of H-bond donors and acceptors than non-CNS active drugs and Pajouhesh and Lenz suggested that CNS targeted drug candidates should have a maximum of eight hydrogen bonds (Goetz *et al.*, 2014; Pajouhesh & Lenz 2005).

c. Polar Surface Area:

This is a measure of the surface area of all the polar atoms in molecule, mainly due to oxygen and nitrogen atoms. The topological polar surface area (TPSA) which is simple and independent on molecular conformation is the most widely reported method for calculating PSA. PSA values of <60 were suggested to be optimal for CNS exposure (Kelder *et al.*, 1999; Ertl *et al.*, 2000).

d. Ionization:

A pK_a value of 7.5-10.5 is necessary for BBB permeation of compounds to prevent ionisation and minimize P-gp interactions (Pajouhesh & Lenz 2005; McDonald *et al.*, 2013).

e. **Molecular Flexibility:**

This permeability descriptor is a measure of the number of rotational bonds in a molecule. Increased molecular flexibility produces a reduction in membrane permeation. A maximum number of 8 rotatable bonds is proposed for CNS targeted drugs (Pajouhesh & Lenz 2005).

f. **Molecular Weight:**

Using results from the analysis of both CNS active and non-CNS active drugs, Van de Waterbeemd suggested that molecular weight should be below 450 (Van de Waterbeemd *et al.*, 1998).

In silico BBB descriptors are relatively easy and cost effective predictors of BBB permeability however, they are highly determined by passive transcellular transport and do not account for the role of active transport mechanisms in the delivery of CNS targeted molecules. *In vitro* models account for both transcellular and paracellular pathways as well as metabolic interactions, therefore providing a more accurate prediction of a drug's transport potential across biological membranes in the early stages of drug development. The parallel artificial membrane permeability assay (PAMPA) is a relatively cost effective and reliable permeability assay that has been successfully used to predict oral absorption of new drugs. *In vitro* cell based permeability models are useful in predicting *in vivo* brain permeation however, they are limited by inconsistency in reproducing results thereby producing unreliable predictions and requiring additional resources (Reichel, A., 2006).

2.5.2 Strategies employed for CNS drug delivery

a. **Direct administration**

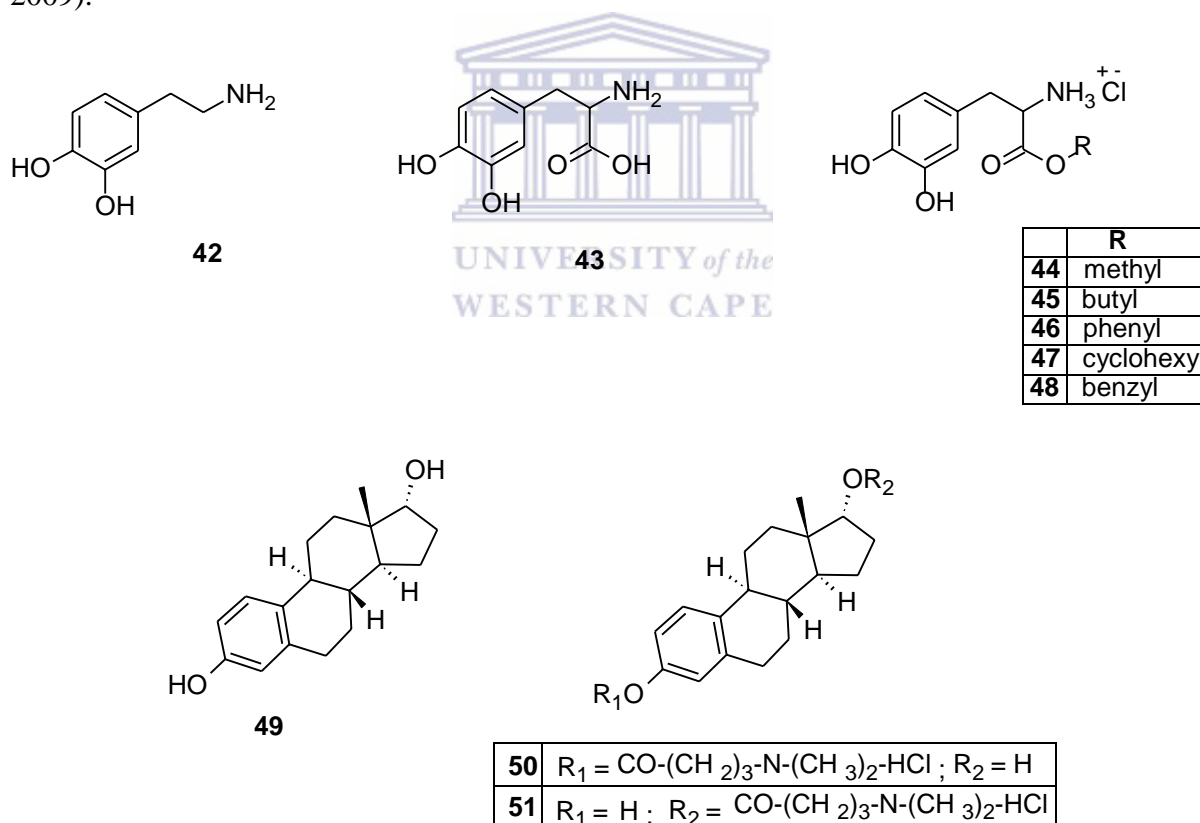
In emergency situations, drug molecules are directly injected into the brain using an intracerebral implant which will permeate the skull. Alternatively, the drug can be delivered to the CSF by intrathecal injection or intracerebroventricular infusion. There is a very high risk of infections and drug toxicity in these invasive approaches. Besides the inconvenience to the patient, the high cost involved limit the use of this method of brain delivery of drugs (Begley 2004; Brasnjevic *et al.*, 2009; Allard *et al.*, 2009).

b. **Nasal or ocular delivery**

Lipophilic molecules with molecular weigh less than 500 Da can diffuse easily through the nasal mucosa which is highly vascularised into the systemic circulation or through the olfactory pathway into the CSF and brain. Successful brain delivery of progesterone,

peptides, proteins and nanovectors has been observed *via* the nasal route of administration (Thorne *et al.*, 2004; Kumar *et al.*, 1982; Celia *et al.*, 2011). Due to erratic absorption and first pass metabolism, oral administration of levodopa (**43**) for brain delivery has been highly unsuccessful in PD management whereas the systemic administration of dopamine (**42**) will precipitate serious peripheral toxicity. The nasal route provides a viable means for the CNS delivery of levodopa, unfortunately its poor water solubility presents a challenge for nasal delivery at a therapeutically significant concentration. Alkyl ester prodrugs of levodopa (**44-48**) have been synthesised and nasal administration of the butyl ester prodrug (**45**) produced improved CNS delivery of dopamine (Kao *et al.*, 2000).

Ester prodrugs of 17 β -estradiol (**50** and **51**) enhanced the nasal delivery of estradiol (**49**) to the brain for AD risk management (Al-Ghananeem *et al.*, 2002). Numerous studies are currently investigating the ocular route for delivering drugs to the CNS (Capsoni *et al.*, 2009).



c. Transient disruption of the BBB

The tight junctions of the BBB can be temporarily opened by infusion of hyperosmotic saccharide solutions *via* the carotid artery. The transient disruption of the BBB is a very expensive procedure and poses a high risk of infection and toxicity to patients. Moreover, the

period of opening of the tight junction is highly unpredictable (Brasnjevic *et al.*, 2009; Deli 2009).

Electromagnetic radiation and focussed ultrasound are used to disrupt selected sites of the BBB to enhance drug penetration to specific regions of the brain. Although this technique is generally less invasive, excessive BBB disruption, necrosis and toxicity are major drawbacks (Vykhodtseva *et al.*, 2008; Madsen & Hirschberg 2010).

d. Efflux transporters' inhibition

Efflux proteins such as multidrug-resistant (MDR) transport proteins actively transport molecules out of the brain. The active efflux transport (AET) system including P-gp, MDR and ATP-binding cassette (ABC) export small, cationic or hydrophobic compounds out of the brain and prevent their accumulation in the brain for significant pharmacological effects. Inhibition of efflux transporters is a viable strategy to improve delivery of CNS targeted drugs (Begley 2004).

Success in anticancer therapy has been previously achieved by targeting efflux proteins expressed by tumour cells (Begley 2004; Zhang *et al.*, 2000). The brain delivery of verapamil has been enhanced by co-administration with P-gp inhibitors such as valsopodar (**52**) (Lee *et al.*, 2006). The cyclic prodrugs (**53-55**) of DADLE, an opioid peptide have also been co-administered with several P-gp inhibitors for improved brain delivery of the opioid peptide on hydrolysis by brain esterases (Ouyang *et al.*, 2009; Stenehjem *et al.*, 2009).

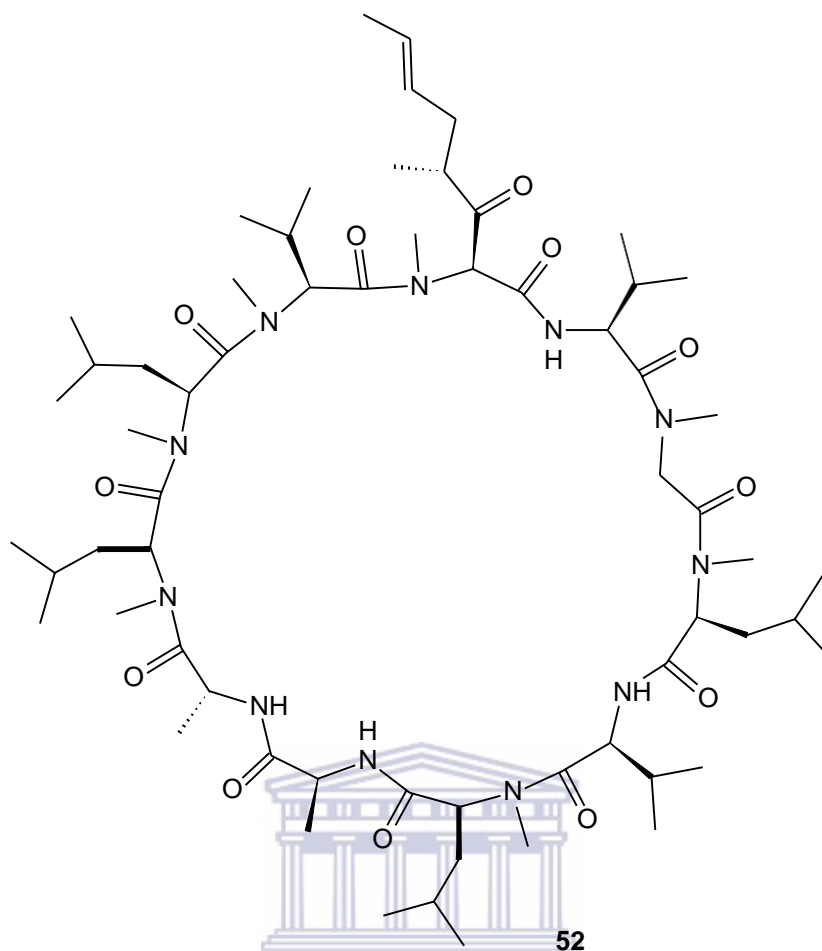


Fig 2.6: Representative active efflux transporter inhibitor

The formation of codrugs of AET inhibitors and drug molecules via covalent linkage is gaining grounds as a means of increasing CNS drug delivery. The codrug (**57**) of entacapone (**56**), a catechol-*O*-methyltransferase (COMT) inhibitor and levodopa increased brain delivery of the latter in PD (Leppanen *et al.*, 2002). The codrug approach may however cause severe toxicity when used in chronic disease management as toxic metabolites will not only accumulate in the brain due to AET inhibition, also peripheral efflux transport system's inhibition will affect drug distribution into peripheral tissues. Drug molecules may also be chemically modified to inhibit their affinity for AET transporters (Taylor 2002).

e. Prodrug delivery

Prodrug strategies have been employed to improve the lipophilicity and BBB permeation of hydrophilic molecules by the use of lipophilic moieties which may be conjugated to a carrier or vector. This approach enhances brain penetration and plasma stability. The prodrug is biotransformed chemically or enzymatically once in the brain to release the parent drug (Rautio *et al.*, 2008).

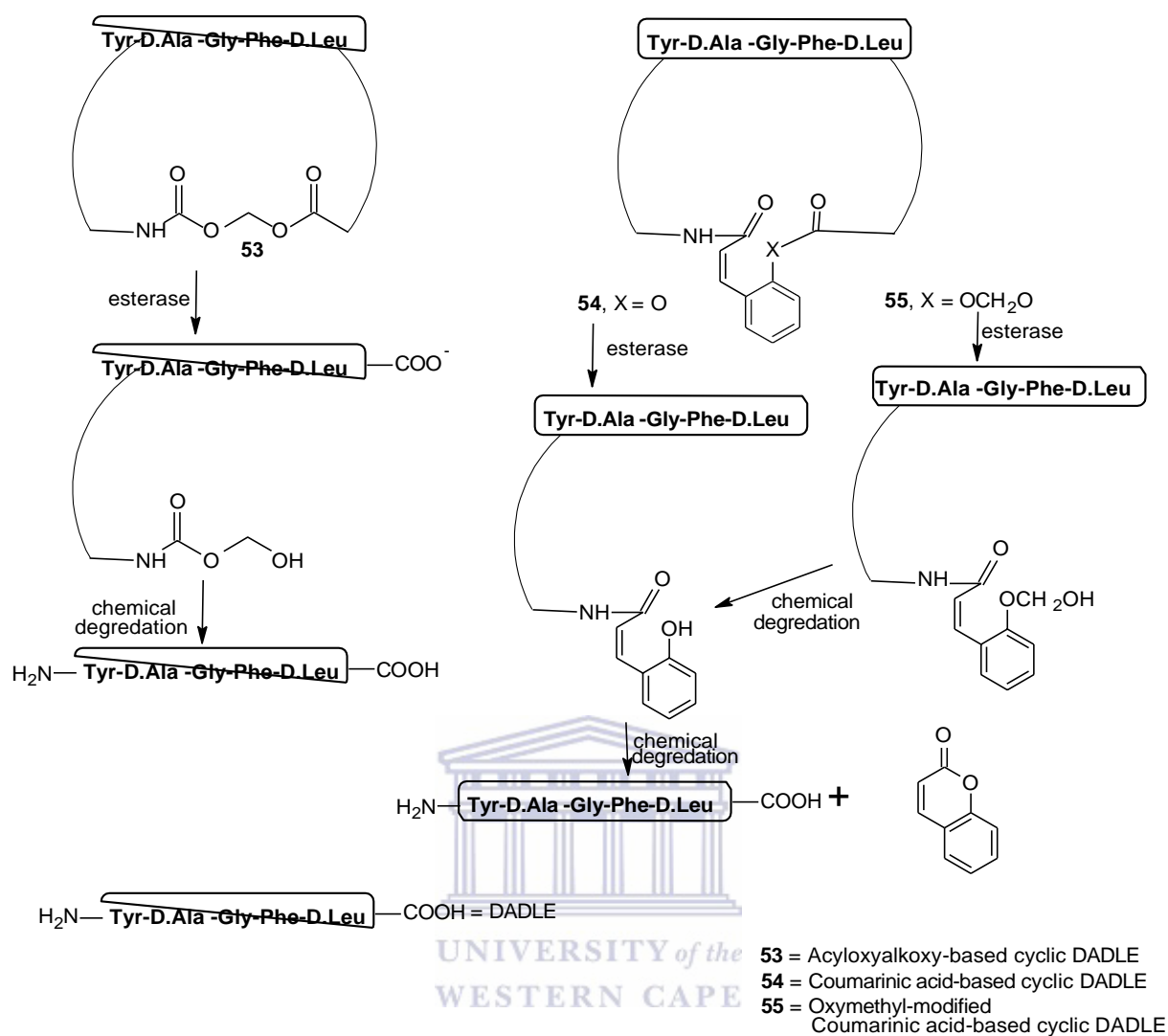
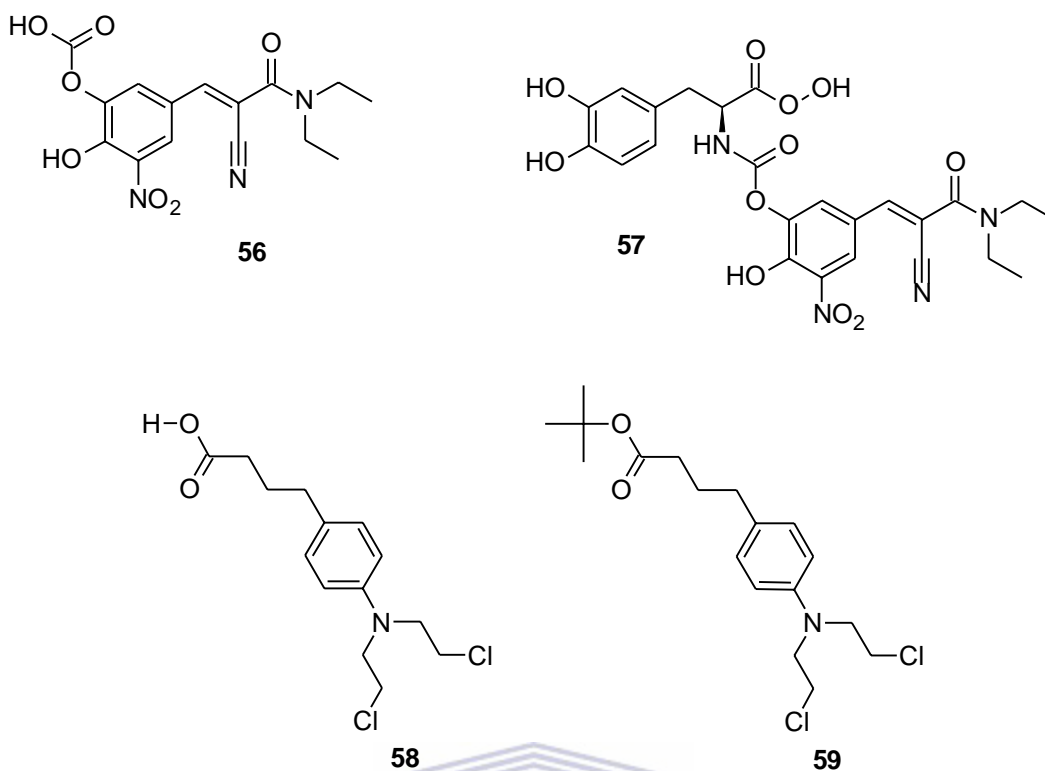
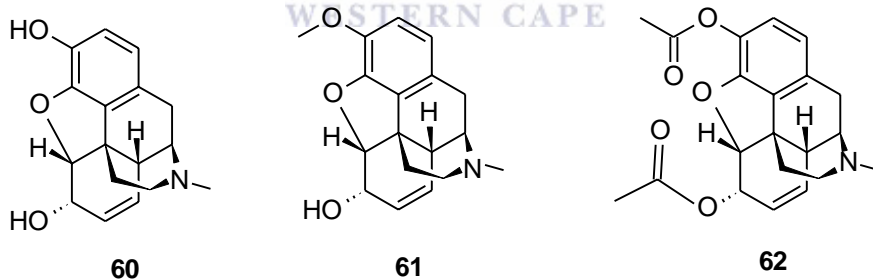


Fig 2.7: Hydrolysis of the cyclic prodrugs of DADLE

Increased brain concentration of various CNS active drugs including the anticancer drug chlorambucil (**58**) have been obtained using the prodrug approach (Genka *et al.*, 1993). The major drawback in the brain delivery of lipophilic prodrugs is the large volume of distribution due to plasma protein and lipid binding, coupled with drug distribution to peripheral tissues due to improved ability to permeate physiological membranes. Furthermore, the active efflux transport systems of the BBB limit the drug concentration at the site of action (Rautio *et al.*, 2008).

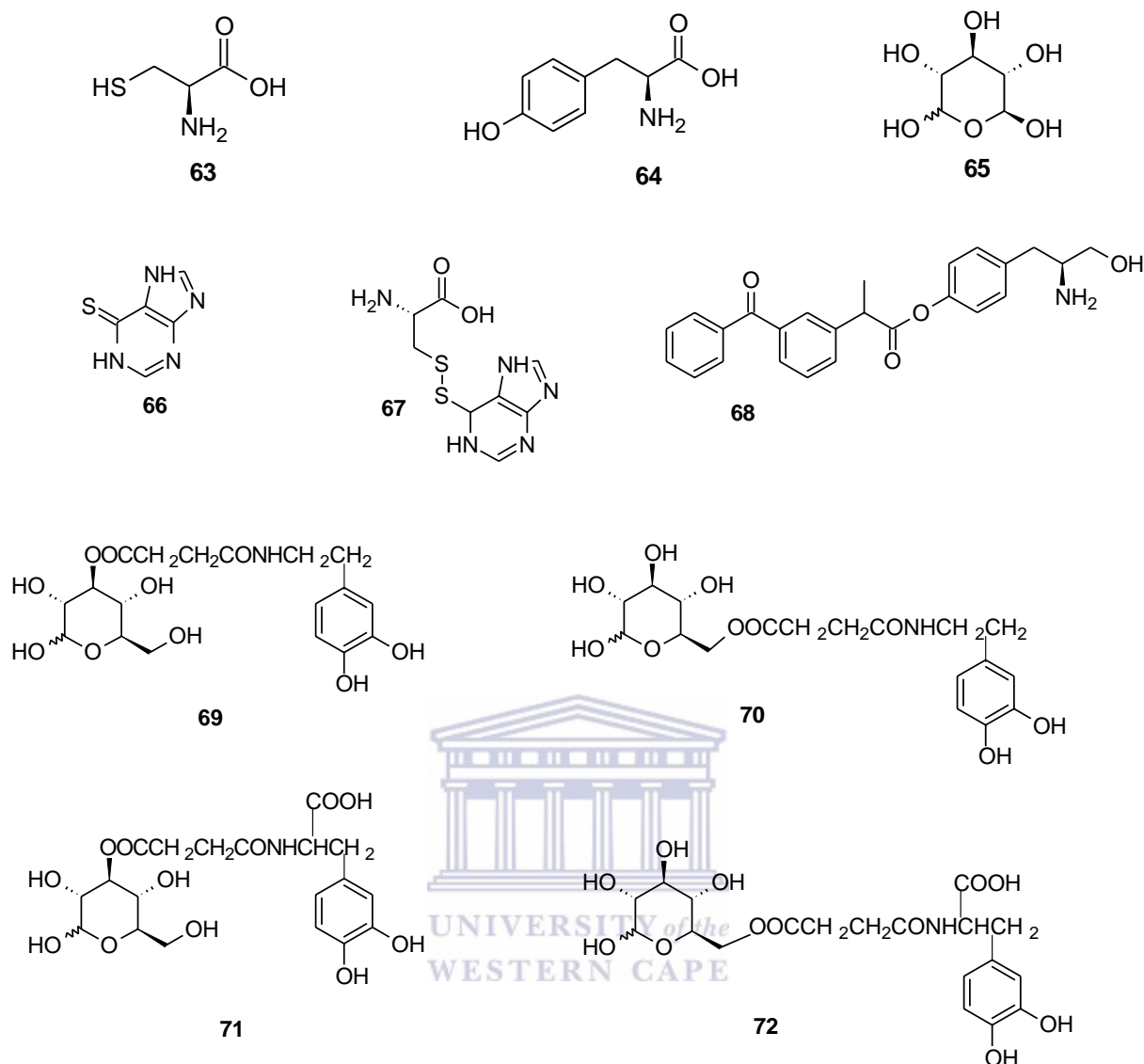


The poor brain distribution of morphine (**60**) has been circumvented by its *O*-methylation and *O*-acetylation to codeine (**61**) and heroin (**62**) respectively. Both molecules are hydrolysed by brain esterases back to the more polar parent drug in the brain (Oldendorf *et al.*, 1972).



f. Carrier-mediated transport (CMT)

Vital nutrients such as glucose, vitamins, hormones and amino acids use specialized transporters to enter the brain *via* facilitated diffusion. Developing drugs with high affinity for BBB endogenous carriers with good pharmacokinetic properties pose a major challenge to medicinal chemists. Furthermore amino acid transporters require free α -amino and α -carboxyl groups to facilitate carrier mediated transport of the prodrugs.



CMT delivery of drugs is based on either its modification into a pseudonutrient prodrug or conjugation with a nutrient substrate to be transported by CMT systems (Tamai & Tsuji 2000). Small molecules with structural similarities to endogenous BBB substrates such as LAT1 and LAT2 in the case of levodopa can be transported into the brain by CMT (Del Amo *et al.*, 2008). LAT1 amino acid substrates such as *L*-cysteine (**63**) and *L*-tyrosine (**64**) were conjugated to 6-mercaptopurine (**66**) and ketoprofen respectively for improved brain delivery of the prodrugs (**67**) and (**68**) (Killian *et al.*, 2007; Gynther *et al.*, 2008). Drugs targeting GLUT1 transporters are a major strategy in CMT drug delivery as *D*-glucose (**65**) is a major endogenous substrate of the BBB endothelia. Glycosylated prodrugs of levodopa and dopamine respectively (**69-72**) are substrates for GLUT1 and have shown improved CNS permeation (Bonina *et al.*, 2003).

g. Adsorptive-mediated transport (AMT)

Cationic molecules and nanovectors deliver drugs to the brain via adsorption and adsorptive endocytosis respectively. The electrostatic interaction between anionic sites on the BBB endothelium and the cations enhances binding of the drugs to the BBB, followed by the formation of vesicles and induction of endocytosis. One of the major limitations of this approach is the disruption of the BBB and lack of receptor specificity for BBB endothelial cell's uptake. Moreover, very large dose of the drug is required which may produce toxic effects. Cationic peptide vectors or polymeric carriers can be conjugated with hydrophilic drugs via the prodrug approach (Järver & Langel 2006). Proteins such as immunoglobulin can also be cationized for AMT mediated delivery to the brain (Hervé *et al.*, 2008; Foged & Nielsen 2008).

h. Receptor-mediated transcytosis (RMT)

This endogenous transport system is utilised by proteins, peptides and macromolecules such as cholesterol to access the brain. Small ligands and nanovectors prodrugs of proteins and antibodies can target specific receptors on the luminal surface of BBB endothelial cells for brain delivery by endocytosis. This approach is independent on the lipophilicity of the drug and may provide the most feasible strategy for brain delivery of drugs due to its high specificity and safety profile (Gabathuler 2010). Prodrugs containing RMT-based vector and drug molecules for brain delivery of small drug molecules and proteins are currently in advanced stages of clinical trials (Demeule *et al.*, 2008; Régina *et al.*, 2008). Chimeric peptides have been genetically engineered to deliver proteins and peptides to the brain by RMT (Pardridge 2003; Boado *et al.*, 2007).

i. Other strategies

Other strategies to improve drug delivery to the brain includes the use of chemical delivery systems (CDS) which is based on the biotransformation of a prodrug into an active drug by sequential metabolism and nanotechnology which employs nanoparticles and liposomes (Bohn *et al.*, 2009; Gourand *et al.*, 2010; Silva 2008; Denora *et al.*, 2009). A prototype of CDS based drug delivery is the dopamine-CDS (**73**) which is chemically converted to a quaternary pyridium salt and subsequent esterification to a precursor of dopamine (Omar *et al.*, 1994).

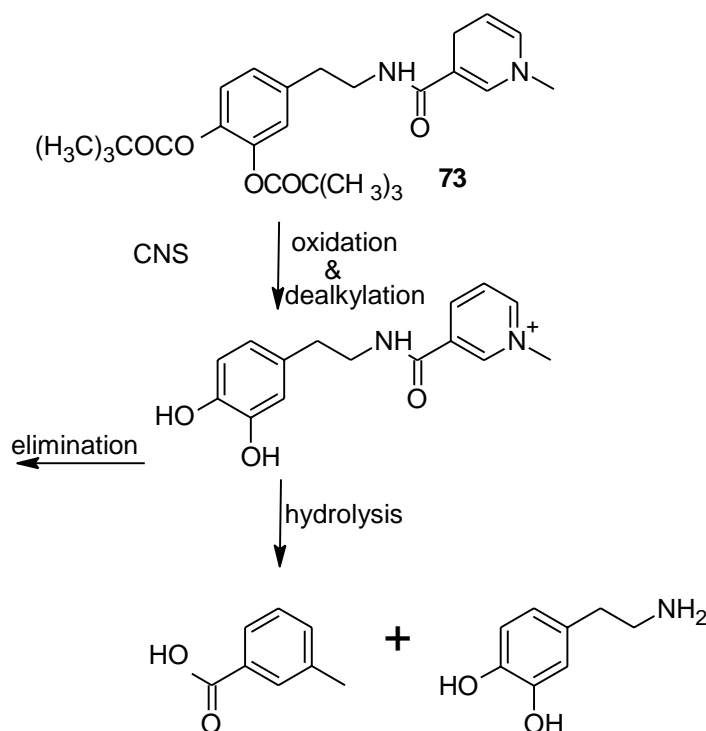


Fig 2.8: Bioconversion of dopamine-CDS

2.6 Non-steroidal anti-inflammatory therapy in neurodegenerative diseases

NSAIDs are used clinically for their antipyretic, analgesic and antirheumatic properties. *In vitro* studies have demonstrated that NSAIDs inhibit both human and mouse microglial neurotoxicity (Silakova & Hewett 2004; Bate *et al.*, 1993). All NSAIDs act through the inhibition of at least one of two isoforms of the cyclooxygenase enzyme which catalyses the metabolism of arachidonic acid released from phospholipids to prostaglandins (PG). COX-1 and COX-2 catalyse the deoxygenation of arachidonic acid to prostaglandin G₂ (PGG₂) in the cyclooxygenase active site and the subsequent reduction of PGG₂ to PGH₂ in the active site of peroxidase. PGH₂ diffuses from the COX enzyme and is biotransformed to prostaglandins (PGE₂, PGD₂, PGF_{2R}, PGI₂) and thromboxane A₂ (TxA₂) by different tissue-specific isomerases. NSAIDs have been shown to inhibit peroxisome proliferators γ (PPAR γ) and nuclear factor kappa B (NF- κ B), transcription factors (Garavito & Mulichak 2003).

Literature suggests that selective COX-1 inhibitors are preferred neuroprotective agents in comparison to COX-2 inhibitors (Aid *et al.*, 2008, Choi *et al.*, 2009). Moreover, COX-2 is expressed mainly in neurons and not by microglia while COX-1 is expressed in microglia and perivascular cells (Garcia-Bueno *et al.*, 2009). However, upregulation of neuronal COX-2

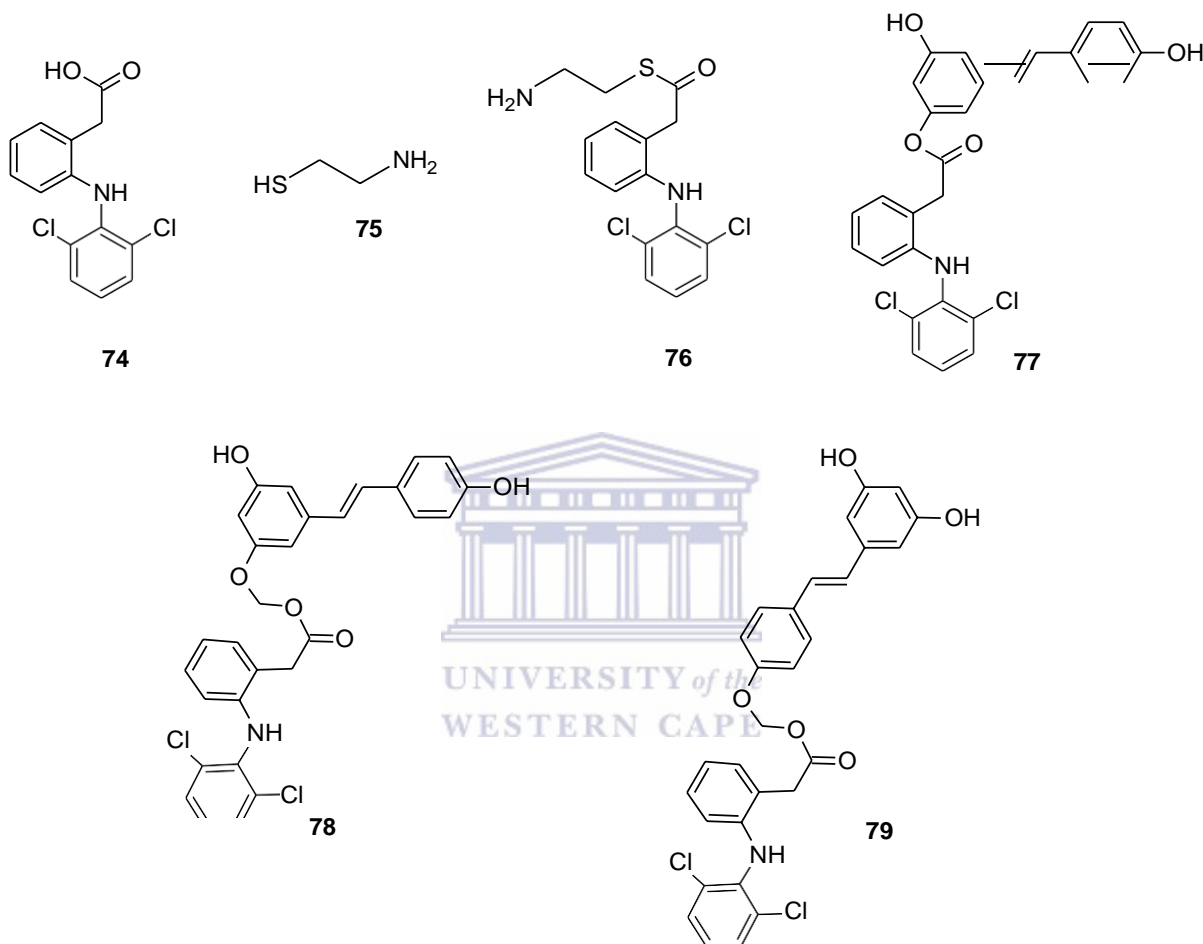
have been observed in the early stage of AD (Andreasson *et al.*, 2001, Hoozemans *et al.*, 2001). Furthermore, COX-2 is involved in the regulation of excitatory synaptic transmission (Slanina & Schweitzer 2005). Recent studies suggest that COX-2 activity is required for neuroinflammation inhibitory effects of neuronal cells (Aid *et al.*, 2010). Moreover, epidemiological studies suggests that chronic use of selective COX-1 inhibitors are beneficial in neurodegenerative disorders whereas COX-2 inhibitors provided no net benefit in neuroprotection (Steven *et al.*, 2008, McGeer *et al.*, 2007, Vlad *et al.*, 2008).

The neuroprotective effects of NSAIDs was thought to be independent on their selectivity for either COX-1 or COX-2 but considering previous studies and arguments from literature, classical COX-1 inhibitors may be the preferred neuroprotective agents. COX-independent mechanisms of NSAIDs action such as PPAR γ activation and inhibition of A β production occurs at concentrations of 100 μ M and above (Lanz *et al.*, 2005, Halliday *et al.*, 2001). The beneficial effect of NSAIDs in neurodegenerative diseases is circumvented by their poor distribution into the brain hence higher doses are required for clinically significant effects which will result in higher risk of side effects (Parepally *et al.*, 2006; Mohan *et al.*, 2006).

The combination of aspirin and acetaminophen provided protection against cyanide-induced superoxide anions (O_2^-) generation by reducing the levels of O_2^- below that of the control basal value. The combination of both agents was found to be more effective in reducing MPP $^+$ -induced increase in O_2^- levels than the individual drugs (Maharaj *et al.*, 2004). The effect of the combination is as a result of its ability to improve cellular respiration and superoxide dismutase activity in the presence of MPP $^+$ at a lower concentration of the individual drug for an additive effect. In a recent study, the NSAID diclofenac (**74**) was successfully conjugated to multi-functional ligands like (**75**), with improved anti-inflammatory effect of the prodrugs (**76-79**) compared with diclofenac alone due to synergy of both drugs (Xu *et al.*, 2015).

Most NSAIDs are lipophilic with a logD_{oct} of 1 to +2 and should cross the BBB by passive diffusion. Conversely, NSAIDs do not cross the BBB due to their polar nature as they are 99% ionised in plasma at physiological pH. Furthermore, organic anion transporters in the BBB inhibit NSAIDs permeability (Kusuhara 2005). Brain uptake of these compounds is further inhibited by their binding to plasma albumin which reduces the fraction of free NSAIDs by over 90% (Davies & Skjodt 2000). Ibuprofen for example has a vascular corrected brain concentration at steady state of 1-2% of that of the total plasma concentration

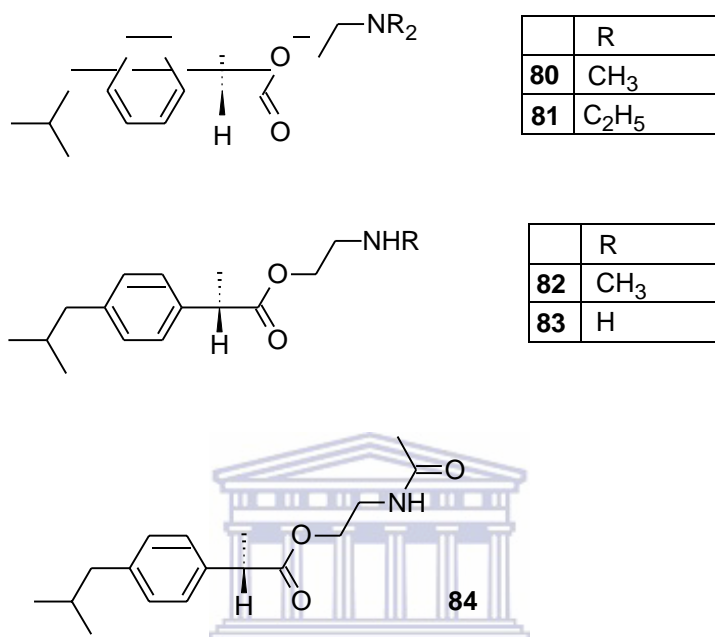
(Mannila *et al.*, 2005). The steady state brain/plasma concentration of ibuprofen, indomethacin, naproxen and ketoprofen was observed to be 0.01-0.05 which is indicative of limited CNS distribution (Eriksen *et al.*, 2005). Increasing the plasma concentration of NSAIDs will precipitate undesirable adverse effects therefore the brain delivery has to be enhanced for effective neuroprotection.



Neuroinflammation as mentioned earlier is a characteristic of most neurodegenerative disorders, it also compromises the integrity of the BBB thereby hasten disease progression as the brain homeostatic regulation is altered. Several prodrugs of NSAIDs have being designed to enhance activity or reduce gastrointestinal toxicity, however very few studies have conducted investigations into CNS delivery of NSAIDs by utilizing the prodrug approach (Meythaler and Peduzzi, 2013; Dahan *et al.*, 2014; Zhao *et al.*, 2014; Zheng *et al.*, 2016).

Using 1,4-dihydro-1-methylpyridine-3-carboxylate as carrier delivery system, prodrugs of selected NSAIDs were synthesised and evaluated for *in vitro* BBB permeation (Perioli *et al.*,

2004). Prodrugs of ibuprofen and a proline moiety or analogues thereof have also been observed to possess anti-inflammatory properties with significant lipooxygenase inhibition (Siskou *et al.*, 2007). Recently, five prodrugs of dexibuprofen (**80-84**) were synthesised and evaluated for *in vivo* biodistribution and pharmacokinetic properties with improved brain distribution observed (Zhang *et al.*, 2012).

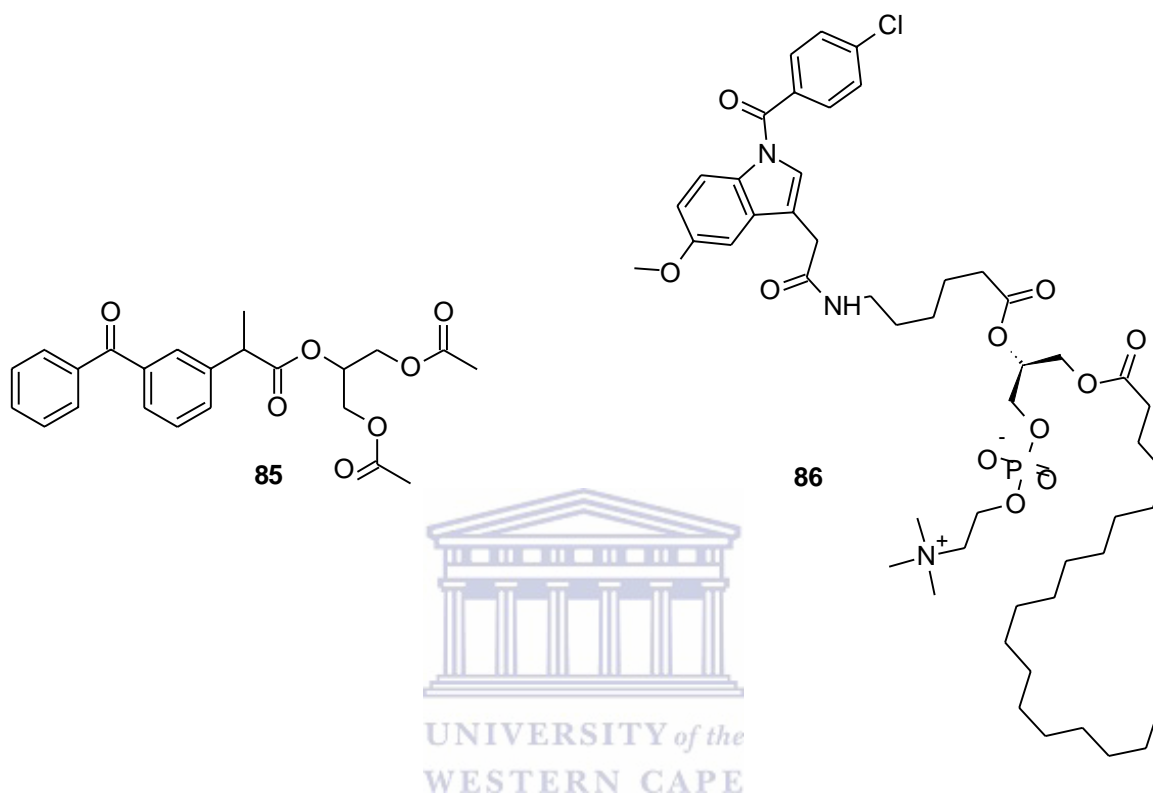


Deguchi *et al.*, 2000 designed a model prodrug for the CNS delivery of NSAIDs by synthesizing the 1,3-diacetyl-2-ketoprofen glyceride (DAKG) prodrug of ketoprofen. The triglyceride prodrug (**85**) was lipophilic enough to cross the BBB but on hydrolysis, ketoprofen was effluxed from the brain and therefore could not act in the CNS. Furthermore, indomethacin was conjugated to lecithin to form the lipophilic prodrug DP-155 (**86**), which is hydrolysed by phospholipase A2 (PLA2) to the parent drug. The brain permeation of indomethacin was significantly increased after oral administration of DP-155 (Dvir *et al.*, 2007).

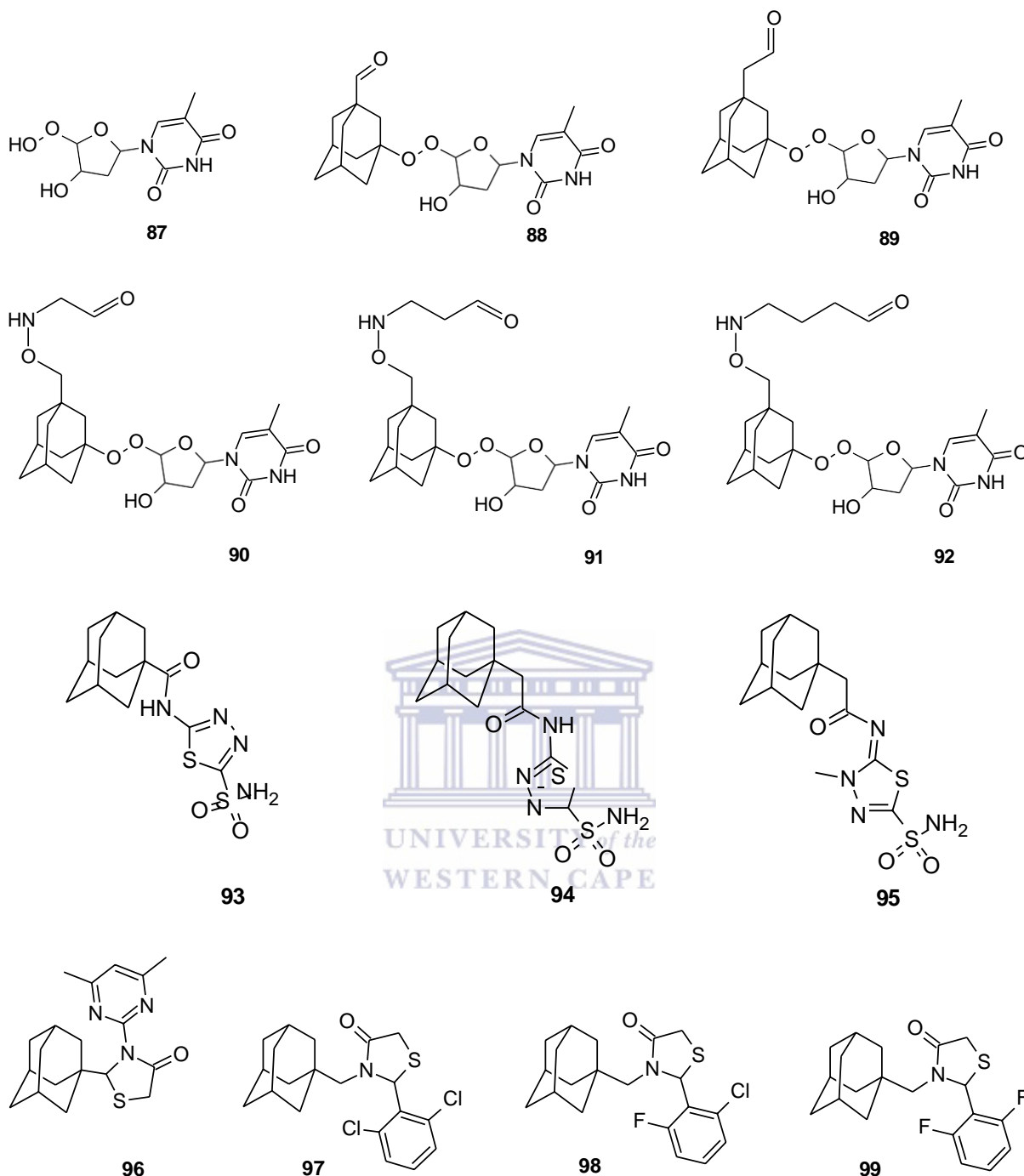
2.7 Polycyclic amines as lipophilic scaffolds

Since the serendipitous discovery of the anti-parkinson effect of the antiviral agent-amantadine (**5**) used in the treatment of influenza-A infections, structurally related compounds have been designed and investigated in drug discovery (Schwab *et al.*, 1972). Polycyclic cage moieties such as the adamantanes and pentacycloundecanes serve as useful

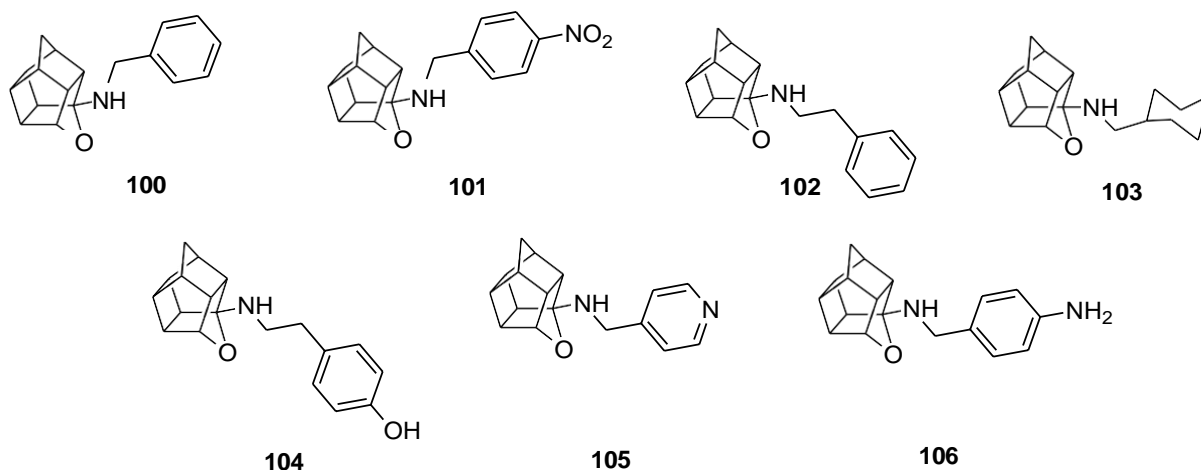
scaffolds in the development of lead compounds in various disease conditions (El-Emam *et al.*, 2004; Harikishore *et al.*, 2013; Van der Schyf & Geldenhuys 2009). Polycyclic scaffolds further possess intrinsic high lipophilicity which can be employed to improve the brain delivery of potential therapeutic agents conjugated to it.



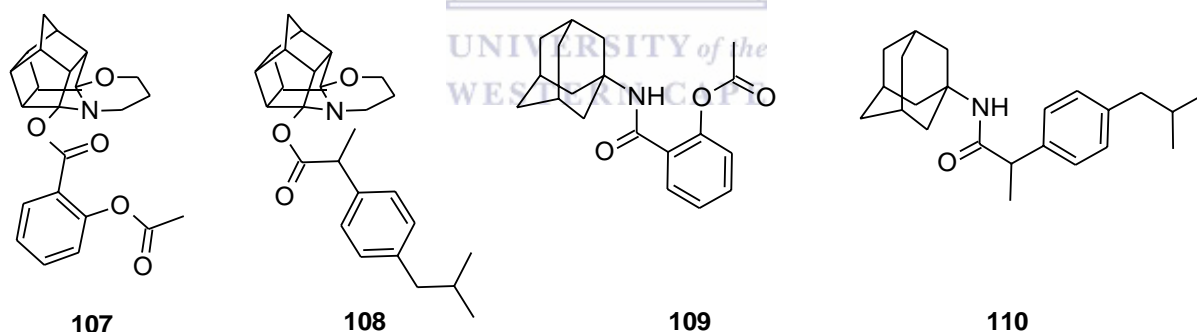
The brain concentration of adamantyl ester prodrugs of the antiretroviral drug azidothymidine (AZT) (**88-92**) was increased up to 18 fold in comparison to intravenous administration of AZT (Tsuzuki *et al.*, 1994). Improved *in vivo* anticonvulsant activity due to increased bioavailability was also obtained on conjugating analogues of carboxamido-thiadiazole-sulfonamide with the lipophilic adamantane cage (**93-95**) (Ilies *et al.*, 2004). Subsequently, the conjugation of amantadine to thiazolidinones (**96-99**) at positions 2 and 3 respectively produced improved lipophilicity and anti-HIV-1 activity although with high cytotoxicity for the 3-position thiazolidinone conjugates (Balzarini *et al.*, 2009).



Polycyclic pentacycloundecanes also impart high lipophilicity to conjugated molecules. Moieties attached to the pentacycloundecane structure (**100-106**) readily permeate through the BBB to reach the CNS within an hour after intra-peritoneal injection. Using experimental values of $\text{Log } P_{\text{oct}}$, solvent accessibility molecular volume (SV) and molecular refractivity (MR) values, hydrophobic interactions were suggested to be largely responsible for the brain permeation of pentacycloundecanes (Zah *et al.*, 2003).



As a follow up to the study by Zah *et al.*, 2003, adamantanes and pentacycloundecanes were employed as lipophilic carriers to synthesise ibuprofen and acetylsalicylic acid prodrugs (107-110) to improve the BBB permeability of parent NSAIDs. The ester prodrugs showed improved brain permeation, however the amide prodrugs produced a low brain concentration to blood concentration ratio which reflects a slower rate of hydrolysis in the brain (Prins *et al.*, 2009). This can be attributed to the stronger amide bond and the ubiquitous nature of amidases in comparison to esterases.



2.8 Conclusion

Neurodegenerative disorders are of a complex pathogenesis therefore targeting neuroinflammation which is a major hallmark in these disorders, may halt disease progression. NSAIDs have intrinsic neuroprotective potentials due to their anti-inflammatory properties, however they do not reach the central nervous system at therapeutically significant concentrations. The blood-brain barrier is the major obstacle to the successful CNS delivery of potential therapeutic agents. Using lipophilic polycyclic carriers, the prodrug approach provides a promising strategy to improve the brain delivery of NSAIDs.

CHAPTER THREE

SYNTHESIS

3.1 Pre-synthesis study

The polycyclic-NSAID conjugates selected for synthesis had to comply with the physicochemical properties required for blood-brain barrier (BBB) permeation and particularly the Lipinski's rule of five for oral bioavailability. *In silico* predictions were done using ChemAxon physico-chemical property predictor.

Lipinski's rule of five

A compound possesses a high probability of good oral bioavailability if it does not violate more than one of the following conditions:

- 1) Molecular weight (Mr) not greater than 500 g/mol
- 2) LogP value not greater than 5
- 3) Not more than five H-bond donors (sum of OH and NH groups)
- 4) Not more than ten H-bond acceptors (sum of nitrogen and oxygen atoms)

Nineteen compounds were selected for synthesis based on the results from the *in silico* predictions (**Table 3.1**). Compound **9.4** was excluded from the synthesis due to its negative Log D value as well as possession of six hydrogen bond acceptors which was in line with other compounds in the aspirin series, however these compounds did not violate more than one Lipinski's criteria.

3.2 Standard synthesis procedures

3.2.1 Chemicals

N,N'-carbonyldiimidazole (CDI), aspirin, ketoprofen, naproxen, ibuprofen, dichloromethane (DCM), tetrahydrofuran (THF), amantadine, sodium borohydride, magnesium sulphate, *p*-benzoquinone, cyclohexane, benzene, cyclopentadiene, ethyl acetate, hexane, ethanol, petroleum ether and acetone were purchased from Sigma-Aldrich (Steinheim, Germany). Unless otherwise specified, all materials were obtained from commercial suppliers and used without further purification. Solvents were dried using standard methods.

3.2.2 Instrumentation

Infrared spectroscopy (IR): The IR spectra were recorded on a Perkin Elmer Spectrum 400 spectrometer, fitted with a diamond attenuated total reflectance (ATR) attachment.

Melting point determination (MP): Melting points were determined using a Stuart[®] SMP-10 instrument and capillary tubes.

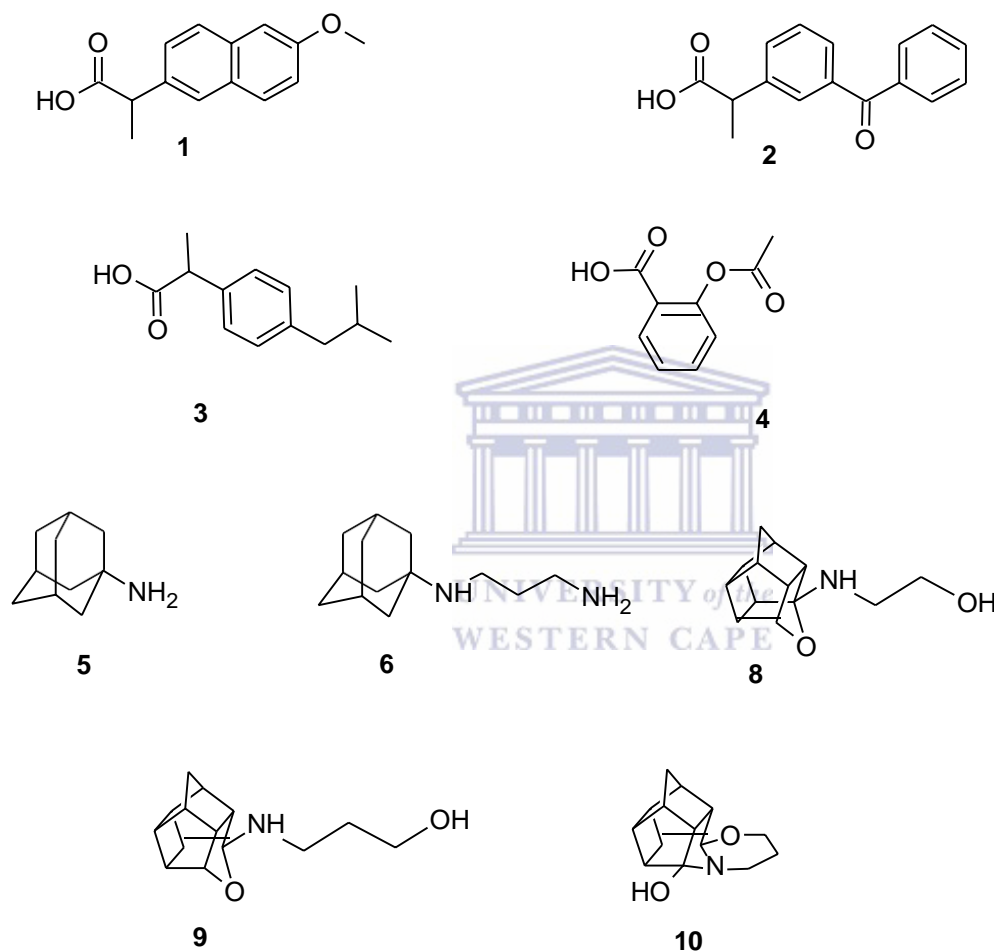


Fig 3.1: Structures selected for conjugation (1-4) to the polycyclic cage scaffolds (5-10)

Nuclear magnetic resonance spectroscopy (NMR): ¹H and ¹³C NMR spectra were acquired using a 400 MHz Avance IIIHD Nanobay spectrometer (Bruker, Rheinstetten, Germany) equipped with a 5 mm BBO probe at 333 K using standard 1D NMR pulse sequence. Tetramethylsilane (TMS) was used as internal standard. All chemical shifts are reported in parts per million (ppm) relative to the signal from TMS ($\delta = 0$) in deuterated chloroform. The multiplicity of the signals is represented by the following symbols: s - singlet, bs - broad

singulet, d - doublet, dd - doublet of doublets, t - triplet, q - quartet and m - multiplet. Spectra of synthesised compounds are included in annexure A.

Table 3.1: *In Silico* analysis of potential prodrugs for blood-brain barrier permeation where the first numbers represent the polycyclic scaffolds and the numbers after the decimal point represents the selected NSAIDs.

Prodrug	Molecular weight	Solubility	Log D	H-bond donors	H-bond acceptors	Toxicity risk
5.1	363.51	-6.5	4.49	1	3	low
6.1	420.59	-2.5	1.05	2	4	low
8.1	431.52	-5.5	1.01	1	5	low
9.1	445.55	-4.1	1.71	1	5	low
10.1	443.51	-6.4	3.85	0	5	low
5.2	387.51	-7.5	5.12	1	3	low
6.2	444.61	-2.1	1.61	2	4	low
8.2	455.54	-5.1	2.25	1	5	low
9.2	469.57	-3.5	1.25	1	5	low
10.2	467.56	-6.8	4.52	0	5	low
5.3	339.51	-7.9	5.35	1	2	low
6.3	396.61	-2.8	1.85	2	3	low
8.3	407.55	-4.8	2.55	1	4	low
9.3	421.57	-3.8	1.51	1	4	low
10.3	419.56	-6.5	4.74	0	4	low
5.4	313.39	-4.8	2.75	1	4	low
6.4	370.49	-0.8	-0.75	2	5	low
8.4	381.42	-2.9	0.31	1	6	low
9.4	395.45	-1.9	-0.62	1	6	low
10.4	393.43	-4.8	2.38	0	6	low

Mass spectroscopy (MS): The MS spectra were recorded on a Perkin Elmer Flexar SQ 300 mass spectrometer by means of direct injection with a syringe pump.

3.2.3 Chromatographic methods

Mobile phases were prepared using different solvents of varying volume-to-volume ratios. Ethyl acetate (ETOAc) 100% was used as primary mobile phase and the polarity adjusted accordingly using hexane (HEX) until the most appropriate mobile phase ($R_f = 0.3$) was obtained. Visualisation was achieved using UV light (254 nm and 366 nm) and iodine vapours.

Thin layer chromatography (TLC): Analytical TLC was performed on 0.20 mm aluminium silica gel sheets (Alugram[®] SIL G/UV254, Kieselgel 60, Macherey-Nagel, Düren, Germany) to monitor all reactions.

Column chromatography: Purification of final products and intermediates was performed using column chromatography in glass columns filled with silica gel (MN Kieselgel 60, 0.063- 0.2mm, 70- 230 mesh ASTM, Separations, Randburg, South Africa).

3.2.4 General synthetic design

The well-described Cookson's diketone, pentacyclo[5.4.0^{2.6}.0^{3,10}.0^{5,9}]undecane-8,11-dione, was synthesised by the photocyclization of the Diels-Alder adduct obtained from the reaction between *p*-benzoquinone and cyclopentadiene (Cookson *et al.*, 1958). Subsequent purification by soxhlet extraction produced the diketone polycyclic compound.

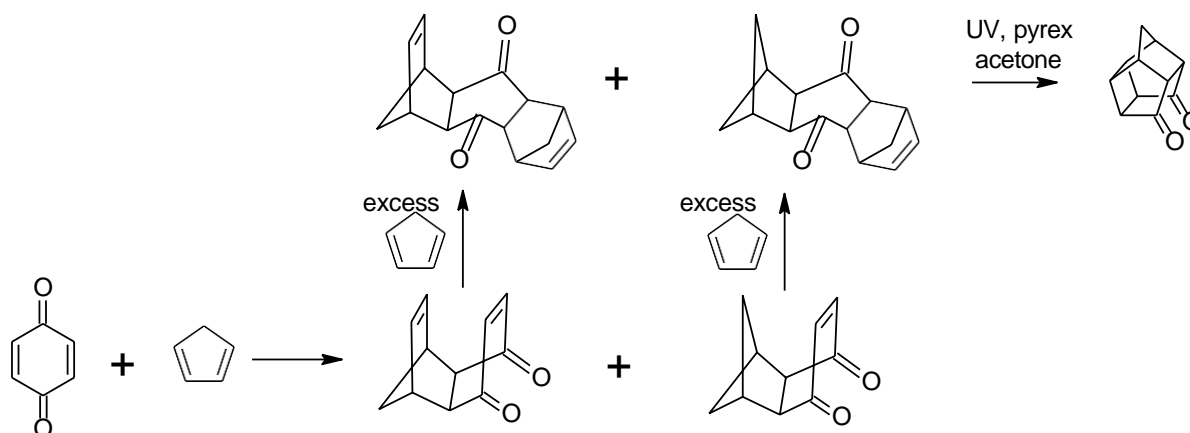
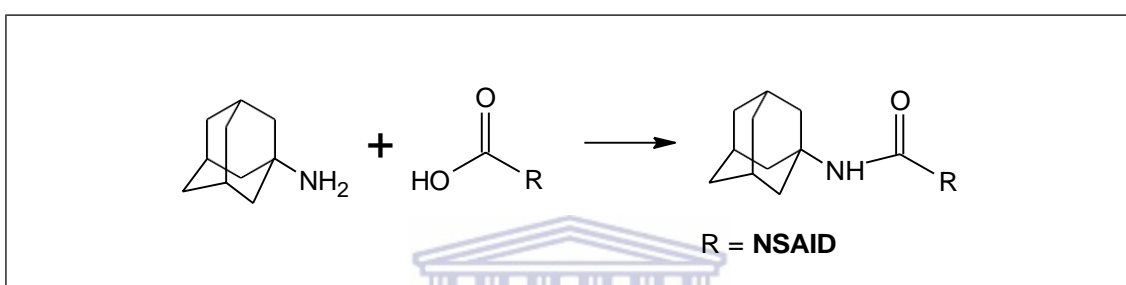


Fig 3.2: Synthesis of Cookson's diketone cage compound (Marchand & Suri 1984)

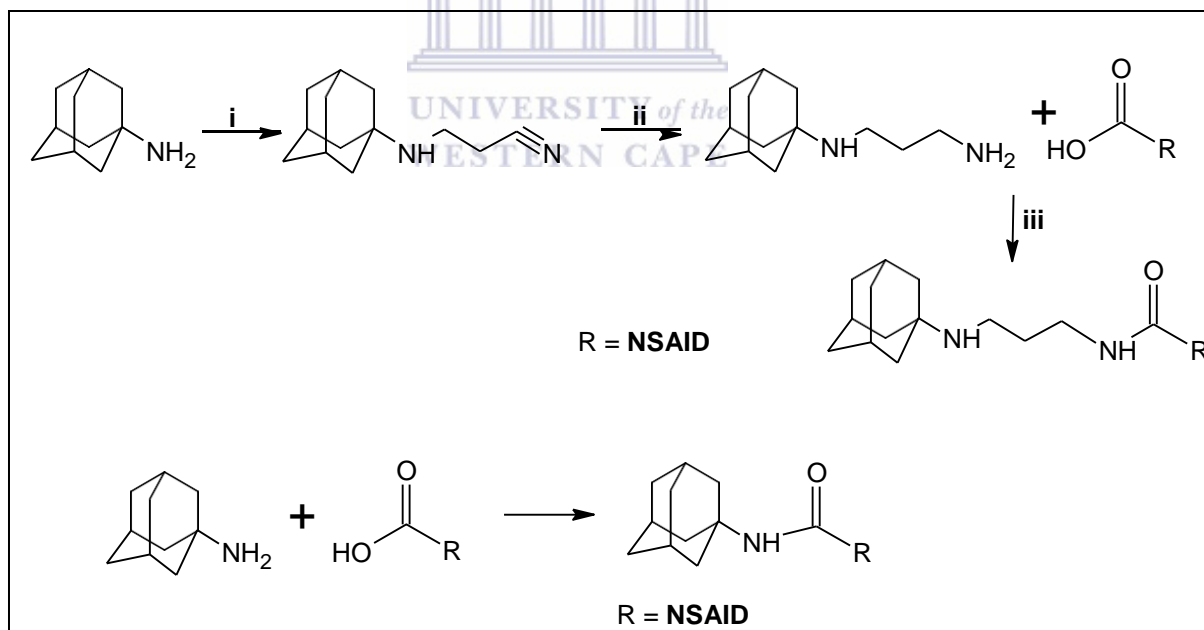
The amantadine-NSAID conjugates were obtained either by directly conjugating free amantadine base with NSAIDs *via* amidation (**Scheme 1**) or through a Michael's addition

reaction of amantadine free base with acrylonitrile and water (**Scheme 2, i**), followed by reduction of the nitrile (**Scheme 2, ii**) with lithium aluminium hydrate (LiAlH) and subsequent amidation with activated NSAID. Activation of the NSAIDs were achieved through the use of activating agent *N,N'*-carbonyldiimidazole (CDI) (**Scheme 2, iii**).

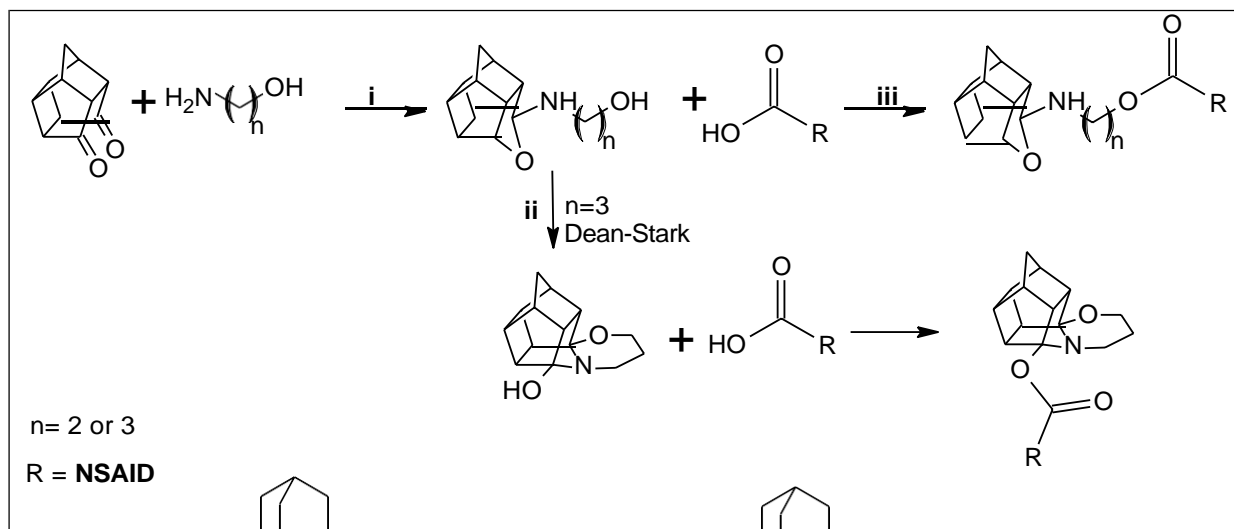
The designed pentacycloundecane-NSAID conjugates were synthesised by conjugating one of the ketone groups in Cookson's diketone with different amines *via* reductive amination to yield the respective pentacycloundecylamines (**scheme 3, i and ii**). The selected NSAIDs were activated using CDI and subsequently conjugated to the respective pentacycloundecylamines derivatives (**scheme 3, iii**).



Scheme 1: Reagents and conditions: **i** = CDI, dichloromethane (DCM), 25°C, 48 hours

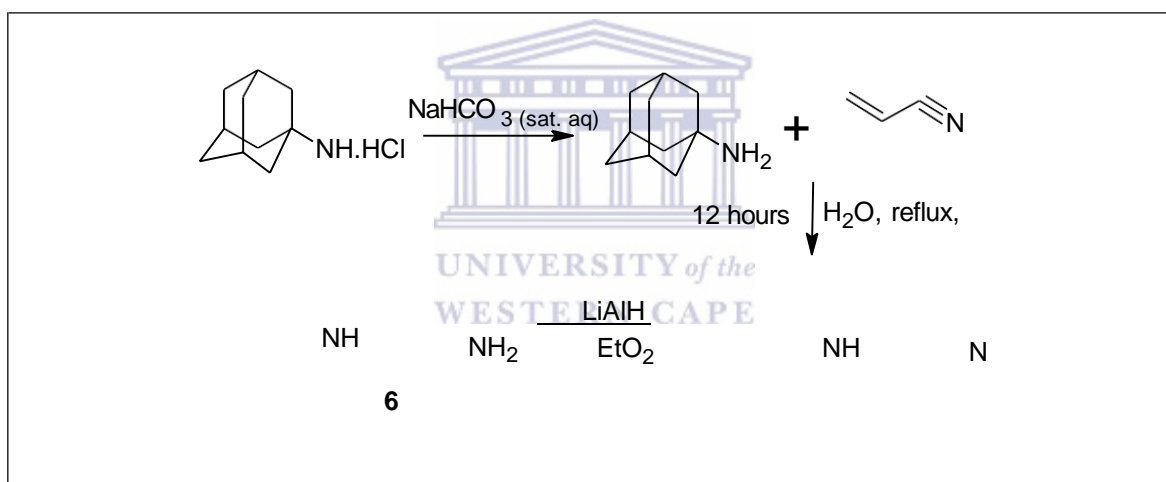


Scheme 2: Reagents and conditions: **i** = acrylonitrile, water (H₂O), reflux, 12 hours; **ii** = lithium aluminium hydrate (LiAlH), diethyl ether (Et₂O); **iii** = CDI, DCM, 48 hours



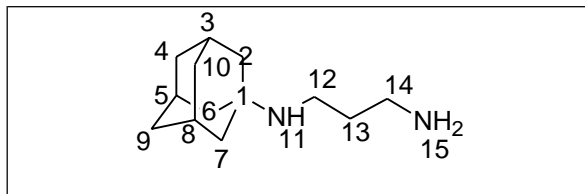
Scheme 3: Reagents and conditions: **i** = anhydrous THF, sodium borohydride (NaBH_4) 5°C , 30 minutes; **ii** = benzene, Dean-Stark, 1 hour; **iii** = CDI, DCM, 72 hours

3.2.4.1 Synthesis of 3-(1-(adamantylamino)propanenitrile) (6)



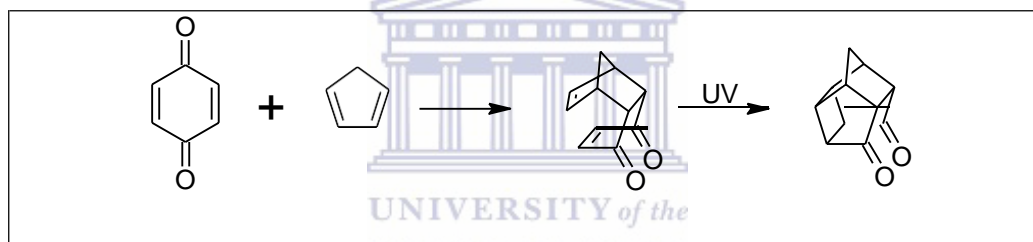
Amantadine hydrochloride was washed with a water solution saturated with sodium hydrogen carbonate (NaHCO_3) to obtain amantadine free base. Amantadine free base (8.151 g, 0.0539 mol) was dissolved in 100 ml of acrylonitrile, 1 ml of H_2O was added and the mixture was allowed to react under reflux for 12 hours. The excess acrylonitrile was removed *in vacuo* and the mixture was washed with 100 ml of brine and extracted with DCM (4 x 25 ml), the organic fraction was dried over anhydrous magnesium sulphate (MgSO_4) filtered and concentrated *in vacuo* to give 9.520 g, of a glassy solid (**scheme 2**). This intermediate (9.520g, 0.0466 mol) was dissolved in 10 ml Et_2O and added drop-wise to a well-cooled suspension of 2.28 g (0.060 mol) of LiAlH_4 in 200 ml of dry Et_2O . The reaction mixture was stirred at room temperature for 3 hours, on cooling 4 ml of H_2O was added, followed by 3 ml

5 N NaOH solution and 14 ml of H₂O. The Et₂O layer was decanted and the solid cake was washed with 4 x 12 ml Et₂O. The combined Et₂O layer was dried over MgSO₄, filtered and the filtrate was concentrated *in vacuo* to produce a white wax as compound **6** (Yield: 6.796 g, 0.033 mol, 70%).



Physical data: C₁₃H₂₄N₂; **mp:** wax; **TLC** (ETOAc 9:1 Hex) R_f 0.3; **¹H-NMR** (400 MHz, CDCl₃) δ_H (spectrum 1): 1.62-1.81 (m, 12H, H-4a, 4b, 6a, 6b, 10a, 10b, 12a, 12b, 13a, 13b, 14a, 14b); 2.10 (bs, 3H, H-11, 15a, 15b); 2.42-2.49 (m, 5H, H-2a, 2b, 7a, 7b, 8) 2.92-2.98 (m, 4H, H-3, 5, 9a, 9b); **IR** (ATR; cm⁻¹) V_{max} (spectrum 2): 3306, 2906, 2846, 1499, 1450, 1313, 817, 794 cm⁻¹.

3.2.4.2 Synthesis of pentacyclo[5.4.0^{2,6}.0^{3,10}.0^{5,9}]undecane-8,11-dione

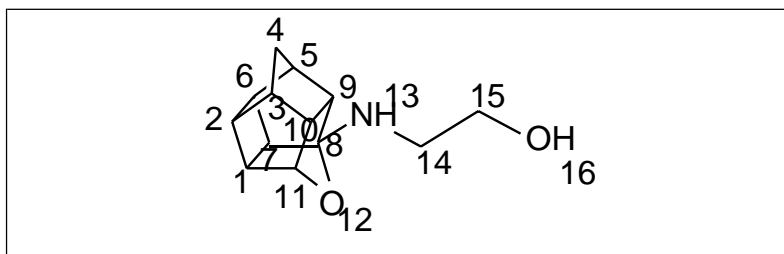


p-Benzoquinone (25.110 g, 0.23 mol) was dissolved in 100 ml dried benzene on an external ice bath (5°C). Freshly monomerised cyclopentadiene was stoichiometrically added in 2 ml aliquots to reaction mixture at 5°C with continuous monitoring by TLC plate until the *p*-benzoquinone spot was no longer visible and a new spot was seen under UV and iodine (mobile phase = HEX 2 : 1 ETOAc; R_f = 0.75). The photo labile reaction mixture was stirred for an additional 60 minutes on the external ice bath (0-5°C). Three spatula measure of activated charcoal was added and the mixture was stirred at room temperature for one hour. The mixture was filtered through Celite[®] to produce a clear yellow solution followed by *in vacuo* evaporation of benzene (BP = 80°C). The amber coloured oil obtained was placed in a dark evaporating hood overnight to remove residual solvent. The yellow Diels-Alder adduct crystals obtained were dissolved in ethyl acetate (4 g per 100 ml of solution) and placed in a photochemical reactor for 6 hours. Cyclisation of the adduct was indicated by decolouration

of the solution. *In vacuo* evaporation of ethyl acetate afforded a light yellow residue. Soxhlet extraction of the residue in 200 ml cyclohexane yielded the diketone cage as fine white powder (Yield: 30.980 g, 0.18 mol, 77%). The physical characteristics of the product correlated with that described in literature (Cookson *et al.* 1958).

3.2.4.3 Synthesis of 8-(2-aminoethanol)-8,11-oxapentacyclo[5.4.0^{2,6,3,10,5,9}.0 .0]-undecane (8)

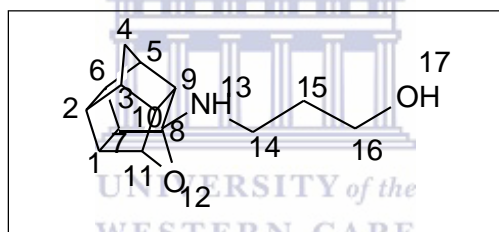
Pentacyclo[5.4.0^{2,6,3,10,5,9}.0 .0]undecane-8,11-dione (5,110 g, 29.33 mmol) was dissolved in 50 ml of dry THF on an external ice bath (0-5°C). 2-Aminoethanol (1.800 g, 29.47 mmol) was dissolved in 6 ml THF and added drop wise to the reaction mixture while maintaining the reaction at 0-5°C by keeping it in an external ice bath. The carbinolamine started to precipitate after 15 minutes and the mixture was stirred for an additional 30 minutes. The carbinolamine was dissolved by adding 30 ml of dry methanol. Sodium borohydride (1.010 g) was slowly added and the mixture was stirred at room temperature for 1 hour to ensure completion. The reaction mixture was concentrated *in vacuo*, washed with water (100 ml), and extracted with dichloromethane (4 x 25 ml). The organic fraction was dried with anhydrous MgSO₄ and evaporated to give light yellow oil. The mixture was purified by column chromatography (eluent: 100% HEX followed by ETOAc 2:1 ETOH) to obtain the desired amine (Yield: 1.430 g, 6.52 mmol, 22%).



Physical data: C₁₃H₁₇NO₂; **mp:** oil; **TLC** (ETOAc 2:1 ETOH) R_f 0.40; **¹H-NMR** (400 MHz, CDCl₃) δ_H (spectrum 3): 4.61 (t, 1H, *J* = 5.22 Hz, H-11), 3.58 (m, 2H, H-15a, 15b), 2.97 (m, 2H, H-14a, 14b), 2.88- 2.69 (m, 4H, H-1, 7, 9, 10), 2.62- 2.45 (m, 5H, H-2, 3, 5, 6, 13), 1.90: 1.48 (AB-q, 2H, *J* = 10.5 Hz, H-4a, 4b).

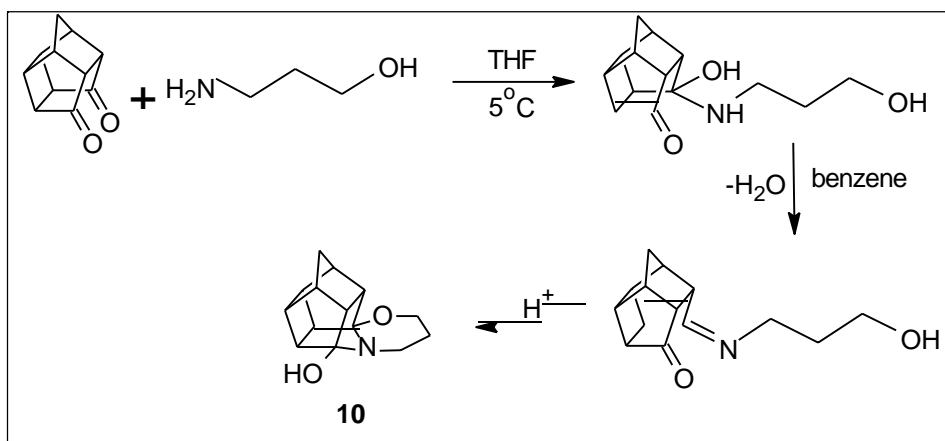
3.2.4.4 Synthesis of 8-(3-aminopropanol)-8,11-oxapentacyclo[5.4.0 .0 .0]-undecane (9)

Pentacyclo[5.4.0 .0 .0]undecane-8,11-dione (5.120 g, 29.39 mmol) was dissolved in 30 ml of THF and cooled down to 5°C on an external ice bath. 3-amino-1-propanol (2.209 g, 29.41 mmol) dissolved in 6 ml THF was added dropwise over 5 minutes while maintaining the reaction mixture at 5°C. The carbinolamine started precipitating after approximately 15 minutes and the reaction was allowed to reach completion for an additional 30 min. The carbinolamine was dissolved by adding 30 ml of dry methanol. Sodium borohydride (1.010 g) was slowly added and the mixture was stirred at room temperature for 1 hour to ensure completion. The reaction mixture was concentrated *in vacuo*, washed with water (100 ml), and extracted with dichloromethane (4 x 25 ml). The organic fraction was dried with anhydrous MgSO₄ and evaporated *in vacuo* to give the light yellow oil. The mixture was purified by column chromatography (eluent: ETOAc 3:2 HEX followed by ETOAc 9:1 HEX) to obtain the desired amine as a light yellow oil (Yield: 1.581 g, 6.78 mmol, 23%).

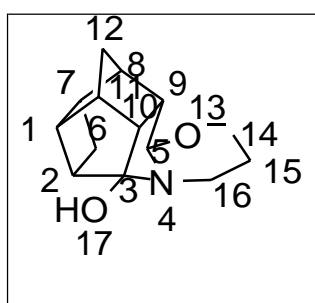


Physical data: C₁₄H₁₉NO₂ ; **mp:** oil; **TLC** (ETOAc 2:1 ETOH) R_f 0.40; **¹H-NMR** (400 MHz, CDCl₃) δ_H (Spectrum 4): 4.96-5.20 (bs, 1H, H-13), 3.72-3.92 (q, 2H, H-16a, 16b), 3.69-3.76 (m, 2H, H-14a, 14b), 2.22-2.80 (4 x m, 9H, H-1, 2, 3, 5, 6, 7, 9, 10, 11), 1.91:1.52 (AB-q, 2H, J = 10.58 Hz, H-4a, 4b), 1.58 (m, 2H, H-15a, 15b).

3.2.4.5 Synthesis of 3-hydroxy-4-aza-8-oxoheptacyclo- [9.4.1.0^{2,10}.0^{3,14}.0^{4,9}.0^{9,13}.0^{12,15}]tetradecane (10)



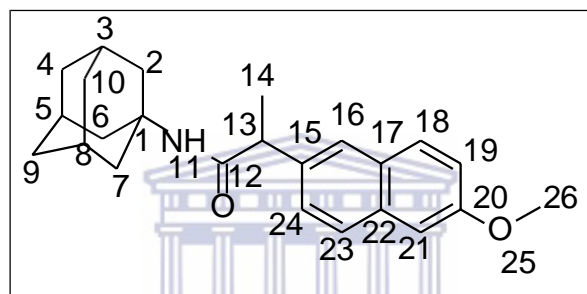
Pentacyclo^{2,6,3,10,5,9}[5.4.0.0.0]undecane-8,11-dione (3.041 g, 17.46 mmol) was dissolved in 30 ml of THF and cooled down to 5°C on an external ice bath. 3-amino-1-propanol (13.129 g, 17.48 mmol) dissolved in 6 ml THF, was added dropwise over 5 minutes while maintaining the reaction mixture at 5°C. The carbinolamine started precipitating after approximately 15 min, but the reaction was allowed to reach completion for an additional 30 min. The solvent was removed by filtration and water was azeotropically removed from the precipitate by refluxing the solution in a Dean-Stark apparatus with 60 ml benzene for 1 hour or until no water was collected in the trap. The benzene was evaporated under reduced pressure and the rearranged cage structure was obtained as yellow oil. Crystallisation and recrystallisation from THF produced the final product as white crystals (Yield: 2.527 g, 12.99 mmol, 62.58%). The physiochemical data correlated with that of literature (Joubert *et al.*, 2008).



Physical data: C₁₄H₁₇NO₂; mp: 169-171°C; TLC (EtOAc 2:1 EtOH) R_f 0.50; ¹H-NMR (400 MHz, CDCl₃) δ_H (spectrum 5): 3.85-3.74 (m, 2H, H-14a, 14b), 3.73-3.67 (m, 2H, H-16a, 16b), 3.02-2.53 (3 x m, 8H, H-1, 2, 6, 7, 8, 9, 10, 11), 1.80:1.52 (AB-q, 2H, J = 10.58 Hz, H-12a, 12b), 1.75-1.55 (m, 2H, H-15a, 15b).

3.2.4.6 Synthesis of 2-(6-methoxy-2-naphthyl)-N-(adamantyl)propanamide (5.1)

Naproxen (0.515 g, 2.24 mmol) was dissolved in 25 ml dry DCM and 0.397 g (2.45 mmol) of CDI was added in molar excess. The reaction mixture was protected from light and stirred at 60°C for 3 hours. Amantadine hydrochloride (0.408 g, 2.17 mmol) and triethylamine (0.698 g, 6.90 mmol) were added to the reaction mixture and the reaction was allowed to proceed at 25°C for 48 hours. Excess solvent was removed under reduced pressure and THF 2:1 ETOAc was added to the product. A white precipitate formed instantaneously and was filtered. TLC of the residue indicated that this was the amantadine free base. Repetition of the precipitation and filtration processes produced a comparatively purer solution of the amide. Purification of the amide by column chromatography (eluent: HEX 2:1 ETOAc, followed by 100% ETOAc) produced the final product as a white powder (Yield: 0.276 g, 0.76 mmol, 35%).

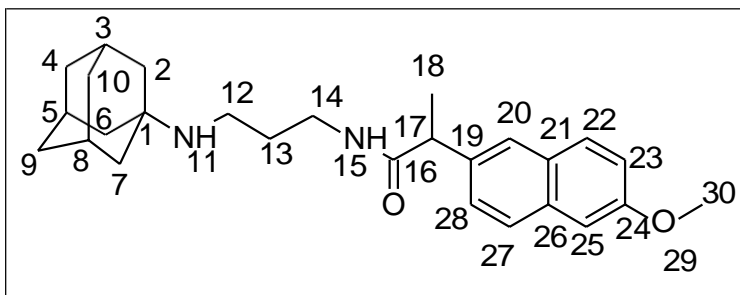


Physical data: C₂₄H₂₉NO₂; **mp:** 156-158°C; **TLC** (ETOAc 1:2 ETOH) R_f 0.6; **¹H-NMR** (400 MHz, CDCl₃) δ_H (spectrum 6): 7.72-7.66 (d, 2H, H-18, 23), 7.44 (d, 2H, H-16, 24), 7.15-7.09 (m, 2H, H-19, 21), 3.93-3.83 (m, 4H, H-13, 26a, 26b, 26c), 1.64-1.54 (m, 4H, H-11, 14a, 14b, 14c), 1.32-1.23 (m, 15H, H-2a, 2b, 3, 4a, 4b, 5, 6a, 6b, 7a, 7b, 8, 9a, 9b, 10a, 10b); **¹³C-NMR** (100 MHz, CDCl₃) δ_C (spectrum 7): 157.67 (C-12), 127.21 (C-20), 126.26 (C-15), 126.10 (C-22), 119.02 (C-18), 105.61 (C-17), 97.24 (1C), 55.32 (C-1), 35.40 (C-2, 6, 10), 31.94 (C-4, 7, 9), 31.85 (C-13), 29.72 (1C), 29.37 (C-3, 5, 8), 27.38 (C-3), 25.73 (1C), 22.71 (C-6), 22.69 (C-14), 18.30 (C-4); **MS** (ESI-MS) *m/z* (spectrum 8): 383.25 [(M+H)⁺, 100%], 384.17 [(M+H+2)⁺, 30%].

3.2.4.7 Synthesis of 2-N-[3-(1-adamantylamino)propyl]-2-(6-methoxy-2-naphthyl)propanamide (6.1)

Naproxen (0.234 g, 1.02 mmol) was dissolved in 15 ml THF and 0.208 g (1.23 mmol) of CDI was added to the mixture. The reaction was allowed to run for 4 hours at 60°C. TLC indicated that naproxen had been completely converted to its activated form. Compound **6** (0.204 g, 0.98 mmol) was added slowly to the solution. The reaction mixture was stirred at room

temperature for 38 hours and concentrated *in vacuo*. The mixture was purified using column chromatography (eluent: HEX 4:1 ETOAc followed by 100% ETOAc) to obtain the oily product (Yield: 0.124 g, 0.29 mmol, 30%).

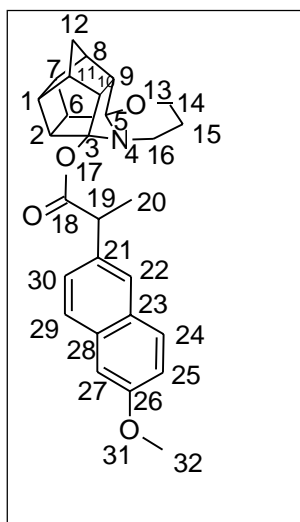


Physical data: $C_{27}H_{36}N_2O_2$; **mp:** oil; **TLC** (ETOAc 1:1 ETOH) R_f 0.5; **1H NMR** (400 MHz, $CDCl_3$) δ_H (spectrum 9): 7.73-7.01 (3 x m, 5H, H-20, 27, 22, 23, 25), 5.51-5.32 (bs, 2H, H-11, 15) 3.95-3.62 (2 x m, 5H, H-13a, 13b, 30a, 30b, 30c), 2.90-2.74 (m, 4H, H-12a, 12b, 14a, 14b), 2.56-2.48 (m, 4H, H-17, 18) 2.05, 1.72-1.44 (m, 15H, H--2a, 2b, 3, 4a, 4b, 5, 6a, 6b, 7a, 7b, 8, 9a, 9b, 10a, 10b), 1.28; **^{13}C NMR** (100MHz, $CDCl_3$) δ_C (spectrum 10): 180.03 (C-16), 157.39 (C-24), 138.03 (1C), 133.40 (C-19), 129.01 (C-26), 128.93 (C-22), 126.82 (C-27), 126.63 (C-20), 125.66 (C-28), 118.86 (1C), 118.06 (C-23), 105.65 (C-25), 55.33 (C-30), 52.79 (C-1), 47.52 (C-17), 41.05 (C-2, 4, 6), 36.14 (C-7, 9, 10), 29.18 (C-3, 5, 8), 18.71 (C-18), 18.05 (1C); **MS** (ESI-MS) m/z . (spectrum 11): 418.17 [(M+H)⁺, 100%], 419.24 [(M+H+2)⁺, 30%].

3248 Synthesis of 3-(4-aza-8-oxo-heptacyclo-

[0.4.1.0^{2,10}.0^{3,14}.0^{4,9,09}.0^{12,15}]tetradecyl)-(6-methoxy-2-naphthyl)propanoate (10.1)

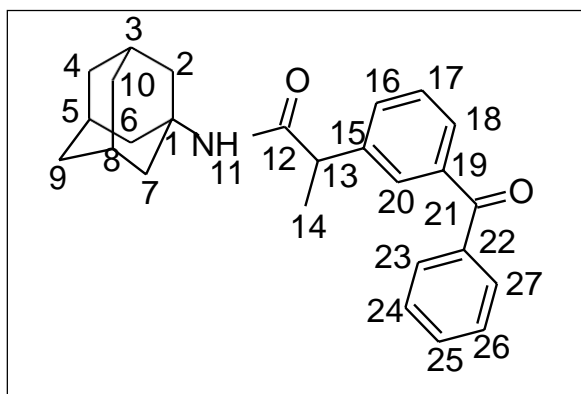
Naproxen (0.304 g, 1.32 mmol) was dissolved in 20 ml of THF and 0.242 g of CDI (1.49 mmol) was added to the mixture. The reaction was allowed to run for 3 hours at 60°C. TLC indicated that naproxen had been completely converted to its activated form. Compound **10** (0.301 g, 1.30 mmol) dissolved in 6 ml of THF was added drop-wise to the activated solution. The reaction mixture was stirred at room temperature for 72 hours and concentrated *in vacuo*. The mixture was purified using column chromatography (eluent: HEX 4:1 ETOAc followed by 100% ETOAc) to obtain the product as an opaque oil (Yield: 0.184 g, 0.42 mmol, 32%).



Physical data: C₂₈H₂₉NO₄; **mp:** oil; **TLC** (ETOAc 2:1 ETOH) R_f 0.4; **¹H NMR** (400 MHz, CDCl₃) δ_H (spectrum 12): 7.78-7.07 (m, 6H, H-22, 29, 24, 25, 27, 30), 3.95-3.78 (m, 7H, H-14a, 14b, 16a, 16b, 32a, 32b, 32c), 3.24-2.66 (4 x m, 5H, H-1, 2, 9, 10, 11), 2.00:1.87 (AB-q, *J* = 10.57 Hz, 2H, H-12a, 12b), 1.61-1.53 (m, 5H, H-6, 7, 8, 15a, 15b), 1.30-1.17 (m, 3H, H-20a, 20b, 20c); **¹³C NMR** (100MHz, CDCl₃) δ_C (spectrum 13): 180.86 (C-18), 157.68 (C-26), 135.06 (C-21), 133.78 (C-28), 129.31 (C-24), 128.90 (C-23), 127.22 (C-29), 126.25 (C-22), 126.11 (C-30), 119.02 (C-25), 105.56 (C-3, 5), 55.32 (C-14), 54.73 (C-6), 45.29 (C-2), 44.65 (1C), 43.16 (C-16); **MS** (ESI-MS) *m/z* (spectrum 14): 444.27 [(M+H)⁺, 100%], 445.86 [(M+H+2)⁺, 30%]; **IR** (ATR, cm⁻¹) V_{max} (spectrum 15): 3175, 2963, 2958, 1481, 1346, 1263 cm⁻¹.

3249 Synthesis of 2-(3-benzoylphenyl)-N-(adamantyl)propanamide (5.2)

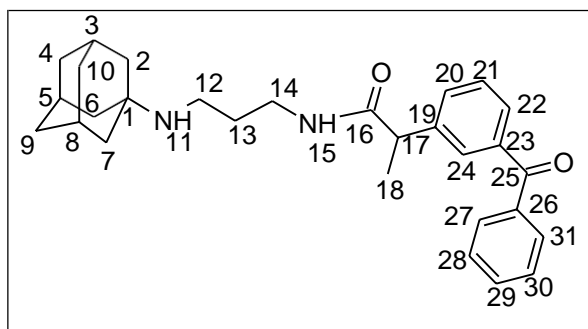
Ketoprofen (0.559 g, 2.20 mmol) was dissolved in 15 ml dry DCM and 0.405 g (2.50 mmol) of CDI was added. The reaction mixture was protected from light and stirred at 60°C for 8 hours. Amantadine hydrochloride (0.408 g, 2.17 mmol) and triethylamine (0.678 g, 6.70 mmol) were added to the reaction mixture and the reaction was allowed to proceed at room 25°C for 38 hours. Excess solvent was removed under reduced pressure and THF 2:1 ETOAc was added to the product. A white precipitate formed instantaneously and was filtered. TLC of the residue indicated that this was the amantadine free base. Repetition of the precipitation and filtration processes produced a comparatively pure solution of the amide product. Purification of the amide by column chromatography (eluent: HEX 3:2 ETOAc followed by 100% ETOAc) produced a white powder (Yield: 0.318 g, 0.82 mmol, 38%).



Physical data: $C_{26}H_{29}NO_2$; **mp:** 136-138°C; **TLC** (ETOAc 1:2 ETOH) R_f 0.6; **1H NMR** (400 MHz, $CDCl_3$) δ_H (spectrum 16): 7.80 (d, 2H, H-23, 27), 7.71 (s, 1H, H-20), 7.69-7.64 (d, 1H, H-25), 7.61-7.55 (t, 2H, H-24, 26), 7.52-7.42 (m, 3H, H-16, 17, 18), 3.73 (q, 1H, H-13), 1.50 (d, 3H, H-14), 1.67-1.61 (m, 6H, H-4a, 4b, 6a, 6b, 10a, 10b), 1.27-1.22 (m, 9H, H-2a, 2b, 3, 5, 7a, 7b, 8, 9a, 9b); **^{13}C NMR** (100MHz, $CDCl_3$) δ_C (spectrum 17): 196.79 (C-21), 172.8 (C-12), 142.39 (C-19), 137.96 (C-15), 137.53 (C-22), 132.61 (1C), 132.54 (C-25), 131.42 (C-27), 131.35 (C-23), 130.10 (C-20), 130.05 (C-17), 129.05 (C-18), 128.34 (C-24, 26), 51.99 (C-1), 47.77 (C-13), 41.52 (C-2, 6, 10), 36.29 (C-4, 7, 9), 29.73 (C-3, 5, 8), 19.91 (C-14); **MS** (ESI-MS) m/z (spectrum 18): 369.52 [(M+H)⁺, 100%], 370.17 [(M+H+2)⁺, 30%]; **IR** (ATR, cm^{-1}) V_{max} (spectrum 19): 3127, 2851, 1567, 1391, 1062, 747 cm^{-1} .

32410 Synthesis of (2R)-N-[3-(1-adamantylamino)propyl]-2-(3-benzoylphenyl)propanamide (6.2)

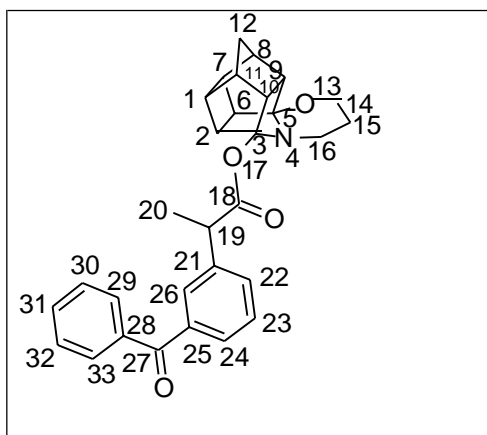
Ketoprofen (0.245 g, 0.96 mmol) was dissolved in 15 ml THF and 0.174 g (1.07 mmol) of CDI was added to the mixture. The reaction was allowed to run for 10 hours at 60°C. TLC indicated that ketoprofen had been completely converted to its activated form. 0.200 g (0.96 mmol) of compound **6** was added slowly to the solution. The reaction mixture was stirred at room temperature for 24 hours and concentrated *in vacuo*. The mixture was purified using column chromatography (eluent: HEX 3:2 ETOAc followed by 100% ETOAc) to obtain the product as a yellow oil (Yield: 0.128 g, 0.29 mmol, 30%).



Physical data: C₂₉H₃₆N₂O₂; **mp:** oil; **TLC** (ETOAc 1:2 ETOH) R_f 0.7; **¹H NMR** (400 MHz, CDCl₃) δ_H (spectrum 20): 7.82-7.77 (d, 2H, H-27, 31), 7.61-7.55 (m, 2H, H-24, 29), 7.50-7.44 (m, 2H, H-28, 30), 3.73-3.66 (m, 3H, H-20, 21, 22), 2.93-2.68 (t, 4H, H-12a, 12b, 14a, 14b), 2.54-2.48 (d, 3H, H-18a, 18b, 18c) 2.06 (m, 5H, H-11, 13a, 13b, 15, 17), 1.70-1.54 (m, 15H, H-2a, 2b, 3, 4a, 4b, 5, 6a, 6b, 7a, 7b, 8, 9a, 9b, 10a, 10b); **¹³C NMR** (100MHz, CDCl₃) δ_C (spectrum 21): 196.71 (C-25), 179.36 (C-16), 143.72 (C-23), 137.60 (C-26), 137.54 (C-22), 132.50 (2C)131.76 (C-29), 131.60 (C-31), 130.06 (C-27), 129.06 (C-24), 128.57 (C-21), 128.29 (1C), 128.14 (C-28, 30), 118.40 (1C), 52.12 (C-1), 47.78 (C-17), 41.68 (C-2, 6, 10), 36.33 (C-4, 7, 9), 29.33 (C-3, 5, 8), 18.92 (C-18); **MS** (ESI-MS) *m/z* (spectrum 22): 444.55 [(M+H)⁺, 100%], 445.73 [(M+H+2)⁺, 30%]; **IR** (ATR, cm⁻¹) V_{max} (spectrum 23): 3011, 2849, 2243, 1654, 1278, 717 cm⁻¹.

3.2.4.11 Synthesis of 3-(4-aza-8-oxo-heptacyclo[0.4.1.0^{2,10}.0^{3,14}.0^{4,9}.0^{12,15}]tetradecyl)-(3-benzoylphenyl)propanoate (10.2)

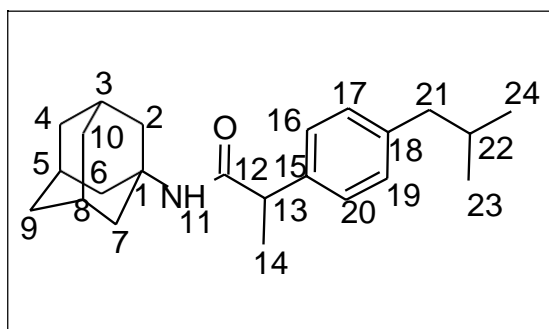
Ketoprofen (0.331 g, 1.30 mmol) was dissolved in 15 ml of THF and 0.238 g of CDI (1.47 mmol) was added to the mixture. The reaction was allowed to run for 9 hours at 60°C. TLC indicated that ketoprofen had been completely converted to its activated form. Compound **10** (0.301 g, 1.30 mmol) dissolved in 6 ml of THF was added drop-wise to the activated solution. The reaction mixture was stirred at room temperature for 72 hours and concentrated *in vacuo*. The mixture was purified using column chromatography (eluent: HEX 1:1 ETOAc followed by 100% ETOAc) to produce the oily product (Yield: 0.165 mg, 0.35 mmol, 27%).



Physical data: C₃₀H₂₉NO₄; **mp:** oil; **TLC** (ETOAc 4:1 ETOH) R_f 0.3; **¹H NMR** (400 MHz, CDCl₃) δ_H (spectrum 24): 7.81-7.376 (m, 3H, H-29, 33, 24), 7.70 (d, 1H, H-22), 7.61-7.54 (m, 2H, H-26, 31), 7.50-7.41 (m, 3H, H-23, 30, 32), 3.80 (m, 1H, H-19), 3.20-2.68 (4 x m, 12H, H-1, 2, 6, 7, 8, 9, 10, 11, 14a, 14b, 16a, 16b), 1.88:2.05 (AB-q, 2H, *J* = 10.56 Hz, H-12a, 12b), 1.55 (d, 3H, H-20a, 20b, 20c), 1.28-1.22 (m, 2H, H-15a, 15b); **¹³C NMR** (100 MHz, CDCl₃) δ_C (spectrum 25): 196.52 (C-27), 178.66 (C-18), 140.31 (C-25), 137.92 (C-21), 137.42 (C-28), 132.60 (C-24), 131.68 (C-31), 130.11 (C-33), 129.33 (C-29), 129.24 (C-26), 128.60 (C-23), 128.33 (C-30, 32) 54.74 (C-6), 45.15 (C-19), 44.67 (1C), 43.81 (1C), 40.51 (1C), 38.76 (1C), 29.71 (1C), 18.21 (C-20); **MS** (ESI-MS) *m/z* (spectrum 26): 458.07 [(M+H)⁺, 100%], 459.28 [(M+H+2)⁺, 30%]; **IR** (ATR, cm⁻¹) V_{max} (spectrum 27): 2975, 1724, 1655, 1202, 701 cm⁻¹.

32412 Synthesis of 2-(4-Isobutylphenyl)-N-(adamantyl)propanamide (5.3)

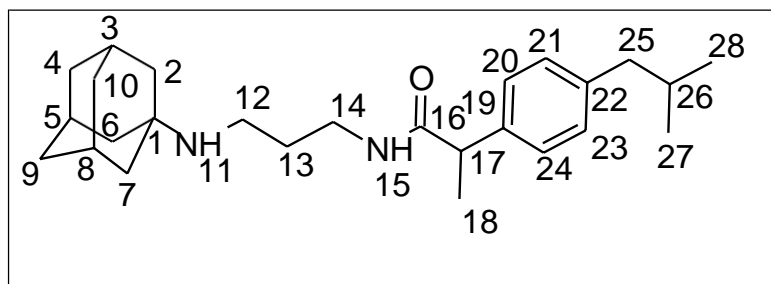
Ibuprofen (0.392 g, 1.90 mmol) was dissolved in 15 ml dry DCM and 0.405 g (2.50 mmol) of CDI was added in molar excess. The reaction mixture was protected from light and stirred at 60°C for 6 hours. Amantadine hydrochloride (0.408 g, 2.17 mmol) and triethylamine (0.660 g, 6.52 mmol) were added to the reaction mixture and the reaction was allowed to proceed at room temperature for 38 hours. Excess solvent was removed under reduced pressure and THF 2:1 ETOAc was added to the product. A white precipitate formed instantaneously and was filtered. TLC of the residue indicated that this was the amantadine free base. Repetition of the precipitation and filtration processes produced a comparatively purer solution of the amide product. Purification of the amide by column chromatography (eluent: HEX 1:19 ETOAc followed by HEX 17:3 ETOAc) produced a white powder (Yield: 0.259 g, 0.76 mmol, 40%).



Physical data: C₂₃H₃₃NO; **mp:** 144-146°C; **TLC** (ETOAc 1:2 ETOH) R_f 0.5; **¹H NMR** (400 MHz, CDCl₃) δ_H (spectrum 28): 7.13-6.98 (m, 4H, H-16, 17, 19, 20), 3.87-3.80 (q, 1H, H-13), 3.38-3.30 (m, 1H, H-22). 2.33-2.40 (m, 2H, H-21a, 21b), 1.977-1.92 (s, 2H, H-2a, 2b), 1.90-1.66 (2 x m, 6H, H-4a, 4b, 6a, 6b, 10a, 10b), 1.58-1.53 (m, 4H, H-7a, 7b, 9a, 9b), 1.40-1.34 (m, 3H, H-14a, 14b, 14c), 1.21 (s, 1H, H-11), 1.124-0.944 (m, 1H, H-8) 0.844-0.780 (m, 6H, H-23a, 23b, 23c, 24a, 24b, 24c); **¹³C NMR** (100 MHz, CDCl₃) δ_C (spectrum 29): 173.3 (C-12), 154.12 (C-15), 140.51 (C-18), 138.88 (C-20), 129.59 (C-16), 127.20 (C-17), 126.90 (C-19), 51.68 (C-1), 49.8 (C-13), 44.99(C-21), 41.46 (C-2, 6, 10), 36.33 (C-4, 7, 9), 32.79 (C-22), 32.51 (C-3, 5, 8), 22.40 (C-14), 22.31 (C-23/24), 21.00 (C-23/24); **MS** (ESI-MS) *m/z* (spectrum 30): 321.11 [(M+H)⁺, 100%], 322.73 [(M+H+2)⁺, 30%]; **IR** (ATR, cm⁻¹) V_{max} (spectrum 31): 3291, 2856, 1699, 1452, 1383, 810 cm⁻¹.

32413 Synthesis of (2S, 2R)-N-[3-(1-adamantylamino)propyl]-2-(4-isobutylphenyl) propanamide (6.3)

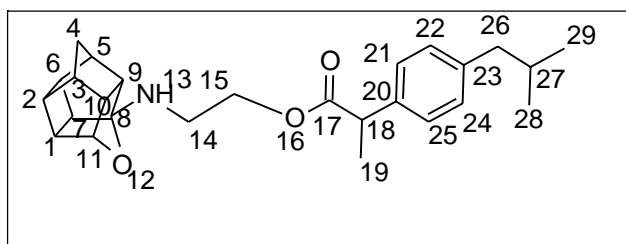
Ibuprofen (0.303 g, 1.47 mmol) was dissolved in 15 ml THF and 0.261 g (1.61 mmol) of CDI was added to the mixture. The reaction was allowed to run for 7 hours at 60°C. TLC indicated that ibuprofen had been completely converted to its activated form. Compound **6** (0.309 g 1.48 mmol) was added slowly to the solution. The reaction mixture was stirred at room temperature for 24 hours and concentrated *in vacuo*. The mixture was purified using column chromatography (eluent: HEX 2:1 ETOAc followed by 100% ETOAc) to obtain the product as a light yellow wax (Yield: 0.154 g, 3.89 mmol, 27%).



Physical data: C₂₆H₄₀N₂O; **mp:** wax; **TLC** (ETOAc 1:1 ETOH) R_f 0.7; **¹H NMR** (400 MHz, CDCl₃) δ_H (spectrum 32): 7.21-7.25 (d, 2H, H-20, 24), 7.10-7.07 (d, 2H, H-21, 23), 2.58 (m, 1H, H-17), 3.93-2.88 (m, 8H, H-2a, 2b, 3, 4a, 4b, 6a, 6b, 8), 2.54-2.49 (m, 7H, H-5, 7a, 7b, 9a, 9b, 10a, 10b), 2.47-1.45 (3 x m, 9H, H-12a, 12b, 13a, 13b, 14a, 14b, 18a, 18b, 18c), 1.27 (bs, 2H, H-11, 15), 0.92-0.88 (d, 7H, H-26, 27, 28); **¹³C NMR** (100MHz, CDCl₃) δ_C (spectrum 33): 179.99 (C-16), 139.99 (C-22), 129.06 (C-19), 127.19 (C-20, 24), 118.9 (C-21, 23), 51.73 (C-1), 47.16 (C-25), 45.00 (C-17), 41.99 (C-2, 6, 10), 36.40 (C-4, 7, 9), 30.13 (C-26), 29.70 (1C), 29.40 (C-3, 5, 8), 22.40 (C-27, 28), 19.18 (1C), 18.71 (C-18); **MS** (ESI-MS) *m/z* (spectrum 34): 413.33 [(M+H)⁺, 100%], 414.34 [(M+H+2)⁺, 30%]; **IR** (ATR, cm⁻¹) V_{max} (spectrum 35): 3307, 2847, 2246, 1615, 1153, 790 cm⁻¹.

3.24.14 ^{2,6,3,10,5,9} Synthesis of 8,11-Oxapentacyclo[5.4.0.0.0]undecane-8-(2-aminoethyl)-(4-isobutylphenyl)-propanoate (8.3)

Ibuprofen (0.283 g, 1.37 mmol) was dissolved in 25 ml of THF and 0.244 g (1.50 mmol) of CDI was added to the mixture. The reaction was allowed to run for 12 hours at 60°C. TLC indicated that ibuprofen had been completely converted to its activated form. Compound **8** (0.300 g, 1.37 mmol) dissolved in 6 ml of THF was added drop-wise to the activated solution. The reaction mixture was stirred at room temperature for 72 hours and concentrated *in vacuo*. The mixture was purified using column chromatography (eluent: 100% ETOAc) to obtain the product as an oil (Yield: 150 mg, 0.37 mmol, 27%).

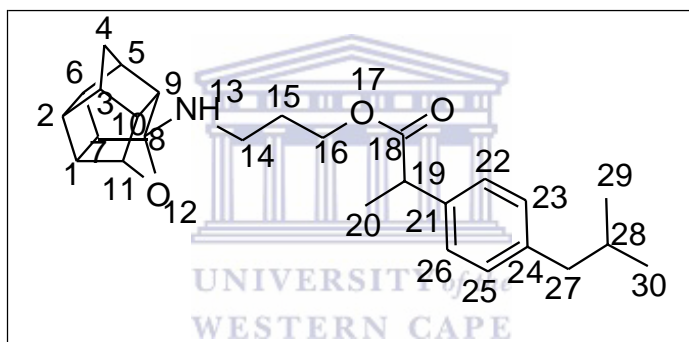


Physical data: C₂₆H₃₃NO₃; **mp:** oil; **TLC** (ETOAc 2:1 ETOH) R_f 0.7; **¹H NMR** (400 MHz, CDCl₃) δ_H (Spectrum 36): 7.3046-7.0475 (m, 4H, H-21, 22, 24, 25), 4.6289 (m, 1H, H-11) 4.1414 (m, 5H, H-14a, 14b, 15a, 15b, 18), 3.618 (2H, H-26a, 26b), 3.5199 (m, 1H, H-27), 3.0603-2.4104 (4 x m 12H, H-1, 2, 3, 5, 6, 7, 9, 10, 13, 19a, 19b, 19c), 1.9293 :1.5702 (AB-q, 2H, *J* = 10.5 Hz, H-4a, 4b), 0.9075 (m, 6H, H-28a, 28b, 28c, 29a, 29b, 29c); **¹³C NMR** (100MHz, CDCl₃) δ_C (spectrum 37): 140.35 (C-23), 139.73 (C-20), 129.09 (C-21, 25), 127.29 (C-22, 24), 82.13 (C-11), 63.26 (C-8), 54.85 (C-16), 54.71 (C-14), 46.46 (C-15), 45.02 (C-26), 44.81 (C-18), 44.53 (C-3), 44.08 (1C), 43.11 (C-4), 41.77 (C-7), 41.60 (C-9),

41.44 (1C), 30.22 (C-27), 22.41 (C-28, 29), 19.11 (C-19); **MS** (ESI-MS) m/z (spectrum 38): 395.75 [(M+H)⁺, 100%], 396.52 [(M+H+2)⁺, 30%]; **IR** (ATR, cm⁻¹) V_{\max} (spectrum 39): 3287, 2960, 1559, 1340, 1067 cm⁻¹.

3.2.4.15 **Synthesis of 8,11-Oxapentacyclo^{2,6 3,10 5,9}[5.4.0 .0 .0]undecane-8-(3-aminopropyl)-(4-isobutylphenyl)-propanoate (9.3)**

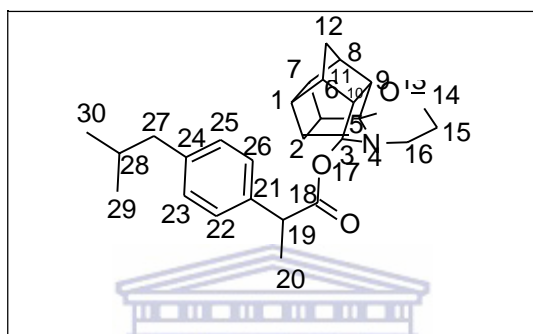
Ibuprofen (0.106 g, 0.51 mmol) was dissolved in 15 ml of THF and 0.0098 g of CDI (0.60 mmol) was added to the mixture. The reaction was allowed to run for 4 hours at 60°C. TLC indicated that ibuprofen had been completely converted to its activated form. Compound **9** (0.118 g, 0.51 mmol) dissolved in 6 ml of THF was added drop-wise to the activated solution. The reaction mixture was stirred at room temperature for 72 hours and concentrated *in vacuo*. The mixture was purified using column chromatography (eluent: HEX 1:4 ETOAc followed by 100% ETOAc) to yield an opaque oil (Yield: 0.060 g, 0.14 mmol, 27%).



Physical data: C₂₇H₃₅NO₃; **mp:** oil; **TLC** (ETOAc 2:1 ETOH) R_f 0.87; **¹H NMR** (400 MHz, CDCl₃) δ_H (spectrum 40): 7.27-7.22 (d, 2H, H-22, 26), 7.15-7.10 (d, 2H, H-23, 25), 3.80-3.47 (m, 2H, H-16a, 16b), 2.45 (d, 2H, H-27a, 27b), 1.95-1.75 (m, 1H, H-28), 1.82:1.52 (AB-q, 2H, $J = 10.56$ Hz, H-4a, 4b) 1.62-1.50 (m, 3H, 20a, 20b, 20c), 1.44-1.23 (2 x m, 8H, H- 1, 2, 3, 5, 6, 7, 9, 10), 0.98-0.84 (m, 9H, H-13, 15a, 15b, 29a, 29b, 29c, 30a, 30b, 30c); **¹³C NMR** (100MHz, CDCl₃) δ_C (spectrum 41): 180.53 (C-18), 140.79 (C-24), 137.06 (C-21), 129.33 (C-22, 26), 127.46 (C-23, 25), 127.19 (1C), 71.99 (C-11), 70.93 (1C), 61.86 (C-15), 45.33 (C-27), 44.53 (C-19), 32.26 (1C), 31.60 (1C), 30.19 (C-28), 29.73 (1C), 29.65 (1C), 29.38 (1C), 22.72 (1C), 22.40 (C-29, 30), 19.28 (1C), 18.12 (C-20), 14.15 (1C), 13.10 (1C); **MS** (ESI-MS) m/z (spectrum 42): 412.55 [(M+H)⁺, 100%], 413.27 [(M+H+2)⁺, 30%]; **IR** (ATR, cm⁻¹) V_{\max} (spectrum 43): 2954, 1724, 1418, 1230, 779 cm⁻¹.

3.2.4.16 Synthesis of 3-(4-aza-8-oxo-heptacyclo-[9.4.1.0^{2,10}.0^{3,14}.0^{4,9}.0^{9,13}.0^{12,15}]tetradecyl)-(4-isobutylphenyl)propanoate (10.3)

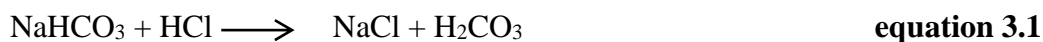
Ibuprofen (0.188 g, 0.91 mmol) was dissolved in 15 ml of THF and 0.154 g of CDI (0.95 mmol) was added to the mixture. The reaction was allowed to run for 5 hours at 60°C. TLC indicated that ibuprofen had been completely converted to its activated form. Compound **10** (0.205 g, 0.89 mmol) dissolved in 6 ml of THF was added drop-wise to the activated solution. The reaction mixture was stirred at room temperature for 72 hours and concentrated *in vacuo*. The mixture was purified using column chromatography (eluent: HEX 4:1 ETOAc) to yield an opaque oil (Yield: 100 mg, 0.24 mmol, 27%).



Physical data: C₂₇H₃₃NO₃; **mp:** oil; **TLC** (ETOAc 1:1 ETOH) R_f 0.7; **¹H NMR** (400 MHz, CDCl₃) δ_H (spectrum 44): 7.26-7.22 (d, 2H, H-22, 26), 7.14-7.10 (d, 2H, H-23, 25), 3.77-3.67 (m, 1H, H-19), 3.11-2.40 (3 x m, 12H, H-1, 2, 6, 7, 8, 9, 10, 11, 14a, 14b, 16a, 16b), 1.80:1.52 (AB-q, 2H, *J* = 10.56 Hz, H-12a, 12b), 2.49-2.45 (d, 2H, H-27a, 27b), 1.93-1.82 (m, 1H, H-28), 1.54-1.50 (d, 3H, H-20), 1.30-1.28 (s, 1H), 0.94-0.90 (d, 8H, H-29a, 29b, 29c, 30a, 30b, 30c, 15a, 15b); **¹³C NMR** (100MHz, CDCl₃) δ_C (spectrum 45): 180.80 (C-18), 140.88 (C-24), 137.07 (C-22, 26), 129.33 (C-23, 25), 127.19 (C-3, 5), 54.73 (1C), 45.05 (C-27), 44.92 (C-19), 44.67 (1C), 43.81 (C-16), 40.51 (C-12), 38.78 (1C), 30.18 (C-28), 29.72 (1C), 22.41 (C-29, 30), 18.13 (C-20); **MS** (ESI-MS) *m/z* (spectrum 46): 410.72 [(M+H)⁺, 100%], 411.56 [(M+H+2)⁺, 30%]; **IR** (ATR, cm⁻¹) V_{max} (spectrum 47): 2954, 1507, 1419, 1230, 779 cm⁻¹.

3.3 Discussion

The commercially available amantadine hydrochloride was converted to amantadine free base by NaHCO₃ with the evolution of CO₂ as indicated by the formation of bubbles in the reaction vessel (**equation 3.2**). The amantadine free base served as the starting material for compounds conjugated with intermediates **5** and **6**.



In the synthesis of compound **6**, LiAlH_4 was employed as the reducing agent due to the presence of weak aluminium-hydrogen bond (Brown, 1951). This increases the efficiency of the reduction reaction as hydrogen is easily released. Brine was used in the extraction process because of the high concentration of electrolytes which will prevent polymerization of the intermediate thereby increasing product yield. Moreover, precipitation of the crude product in diethyl ether afforded the recovery of the pure intermediate.

A major challenge in the synthesis was inadequate activation of the NSAIDs due to the presence of the carboxylic poor leaving functional groups. Several activating agents were employed but they failed to produce the desired activated intermediate.

On reacting the NSAIDs with thionyl chloride and subsequent conjugation with polycyclic scaffolds, TLC plates indicated that the reaction proceeded, however NMR spectroscopy of the product did not produce the desired peaks. This can be attributed to the high reactivity of thionyl chloride and the generation of polycyclic chloride derivatives. Thionyl chloride is also very toxic and difficult to handle (Zuffanti, 1948).

The use of DCC in the presence of a catalytic amount of DMAP produced unwanted by-products that were difficult to separate by column chromatography. The chromatogram produced a minimum of five spots in diverse mobile phases.

Activation with CDI generated the reactive carboxylic acid imidazolide with the production of CO_2 and imidazole which are relatively non-toxic and easily removed (Armstrong, 2007). Four compounds were not successfully synthesised due to the formation of insoluble by-products as a result of cross-linking of excess CDI with the linker. Eleven compounds were successfully synthesised with yields ranging from 15% to 43%. Low yields can be attributed to incomplete activation of the parent NSAIDs resulting in incomplete conjugation. Activation of carboxylic acids requires the presence of heat and the activation complex differs amongst the selected NSAIDs. The average time of activation is 8 hours as observed in the ibuprofen series. The presence of water in the solvents may also account for the ineffective activation of NSAIDs due to the degradation of CDI as indicated by the formation

of bubbles. Using excess CDI may also play a role in the unsuccessful synthesis of these compounds and this should be avoided in future synthesis.

3.4 Conclusion

A series of polycyclic-NSAID conjugates were synthesised by using the pentacycloundecane cage moiety or amantadine scaffolds conjugated to various NSAIDs. Through reductive amination, different linkers were attached to the primary pentacycloundecane structure to obtain various pentacyclamine intermediates. The adamantane conjugate moiety was synthesised *via* a Michael's addition reaction. The polycyclic intermediates were then conjugated with the selected NSAIDs using activation chemistry with CDI. Structural confirmation of the eleven novel compounds was performed by one dimensional NMR spectroscopy and mass spectrometry. Characterisation of the functional groups, particularly the ester and amide moieties were performed using IR spectroscopy.



CHAPTER FOUR

BIOLOGICAL EVALUATION

The hypothesis that the synthesised polycyclic NSAIDs (chapter 3) will retain the activity of the parent NSAIDs while possessing good brain permeability was investigated by three biological assays. In the first two assays, the compounds were evaluated for antioxidant activity. *In vitro* BBB permeability studies of the polycyclic ibuprofen series were also conducted as a proof of concept to demonstrate the effect of side chain attachments on possible brain permeation.

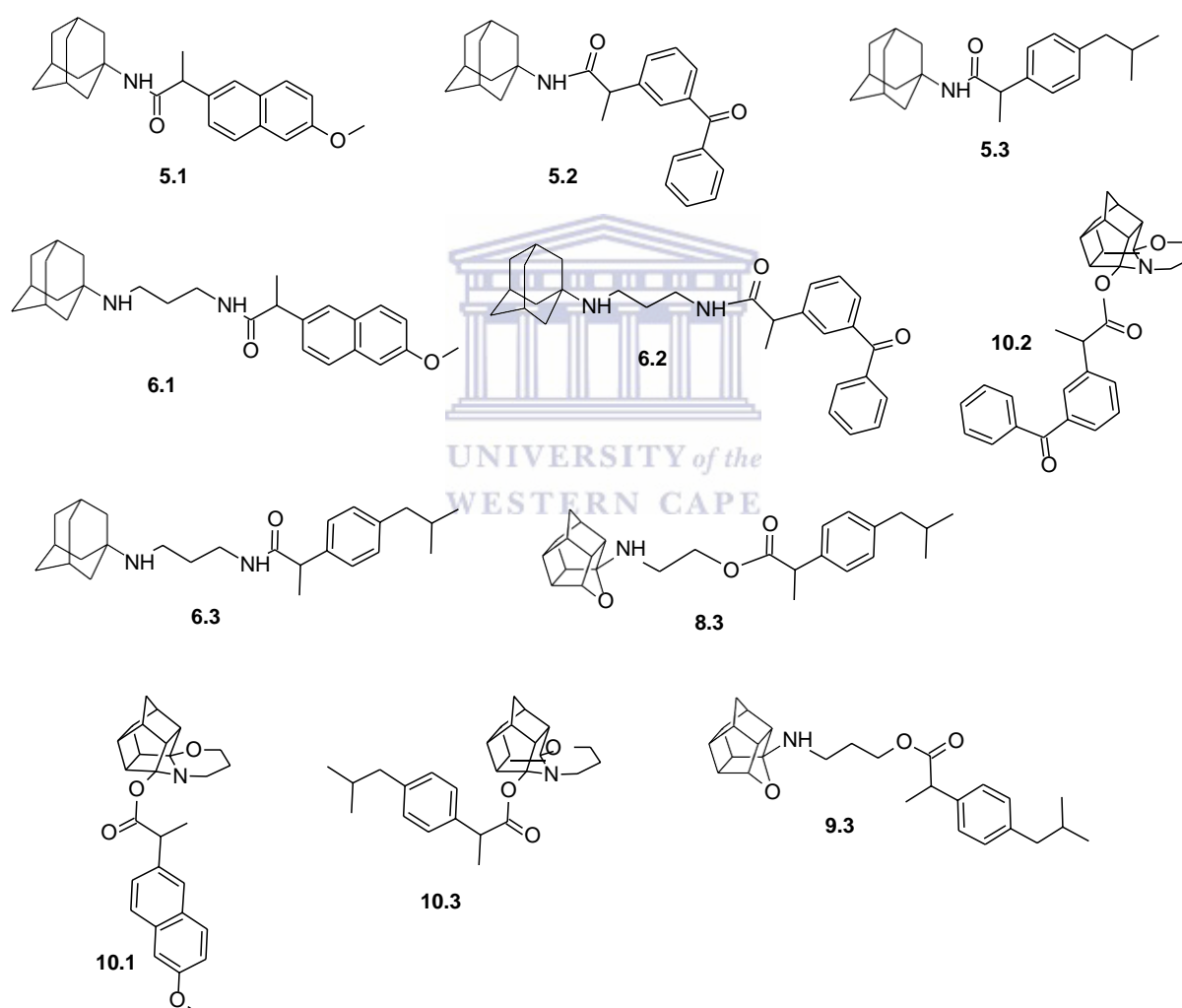


Fig 4.1: Polycyclic-NSAID conjugates evaluated in this study

4.1 Materials and method for the antioxidant assays

Stock solutions of the synthesised compounds (1 ml of a 10 mM solution), parent NSAIDs and trolox were prepared in DMSO. Serial dilutions were subsequently made with DMSO to

obtain concentrations of 1 mM, 0.1 mM and 0.01mM respectively. The assays were done in triplicate using the same procedures for reproducibility of results. The results were analysed by GraphPad Prism 7 and recorded as mean and standard deviation. ANOVA was used to determine the significant difference in mean values ($P < 0.05$).

4.1.1 2,2-Diphenyl-1-picrylhydrazyl (DPPH) assay

The DPPH assay was done according to the method of Brand-Williams group with some modifications (Brand-Williams *et al.*, 1995). A 60 ml DPPH solution (0.041 mM) was prepared with methanol. This solution was further diluted with methanol until an absorbance of 0.7 ± 0.02 units at 515 nm in a 1 cm cuvette using a UV spectrophotometer was obtained. This served as the working solution (Lee *et al.*, 2003).

The test compounds (20 μ l) were added to 180 μ l of the DPPH⁺ solution and incubated for 30 minutes at room temperature. The absorbance reading at 515 nm was measured in a UV multiplate reader. Trolox and DMSO (20 μ l each) were also exposed to the same conditions and served as reference standard and control respectively.

4.1.2 2,2-Azinobis (3-ethyl-benzothiazoline-6-sulfonic acid) (ABTS) assay

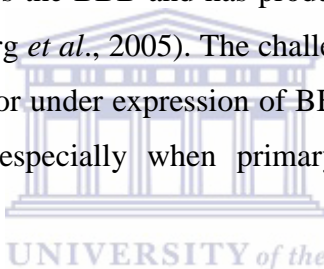
The procedure described by Arnao's group was used with some modifications to determine the ABTS radical scavenging activity of the synthesised compounds (Arnao *et al.*, 2001). ABTS solution (7.4 mM) and 2.6 mM potassium persulfate solution were prepared as stock solutions. The two stock solutions (5 ml each) were mixed together. The mixture was protected from light and stirred for 12 hours at room temperature. The ABTS⁺ solution obtained after 12 hours was observed to be stable for two to three days when stored at 5°C and protected from light. The activated ABTS⁺ solution (1 ml) was diluted with dry methanol to obtain an absorbance of 0.7 ± 0.02 units at 734 nm in a 1 cm cuvette using a UV spectrophotometer.

The test compounds (20 μ l per compound) were added to 180 μ l of the ABTS⁺ and incubated for 30 minutes at room temperature. The absorbance reading at 405 nm was measured in a UV multiplate reader. Trolox and DMSO (20 μ l each) were also exposed to the same conditions and served as standard and control respectively.

4.1.3 Materials and method for BBB permeability assay

Dulbecco's modified Eagle's medium (DMEM) and DMEM/Ham's nutrient mixture F-12 medium (DMEM/F12) and RBE4 rat brain capillary endothelial cells (RBE4) were obtained from the Medical and Biological Sciences (MBS) laboratory of the University of the Western Cape.

The rate of brain uptake at initial concentration expressed as permeability surface area (PS) and extent of brain exposure at static state (brain to blood ratio) are two common methods of assessing brain permeation. PS is not affected by other pharmacokinetic parameters and is therefore a more reliable measure of a drug's BBB permeability in the early stage of drug development (Partridge WM, 2004). An array of methods has been developed for PS measurements (Di et al., 2008). *In vitro* cell based assays provide an accurate and cost effective means of measuring the rate of drug permeation. RBE4 is an immortalized brain endothelial cell line which mimics the BBB and has produced good correlation with *in vivo* BBB permeability studies (Garberg *et al.*, 2005). The challenges in cell based assays includes batch variability, overexpression or under expression of BBB transporters, more porous tight junctions and labour intensity especially when primary cultures have to be prepared (Gumbleton and Audus, 2001).



4.2 *In vitro* blood-brain barrier permeability study

The PAMPA-BBB method which was previously published (Di *et al.*, 2003) was modified and adapted accordingly. The mice endothelial cell line was pre-incubated at 37 °C in 5% CO₂ conditions for 4 days to establish highly reconstructed tight-junctions in the BBB model. The trans-endothelial electrical resistance (TEER) was measured before and after the assay to confirm the integrity of the tight-junctions. The assay was performed using the BBB cell layers with TEER values of approximately 200 Ωcm².

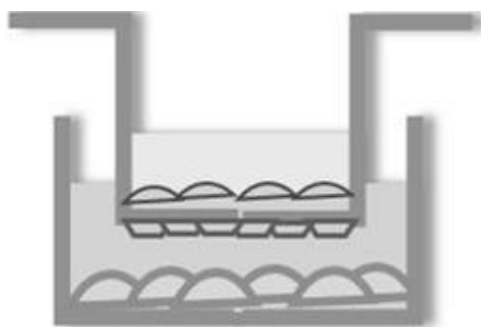


Fig 4.2: Blood-brain barrier model using rat brain endothelial cells

The cells were seeded into 24-well tissue culture inserts (3.0 μm pore size, 0.6×10^6 pores/cm²). Test compounds were dissolved in DMSO at 5 mg/ml as primary stock solution. The stock solutions (20 μl) were diluted with DMSO to make secondary stock solution (final concentration 10 μM). The secondary stock solution (300 μL) and 500 μL of the nutrient medium were added to the donor and acceptor wells respectively. The donor filter plate (apical region) was carefully put on the acceptor plate (basolateral region). The “sandwich” consisted of the aqueous donor well with test compound on the top, artificial blood-brain membrane in the middle, and aqueous acceptor on the bottom (**Fig 4.2**). The test compound diffused from the donor well through the lipid membrane into the acceptor well. The setup was incubated at 37°C for 18 hours (5% CO₂) while the permeation occurred. P_{app} is greatly affected by both the area of the filter membrane used and the time period. In this study, these parameters were carefully considered and 18 hours was considered optimal as prolonged incubation time could compromise the integrity of the BBB model.

The concentration of drug in the acceptor well was determined using a UV plate reader. Samples were analysed in triplicate for statistical viability and the average is reported. Quality control standards using only the nutrient medium in both the donor and acceptor well was also run to monitor the integrity of the membrane.

4.3 Result and discussion

4.3.1 Antioxidant evaluation

In the ABTS assay, ABTS solution undergoes oxidation in the presence of potassium persulphate to form the intensely coloured blue/green ABTS⁺ chromophore. The ability of the test compounds to react with the ABTS radical cation is indicated by the extent of ABTS radical deactivation as indicated by decolourisation of the ABTS⁺ solution (Miller & Rice-Evans, 1996). The absorbance reading is an indication of free radical scavenging activity. High absorbance readings indicate the presence of active ABTS radicals and therefore low free radical scavenging activity and vice-versa. The percentage inhibition of the ABTS radical solution is calculated relative to that of control under the same conditions.

In the DPPH assay, the stable DPPH radical possess an odd electron which can be paired to a free radical scavenging antioxidant or a hydrogen donor to produce the reduced (non radical) form of DPPH. This is indicated by decolourisation of the purple DPPH relative to the amount of electrons being captured.

The results (**Table 4.2** and **Table 4.3**) were expressed as % inhibition of ABTS⁺ or DPPH free radicals and were calculated according to equation 4.1 below (**Fig 4.3** and **Fig 4.4**).

$$\% \text{ inhibition} = \left(\frac{A_c - A_s}{A_c} \right) \times 100\% \quad \left(\text{equation 4.1} \right)$$

Where: A_c = Absorbance value of control

A_s = Absorbance value of test solution

Table 4.1: Result of antioxidant evaluation of test compounds showing level of statistical significance in comparison to trolox (* $p < 0.05$, ** $p < 0.01$, *** $p < 0.001$) and IC₅₀ values of compounds showing more than 50 % scavenging activity.

		P value	R squared	P value summary	95% Confidence Interval for Mean		Mean IC ₅₀ (μM)	LogIC ₅₀
					Lower Bound	Upper Bound		
ABTS	1	0.0084	0.9833	**	0.6494	0.9998		
	5.1	0.0046	0.9908	**	0.7907	0.9999		
	6.1	0.0006	0.9988	***	0.9710	1.0000	149 ± 11.23	-4.827
	10.1	0.0119	0.9764	*	0.5371	0.9998		
	2	0.0075	0.9850	**	0.6795	0.9998		
	5.2	0.0063	0.9875	**	0.7261	0.9999	656 ± 175.61	-4.183
	6.2	0.0014	0.9973	**	0.9340	1.0000	61.1 ± 16.10	-5.214
	10.2	0.0023	0.9954	**	0.8911	1.0000		
	3	0.0039	0.9923	**	0.8215	0.9999		
	5.3	0.0165	0.9672	*	0.4084	0.9997		
	6.3	0.0339	0.9334	*	0.07029	0.9993	180 ± 32.26	-4.744
	8.3	0.0229	0.9548	*	0.2638	0.9995		
	9.3	0.0328	0.9355	*	0.08707	0.9993		
	10.3	0.0031	0.9939	**	0.856	0.9999	846 ± 160.23	-4.073
Trolox	0.0054	0.9893	**	0.7608	0.9999	27.2 ± 6.33	-4.566	
DPPH	1	0.0193	0.9618	*	0.3419	0.9996		
	5.1	0.0010	0.998	**	0.9498	1.0000		
	6.1	0.0042	0.9916	**	0.8086	0.9999		
	10.1	0.0023	0.9953	**	0.8886	1.0000		
	2	0.0003	0.9995	***	0.9864	1.0000	45.5 ± 11.06	-6.342
	5.2	0.0227	0.9552	*	0.2677	0.9995	70.4 ± 12.48	-5.153
	6.2	0.0157	0.9689	*	0.4307	0.9997	718 ± 214.54	-4.144
	10.2	0.0158	0.9687	*	0.4283	0.9997		
	3	0.0144	0.9715	*	0.4655	0.9997		
	5.3	0.0309	0.9391	*	0.1167	0.9994		
	6.3	0.0054	0.9893	**	0.7615	0.9999	700 ± 223.02	-4.155
	8.3	0.0371	0.9272	*	0.02461	0.9993		
	9.3	0.0007	0.9987	***	0.9676	1.0000	467 ± 43.57	-4.331
	10.3	0.0449	0.9123	*	-0.0726	0.9991		
Trolox	0.0464	0.9094	*	-0.8964	0.9991	26.8 ± 8.56	-6.572	

Table 4.2: Absorbance reading of test compounds after incubation with ABTS⁺ solution

Concentration (mM)	reading	Compound														
		1	5.1	6.1	10.1	2	5.2	6.2	10.2	3	5.3	6.3	8.3	9.3	10.3	trolox
1	1	0.607	0.405	0.221	0.393	0.552	0.318	0.121	0.397	0.581	0.401	0.163	0.361	0.484	0.317	0.062
	2	0.603	0.396	0.218	0.386	0.561	0.319	0.111	0.372	0.574	0.397	0.175	0.381	0.466	0.307	0.059
	3	0.612	0.401	0.207	0.397	0.557	0.315	0.117	0.384	0.579	0.388	0.158	0.386	0.479	0.324	0.061
0.1	1	0.603	0.596	0.334	0.411	0.601	0.433	0.286	0.491	0.627	0.507	0.351	0.407	0.557	0.431	0.203
	2	0.606	0.581	0.326	0.409	0.596	0.417	0.272	0.485	0.623	0.517	0.381	0.404	0.565	0.418	0.199
	3	0.602	0.575	0.319	0.406	0.611	0.426	0.289	0.478	0.626	0.511	0.373	0.411	0.563	0.423	0.198
0.01	1	0.639	0.607	0.461	0.501	0.627	0.535	0.457	0.638	0.634	0.597	0.601	0.525	0.601	0.513	0.441
	2	0.641	0.598	0.456	0.529	0.623	0.528	0.471	0.626	0.629	0.578	0.598	0.516	0.614	0.499	0.416
	3	0.638	0.601	0.471	0.511	0.628	0.531	0.459	0.613	0.632	0.566	0.609	0.532	0.611	0.532	0.427
0.001	1	0.642	0.631	0.596	0.595	0.641	0.607	0.601	0.648	0.641	0.635	0.649	0.631	0.627	0.597	0.566
	2	0.639	0.628	0.601	0.601	0.638	0.609	0.597	0.651	0.638	0.638	0.657	0.633	0.617	0.578	0.563
	3	0.641	0.626	0.588	0.598	0.642	0.601	0.611	0.637	0.639	0.637	0.658	0.628	0.625	0.601	0.571

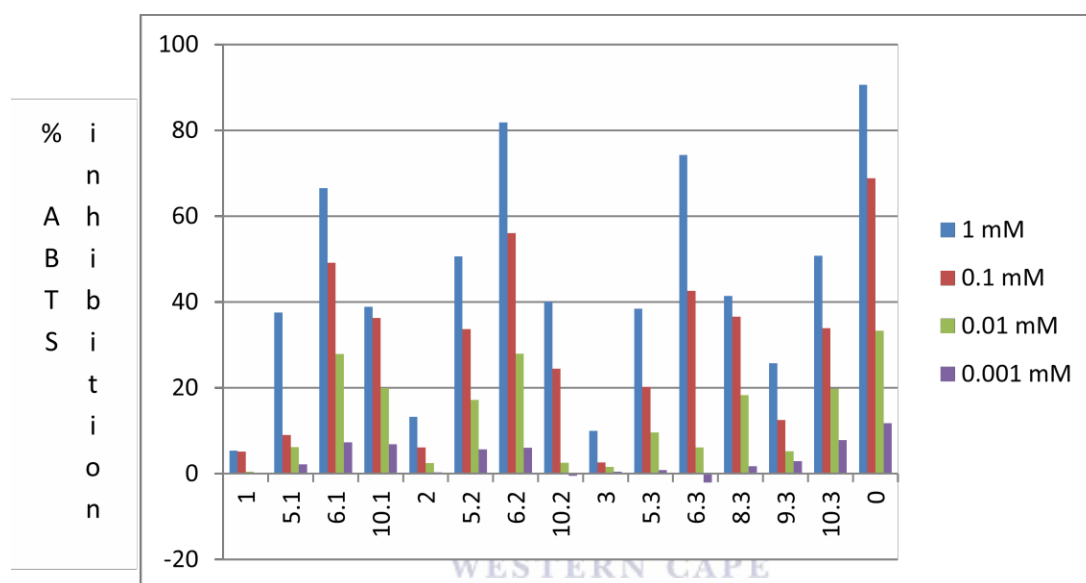


Fig 4.3: ABTS⁺ scavenging assay of parent NSAIDs (1, 2 and 3) and synthesised compounds in comparison to trolox (0) showing average % inhibition recorded at 732 nM

Table 4.3: Absorbance reading of test compounds after incubation with DPPH solution

Concentration (mM)	reading	Compound														
		1	5.1	6.1	10.1	2	5.2	6.2	10.2	3	5.3	6.3	8.3	9.3	10.3	trolox
1	1	1.289	1.1	1.08	1.203	0.195	0.404	0.211	0.806	1.352	1.161	0.667	0.754	0.621	0.701	0.115
	2	1.285	1.11	1.067	1.194	0.214	0.411	0.198	0.797	1.35	1.16	0.691	0.766	0.6	0.687	0.103
	3	1.287	1.112	1.099	1.185	0.186	0.386	0.203	0.799	1.346	1.156	0.677	0.781	0.616	0.675	0.111
0.1	1	1.3	1.205	1.119	1.31	0.306	0.851	0.406	1.314	1.36	1.17	0.916	0.999	0.871	1.006	0.212
	2	1.31	1.196	1.114	1.296	0.298	0.866	0.388	1.299	1.358	1.168	0.899	0.985	0.886	0.985	0.204
	3	1.297	1.177	1.13	1.3	0.312	0.889	0.411	1.306	1.361	1.176	0.897	0.974	0.893	0.977	0.199
0.01	1	1.339	1.303	1.13	1.31	0.697	1.204	0.981	1.363	1.364	1.196	1.105	1.119	1.209	1.279	0.415
	2	1.336	1.287	1.13	1.316	0.701	1.207	0.978	1.365	1.366	1.188	1.096	1.105	1.195	1.271	0.421
	3	1.335	1.262	1.13	1.314	0.687	1.193	0.959	1.366	1.363	1.197	1.077	1.112	1.212	1.289	0.407
0.001	1	1.35	1.36	1.13	1.329	1.011	1.303	1.001	1.37	1.372	1.205	1.117	1.14	1.37	1.282	0.899
	2	1.356	1.357	1.13	1.327	0.997	1.308	0.995	1.374	1.374	1.214	1.104	1.128	1.368	1.299	0.898
	3	1.349	1.356	1.13	1.324	0.999	1.294	0.974	1.372	1.377	1.199	1.112	1.119	1.369	1.309	0.909

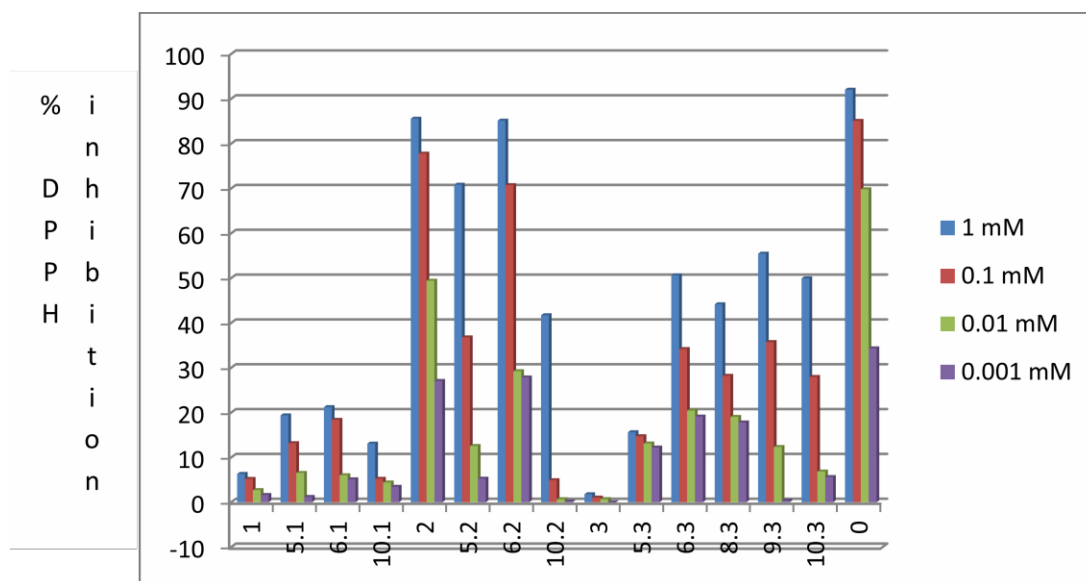


Fig 4.4: DPPH radical scavenging assay of parent NSAIDs (**1**, **2** and **3**) and synthesised compounds in comparison to trolox (**0**) showing % inhibition recorded at 517 nM

The radical scavenging ability of test compounds was evaluated by their ability to react with and deactivate stable $ABTS^+$ and DPPH free radicals. These antioxidant assays are easily reproducible and are accurately used to determine the radical scavenging properties of new drug candidates and food (Brand-Williams *et al.*, 1995). The results for the ABTS and DPPH antioxidant assays are represented in tables 4.1, 4.2 and 4.3 respectively. The activities of the synthesised compounds and parent NSAIDs were compared to that of trolox, which is a known potent antioxidant. The compounds were more reactive to the DPPH free radical than the stable $ABTS^+$ as they displayed a higher DPPH scavenging activity in comparison to the $ABTS^+$. This behaviour has been previously reported as some compounds have been observed to possess DPPH reactivity with no significant $ABTS^+$ scavenging activity. The selective reactivity of compounds for $ABTS^+$ or DPPH radicals have been linked to stereochemical relationships and solubility difference of test compounds in the different systems (Yu *et al.*, 2002).

The result of the post hoc analysis indicates that in the ABTS assay, compounds **6.1**, **5.2**, **6.2**, **6.3**, and **10.3** produced inhibition of more than 50 % of the ABTS free radical at the concentrations tested. In the DPPH assay, compounds **5.2**, **6.2**, **6.3** and **9.3** produced DPPH radical scavenging activity above 50 % between 1000 μ M and 1 μ M concentrations. The IC_{50} values of the active compounds are shown in table 4.3. The conjugation of polycyclic moieties to ketoprofen (**5.2**, **6.2** and **10.2**) slightly reduced the DPPH radical scavenging

activity, although this reduction is not statistically relevant ($p > 0.05$). This conjugation should not be disregarded as the benefit of potential BBB permeation supersedes the reduction in antioxidant effect. The results from the antioxidant study shows that in general the conjugation of the polycyclic moieties to NSAIDs enhanced the antioxidant properties compared to the parent NSAIDs (**Fig 4.3** and **Fig 4.4**). This could be an additional advantage of these compounds by acting as improved radical scavengers that should be able to cross the BBB and have neuroprotective effect before potential enzymatic cleavage of the parent NSAID from the polycyclic moiety.

4.3.2 Permeability Coefficient (Papp)

Permeability coefficient (Papp) is the measure of the amount of a compound passing through a membrane per unit time thereby providing an indication of the rate of transport of compounds across biological membranes (Dehouck *et al.*, 1992). The polycyclic ibuprofen prodrugs were evaluated for *in vitro* BBB permeability as a proof of concept that polycyclic moieties will improve the BBB permeation of therapeutic agents. At the end of the BBB assay, the content of the basolateral region of the BBB model was collected and the absorbance was measured at 274 nm using a UV spectrophotometer. The concentration on the basolateral side was determined from Beer Lambert's law that absorbance is directly proportional to the concentration (**equation 4.2**). Apparent permeability coefficient (Papp) was calculated according to equation 4.3 to evaluate the rate of drug permeation.

$$C_B = A_B \times C_A / A_A \quad \text{equation 4.2}$$

$$P_{app} \text{ (cm/s)} = V_B / A C_A \times \Delta C_B / \Delta t \quad \text{equation 4.3}$$

Where: A_A = absorbance value of apical compartment

A_B = absorbance value in basolateral compartment

Papp = apparent permeability coefficient

V_B = volume in the basolateral compartment

A = Surface area of the filter membrane

C_A = initial concentration in the apical compartment = 10 μM

ΔC = Change in concentration of basolateral compartment over time

Percentage recovery was calculated using equation 4.4 and this value was used to evaluate the BBB permeation of the ibuprofen conjugates relative to the parent ibuprofen (**Table 4.4**).

$$\% \text{ recovery} = \Delta C_B / C_A \times 100\% \quad \text{equation 4.4}$$

The mean P_{app} value for the ibuprofen polycyclic conjugates was $2.8083 \times 10^{-6} \text{ cm s}^{-1}$ representing an average increase in P_{app} by 86.72% across the ibuprofen series. This result correlates with our initial hypothesis that lipophilic moieties will increase the membrane permeation of privileged compounds. Compound **5.3** and **6.3** increased P_{app} by 57.10% and 119.71% respectively. This suggests that increasing the chain length between the amantadine cage and NSAID confers higher permeability on the parent molecule. This can be attributed to the higher lipophilicity and decreased steric interactions conferred by the carbon linker. The effect of chain length can further be studied as increasing it beyond a threshold can result in instability and prevent the lipophilic moiety from serving as a suitable carrier for the NSAIDs.

Table 4.4: % recovery of test compounds from rat endothelial BBB model

Compound	Average absorbance	P value	Apparent permeability coefficient ($\mu\text{cm/s}$)	Concentration (μM)	% recovery
3	0.034 ± 0.004	-	1.504 ± 0.009	3.4446	34.45%
5.3	0.052 ± 0.004	0.0005	2.363 ± 0.032	5.4110	54.11%
6.3	0.121 ± 0.008	0.0075	3.304 ± 0.002	7.5672	75.67%
8.3	0.041 ± 0.001	0.1305	1.749 ± 0.004	4.0058	40.06%
9.3	0.057 ± 0.001	0.0033	3.002 ± 0.001	6.8735	68.74%
10.3	0.078 ± 0.001	0.0002	3.624 ± 0.001	8.2981	82.98%

In the pentacycloundecane series, increasing the number of carbon spacers (compound **9.3**) also produced significant increase in P_{app} by up to 140.93 % as compared to 16.30 % by the 2 carbon spacer analogue, compound **8.3**. This as stated earlier, may be caused by increased lipophilicity and the ability of increased chain length to reduce steric hindrance between the conjugated molecules and thereby fostering interactions with biological membranes. The

rearranged cage structure (compound **10.3**) was observed to be the most promising lipophilic scaffold in the series. Our findings are in accord with those of Prins et al., 2009. The rearrangement of the carbon chain significantly increases the hydrophobicity of the polycyclic scaffold. Interestingly, our findings contradict the same group with respect to the amide series as P_{app} was not reduced by conjugation with amantadine. This is however expected as this study focused on increasing brain permeation and did not account for enzymatic hydrolysis unlike the previous study where the action of amidase enzymes affected the brain permeation of the amide prodrugs.

4.4 Conclusion

The polycyclic NSAID conjugates in this study showed significant antioxidant properties. The results indicate that the compounds have relatively weaker ABTS radical scavenging activity compared to DPPH radical deactivating properties. Antioxidant inhibition as well as BBB permeation of statistical significance ($P < 0.05$) was observed across the series synthesised. In general, the conjugation of the polycyclic moieties to NSAIDs enhanced the antioxidant properties compared to the parent NSAIDs. The BBB assay result suggests that the polycyclic moieties employed in this study can improve the pharmacokinetic profile of NSAIDs and enable BBB penetration as the ibuprofen cage conjugates showed improved permeability compared to the parent NSAID (**3**).

CHAPTER FIVE

SUMMARY AND CONCLUSION

5.1 Introduction

Neurodegenerative disorders (ND) have immense economic consequences on nations as they affect productivity and impede motor and cognitive functions (Gustavsson *et al.*, 2011). The recent surge in the prevalence of ND has prompted the scientific body to extensively investigate the processes that propagate the development of these disorders. A combination of neurotoxic events involving inflammation, protein aggregation, oxidative stress and excitotoxicity promote neuronal damage and loss thereof (Zádori *et al.*, 2012).

Inflammatory response is essential for tissue survival as it protects against infections and injuries. Unregulated inflammatory response can however damage healthy tissues as in the case of neurons in ND (Glass *et al.*, 2010). Agents that modulate inflammatory responses have potential neuroprotective properties as uncontrolled inflammation drives ND progression (Choi *et al.*, 2013).

NSAIDs exert their neuroprotective properties by reducing the biosynthesis of pro-inflammatory prostaglandins *via* the inhibition of cyclooxygenase enzymes (Vlad *et al.*, 2008). NSAIDs however cause gastric irritation at therapeutically relevant doses for ND management. Moreover, the carboxylic group of NSAIDs readily ionises at physiological pH thereby limiting brain permeation and efficacy (Eriksen *et al.*, 2003).

Following the discovery of the neuroprotective effects of the adamantanes, the structural similarities of polycyclic compounds have been extensively investigated. These compounds can be used as scaffolds to improve the pharmacological profile of known therapeutic agents and develop lead compounds for the management of ND (Van der Schyf *et al.*, 2009; Joubert *et al.*, 2011).

Currently, all the therapeutic agents used in ND management only offer palliative relief of symptoms for a short period of time and no effect in halting disease progression (Obeso *et al.*, 2010). Effective delivery of pharmacological agents into the CNS is restricted by the Blood-Brain Barrier (BBB). The design of compounds with favourable physicochemical properties for BBB permeation is of paramount importance in the treatment of diseases of the CNS.

The development of CNS active NSAIDs formed the basis for this study. The study objective was met by synthesising a series of novel polycyclic prodrugs of NSAIDs, which were further evaluated for antioxidant properties and potential BBB permeation. These compounds demonstrated promising potentials as therapeutic agents in ND management. The compounds can be further evaluated for COX inhibitory activities, stability and metabolism profile to improve the knowledge base for effective brain delivery of NSAIDs in neurodegenerative conditions.

5.2 Synthesis

Polycyclic intermediates including amantadine cage (**5-6**) and pentacycloundecane backbones (**8-10**) were successfully synthesised. Synthesis of the diketone cage as described in literature produced a yield of 77% and this served as the foundation for derivatization of various polycyclic amines. Polycyclic intermediates (**8-10**) were synthesised by reductive amination reaction of the ketone groups of the diketone cage with selected amines. A series of polycyclic-NSAID conjugates were synthesised by using the pentacycloundecane cage moiety or amantadine scaffolds conjugated to various NSAIDs *via* reductive amination with different linkers and activation chemistry with CDI. Eleven polycyclic conjugates of NSAIDs (**Fig 5.1**) were synthesised with percentage yields ranging between 16 % and 44 %. The low product yield may be attributed to incomplete activation of parent NSAIDs before conjugation as well as product loss during purification through column chromatography. Structural confirmation was performed by NMR and IR spectroscopy as well as mass spectrometry.

5.3 Biological Evaluation

The polycyclic NSAID conjugates in this study showed significant antioxidant properties. The results indicate that the compounds have relatively weaker ABTS radical scavenging activity compared to DPPH radical deactivating properties. In general the conjugation of the polycyclic moieties to NSAIDs enhanced the antioxidant properties compared to the parent NSAIDs. The BBB assay indicated that the polycyclic moieties employed in this study can improve the pharmacokinetic profile of NSAIDs and enable BBB penetration as the ibuprofen prodrugs showed improved activities compared to the parent NSAID (**3**).

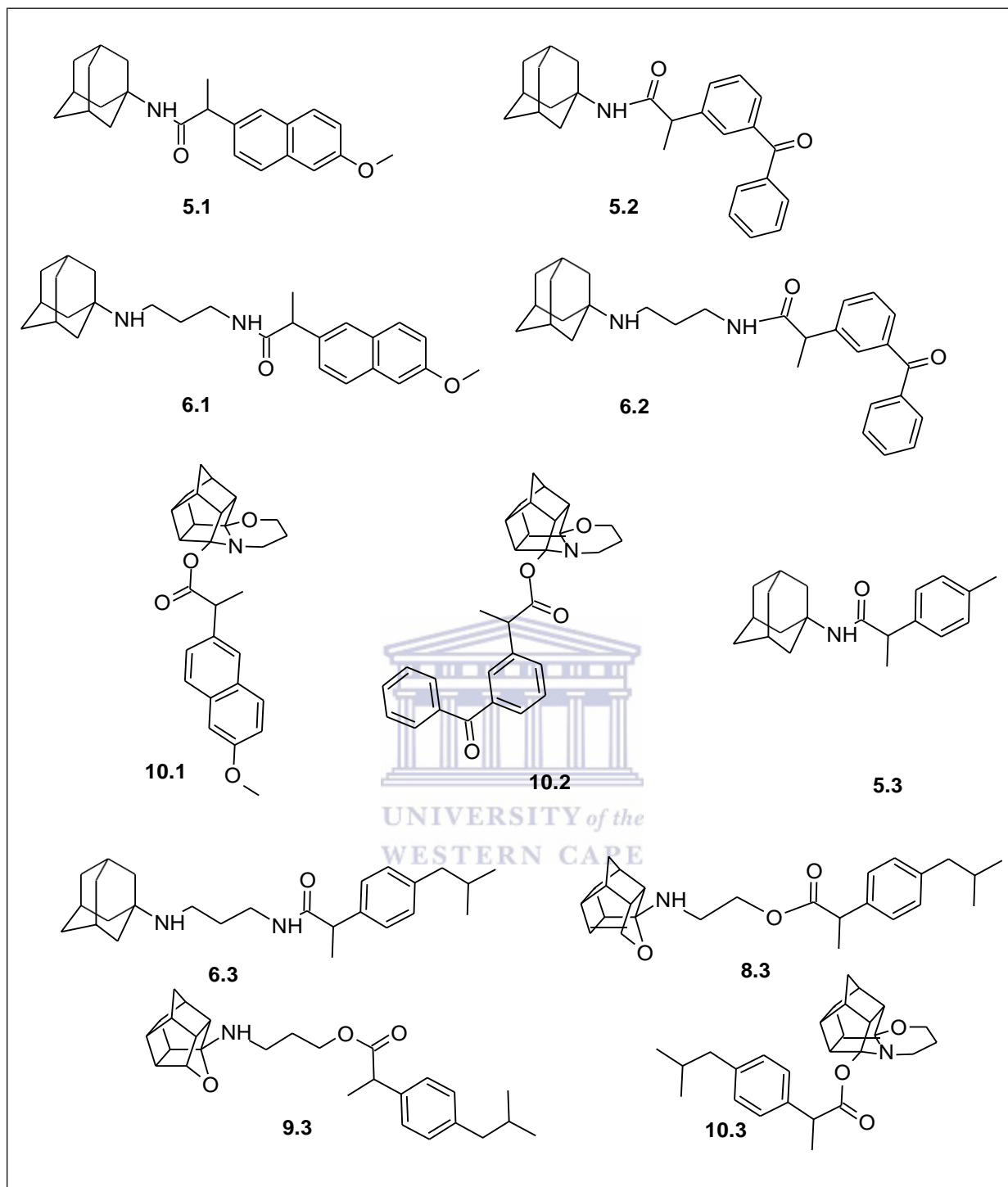


Fig 5.1: Polycyclic NSAIDs synthesised

5.4 Conclusion

A series of polycyclic NSAIDs prodrugs were successfully synthesised and their radical scavenging properties as well as potential BBB properties evaluated. The results show that the compounds synthesised can serve as potential therapeutic agents in halting

neurodegenerative disease progression. It is recommended that a broader series of polycyclic NSAIDs be synthesised encompassing a diverse groups of polycyclic scaffolds and NSAIDs. Other biological assays that can be explored include COX inhibition and ADME studies to further investigate the potential of these NSAID-polycyclic conjugates as therapeutic agents in halting neurodegeneration.



REFERENCES

- Abbott, N.J., Rönnebeck, L. and Hansson, E., 2006. Astrocyte–endothelial interactions at the blood–brain barrier. *Nature reviews neuroscience*, 7(1), pp.41-53.
- Abramov, A.Y. and Duchen, M.R., 2008. Mechanisms underlying the loss of mitochondrial membrane potential in glutamate excitotoxicity. *Biochimica et biophysica acta bioenergetics*, 1777(7), pp.953-964.
- ADAPT Research Group, 2008. Cognitive function over time in the Alzheimer's Disease Anti-inflammatory Prevention Trial (ADAPT): results of a randomized, controlled trial of naproxen and celecoxib. *Archives of neurology*, 65(7), pp.896.
- Adibhatla, R.M. and Hatcher, J.F., 2010. Lipid oxidation and peroxidation in CNS health and disease: from molecular mechanisms to therapeutic opportunities. *Antioxidants and redox signaling*, 12(1), pp.125-169.
- Aggarwal, B.B. and Harikumar, K.B., 2009. Potential therapeutic effects of curcumin, the anti-inflammatory agent, against neurodegenerative, cardiovascular, pulmonary, metabolic, autoimmune and neoplastic diseases. *The international journal of biochemistry and cell biology*, 41(1), pp.40-59.
- Aid, S., Langenbach, R. and Bosetti, F., 2008. Neuroinflammatory response to lipopolysaccharide is exacerbated in mice genetically deficient in cyclooxygenase-2. *Journal of neuroinflammation*, 5(1), pp.17.
- Aid, S., Silva, A.C., Candelario-Jalil, E., Choi, S.H., Rosenberg, G.A. and Bosetti, F., 2010. Cyclooxygenase-1 and-2 differentially modulate lipopolysaccharide-induced blood–brain barrier disruption through matrix metalloproteinase activity. *Journal of cerebral blood flow and metabolism*, 30(2), pp.370-380.
- Alavian, S.M., Ande, S.R., Coombs, K.M., Yeganeh, B., Davoodpour, P., Hashemi, M., Los, M. and Ghavami, S., 2011. Virus-triggered autophagy in viral hepatitis–possible novel strategies for drug development. *Journal of viral hepatitis*, 18(12), pp.821-830.
- Al-Ghananeem, A.M., Traboulsi, A.A., Dittert, L.W. and Hussain, A.A., 2002. Targeted brain delivery of 17 β -estradiol via nasally administered water soluble prodrugs. *American association of pharmaceutical scientists pharmscitech*, 3(1), pp.40-47.
- Allard, E., Passirani, C. and Benoit, J.P., 2009. Convection-enhanced delivery of nanocarriers for the treatment of brain tumors. *Biomaterials*, 30(12), pp.2302-2318.

- Alleyne, T., Mohan, N., Joseph, J. and Adogwa, A., 2011. Unraveling the role of metal ions and low catalytic activity of cytochrome C oxidase in Alzheimer's disease. *Journal of molecular neuroscience*, 43(3), pp.284-289.
- Amor, S., Puentes, F., Baker, D. and Van Der Valk, P., 2010. Inflammation in neurodegenerative diseases. *Immunology*, 129(2), pp.154-169.
- Anglade, P., Vyas, S., Javoy-Agid, F., Herrero, M.T., Michel, P.P., Marquez, J., Mouatt-Prigent, A., Ruberg, M., Hirsch, E.C. and Agid, Y., 1997. Apoptosis and autophagy in nigral neurons of patients with Parkinson's disease. *Histology and histopathology*, 12(1), pp.25-32.
- Arawaka, S., Machiya, Y. and Kato, T., 2010. Heat shock proteins as suppressors of accumulation of toxic prefibrillar intermediates and misfolded proteins in neurodegenerative diseases. *Current pharmaceutical biotechnology*, 11(2), pp.158-166.
- Arnao, M.B., Cano, A. and Acosta, M., 2001. The hydrophilic and lipophilic contribution to total antioxidant activity. *Food chemistry*, 73(2), pp.239-244.
- Arrasate, M., Mitra, S., Schweitzer, E.S., Segal, M.R. and Finkbeiner, S., 2004. Inclusion body formation reduces levels of mutant huntingtin and the risk of neuronal death. *Nature*, 431(7010), pp.805-810.
- Artal-Sanz, M., Samara, C., Syntichaki, P. and Tavernarakis, N., 2006. Lysosomal biogenesis and function is critical for necrotic cell death in *Caenorhabditis elegans*. *Journal of cell biology*, 173(2), pp.231-239.
- Balistreri, C.R., Colonna-Romano, G., Lio, D., Candore, G. and Caruso, C., 2009. TLR4 polymorphisms and ageing: implications for the pathophysiology of age-related diseases. *Journal of clinical immunology*, 29(4), pp.406-415.
- Balzarini, J., Orzeszko, B., Maurin, J.K. and Orzeszko, A., 2007. Synthesis and anti-HIV studies of 2-adamantyl-substituted thiazolidin-4-ones. *European journal of medicinal chemistry*, 42(7), pp.993-1003.
- Begley, D.J., 2004. Delivery of therapeutic agents to the central nervous system: the problems and the possibilities. *Pharmacology and therapeutics*, 104(1), pp.29-45.
- Bhat, V. and Weiner, W.J., 2005. Parkinson's disease. Diagnosis and the initiation of therapy. *Minerva medica*, 96(3), pp.145-154.

- Boado, R.J., Zhang, Y., Zhang, Y. and Pardridge, W.M., 2007. Humanization of anti-human insulin receptor antibody for drug targeting across the human blood–brain barrier. *Biotechnology and bioengineering*, 96(2), pp.381-391.
- Bohn, P., Le Fur, N., Hagues, G., Costentin, J., Torquet, N., Papamicaël, C., Marsais, F. and Levacher, V., 2009. Rational design of central selective acetylcholinesterase inhibitors by means of a “bio-oxidisable prodrug” strategy. *Organic and biomolecular chemistry*, 7(12), pp.2612-2618.
- Bolognesi, B., Kumita, J.R., Barros, T.P., Esbjorner, E.K., Luheshi, L.M., Crowther, D.C., Wilson, M.R., Dobson, C.M., Favrin, G. and Yerbury, J.J., 2010. ANS binding reveals common features of cytotoxic amyloid species. *ACS chemical biology*, 5(8), pp.735-740.
- Bonina, F., Puglia, C., Rimoli, M.G., Melisi, D., Boatto, G., Nieddu, M., Calignano, A., Rana, G.L. and Caprariis, P.D., 2003. Glycosyl derivatives of dopamine and L-dopa as anti-Parkinson prodrugs: synthesis, pharmacological activity and in vitro stability studies. *Journal of drug targeting*, 11(1), pp.25-36.
- Brambilla, R. and Abbracchio, M.P., 2001. Modulation of Cyclooxygenase-2 and Brain Reactive Astrogliosis by Purinergic P2 Receptors. *Annals of the new york academy of sciences*, 939(1), pp.54-62.
- Brand-Williams, W., Cuvelier, M.E. and Berset, C.L.W.T., 1995. Use of a free radical method to evaluate antioxidant activity. *Lebensmittel-wissenschaft and technologie- Food science and Technology*, 28(1), pp.25-30.
- Brasnjevic, I., Steinbusch, H.W., Schmitz, C., Martinez-Martinez, P. and European NanoBioPharmaceutics Research Initiative, 2009. Delivery of peptide and protein drugs over the blood–brain barrier. *Progress in neurobiology*, 87(4), pp.212-251.
- Brown, W.G., 1951. Reductions by lithium aluminum hydride. *Organic reactions*. pp.469.
- Bruijn, L.I., Houseweart, M.K., Kato, S., Anderson, K.L., Anderson, S.D., Ohama, E., Reaume, A.G., Scott, R.W. and Cleveland, D.W., 1998. Aggregation and motor neuron toxicity of an ALS-linked SOD1 mutant independent from wild-type SOD1. *Science*, 281(5384), pp.1851-1854.
- Brundin, P., Melki, R. and Kopito, R., 2010. Prion-like transmission of protein aggregates in neurodegenerative diseases. *Nature reviews molecular and cell biology*, 11(4), pp.301-307.

REFERENCE

- Bucciantini, M., Giannoni, E., Chiti, F., Baroni, F., Formigli, L., Zurdo, J., Taddei, N., Ramponi, G., Dobson, C.M. and Stefani, M., 2002. Inherent toxicity of aggregates implies a common mechanism for protein misfolding diseases. *Nature*, 416(6880), pp.507-511.
- Bunch, L., Erichsen, M.N. and Jensen, A.A., 2009. Excitatory amino acid transporters as potential drug targets. *Expert opinion on therapeutic targets*, 13(6), pp.719-731.
- Candé, C., Cecconi, F., Dessen, P. and Kroemer, G., 2002. Apoptosis-inducing factor (AIF): key to the conserved caspase-independent pathways of cell death?. *Journal of cell science*, 115(24), pp.4727-4734.
- Candore, G., Balistreri, C.R., Grimaldi, M.P., Listì, F., Vasto, S., Chiappelli, M., Licastro, F., Colonna-Romano, G., Lio, D. and Caruso, C., 2007. Polymorphisms of pro-inflammatory genes and Alzheimer's disease risk: a pharmacogenomic approach. *Mechanisms of ageing and development*, 128(1), pp.67-75.
- Capsoni, S., Covaceuszach, S., Ugolini, G., Spirito, F., Vignone, D., Stefanini, B., Amato, G. and Cattaneo, A., 2009. Delivery of NGF to the brain: intranasal versus ocular administration in anti-NGF transgenic mice. *Journal of alzheimer's disease*, 16(2), pp.371-388.
- Caraci, F., Battaglia, G., Sortino, M.A., Spampinato, S., Molinaro, G., Copani, A., Nicoletti, F. and Bruno, V., 2012. Metabotropic glutamate receptors in neurodegeneration/neuroprotection: still a hot topic?. *Neurochemistry international*, 61(4), pp.559-565.
- Castillo-Trivino, T., Braithwaite, D., Bacchetti, P. and Waubant, E., 2013. Rituximab in relapsing and progressive forms of multiple sclerosis: a systematic review. *Public library of science one*, 8(7), pp.e66308.
- Cataldo, A.M., Hamilton, D.J., Barnett, J.L., Paskevich, P.A. and Nixon, R.A., 1996. Properties of the endosomal-lysosomal system in the human central nervous system: disturbances mark most neurons in populations at risk to degenerate in Alzheimer's disease. *Journal of neuroscience*, 16(1), pp.186-199.
- Catterall, W.A., Striessnig, J., Snutch, T.P. and Perez-Reyes, E., 2003. International Union of Pharmacology. XL. Compendium of voltage-gated ion channels: calcium channels. *Pharmacological reviews*, 55(4), pp.579-581.

- Cavalli, A., Bolognesi, M.L., Minarini, A., Rosini, M., Tumiatti, V., Recanatini, M. and Melchiorre, C., 2008. Multi-target-directed ligands to combat neurodegenerative diseases. *Journal of medicinal chemistry*, 51(3), pp.347-372.
- Celia, C., Cosco, D., Paolino, D. and Fresta, M., 2011. Nanoparticulate devices for brain drug delivery. *Medicinal research reviews*, 31(5), pp.716-756.
- Chan, C.S., Guzman, J.N., Ilijic, E., Mercer, J.N., Rick, C., Tkatch, T., Meredith, G.E. and Surmeier, D.J., 2007. 'Rejuvenation' protects neurons in mouse models of Parkinson's disease. *Nature*, 447(7148), pp.1081-1086.
- Chang, C.C., Cao, S., Kang, S., Kai, L., Tian, X., Pandey, P., Dunne, S.F., Luan, C.H., Surmeier, D.J. and Silverman, R.B., 2010. Antagonism of 4-substituted 1, 4-dihydropyridine-3, 5-dicarboxylates toward voltage-dependent L-type Ca²⁺ channels Ca_v1.3 and Ca_v1.2. *Bioorganic and medicinal chemistry*, 18(9), pp.3147-3158.
- Chen, H., Yoshioka, H., Kim, G.S., Jung, J.E., Okami, N., Sakata, H., Maier, C.M., Narasimhan, P., Goeders, C.E. and Chan, P.H., 2011. Oxidative stress in ischemic brain damage: mechanisms of cell death and potential molecular targets for neuroprotection. *Antioxidants & redox signaling*, 14(8), pp.1505-1517.
- Chen, H.S.V. and Lipton, S.A., 2006. The chemical biology of clinically tolerated NMDA receptor antagonists. *Journal of neurochemistry*, 97(6), pp.1611-1626.
- Choi, S.H., Aid, S. and Bosetti, F., 2009. The distinct roles of cyclooxygenase-1 and-2 in neuroinflammation: implications for translational research. *Trends in pharmacological sciences*, 30(4), pp.174-181.
- Choi, S.H., Aid, S., Caracciolo, L., Sakura Minami, S., Niikura, T., Matsuoka, Y., Turner, R.S., Mattson, M.P. and Bosetti, F., 2013. Cyclooxygenase-1 inhibition reduces amyloid pathology and improves memory deficits in a mouse model of Alzheimer's disease. *Journal of neurochemistry*, 124(1), pp.59-68.
- Chung, K.K. and David, K.K., 2010. Emerging roles of nitric oxide in neurodegeneration. *Nitric Oxide*, 22(4), pp.290-295.
- Chung, K.K., Thomas, B., Li, X., Pletnikova, O., Troncoso, J.C., Marsh, L., Dawson, V.L. and Dawson, T.M., 2004. S-nitrosylation of parkin regulates ubiquitination and compromises parkin's protective function. *Science*, 304(5675), pp.1328-1331.

- Collins, L.M., Toulouse, A., Connor, T.J. and Nolan, Y.M., 2012. Contributions of central and systemic inflammation to the pathophysiology of Parkinson's disease. *Neuropharmacology*, 62(7), pp.2154-2168.
- Cookson, R.C., Crundwell, E., Hill, R.R. and Hudec, J., 1964. 586. Photochemical cyclisation of diels–alder adducts. *Journal of the chemical society (resumed)*, pp.3062-3075.
- Cowan, W.M. and Kandel, E.R., 2001. Prospects for neurology and psychiatry. *Journal of the american medical association*, 285(5), pp.594-600.
- Crossman, A.R., Peggs, D., Boyce, S., Luquin, M.R. and Sambrook, M.A., 1989. Effect of the NMDA antagonist MK-801 on MPTP-induced parkinsonism in the monkey. *Neuropharmacology*, 28(11), pp.1271-1273.
- Czirr, E. and Wyss-Coray, T., 2012. The immunology of neurodegeneration. *The Journal of clinical investigation*, 122(4), pp.1156-1163.
- Dahan, A., Zimmermann, E.M. and Ben-Shabat, S., 2014. Modern prodrug design for targeted oral drug delivery. *Molecules*, 19(10), pp.16489-16505.
- Damiano, M., Galvan, L., Déglon, N. and Brouillet, E., 2010. Mitochondria in Huntington's disease. *Biochimica et Biophysica acta molecular basis of disease*, 1802(1), pp.52-61.
- de Calignon, A., Polydoro, M., Suárez-Calvet, M., William, C., Adamowicz, D.H., Kopeikina, K.J., Pitstick, R., Sahara, N., Ashe, K.H., Carlson, G.A. and Spire-Jones, T.L., 2012. Propagation of tau pathology in a model of early Alzheimer's disease. *Neuron*, 73(4), pp.685-697.
- De Vos, K.J., Chapman, A.L., Tennant, M.E., Manser, C., Tudor, E.L., Lau, K.F., Brownlee, J., Ackerley, S., Shaw, P.J., McLoughlin, D.M. and Shaw, C.E., 2007. Familial amyotrophic lateral sclerosis-linked SOD1 mutants perturb fast axonal transport to reduce axonal mitochondria content. *Human molecular genetics*, 16(22), pp.2720-2728.
- Deguchi, Y., Hayashi, H., Fujii, S., Naito, T., Yokoyama, Y., Yamada, S. and Kimura, R., 2000. Improved brain delivery of a nonsteroidal anti-inflammatory drug with a synthetic glyceride ester: a preliminary attempt at a CNS drug delivery system for the therapy of Alzheimer's disease. *Journal of drug targeting*, 8(6), pp.371-381.
- Dehouck, M.P., Jolliet-Riant, P., Brée, F., Fruchart, J.C., Cecchelli, R. and Tillement, J.P., 1992. Drug Transfer Across the Blood-Brain Barrier: Correlation Between In Vitro and In Vivo Models. *Journal of neurochemistry*, 58(5), pp.1790-1797.

- Deli, M.A., 2009. Potential use of tight junction modulators to reversibly open membranous barriers and improve drug delivery. *Biochimica et Biophysica acta biomembranes*, 1788(4), pp.892-910.
- Demeule, M., Currie, J.C., Bertrand, Y., Che, C., Nguyen, T., Regina, A., Gabathuler, R., Castaigne, J.P. and Beliveau, R., 2008. Involvement of the low-density lipoprotein receptor-related protein in the transcytosis of the brain delivery vector Angiopep-2. *Journal of neurochemistry*, 106(4), pp.1534-1544.
- Denora, N., Trapani, A., Laquintana, V., Lopedota, A. and Trapani, G., 2009. Recent advances in medicinal chemistry and pharmaceutical technology-strategies for drug delivery to the brain. *Current topics in medicinal chemistry*, 9(2), pp.182-196.
- Denton, R.M., 2009. Regulation of mitochondrial dehydrogenases by calcium ions. *Biochimica Et biophysica acta bioenergetics*, 1787(11), pp.1309-1316.
- Di Giorgio, F.P., Boulting, G.L., Bobrowicz, S. and Eggan, K.C., 2008. Human embryonic stem cell-derived motor neurons are sensitive to the toxic effect of glial cells carrying an ALS-causing mutation. *Cell stem cell*, 3(6), pp.637-648.
- Di, L., Kerns, E.H. and Carter, G.T., 2008. Strategies to assess blood–brain barrier penetration. *Expert opinion on drug discovery*, 3(6), pp.677-687.
- Di, L., Kerns, E.H., Fan, K., McConnell, O.J. and Carter, G.T., 2003. High throughput artificial membrane permeability assay for blood–brain barrier. *European journal of medicinal chemistry*, 38(3), pp.223-232.
- Dikic, I., Wakatsuki, S. and Walters, K.J., 2009. Ubiquitin-binding domains—from structures to functions. *Nature reviews molecular cell biology*, 10(10), pp.659-671.
- Doens, D. and Fernández, P.L., 2014. Microglia receptors and their implications in the response to amyloid β for Alzheimer's disease pathogenesis. *Journal of neuroinflammation*, 11(1), pp.48.
- Drouin-Ouellet, J. and Cicchetti, F., 2012. Inflammation and neurodegeneration: the story 'retolled'. *Trends in pharmacological sciences*, 33(10), pp.542-551.
- Dvir, E., Elman, A., Simmons, D., Shapiro, I., Duvdevani, R., Dahan, A., Hoffman, A. and Friedman, J.E., 2007. DP-155, a Lecithin Derivative of Indomethacin, is a Novel Nonsteroidal Antiinflammatory Drug for Analgesia and Alzheimer's Disease Therapy. *Central nervous system drug reviews*, 13(2), pp.260-277.

- El-Emam, A.A., Al-Deeb, O.A., Al-Omar, M. and Lehmann, J., 2004. Synthesis, antimicrobial, and anti-HIV-1 activity of certain 5-(1-adamantyl)-2-substituted thio-1, 3, 4-oxadiazoles and 5-(1-adamantyl)-3-substituted aminomethyl-1, 3, 4-oxadiazoline-2-thiones. *Bioorganic and medicinal chemistry*, 12(19), pp.5107-5113.
- Ertl, P., Rohde, B. and Selzer, P., 2000. Fast calculation of molecular polar surface area as a sum of fragment-based contributions and its application to the prediction of drug transport properties. *Journal of medicinal chemistry*, 43(20), pp.3714-3717.
- Fairman, W.A. and Amara, S.G., 1999. Functional diversity of excitatory amino acid transporters: ion channel and transport modes. *American journal of physiology-renal physiology*, 277(4), pp.F481-F486.
- Farooqui, T. and Farooqui, A.A., 2009. Aging: an important factor for the pathogenesis of neurodegenerative diseases. *Mechanisms of ageing and development*, 130(4), pp.203-215.
- Firdaus, W.J., Wytenbach, A., Giuliano, P., Kretz-Remy, C., Currie, R.W. and Arrigo, A.P., 2006. Huntingtin inclusion bodies are iron-dependent centers of oxidative events. *The federation of european biochemical societies journal*, 273(23), pp.5428-5441.
- Foged, C. and Nielsen, H.M., 2008. Cell-penetrating peptides for drug delivery across membrane barriers. *Expert opinion on drug delivery*, 5(1), pp.105-117.
- Forman, M.S., Trojanowski, J.Q. and Lee, V.M., 2004. Neurodegenerative diseases: a decade of discoveries paves the way for therapeutic breakthroughs. *Nature medicine*, 10(10), pp.1055-1063.
- Fratiglioni, L. and Qiu, C., 2009. Prevention of common neurodegenerative disorders in the elderly. *Experimental gerontology*, 44(1), pp.46-50.
- Fridovich, I., 1997. Superoxide anion radical (O_2^-), superoxide dismutases, and related matters. *Journal of biological chemistry*, 272(30), pp.18515-18517.
- Frost, B. and Diamond, M.I., 2010. Prion-like mechanisms in neurodegenerative diseases. *Nature reviews neuroscience*, 11(3), pp.155-159.
- Fuchs, Y. and Steller, H., 2011. Programmed cell death in animal development and disease. *Cell*, 147(4), pp.742-758.
- Gabathuler, R., 2010. Approaches to transport therapeutic drugs across the blood-brain barrier to treat brain diseases. *Neurobiology of disease*, 37(1), pp.48-57.

- Garavito, R.M. and Mulichak, A.M., 2003. The structure of mammalian cyclooxygenases. *Annual review of biophysics and biomolecular structure*, 32(1), pp.183-206.
- Garberg, P., Ball, M., Borg, N., Cecchelli, R., Fenart, L., Hurst, R.D., Lindmark, T., Mabondzo, A., Nilsson, J.E., Raub, T.J. and Stanimirovic, D., 2005. In vitro models for the blood–brain barrier. *Toxicology in vitro*, 19(3), pp.299-334.
- García-Bueno, B., Serrats, J. and Sawchenko, P.E., 2009. Cerebrovascular cyclooxygenase-1 expression, regulation, and role in hypothalamic-pituitary-adrenal axis activation by inflammatory stimuli. *Journal of neuroscience*, 29(41), pp.12970-12981.
- Garcia-Garcia, A., Zavala-Flores, L., Rodriguez-Rocha, H. and Franco, R., 2012. Thiol-redox signaling, dopaminergic cell death, and Parkinson's disease. *Antioxidants and redox signaling*, 17(12), pp.1764-1784.
- Garthwaite, J., Charles, S.L. and Chess-Williams, R., 1988. Endothelium-derived relaxing factor release on activation of NMDA receptors suggests role as intercellular messenger in the brain. *Nature*, 336(6197), pp.385-388.
- Geldenhuys, W.J., Youdim, M.B., Carroll, R.T. and Van der Schyf, C.J., 2011. The emergence of designed multiple ligands for neurodegenerative disorders. *Progress in neurobiology*, 94(4), pp.347-359.
- Genka, S., Deutsch, J., Shetty, U.H., Stahle, P.L., John, V., Lieberburg, I.M., Ali-Osmant, F., Rapoport, S.I. and Greig, N.H., 1993. Development of lipophilic anticancer agents for the treatment of brain tumors by the esterification of water-soluble chlorambucil. *Clinical and experimental metastasis*, 11(2), pp.131-140.
- Ghavami, S., Kerkhoff, C., Chazin, W.J., Kadkhoda, K., Xiao, W., Zuse, A., Hashemi, M., Eshraghi, M., Schulze-Osthoff, K., Klonisch, T. and Los, M., 2008. S100A8/9 induces cell death via a novel, RAGE-independent pathway that involves selective release of Smac/DIABLO and Omi/HtrA2. *Biochimica et biophysica acta molecular cell research*, 1783(2), pp.297-311.
- Ghose, A.K., Viswanadhan, V.N. and Wendoloski, J.J., 1999. A knowledge-based approach in designing combinatorial or medicinal chemistry libraries for drug discovery. 1. A qualitative and quantitative characterization of known drug databases. *Journal of combinatorial chemistry*, 1(1), pp.55-68.

- Giasson, B.I., Duda, J.E., Murray, I.V., Chen, Q., Souza, J.M., Hurtig, H.I., Ischiropoulos, H., Trojanowski, J.Q. and Lee, V.M.Y., 2000. Oxidative damage linked to neurodegeneration by selective α -synuclein nitration in synucleinopathy lesions. *Science*, 290(5493), pp.985-989.
- Gilgun-Sherki, Y., Melamed, E. and Offen, D., 2006. Anti-inflammatory drugs in the treatment of neurodegenerative diseases: current state. *Current pharmaceutical design*, 12(27), pp.3509-3519.
- Glass, C.K., Saijo, K., Winner, B., Marchetto, M.C. and Gage, F.H., 2010. Mechanisms underlying inflammation in neurodegeneration. *Cell*, 140(6), pp.918-934.
- Gleichmann, M. and Mattson, M.P., 2010. Alzheimer's disease and neuronal network activity. *Neuromolecular medicine*, 12(1), pp.44-47.
- Glick, D., Barth, S. and Macleod, K.F., 2010. Autophagy: cellular and molecular mechanisms. *The Journal of pathology*, 221(1), pp.3-12.
- Goetz, G.H., Farrell, W., Shalaeva, M., Sciabola, S., Anderson, D., Yan, J., Philippe, L. and Shapiro, M.J., 2014. High throughput method for the indirect detection of intramolecular hydrogen bonding. *Journal of medicinal chemistry*, 57(7), pp.2920-2929.
- Golde, T.E. and Miller, V.M., 2009. Proteinopathy-induced neuronal senescence: a hypothesis for brain failure in Alzheimer's and other neurodegenerative diseases. *Alzheimers research and therapy*, 1(2), pp.5.
- Gourand, F., Mercey, G., Ibazizène, M., Tirel, O., Henry, J., Levacher, V., Perrio, C. and Barré, L., 2010. Chemical delivery system of metaiodobenzylguanidine (MIBG) to the central nervous system. *Journal of medicinal chemistry*, 53(3), pp.1281-1287.
- Green, D.R. and Reed, J.C., 1998. Mitochondria and apoptosis. *Science- american association for the advancement of science-Weekly Paper Edition*, 281(5381), pp.1309-1311.
- Grobler, E., Grobler, A., Van der Schyf, C.J. and Malan, S.F., 2006. Effect of polycyclic cage amines on the transmembrane potential of neuronal cells. *Bioorganic and medicinal chemistry*, 14(4), pp.1176-1181.
- Grosskreutz, J., Van Den Bosch, L. and Keller, B.U., 2010. Calcium dysregulation in amyotrophic lateral sclerosis. *Cell calcium*, 47(2), pp.165-174.

- Gumbleton, M. and Audus, K.L., 2001. Progress and limitations in the use of in vitro cell cultures to serve as a permeability screen for the blood-brain barrier. *Journal of pharmaceutical sciences*, 90(11), pp.1681-1698.
- Gustavsson, A., Svensson, M., Jacobi, F., Allgulander, C., Alonso, J., Beghi, E., Dodel, R., Ekman, M., Faravelli, C., Fratiglioni, L. and Gannon, B., 2011. Cost of disorders of the brain in Europe 2010. *European journal of neuropsychopharmacology*, 21(10), pp.718-779.
- Gynther, M., Laine, K., Ropponen, J., Leppänen, J., Mannila, A., Nevalainen, T., Savolainen, J., Järvinen, T. and Rautio, J., 2008. Large neutral amino acid transporter enables brain drug delivery via prodrugs. *Journal of medicinal chemistry*, 51(4), pp.932-936.
- Habgood, M.D., Begley, D.J. and Abbott, N.J., 2000. Determinants of passive drug entry into the central nervous system. *Cellular and molecular neurobiology*, 20(2), pp.231-253.
- Habibi, E., Masoudi-Nejad, A., Abdolmaleky, H.M. and Haggarty, S.J., 2011. Emerging roles of epigenetic mechanisms in Parkinson's disease. *Functional and integrative genomics*, 11(4), pp.523-537.
- Hammarlund-Udenaes, M., Fridén, M., Syvänen, S. and Gupta, A., 2008. On the rate and extent of drug delivery to the brain. *Pharmaceutical research*, 25(8), pp.1737-1750.
- Hanisch, U.K., Johnson, T.V. and Kipnis, J., 2008. Toll-like receptors: roles in neuroprotection?. *Trends in neurosciences*, 31(4), pp.176-182.
- Harikishore, A., Leow, M.L., Niang, M., Rajan, S., Pasunooti, K.K., Preiser, P.R., Liu, X. and Yoon, H.S., 2013. Adamantyl derivative as a potent inhibitor of Plasmodium FK506 binding protein 35. *American chemical society medicinal chemistry letters*, 4(11), pp.1097-1101.
- Hartl, F.U., Bracher, A. and Hayer-Hartl, M., 2011. Molecular chaperones in protein folding and proteostasis. *Nature*, 475(7356), pp.324-332.
- Häusser, M., 2000. The Hodgkin-Huxley theory of the action potential. *Nature neuroscience*, 3, pp.1165-1165.
- Helton, T.D., Xu, W. and Lipscombe, D., 2005. Neuronal L-type calcium channels open quickly and are inhibited slowly. *Journal of neuroscience*, 25(44), pp.10247-10251.
- Herrero-Mendez, A., Almeida, A., Fernández, E., Maestre, C., Moncada, S. and Bolaños, J.P., 2009. The bioenergetic and antioxidant status of neurons is controlled by continuous

- degradation of a key glycolytic enzyme by APC/C–Cdh1. *Nature cell biology*, 11(6), pp.747-752.
- Hervé, F., Ghinea, N. and Scherrmann, J.M., 2008. CNS delivery via adsorptive transcytosis. *The American association of pharmaceutical scientists journal*, 10(3), pp.455-472.
- Hitchcock, S.A., 2012. Structural modifications that alter the P-glycoprotein efflux properties of compounds. *Journal of medicinal chemistry*, 55(11), pp.4877-4895.
- Ilies, M.A., Masereel, B., Rolin, S., Scozzafava, A., Câmpeanu, G., Câmpeanu, V. and Supuran, C.T., 2004. Carbonic anhydrase inhibitors: aromatic and heterocyclic sulfonamides incorporating adamantyl moieties with strong anticonvulsant activity. *Bioorganic and medicinal chemistry*, 12(10), pp.2717-2726.
- Ivanoiu, A., Adam, S., Van der Linden, M., Salmon, E., Juillerat, A.C., Mulligan, R. and Seron, X., 2005. Memory evaluation with a new cued recall test in patients with mild cognitive impairment and Alzheimer's disease. *Journal of neurology*, 252(1), pp.47-55.
- Jain, K.K., 2010. An Overview of Drug Delivery to the CNS. *Drug delivery to the central nervous system*, pp.1-13.
- Jankovic, J., 2008. Parkinson's disease: clinical features and diagnosis. *Journal of neurology, neurosurgery and psychiatry*, 79(4), pp.368-376.
- Järver, P. and Langel, Ü., 2006. Cell-penetrating peptides—a brief introduction. *Biochimica et Biophysica Acta biomembranes*, 1758(3), pp.260-263.
- Jaturapatporn, D., Isaac, M.G.E.K.N., McCleery, J. and Tabet, N., 2012. Aspirin, steroidal and non-steroidal anti-inflammatory drugs for the treatment of Alzheimer's disease. *The cochrane library*.
- Joubert, J., van Dyk, S. and Malan, S.F., 2008. Fluorescent polycyclic ligands for nitric oxide synthase (NOS) inhibition. *Bioorganic and medicinal chemistry*, 16(19), pp.8952-8958.
- Joubert, J., van Dyk, S., Green, I.R. and Malan, S.F., 2011. Synthesis, evaluation and application of polycyclic fluorescent analogues as N-methyl-D-aspartate receptor and voltage gated calcium channel ligands. *European journal of medicinal chemistry*, 46(10), pp.5010-5020.
- Kalaria, R.N., Maestre, G.E., Arizaga, R., Friedland, R.P., Galasko, D., Hall, K., Luchsinger, J.A., Ogunniyi, A., Perry, E.K., Potocnik, F. and Prince, M., 2008. Alzheimer's disease

- and vascular dementia in developing countries: prevalence, management, and risk factors. *The lancet neurology*, 7(9), pp.812-826.
- Kanai, Y. and Hediger, M.A., 2003. The glutamate and neutral amino acid transporter family: physiological and pharmacological implications. *European journal of pharmacology*, 479(1), pp.237-247.
- Kao, H.D., Traboulsi, A., Itoh, S., Dittert, L. and Hussain, A., 2000. Enhancement of the systemic and CNS specific delivery of L-dopa by the nasal administration of its water soluble prodrugs. *Pharmaceutical research*, 17(8), pp.978-984.
- Kapùs, A., Szászi, K., Káldi, K., Ligeti, E. and Fonyó, A., 1991. Is the mitochondrial Ca²⁺ uniporter a voltage-modulated transport pathway?. *Federation of european biochemical societies letters*, 282(1), pp.61-64.
- Kegel, K.B., Kim, M., Sapp, E., McIntyre, C., Castaño, J.G., Aronin, N. and DiFiglia, M., 2000. Huntingtin expression stimulates endosomal–lysosomal activity, endosome tubulation, and autophagy. *Journal of neuroscience*, 20(19), pp.7268-7278.
- Kelder, J., Grootenhuis, P.D., Bayada, D.M., Delbressine, L.P. and Ploemen, J.P., 1999. Polar molecular surface as a dominating determinant for oral absorption and brain penetration of drugs. *Pharmaceutical research*, 16(10), pp.1514-1519.
- Killian, D.M., Hermeling, S. and Chikhale, P.J., 2007. Targeting the cerebrovascular large neutral amino acid transporter (LAT1) isoform using a novel disulfide-based brain drug delivery system. *Drug delivery*, 14(1), pp.25-31.
- Klaic, L., Trippier, P.C., Mishra, R.K., Morimoto, R.I. and Silverman, R.B., 2011. Remarkable stereospecific conjugate additions to the Hsp90 inhibitor celastrol. *Journal of the american chemical society*, 133(49), pp.19634-19637.
- Kokaia, Z., Martino, G., Schwartz, M. and Lindvall, O., 2012. Cross-talk between neural stem cells and immune cells: the key to better brain repair [quest]. *Nature neuroscience*, 15(8), pp.1078-1087.
- Komatsu, M., Waguri, S., Chiba, T., Murata, S., Iwata, J.I., Tanida, I., Ueno, T., Koike, M., Uchiyama, Y., Kominami, E. and Tanaka, K., 2006. Loss of autophagy in the central nervous system causes neurodegeneration in mice. *Nature*, 441(7095), pp.880-884.
- Krantic, S., Mechawar, N., Reix, S. and Quirion, R., 2005. Molecular basis of programmed cell death involved in neurodegeneration. *Trends in neurosciences*, 28(12), pp.670-676.

- Krueger, M. and Bechmann, I., 2010. CNS pericytes: concepts, misconceptions, and a way out. *Glia*, 58(1), pp.1-10.
- Kwan, W., Träger, U., Davalos, D., Chou, A., Bouchard, J., Andre, R., Miller, A., Weiss, A., Giorgini, F., Cheah, C. and Möller, T., 2012. Mutant huntingtin impairs immune cell migration in Huntington disease. *The Journal of clinical investigation*, 122(12), pp.4737.
- Lee, E.W., Seo, J.H., Jeong, M.H., Lee, S.S. and Song, J.W., 2012. The roles of FADD in extrinsic apoptosis and necroptosis. *Biochemistry and molecular biology reports*, 45(9), pp.496-508.
- Lee, S.C., Kim, J.H., Jeong, S.M., Kim, D.R., Ha, J.U., Nam, K.C. and Ahn, D.U., 2003. Effect of far-infrared radiation on the antioxidant activity of rice hulls. *Journal of agricultural and food chemistry*, 51(15), pp.4400-4403.
- Lee, S.G., Su, Z.Z., Emdad, L., Gupta, P., Sarkar, D., Borjabad, A., Volsky, D.J. and Fisher, P.B., 2008. Mechanism of ceftriaxone induction of excitatory amino acid transporter-2 expression and glutamate uptake in primary human astrocytes. *Journal of biological chemistry*, 283(19), pp.13116-13123.
- Lee, V.M.Y. and Trojanowski, J.Q., 2006. Mechanisms of Parkinson's disease linked to pathological α -synuclein: new targets for drug discovery. *Neuron*, 52(1), pp.33-38.
- Lee, Y.J., Maeda, J., Kusuhara, H., Okauchi, T., Inaji, M., Nagai, Y., Obayashi, S., Nakao, R., Suzuki, K., Sugiyama, Y. and Suhara, T., 2006. In vivo evaluation of P-glycoprotein function at the blood-brain barrier in nonhuman primates using [11C] verapamil. *Journal of pharmacology and experimental therapeutics*, 316(2), pp.647-653.
- Leeson, P.D. and Springthorpe, B., 2007. The influence of drug-like concepts on decision-making in medicinal chemistry. *Nature reviews drug discovery*, 6(11), pp.881-890.
- Leo, A., Hansch, C. and Elkins, D., 1971. Partition coefficients and their uses. *Chemical reviews*, 71(6), pp.525-616.
- Leppänen, J., Huuskonen, J., Nevalainen, T., Gynther, J., Taipale, H. and Järvinen, T., 2002. Design and Synthesis of a Novel L-Dopa- Entacapone Codrug. *Journal of medicinal chemistry*, 45(6), pp.1379-1382.
- Levine, B. and Yuan, J., 2005. Autophagy in cell death: an innocent convict?. *The journal of clinical investigation*, 115(10), pp.2679.
- Li, C., Yuan, K. and Schluesener, H., 2013. Impact of minocycline on neurodegenerative diseases in rodents: a meta-analysis. *Reviews in the neurosciences*, 24(5), pp.553-562.

- Liberski, P.P., Sikorska, B., Bratosiewicz-Wasik, J., Gajdusek, D.C. and Brown, P., 2004. Neuronal cell death in transmissible spongiform encephalopathies (prion diseases) revisited: from apoptosis to autophagy. *The international journal of biochemistry and cell biology*, 36(12), pp.2473-2490.
- Lin, X., Parisiadou, L., Gu, X.L., Wang, L., Shim, H., Sun, L., Xie, C., Long, C.X., Yang, W.J., Ding, J. and Chen, Z.Z., 2009. Leucine-rich repeat kinase 2 regulates the progression of neuropathology induced by Parkinson's-disease-related mutant α -synuclein. *Neuron*, 64(6), pp.807-827.
- Lipinski, C.A., Lombardo, F., Dominy, B.W. and Feeney, P.J., 1997. Experimental and computational approaches to estimate solubility and permeability in drug discovery and development settings. *Advanced drug delivery reviews*, 23(1-3), pp.3-25.
- Lipton, S.A., 2006. Paradigm shift in neuroprotection by NMDA receptor blockade: memantine and beyond. *Nature reviews drug discovery*, 5(2), pp.160-170.
- Los, M., Wesselborg, S. and Schulze-Osthoff, K., 1999. The role of caspases in development, immunity, and apoptotic signal transduction: lessons from knockout mice. *Immunity*, 10(6), pp.629-639.
- Luginger, E., Wenning, G.K., Bösch, S. and Poewe, W., 2000. Beneficial effects of amantadine on L-dopa-induced dyskinesias in Parkinson's disease. *Movement disorders*, 15(5), pp.873-878.
- Lugo-Huitrón, R., Blanco-Ayala, T., Ugalde-Muniz, P., Carrillo-Mora, P., Pedraza-Chaverri, J., Silva-Adaya, D., Maldonado, P.D., Torres, I., Pinzon, E., Ortiz-Islas, E. and López, T., 2011. On the antioxidant properties of kynurenic acid: free radical scavenging activity and inhibition of oxidative stress. *Neurotoxicology and teratology*, 33(5), pp.538-547.
- Macchio, G.J., Ito, V. and Sahgal, V., 1993. Amantadine-induced coma. *Archives of physical medicine and rehabilitation*, 74(10), pp.1119-1120.
- Madsen, S.J. and Hirschberg, H., 2010. Site-specific opening of the blood-brain barrier. *Journal of biophotonics*, 3(5-6), pp.356-367.
- Malan, S.F., der Walt, V., Jurgens, J. and Van der Schyf, C.J., 2000. Structure-Activity Relationships of Polycyclic Aromatic Amines with Calcium Channel Blocking Activity. *Archiv der pharmazie*, 333(1), pp.10-16.

- Mandel, S., Grünblatt, E., Riederer, P., Gerlach, M., Levites, Y. and Youdim, M.B., 2003. Neuroprotective strategies in Parkinson's disease. *Central nervous system drugs*, 17(10), pp.729-762.
- Marchetto, M.C., Muotri, A.R., Mu, Y., Smith, A.M., Cezar, G.G. and Gage, F.H., 2008. Non-cell-autonomous effect of human SOD1 G37R astrocytes on motor neurons derived from human embryonic stem cells. *Cell stem cell*, 3(6), pp.649-657.
- Martin, J.B., 1999. Molecular basis of the neurodegenerative disorders. *New england journal of medicine*, 340(25), pp.1970-1980.
- McDonald, I.M., Mate, R.A., Zusi, F.C., Huang, H., Post-Munson, D.J., Ferrante, M.A., Gallagher, L., Bertekap, R.L., Knox, R.J., Robertson, B.J. and Harden, D.G., 2013. Discovery of a novel series of quinolone $\alpha 7$ nicotinic acetylcholine receptor agonists. *Bioorganic and medicinal chemistry letters*, 23(6), pp.1684-1688.
- McGeer, P.L. and McGeer, E.G., 2007. NSAIDs and Alzheimer disease: epidemiological, animal model and clinical studies. *Neurobiology of aging*, 28(5), pp.639-647.
- Mehdipour, A.R. and Hamidi, M., 2009. Brain drug targeting: a computational approach for overcoming blood-brain barrier. *Drug discovery today*, 14(21), pp.1030-1036.
- Meijer, L., Thunnissen, A.M., White, A.W., Garnier, M., Nikolic, M., Tsai, L.H., Walter, J., Cleverley, K.E., Salinas, P.C., Wu, Y.Z. and Biernat, J., 2000. Inhibition of cyclin-dependent kinases, GSK-3 β and CK1 by hymenialdisine, a marine sponge constituent. *Chemistry and biology*, 7(1), pp.51-63.
- Melnikova, I., 2007. Therapies for Alzheimer's disease. *Nature reviews drug discovery*, 6(5), pp.341-342.
- Meythaler, J.M. and Peduzzi, J., Landon CG Miller, 2013. *Method of treating traumatic brain and spinal cord injuries and other neurogenic conditions using non-steroidal anti-inflammatory drugs and naturally occurring conotoxins*. U.S. Patent 8,513, pp.281.
- Miller, N.J. and Rice-Evans, C.A., 1996. Spectrophotometric determination of antioxidant activity. *Redox report*, 2(3), pp.161-171.
- Minati, L., Edginton, T., Grazia Bruzzone, M. and Giaccone, G., 2009. Reviews: current concepts in Alzheimer's disease: a multidisciplinary review. *American Journal of alzheimer's disease and other dementias*, 24(2), pp.95-121.
- Miura, M., 2011. Apoptotic and non-apoptotic caspase functions in neural development. *Neurochemical research*, 36(7), pp.1253-1260.

- Monaghan, D.T., Irvine, M.W., Costa, B.M., Fang, G. and Jane, D.E., 2012. Pharmacological modulation of NMDA receptor activity and the advent of negative and positive allosteric modulators. *Neurochemistry international*, 61(4), pp.581-592.
- Monson, N.L., Ireland, S.J., Ligocki, A.J., Chen, D., Rounds, W.H., Li, M., Huebinger, R.M., Munro Cullum, C., Greenberg, B.M., Stowe, A.M. and Zhang, R., 2014. Elevated CNS inflammation in patients with preclinical Alzheimer's disease. *Journal of cerebral blood flow and metabolism*, 34(1), pp.30-33.
- Morsali, D., Bechtold, D., Lee, W., Chauhdry, S., Palchaudhuri, U., Hassoon, P., Snell, D.M., Malpass, K., Piers, T., Pocock, J. and Roach, A., 2013. Safinamide and flecainide protect axons and reduce microglial activation in models of multiple sclerosis. *Brain*, 136(4), pp.1067-1082.
- Mosley, R.L. and Gendelman, H.E., 2010. Control of neuroinflammation as a therapeutic strategy for amyotrophic lateral sclerosis and other neurodegenerative disorders. *Experimental neurology*, 222(1), pp.1-5.
- Mount, C. and Downton, C., 2006. Alzheimer disease: progress or profit?. *Nature medicine*, 12(7), pp.780-784.
- Nakamura, T. and Lipton, S.A., 2009. Cell death: protein misfolding and neurodegenerative diseases. *Apoptosis*, 14(4), pp.455-468.
- Neuwelt, E., Abbott, N.J., Abrey, L., Banks, W.A., Blakley, B., Davis, T., Engelhardt, B., Grammas, P., Nedergaard, M., Nutt, J. and Pardridge, W., 2008. Strategies to advance translational research into brain barriers. *The Lancet neurology*, 7(1), pp.84-96.
- Neuwelt, E.A., 2004. Mechanisms of disease: the blood-brain barrier. *Neurosurgery*, 54(1), pp.131-142.
- Nicoletti, F., Bruno, V., Copani, A., Casabona, G. and Knöpfel, T., 1996. Metabotropic glutamate receptors: a new target for the therapy of neurodegenerative disorders?. *Trends in neurosciences*, 19(7), pp.267-271.
- Norinder, U. and Haeberlein, M., 2002. Computational approaches to the prediction of the blood-brain distribution. *Advanced drug delivery reviews*, 54(3), pp.291-313.
- Obeso, J.A., Rodriguez-Oroz, M.C., Goetz, C.G., Marin, C., Kordower, J.H., Rodriguez, M., Hirsch, E.C., Farrer, M., Schapira, A.H. and Halliday, G., 2010. Missing pieces in the Parkinson's disease puzzle. *Nature medicine*, 16(6), pp.653-661.

- Oldendorf, W.H., Hyman, S., Braun, L. and Oldendorf, S.Z., 1972. Blood-brain barrier: penetration of morphine, codeine, heroin, and methadone after carotid injection. *Science*, 178(4064), pp.984-986.
- Omar, F.A., Farag, H.H. and Bodor, N., 1994. Synthesis and evaluation of a redox chemical delivery system for brain-enhanced dopamine containing an activated carbamate-type ester. *Journal of drug targeting*, 2(4), pp.309-316.
- Ouyang, H., Andersen, T.E., Chen, W., Nofsinger, R., Steffansen, B. and Borchardt, R.T., 2009. A comparison of the effects of p-glycoprotein inhibitors on the blood–brain barrier permeation of cyclic prodrugs of an opioid peptide (DADLE). *Journal of pharmaceutical sciences*, 98(6), pp.2227-2236.
- Pajouhesh, H. and Lenz, G.R., 2005. Medicinal chemical properties of successful central nervous system drugs. *NeuroRx*, 2(4), pp.541-553.
- Palomo, V., I Perez, D., Gil, C. and Martinez, A., 2011. The potential role of glycogen synthase kinase 3 inhibitors as amyotrophic lateral sclerosis pharmacological therapy. *Current medicinal chemistry*, 18(20), pp.3028-3034.
- Panov, A.V., Gutekunst, C.A., Leavitt, B.R., Hayden, M.R., Burke, J.R., Strittmatter, W.J. and Greenamyre, J.T., 2002. Early mitochondrial calcium defects in Huntington's disease are a direct effect of polyglutamines. *Nature neuroscience*, 5(8), pp.731-736.
- Panza, F., Solfrizzi, V., Frisardi, V., Capurso, C., D'introno, A., Colacicco, A.M., Vendemiale, G., Capurso, A. and Imbimbo, B.P., 2009. Disease-Modifying Approach to the Treatment of Alzheimer's Disease. *Drugs and aging*, 26(7), pp.537-555.
- Paoletti, P. and Neyton, J., 2007. NMDA receptor subunits: function and pharmacology. *Current opinion in pharmacology*, 7(1), pp.39-47.
- Pardridge, W.M., 2001. *Brain drug targeting: the future of brain drug development*. Cambridge University Press, pp.353.
- Pardridge, W.M., 2003. Blood-brain barrier drug targeting: the future of brain drug development. *Molecular interventions*, 3(2), pp.90-105.
- Peng, J., Stevenson, F.F., Doctrow, S.R. and Andersen, J.K., 2005. Superoxide Dismutase/Catalase Mimetics Are Neuroprotective against Selective Paraquat-mediated Dopaminergic Neuron Death in the Substantial Nigra IMPLICATIONS FOR PARKINSON DISEASE. *Journal of biological chemistry*, 280(32), pp.29194-29198.

- Perioli, L., Ambrogi, V., Bernardini, C., Grandolini, G., Ricci, M., Giovagnoli, S. and Rossi, C., 2004. Potential prodrugs of non-steroidal anti-inflammatory agents for targeted drug delivery to the CNS. *European journal of medicinal chemistry*, 39(8), pp.715-727.
- Pietta, P.G., 2000. Flavonoids as antioxidants. *Journal of natural products*, 63(7), pp.1035-1042.
- Prahlad, V. and Morimoto, R.I., 2009. Integrating the stress response: lessons for neurodegenerative diseases from *C. elegans*. *Trends in cell biology*, 19(2), pp.52-61.
- Prins, L.H., Du Preez, J.L., Van Dyk, S. and Malan, S.F., 2009. Polycyclic cage structures as carrier molecules for neuroprotective non-steroidal anti-inflammatory drugs. *European journal of medicinal chemistry*, 44(6), pp.2577-2582.
- Rashedi, I., Panigrahi, S., Ezzati, P., Ghavami, S. and Los, M., 2007. Autoimmunity and apoptosis-therapeutic implications. *Current medicinal chemistry*, 14(29), pp.3139-3151.
- Rautio, J., Kumpulainen, H., Heimbach, T., Oliyai, R., Oh, D., Järvinen, T. and Savolainen, J., 2008. Prodrugs: design and clinical applications. *Nature reviews drug discovery*, 7(3), pp.255-270.
- Regina, A., Demeule, M., Che, C., Lavalley, I., Poirier, J., Gabathuler, R., Beliveau, R. and Castaigne, J.P., 2008. Antitumour activity of ANG1005, a conjugate between paclitaxel and the new brain delivery vector Angiopep-2. *British journal of pharmacology*, 155(2), pp.185-197.
- Reichel, A., 2006. The role of blood-brain barrier studies in the pharmaceutical industry. *Current drug metabolism*, 7(2), pp.183-203.
- Reichel, A., 2009. Addressing central nervous system (CNS) penetration in drug discovery: basics and implications of the evolving new concept. *Chemistry and biodiversity*, 6(11), pp.2030-2049.
- Richard, T., Pawlus, A.D., Iglésias, M.L., Pedrot, E., Waffo-Teguo, P., Mérillon, J.M. and Monti, J.P., 2011. Neuroprotective properties of resveratrol and derivatives. *Annals of the new york academy of sciences*, 1215(1), pp.103-108.
- Rizzuto, R. and Pozzan, T., 2006. Microdomains of intracellular Ca²⁺: molecular determinants and functional consequences. *Physiological reviews*, 86(1), pp.369-408.
- Rizzuto, R., Bernardi, P. and Pozzan, T., 2000. Mitochondria as all-round players of the calcium game. *The Journal of physiology*, 529(1), pp.37-47.
- Ross, C.A. and Poirier, M.A., 2004. Protein aggregation and neurodegenerative disease.

REFERENCE

- Rossi, D. and Volterra, A., 2009. Astrocytic dysfunction: insights on the role in neurodegeneration. *Brain research bulletin*, 80(4), pp.224-232.
- Salter, M.W. and Beggs, S., 2014. Sublime microglia: expanding roles for the guardians of the CNS. *Cell*, 158(1), pp.15-24.
- Savitt, J.M., Dawson, V.L. and Dawson, T.M., 2006. Diagnosis and treatment of Parkinson disease: molecules to medicine. *Journal of clinical investigation*, 116(7), pp.1744.
- Schubert, U., Anton, L.C., Gibbs, J., Norbury, C.C., Yewdell, J.W. and Bennink, J.R., 2000. Rapid degradation of a large fraction of newly synthesized proteins by proteasomes. *Nature a-z index*, 404(6779), pp.770-774.
- Schwab, R.S., Poskanzer, D.C., England, A.C. and Young, R.R., 1972. Amantadine in Parkinson's disease: review of more than two years' experience. *Journal of the american medical association*, 222(7), pp.792-795.
- Schwarcz, R., Bruno, J.P., Muchowski, P.J. and Wu, H.Q., 2012. Kynurenines in the mammalian brain: when physiology meets pathology. *Nature reviews neuroscience*, 13(7), pp.465-477.
- Shachar, D.B., Kahana, N., Kampel, V., Warshawsky, A. and Youdim, M.B., 2004. Neuroprotection by a novel brain permeable iron chelator, VK-28, against 6-hydroxydopamine lesion in rats. *Neuropharmacology*, 46(2), pp.254-263.
- Shanbhag, V.R., Crider, A.M., Gokhale, R., Harpalani, A. and Dick, R.M., 1992. Ester and amide prodrugs of ibuprofen and naproxen: synthesis, anti-inflammatory activity, and gastrointestinal toxicity. *Journal of pharmaceutical sciences*, 81(2), pp.149-154.
- Sherman, M.Y. and Goldberg, A.L., 2001. Cellular defenses against unfolded proteins: a cell biologist thinks about neurodegenerative diseases. *Neuron*, 29(1), pp.15-32.
- Silakova, J.M., Hewett, J.A. and Hewett, S.J., 2004. Naproxen reduces excitotoxic neurodegeneration in vivo with an extended therapeutic window. *Journal of pharmacology and experimental therapeutics*, 309(3), pp.1060-1066.
- Silva, G.A., 2008. Nanotechnology approaches to crossing the blood-brain barrier and drug delivery to the CNS. *Biomed central neuroscience*, 9(3), pp.S4.
- Sinnegger-Brauns, M.J., Huber, I.G., Koschak, A., Wild, C., Obermair, G.J., Einzinger, U., Hoda, J.C., Sartori, S.B. and Striessnig, J., 2009. Expression and 1, 4-dihydropyridine-binding properties of brain L-type calcium channel isoforms. *Molecular pharmacology*, 75(2), pp.407-414.

- Skaper, S.D., Facci, L. and Giusti, P., 2014. Mast cells, glia and neuroinflammation: partners in crime?. *Immunology*, 141(3), pp.314-327.
- Skulachev, V.P., 2012. Mitochondria-targeted antioxidants as promising drugs for treatment of age-related brain diseases. *Journal of alzheimer's disease*, 28(2), pp.283-289.
- Squadrito, G.L. and Pryor, W.A., 1998. Oxidative chemistry of nitric oxide: the roles of superoxide, peroxynitrite, and carbon dioxide. *Free radical biology and medicine*, 25(4), pp.392-403.
- Stenehjem, D.D., Hartz, A.M., Bauer, B. and Anderson, G.W., 2009. Novel and emerging strategies in drug delivery for overcoming the blood–brain barrier. *Future*, 1(9), pp.1623-1641.
- Striessnig, J., Koschak, A., Sinnegger-Brauns, M.J., Hetzenauer, A., Nguyen, N.K., Busquet, P., Pelster, G. and Singewald, N., 2006. Role of voltage-gated L-type Ca²⁺ channel isoforms for brain function.
- Strigrow, F. and Ehrlich, B.E., 1996. Ligand-gated calcium channels inside and out. *Current opinion in cell biology*, 8(4), pp.490-495.
- Surmeier, D.J., Guzman, J.N., Sanchez-Padilla, J. and Goldberg, J.A., 2011. The origins of oxidant stress in Parkinson's disease and therapeutic strategies. *Antioxidants and redox signaling*, 14(7), pp.1289-1301.
- Syntichaki, P., Xu, K., Driscoll, M. and Tavernarakis, N., 2002. Specific aspartyl and calpain proteases are required for neurodegeneration in *C. elegans*. *Nature*, 419(6910), pp.939-944.
- Szeto, H.H. and Schiller, P.W., 2011. Novel therapies targeting inner mitochondrial membrane—from discovery to clinical development. *Pharmaceutical research*, 28(11), pp.2669-2679.
- T Hellwig, C., Passante, E. and Rehm, M., 2011. The molecular machinery regulating apoptosis signal transduction and its implication in human physiology and pathophysiology. *Current molecular medicine*, 11(1), pp.31-47.
- Tavernarakis, N. and Samara, C., 2008. Autophagy and cell death in *Caenorhabditis elegans*. *Current pharmaceutical design*, 14(2), pp.97-115.
- Taylor, E.M., 2002. The impact of efflux transporters in the brain on the development of drugs for CNS disorders. *Clinical pharmacokinetics*, 41(2), pp.81-92.

- Taylor, J.P., Hardy, J. and Fischbeck, K.H., 2002. Toxic proteins in neurodegenerative disease. *Science*, 296(5575), pp.1991-1995.
- Tendi, E.A., Cunsolo, R., Bellia, D., Messina, R.L., Paratore, S., Calissano, P. and Cavallaro, S., 2010. Drug target identification for neuronal apoptosis through a genome scale screening. *Current medicinal chemistry*, 17(26), pp.2906-2920.
- Thorne, R.G., Pronk, G.J., Padmanabhan, V. and Frey, W.2., 2004. Delivery of insulin-like growth factor-I to the rat brain and spinal cord along olfactory and trigeminal pathways following intranasal administration. *Neuroscience*, 127(2), pp.481-496.
- Tooze, S.A. and Schiavo, G., 2008. Liaisons dangereuses: autophagy, neuronal survival and neurodegeneration. *Current opinion in neurobiology*, 18(5), pp.504-515.
- Trott, A., West, J.D., Klaić, L., Westerheide, S.D., Silverman, R.B., Morimoto, R.I. and Morano, K.A., 2008. Activation of heat shock and antioxidant responses by the natural product celastrol: transcriptional signatures of a thiol-targeted molecule. *Molecular biology of the cell*, 19(3), pp.1104-1112.
- Tsang, A.H. and Chung, K.K., 2009. Oxidative and nitrosative stress in Parkinson's disease. *Biochimica et Biophysica acta molecular basis of disease*, 1792(7), pp.643-650.
- Tsuzuki, N., Hama, T., Kawada, M., Hasui, A., Konishi, R., Shiwa, S., Ochi, Y., Futaki, S. and Kitagawa, K., 1994. Adamantane as a brain-directed drug carrier for poorly absorbed drug. 2. AZT derivatives conjugated with the 1-adamantane moiety. *Journal of pharmaceutical sciences*, 83(4), pp.481-484.
- Van Damme, P., Bogaert, E., Dewil, M., Hersmus, N., Kiraly, D., Scheveneels, W., Bockx, I., Braeken, D., Verpoorten, N., Verhoeven, K. and Timmerman, V., 2007. Astrocytes regulate GluR2 expression in motor neurons and their vulnerability to excitotoxicity. *Proceedings of the national academy of sciences*, 104(37), pp.14825-14830.
- van de Waterbeemd, H., Camenisch, G., Folkers, G., Chretien, J.R. and Raevsky, O.A., 1998. Estimation of blood-brain barrier crossing of drugs using molecular size and shape, and H-bonding descriptors. *Journal of drug targeting*, 6(2), pp.151-165.
- Van der Schyf, C.J. and Geldenhuys, W.J., 2009. Polycyclic compounds: Ideal drug scaffolds for the design of multiple mechanism drugs?. *Neurotherapeutics*, 6(1), pp.175-186.
- Varma, M.V., Obach, R.S., Rotter, C., Miller, H.R., Chang, G., Steyn, S.J., El-Kattan, A. and Troutman, M.D., 2010. Physicochemical space for optimum oral bioavailability:

- contribution of human intestinal absorption and first-pass elimination. *Journal of medicinal chemistry*, 53(3), pp.1098-1108.
- Veber, D.F., Johnson, S.R., Cheng, H.Y., Smith, B.R., Ward, K.W. and Kopple, K.D., 2002. Molecular properties that influence the oral bioavailability of drug candidates. *Journal of medicinal chemistry*, 45(12), pp.2615-2623.
- Vlad, S.C., Miller, D.R., Kowall, N.W. and Felson, D.T., 2008. Protective effects of NSAIDs on the development of Alzheimer disease. *Neurology*, 70(19), pp.1672-1677.
- Vykhodtseva, N., McDannold, N. and Hynynen, K., 2008. Progress and problems in the application of focused ultrasound for blood–brain barrier disruption. *Ultrasonics*, 48(4), pp.279-296.
- Wager, T.T., Chandrasekaran, R.Y., Hou, X., Troutman, M.D., Verhoest, P.R., Villalobos, A. and Will, Y., 2010. Defining desirable central nervous system drug space through the alignment of molecular properties, in vitro ADME, and safety attributes. *American chemical society chemical neuroscience*, 1(6), pp.420-434.
- Walker, L.C. and LeVine, H., 2012. Corruption and spread of pathogenic proteins in neurodegenerative diseases. *Journal of biological chemistry*, 287(40), pp.33109-33115.
- Wallach, D., Varfolomeev, E.E., Malinin, N.L., Goltsev, Y.V., Kovalenko, A.V. and Boldin, M.P., 1999. Tumor necrosis factor receptor and Fas signaling mechanisms. *Annual review of immunology*, 17(1), pp.331-367.
- Wang, P., Lazarus, B.D., Forsythe, M.E., Love, D.C., Krause, M.W. and Hanover, J.A., 2012. O-GlcNAc cycling mutants modulate proteotoxicity in *Caenorhabditis elegans* models of human neurodegenerative diseases. *Proceedings of the national academy of sciences*, 109(43), pp.17669-17674.
- Wolf, E., Seppi, K., Katzenschlager, R., Hochschorner, G., Ransmayr, G., Schwingenschuh, P., Ott, E., Kloiber, I., Haubenberger, D., Auff, E. and Poewe, W., 2010. Long-term antidyskinetic efficacy of amantadine in Parkinson's disease. *Movement disorders*, 25(10), pp.1357-1363.
- X Sureda, F., Junyent, F., Verdager, E., Auladell, C., Pelegri, C., Vilaplana, J., Folch, J., Maria Canudas, A., Beas Zarate, C., Pallàs, M. and Camins, A., 2011. Antiapoptotic drugs: a therapeutic strategy for the prevention of neurodegenerative diseases. *Current pharmaceutical design*, 17(3), pp.230-245.

- Xu, Z., Wu, J., Zheng, J., Ma, H., Zhang, H., Zhen, X., Zheng, L.T. and Zhang, X., 2015. Design, synthesis and evaluation of a series of non-steroidal anti-inflammatory drug conjugates as novel neuroinflammatory inhibitors. *International immunopharmacology*, 25(2), pp.528-537.
- Youdim, M.B., Geldenhuys, W.J. and Van der Schyf, C.J., 2007. Why should we use multifunctional neuroprotective and neurorestorative drugs for Parkinson's disease?. *Parkinsonism and related disorders*, 13, pp.S281-S291.
- Yu, L., Haley, S., Perret, J., Harris, M., Wilson, J. and Qian, M., 2002. Free radical scavenging properties of wheat extracts. *Journal of agricultural and food chemistry*, 50(6), pp.1619-1624.
- Yue, Z., Friedman, L., Komatsu, M. and Tanaka, K., 2009. The cellular pathways of neuronal autophagy and their implication in neurodegenerative diseases. *Biochimica et biophysica acta molecular cell research*, 1793(9), pp.1496-1507.
- Zádori, D., Klivényi, P., Szalárdy, L., Fülöp, F., Toldi, J. and Vécsei, L., 2012. Mitochondrial disturbances, excitotoxicity, neuroinflammation and kynurenines: novel therapeutic strategies for neurodegenerative disorders. *Journal of the neurological sciences*, 322(1), pp.187-191.
- Zah, J., Terre'Blanche, G., Erasmus, E. and Malan, S.F., 2003. Physicochemical prediction of a brain–blood distribution profile in polycyclic amines. *Bioorganic and medicinal chemistry*, 11(17), pp.3569-3578.
- Zecca, L., Youdim, M.B., Riederer, P., Connor, J.R. and Crichton, R.R., 2004. Iron, brain ageing and neurodegenerative disorders. *Nature reviews neuroscience*, 5(11), pp.863-873.
- Zhang, X., Liu, X., Gong, T., Sun, X. and Zhang, Z.R., 2012. In vitro and in vivo investigation of dexibuprofen derivatives for CNS delivery. *Acta pharmacologica sinica*, 33(2), pp.279-288.
- Zhang, Y., Han, H., Elmquist, W.F. and Miller, D.W., 2000. Expression of various multidrug resistance-associated protein (MRP) homologues in brain microvessel endothelial cells. *Brain research*, 876(1), pp.148-153.
- Zhao, Y., Qu, B., Wu, X., Li, X., Liu, Q., Jin, X., Guo, L., Hai, L. and Wu, Y., 2014. Design, synthesis and biological evaluation of brain targeting l-ascorbic acid prodrugs of

REFERENCE

- ibuprofen with “lock-in” function. *European journal of medicinal chemistry*, 82, pp.314-323.
- Zheng, D., Shuai, X., Li, Y., Zhou, P., Gong, T., Sun, X. and Zhang, Z., 2016. Novel flurbiprofen derivatives with improved brain delivery: synthesis, in vitro and in vivo evaluations. *Drug delivery*, 23(7), pp.2183-2192.
- Zuffanti, S., 1948. Preparation of acyl chlorides with thionyl chloride. *Journal of chemical education*, 25(9), pp.481.

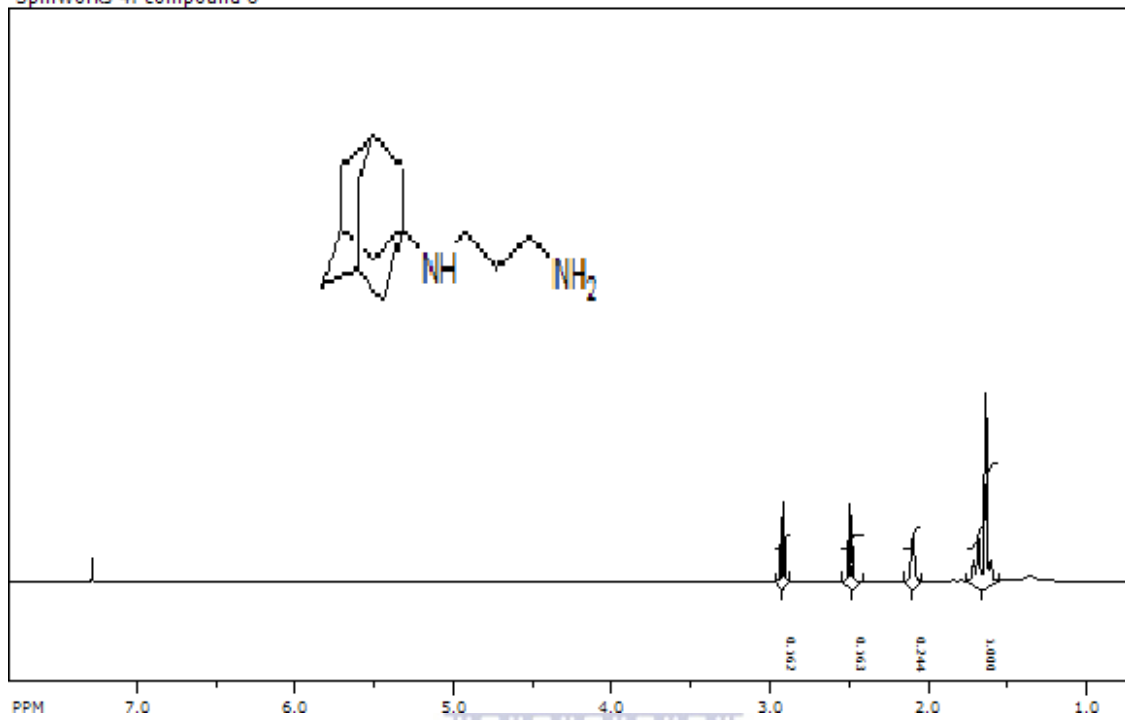


ANNEXURE A
SPECTRAL DATA: INFRARED, MASS AND NUCLEAR MAGNETIC
RESONANCE SPECTRA

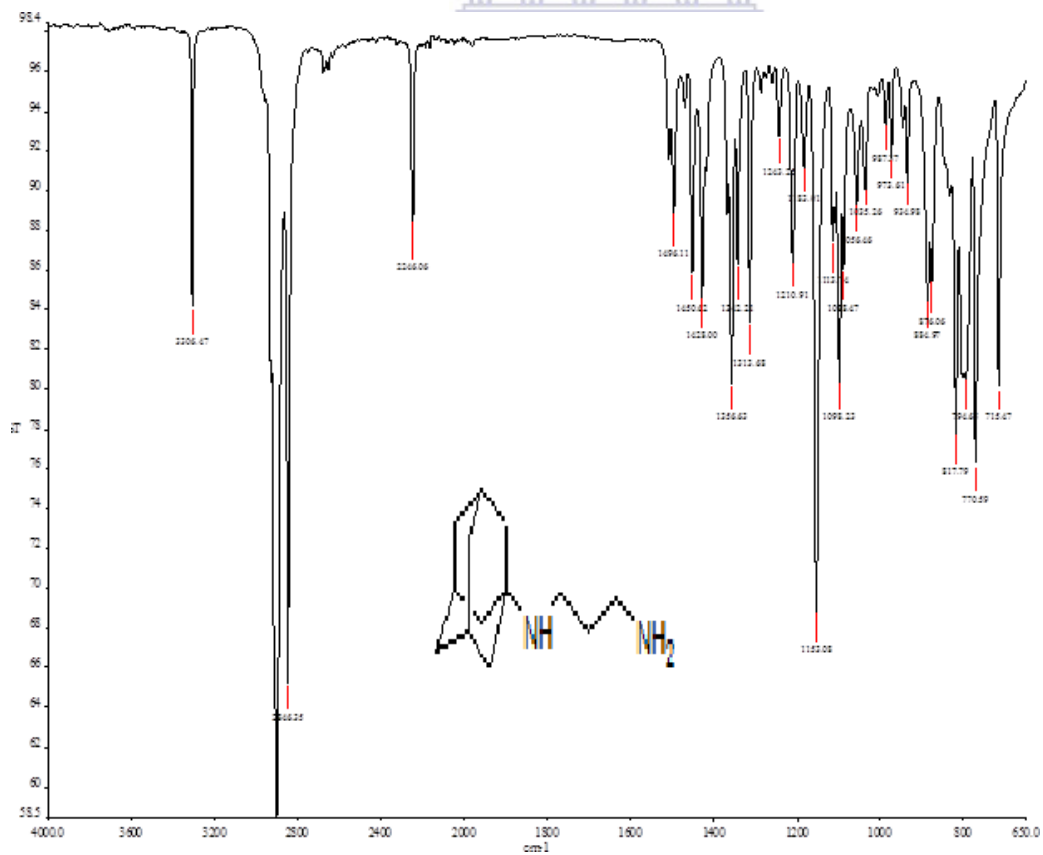


Spectrum 1

SpinWorks 4: compound 6

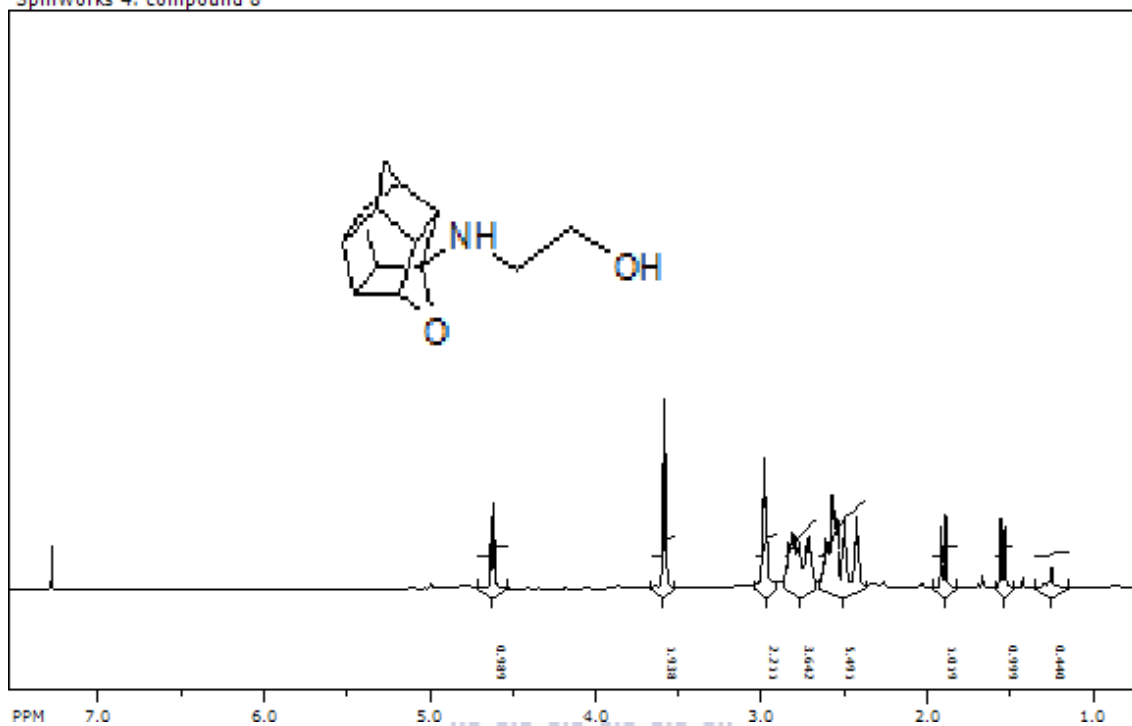


Spectrum 2



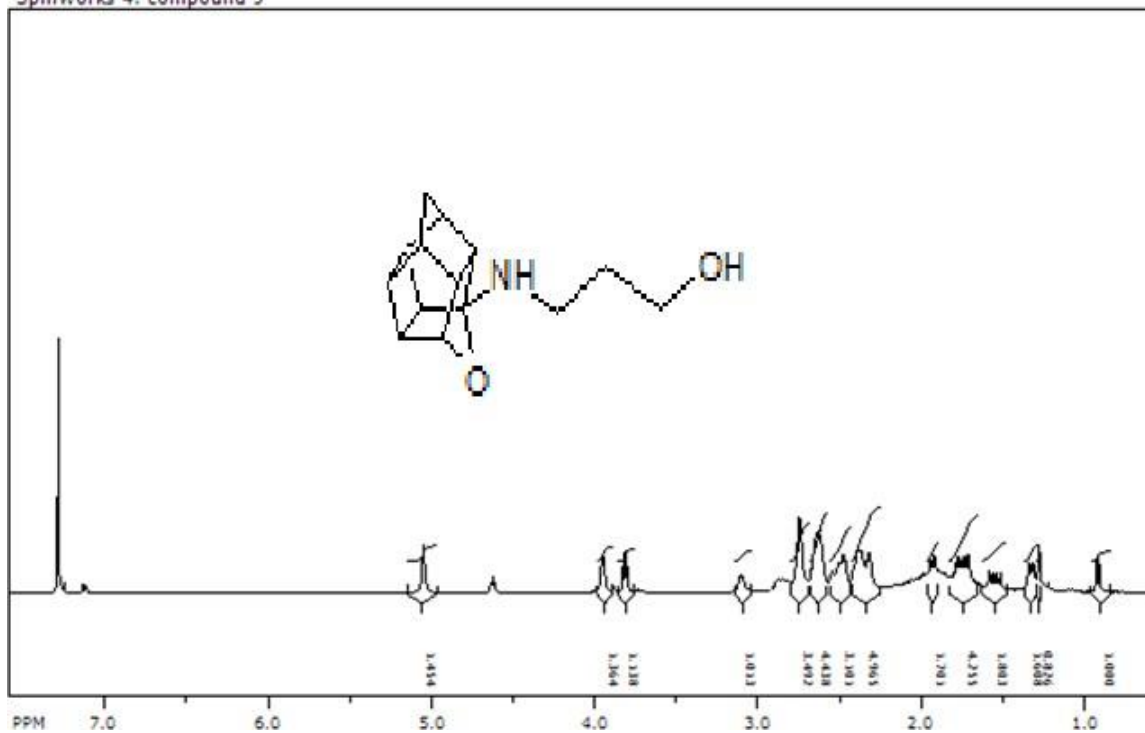
Spectrum 3

SpinWorks 4: compound 8



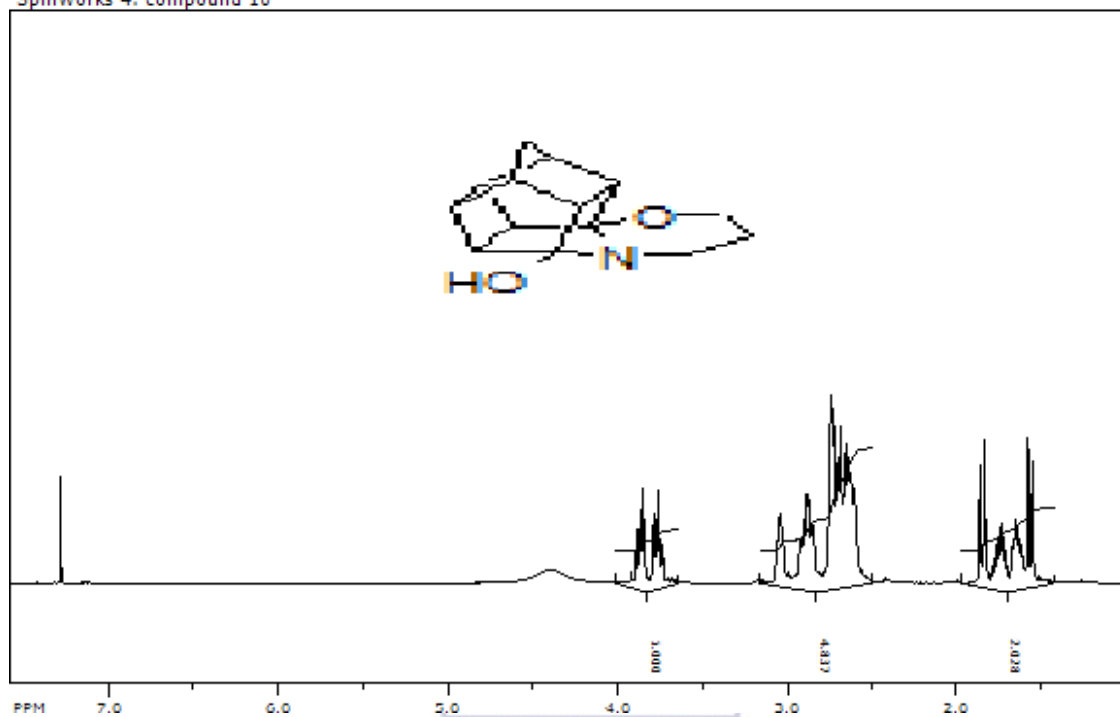
Spectrum 4

SpinWorks 4: compound 9



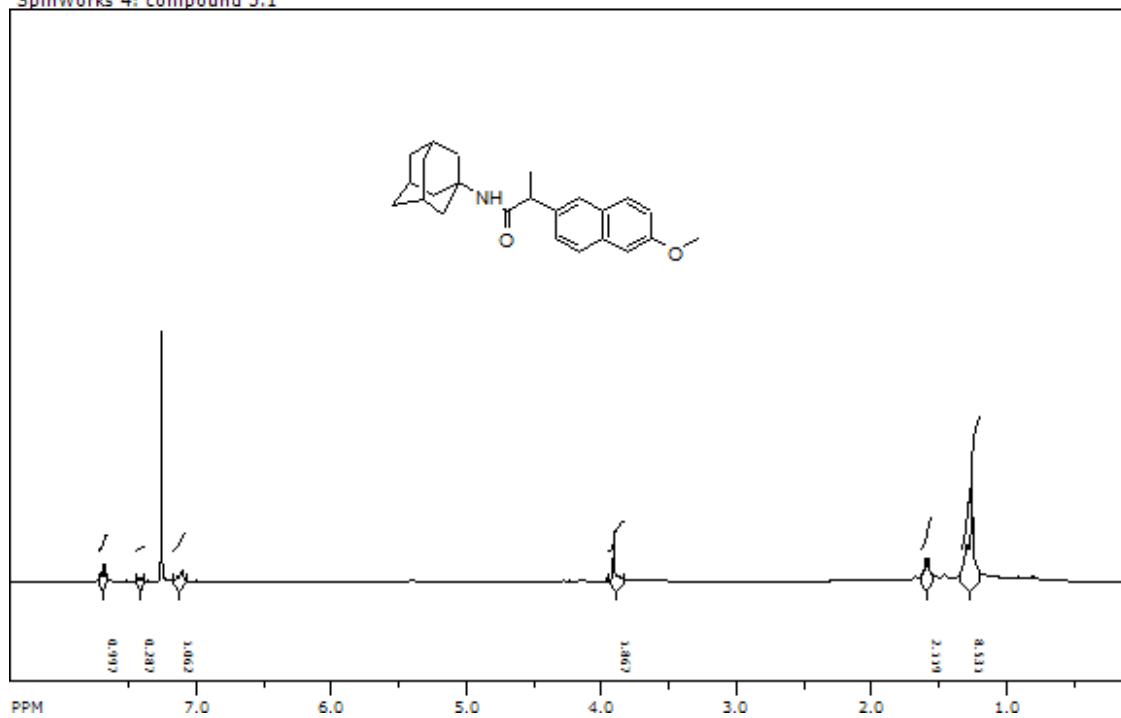
Spectrum 5

SpinWorks 4: compound 10



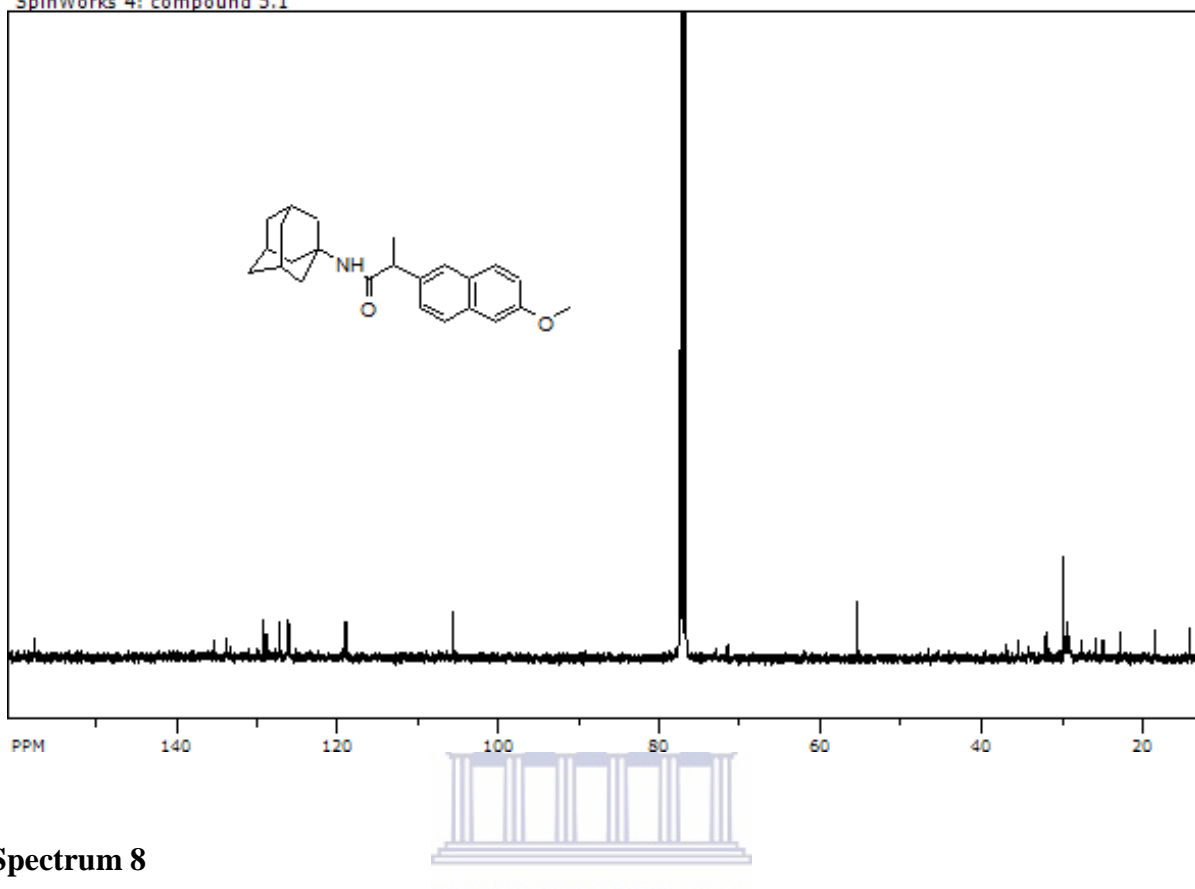
Spectrum 6

SpinWorks 4: compound 5.1

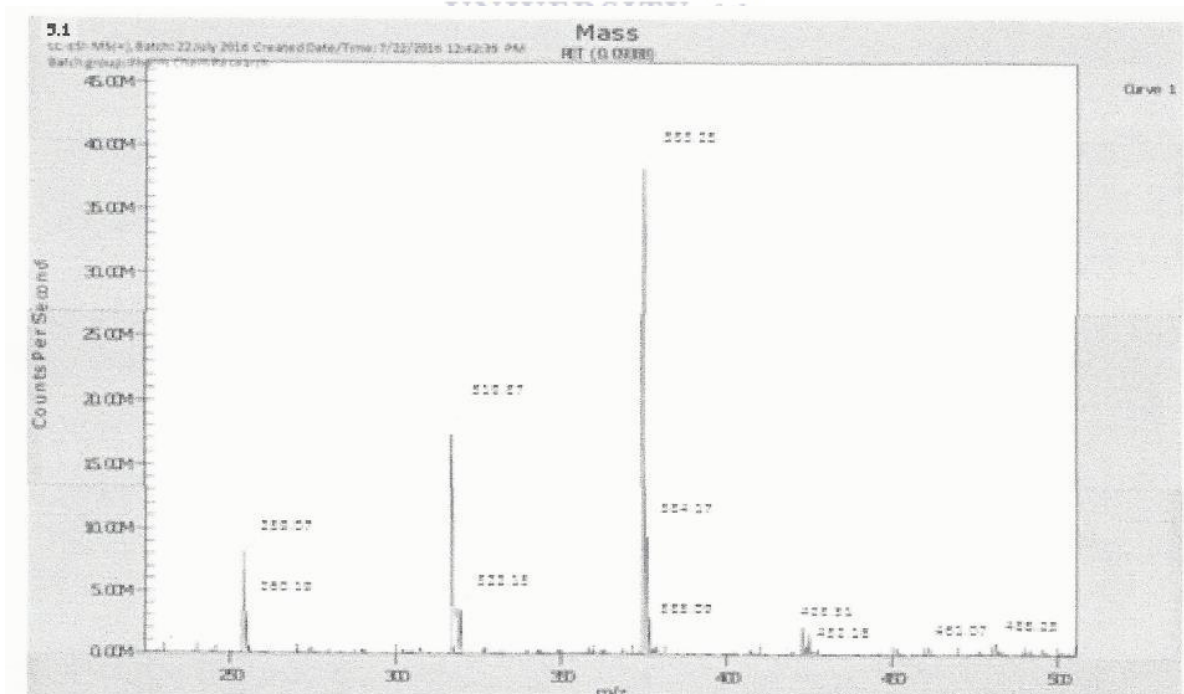


Spectrum 7

SpinWorks 4: compound 5.1

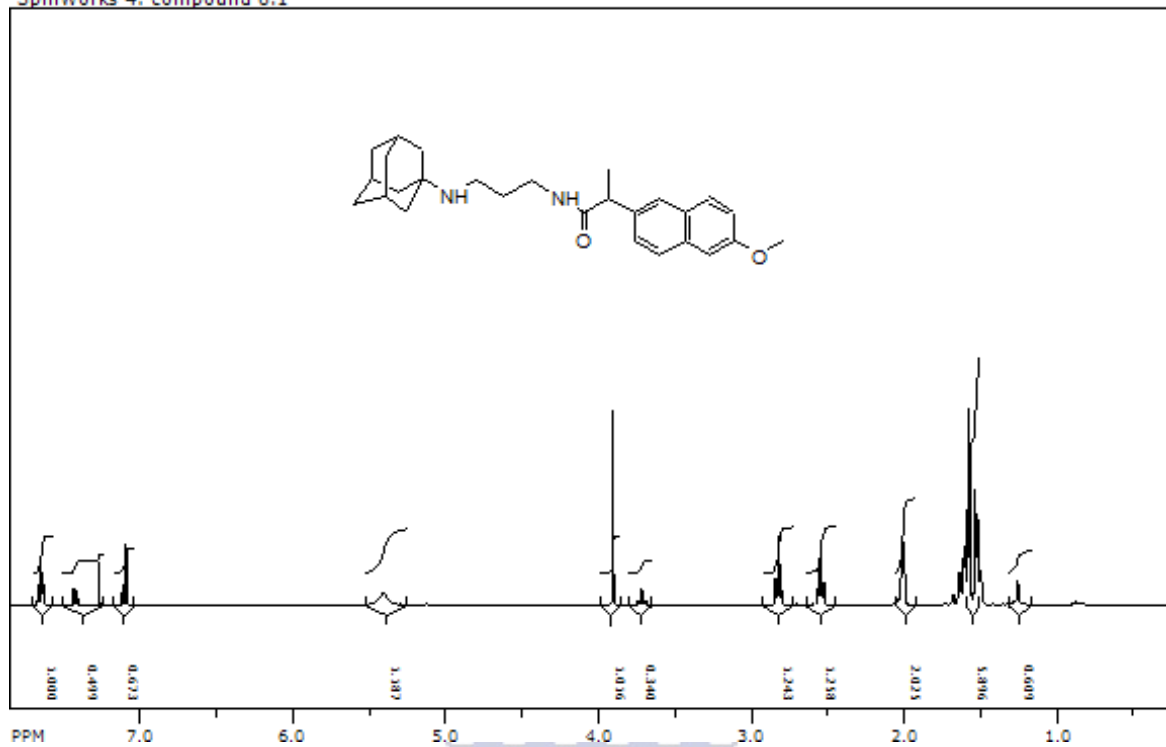


Spectrum 8



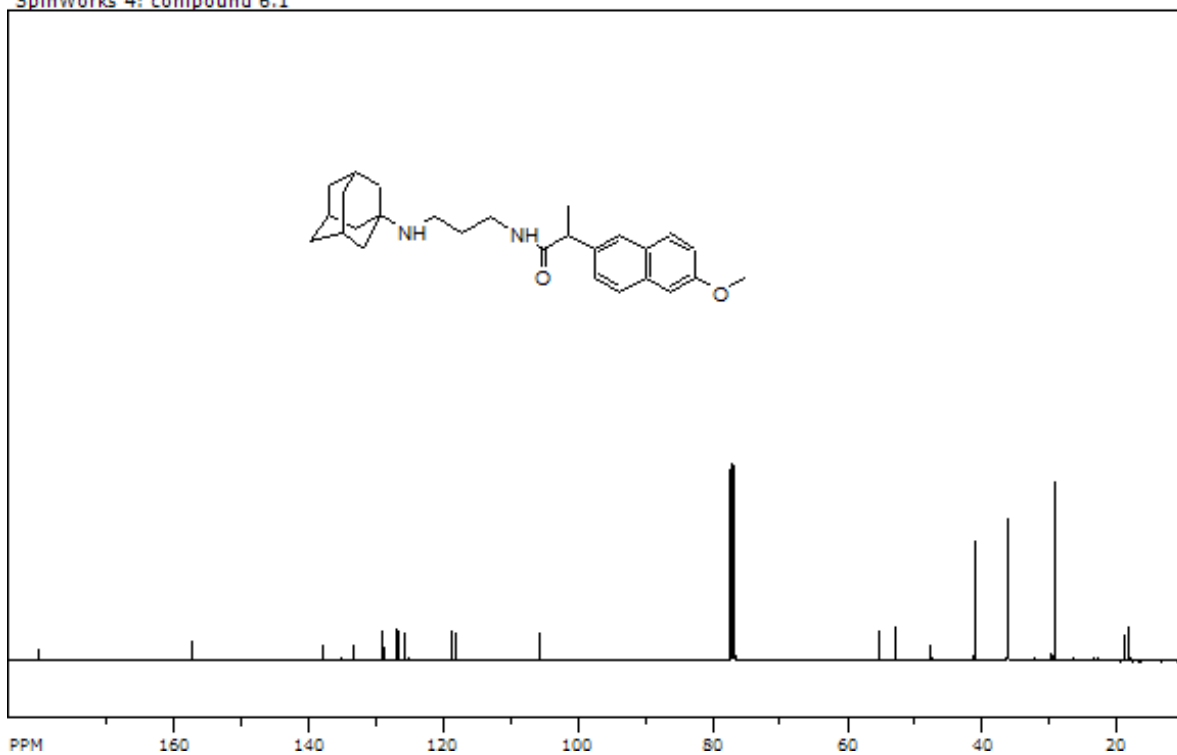
Spectrum 9:

SpinWorks 4: compound 6.1

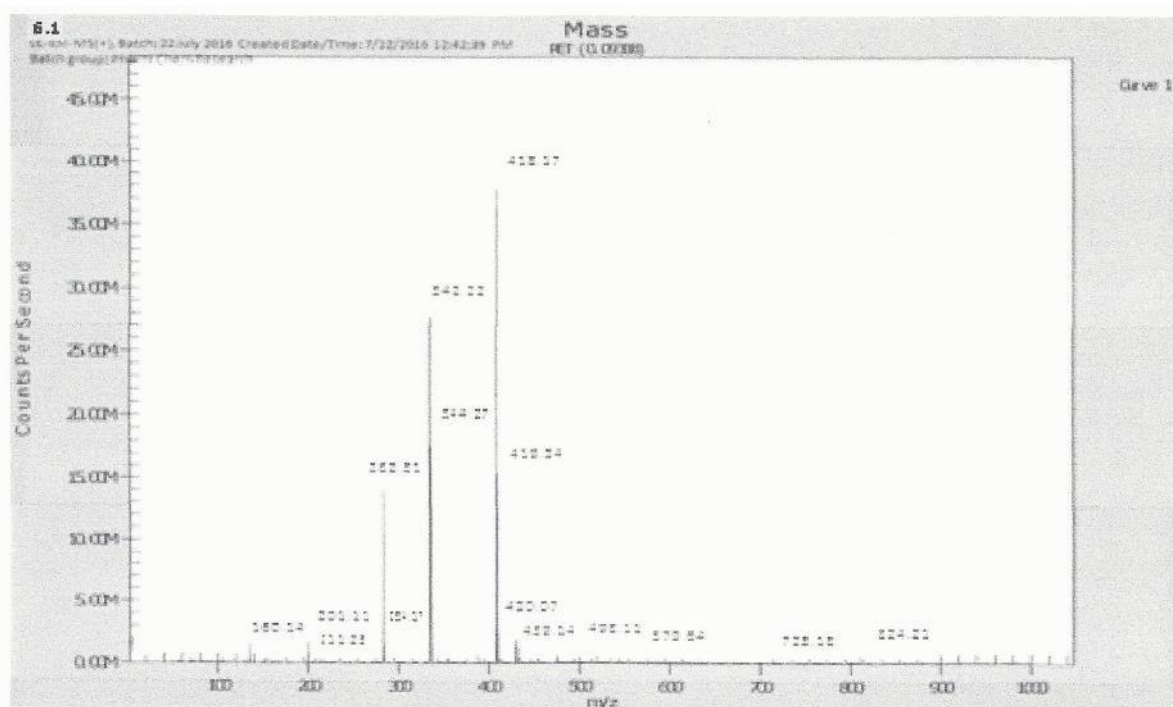


Spectrum 10

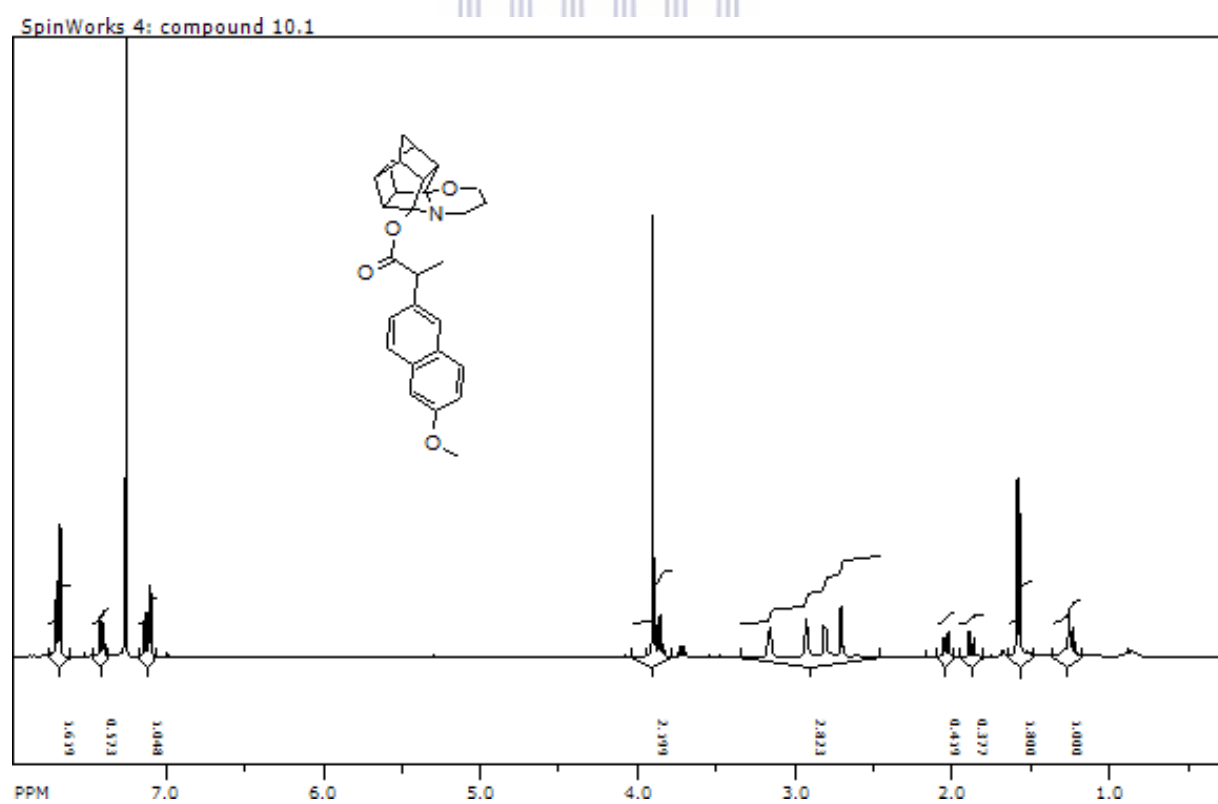
SpinWorks 4: compound 6.1



Spectrum 11

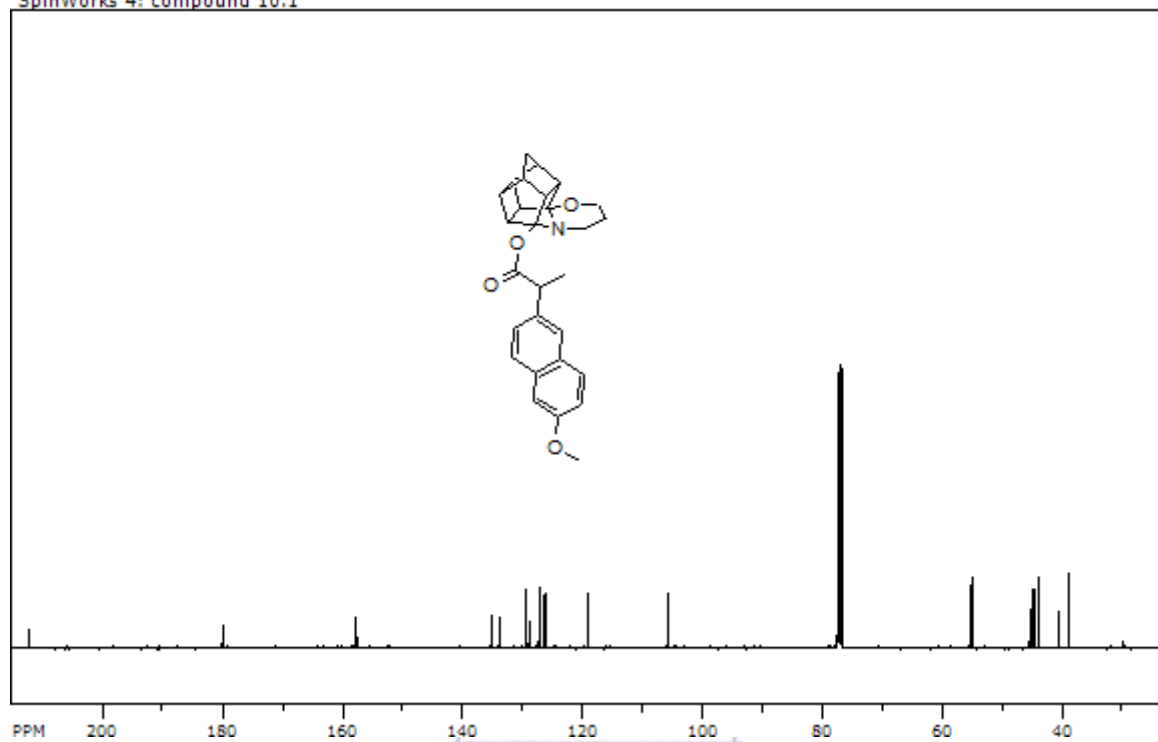


Spectrum 12

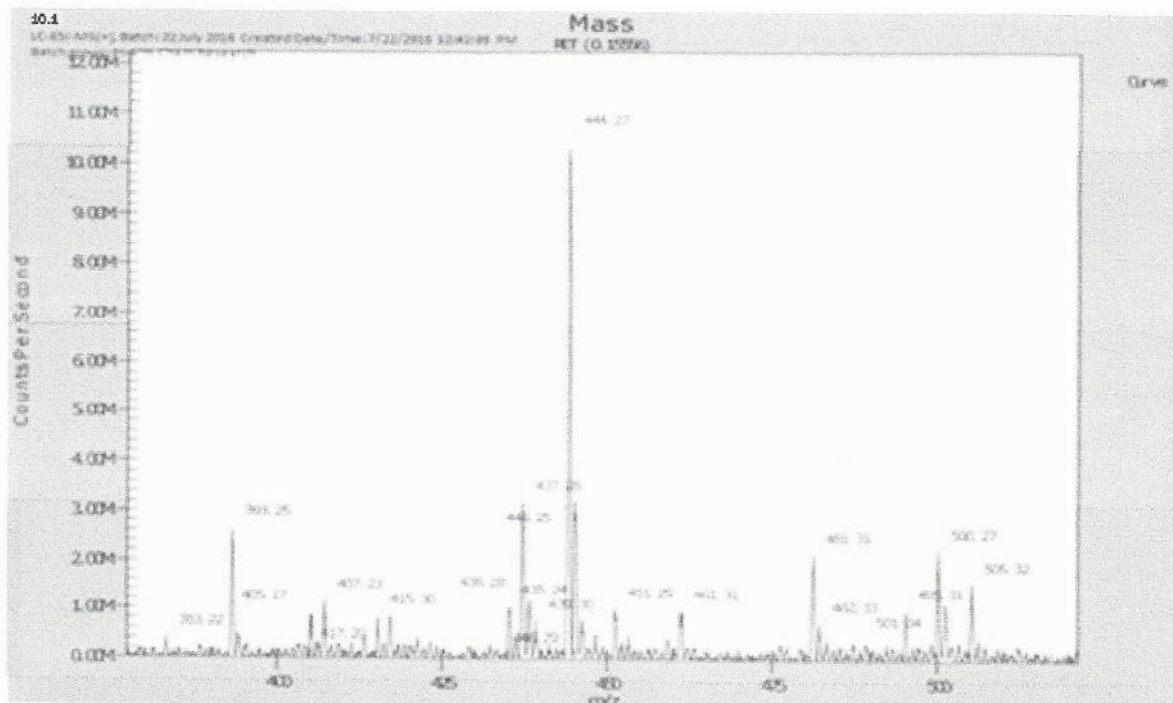


Spectrum 13

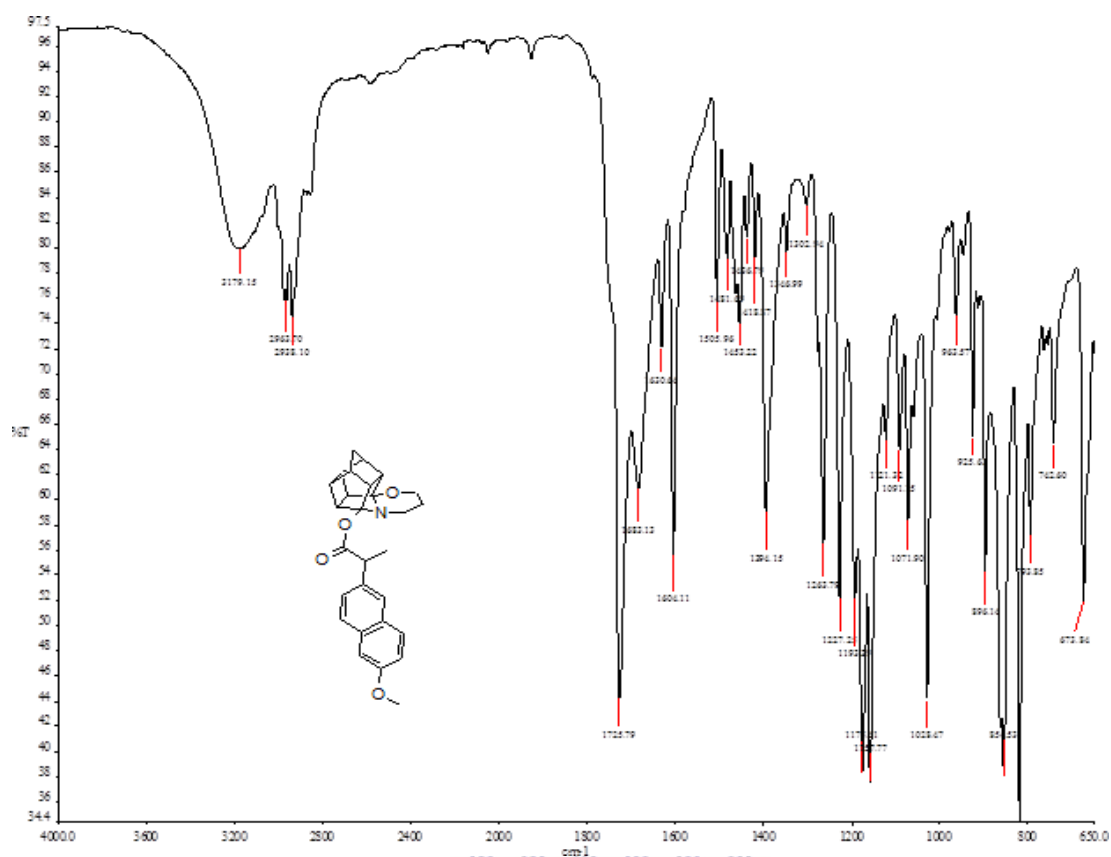
SpinWorks 4: compound 10.1



Spectrum 14



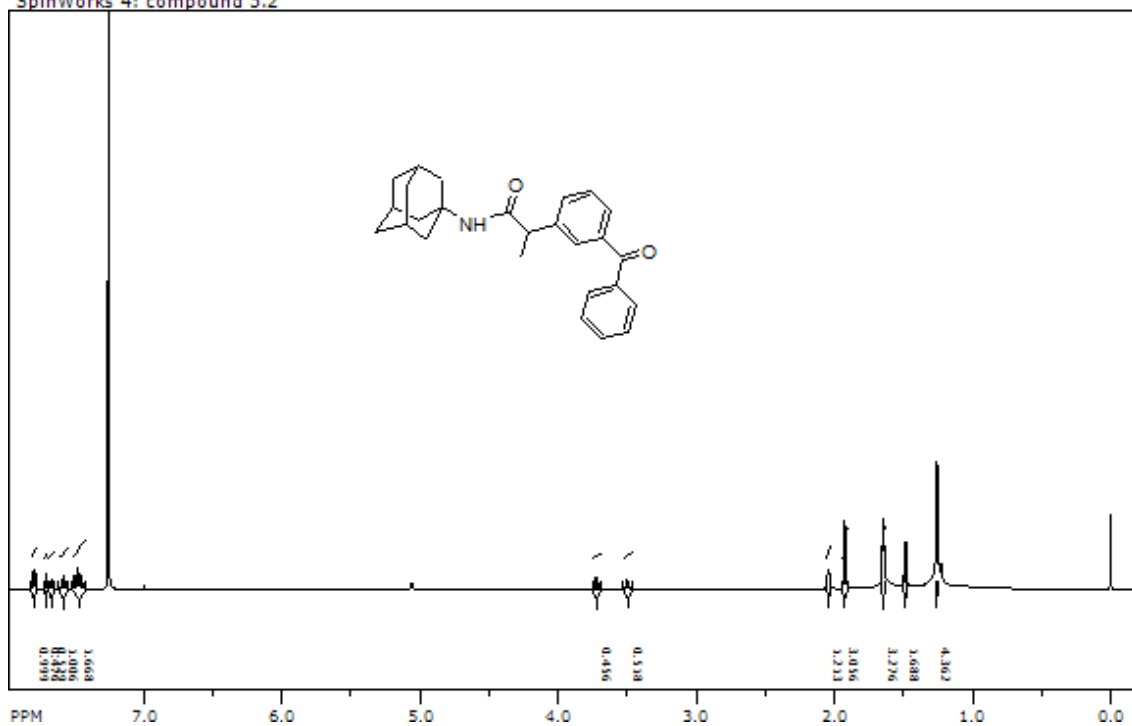
Spectrum 15



UNIVERSITY of the
WESTERN CAPE

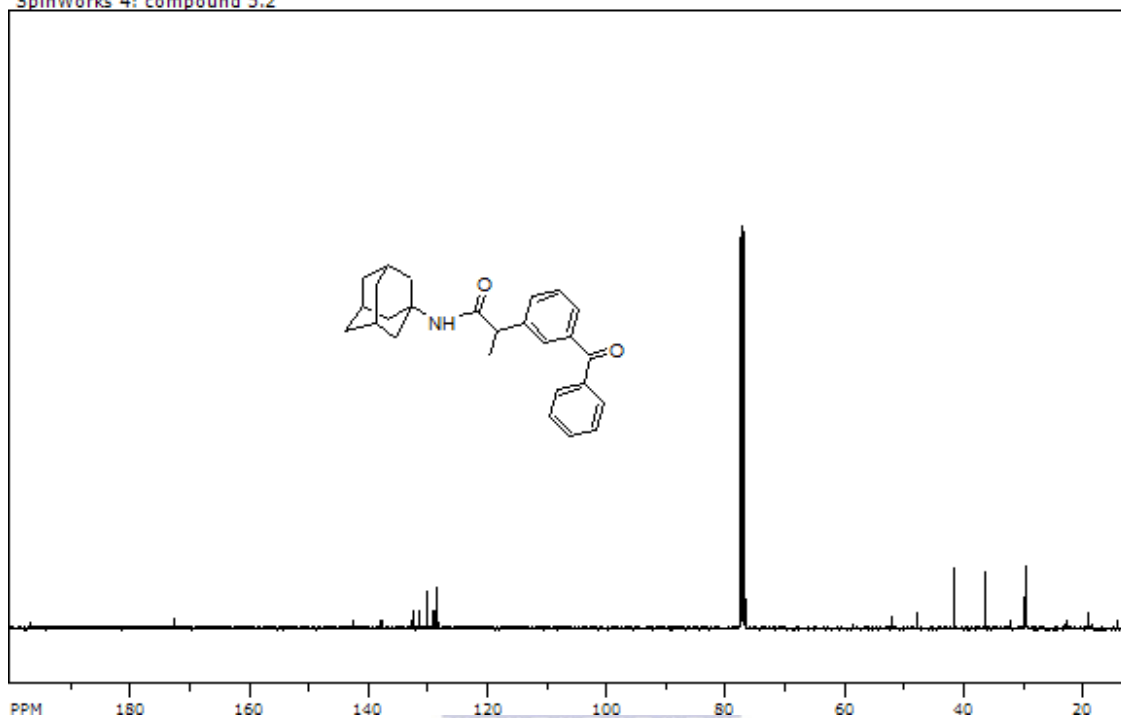
Spectrum 16

SpinWorks 4: compound 5.2

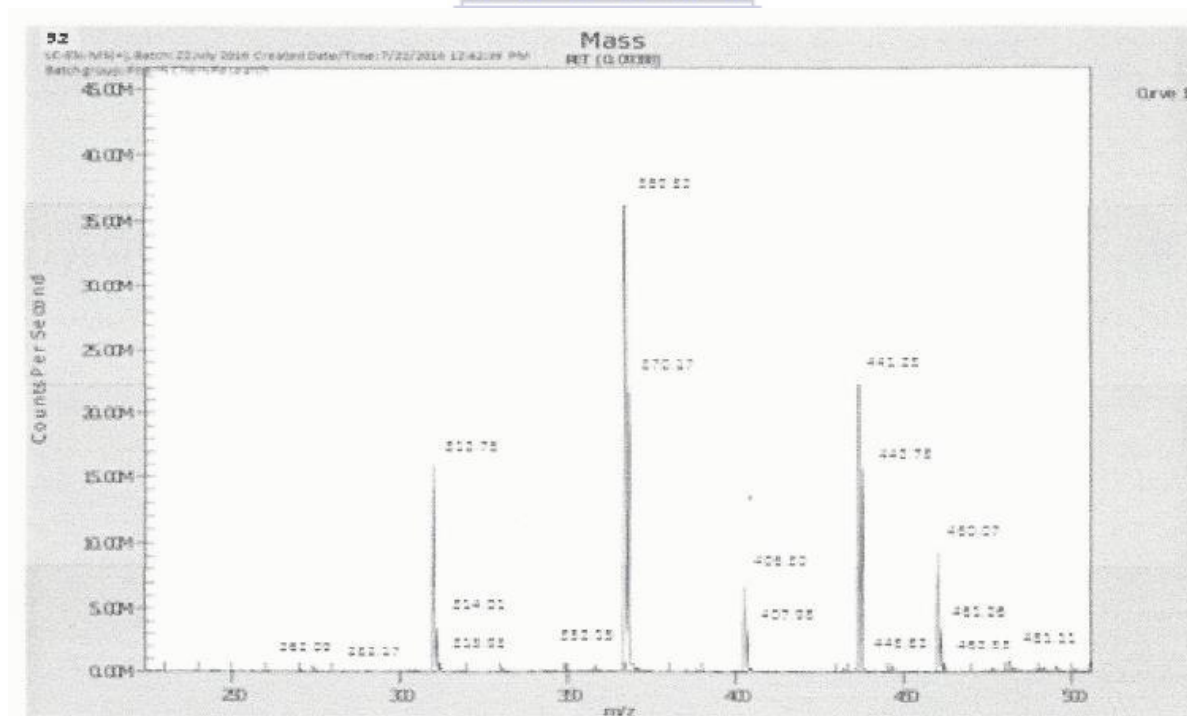


Spectrum 17

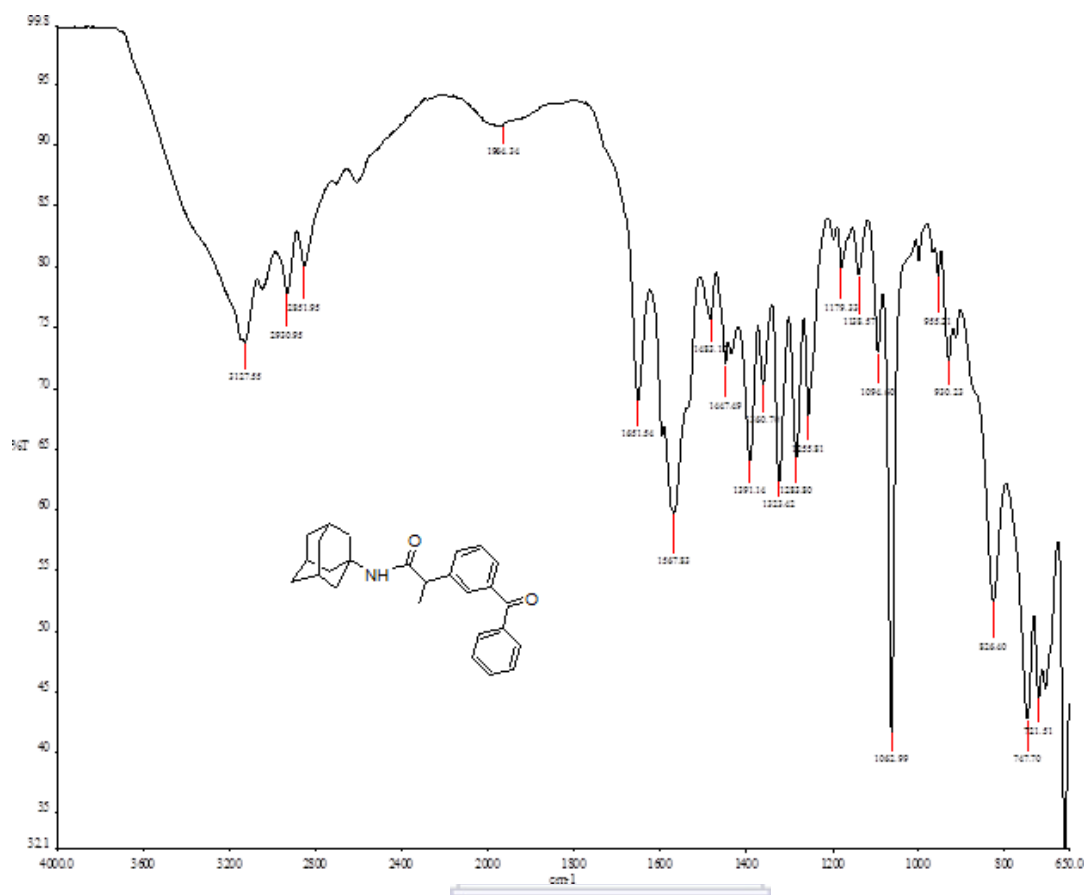
SpinWorks 4: compound 5.2



Spectrum 18



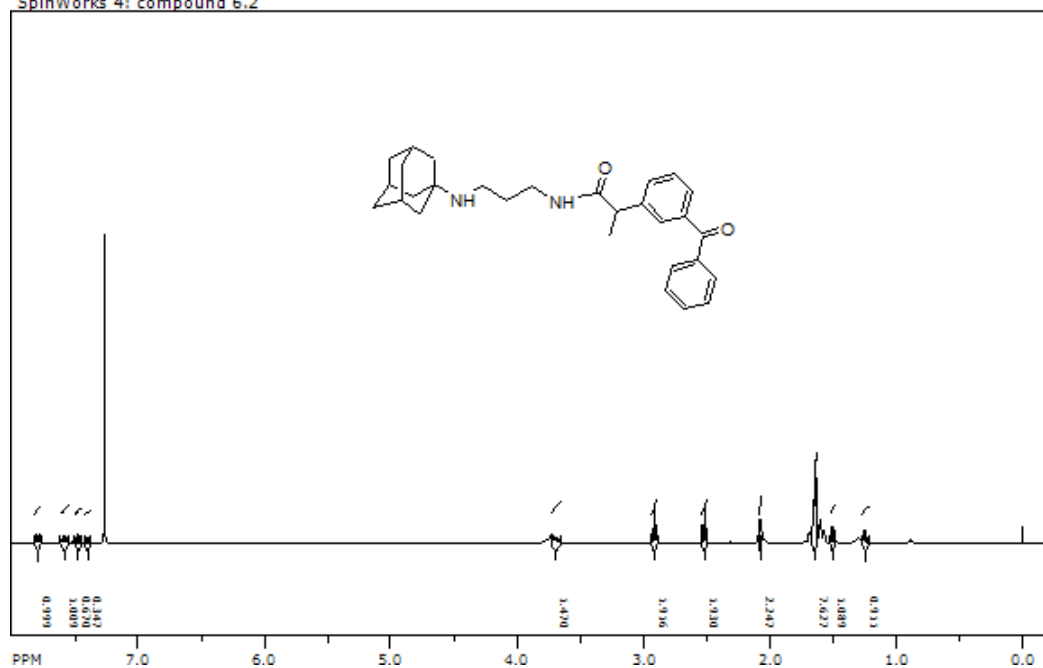
Spectrum 19



UNIVERSITY of the
WESTERN CAPE

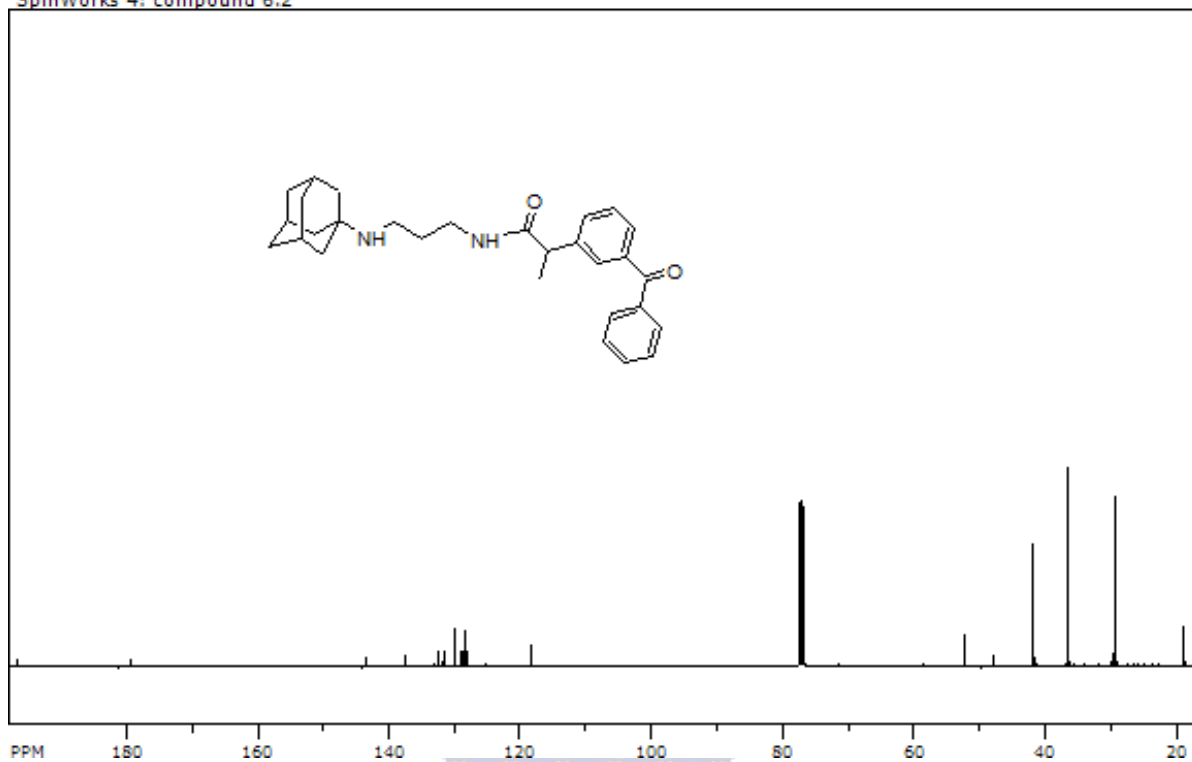
Spectrum 20

SpinWorks 4: compound 6.2

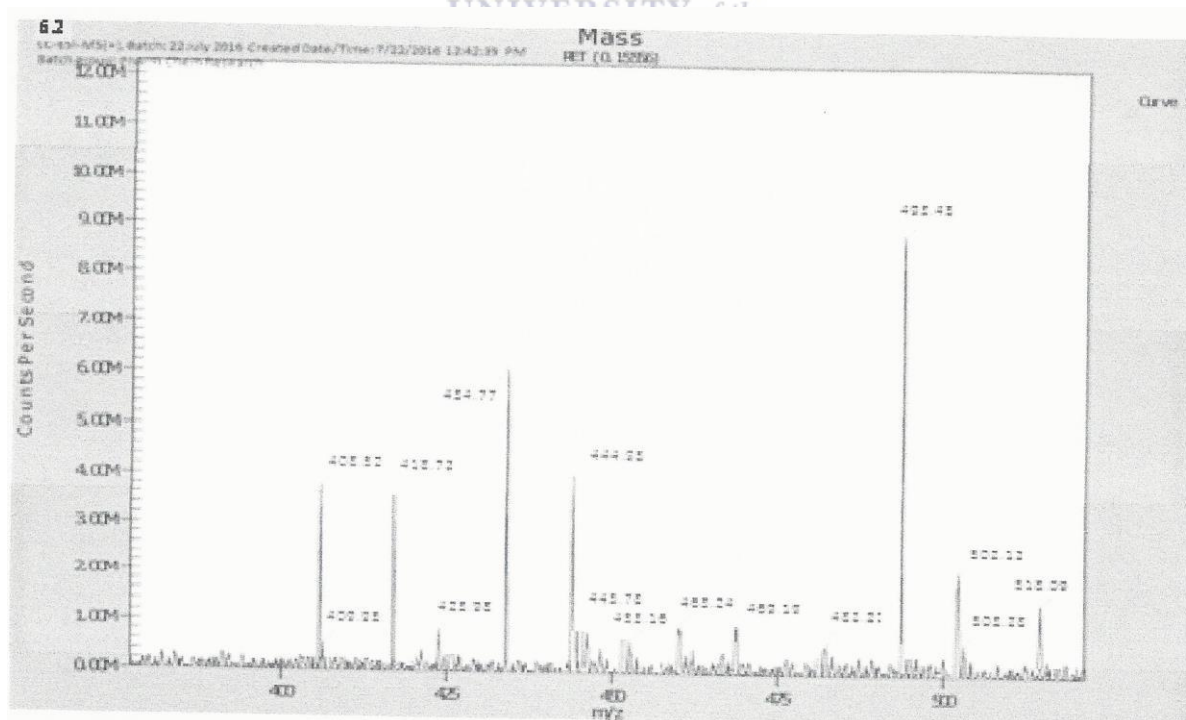


Spectrum 21

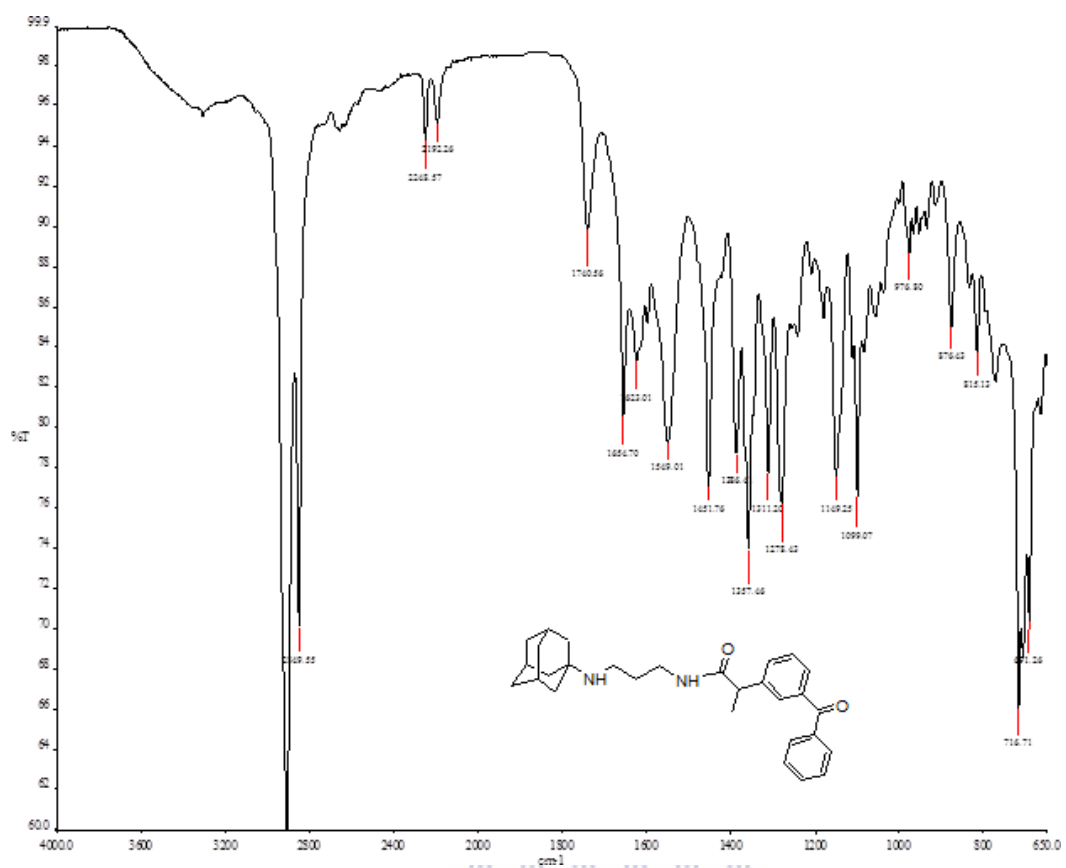
SpinWorks 4: compound 6.2



Spectrum 22

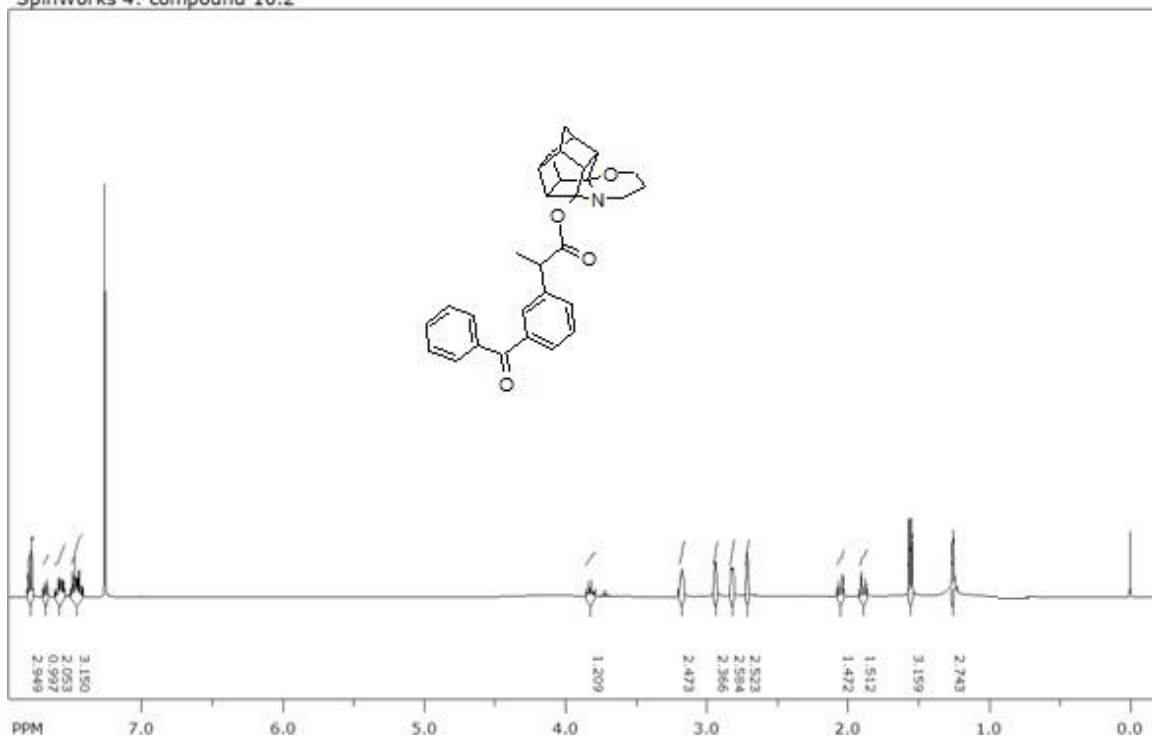


Spectrum 23



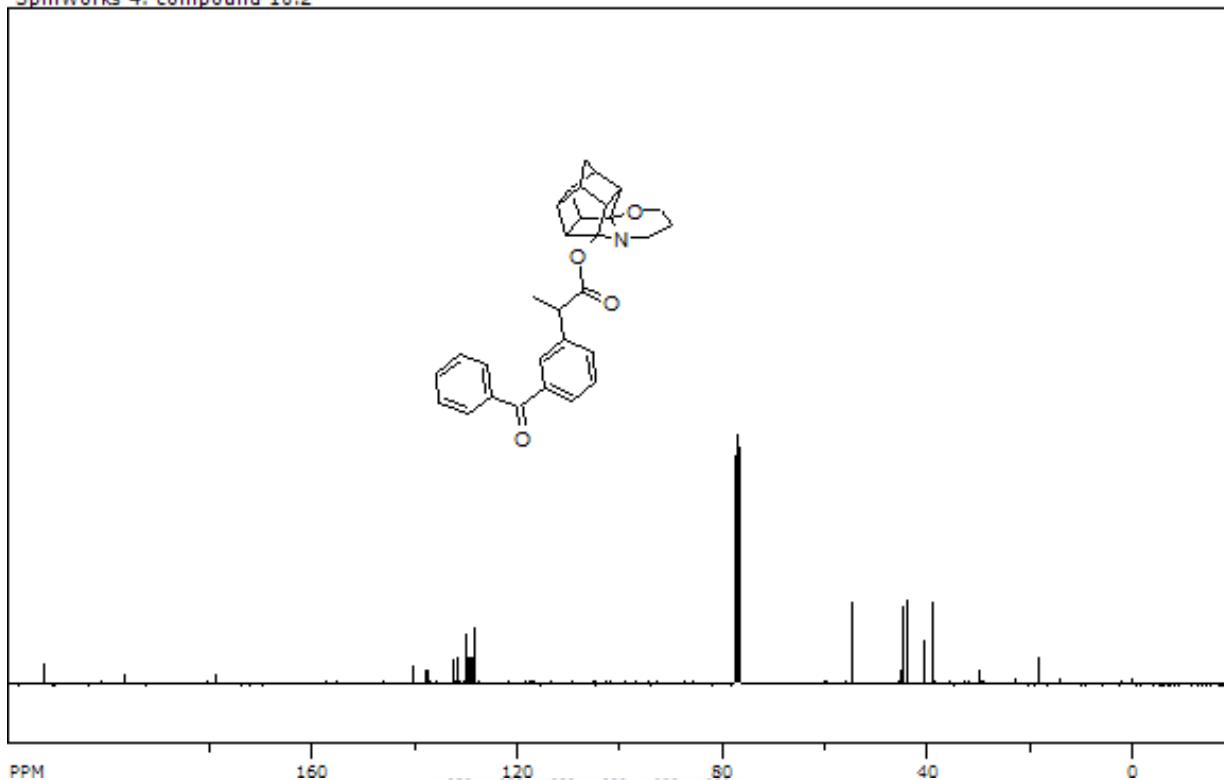
Spectrum 24

SpinWorks 4: compound 10.2

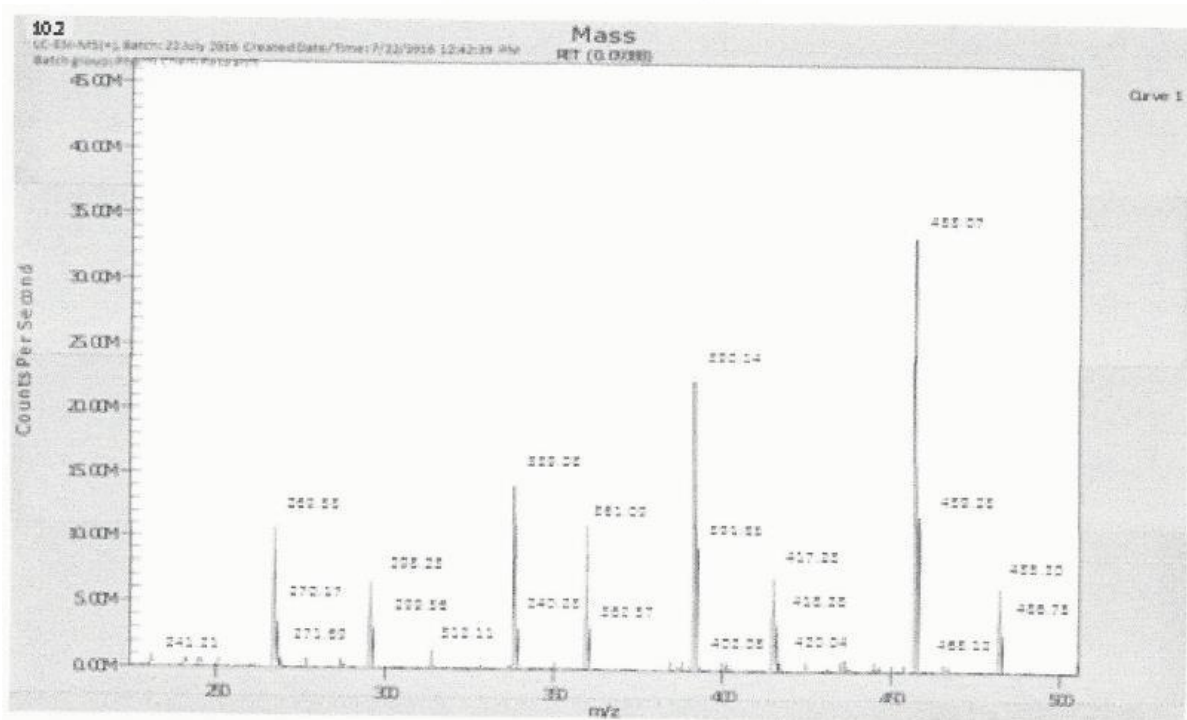


Spectrum 25

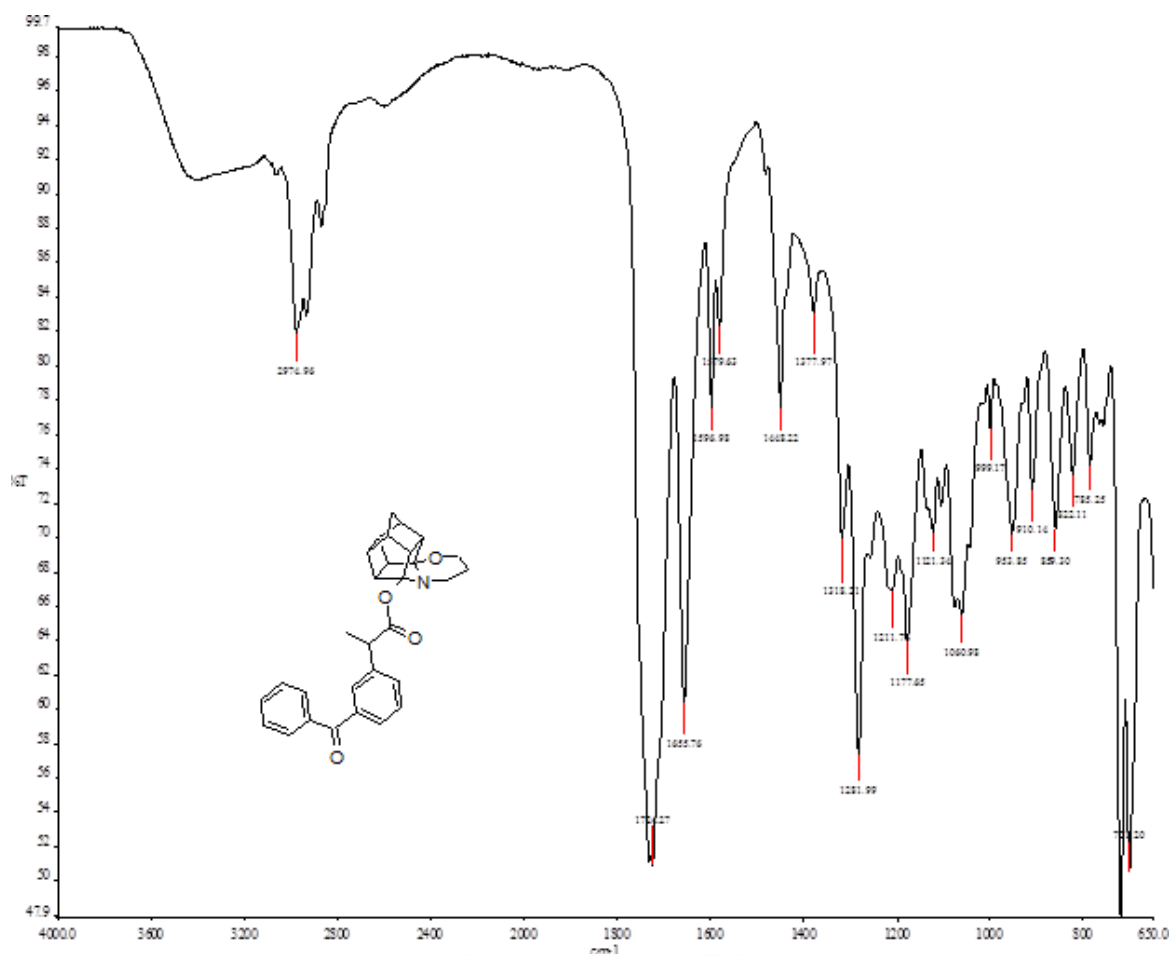
SpinWorks 4: compound 10.2



Spectrum 26



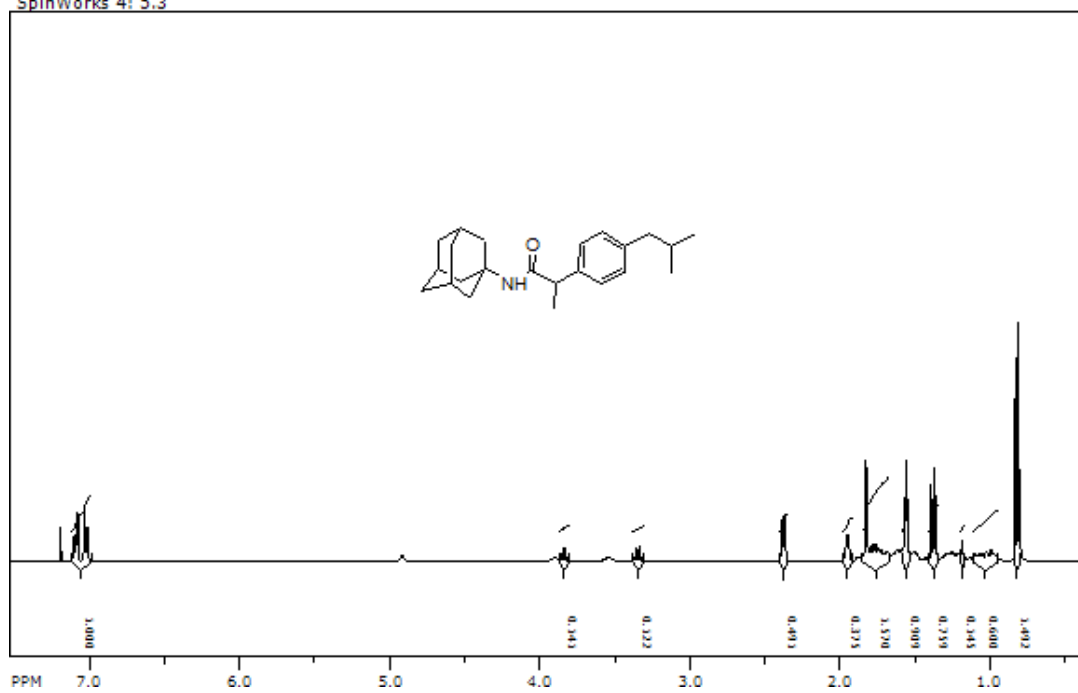
Spectrum 27



Spectrum 28

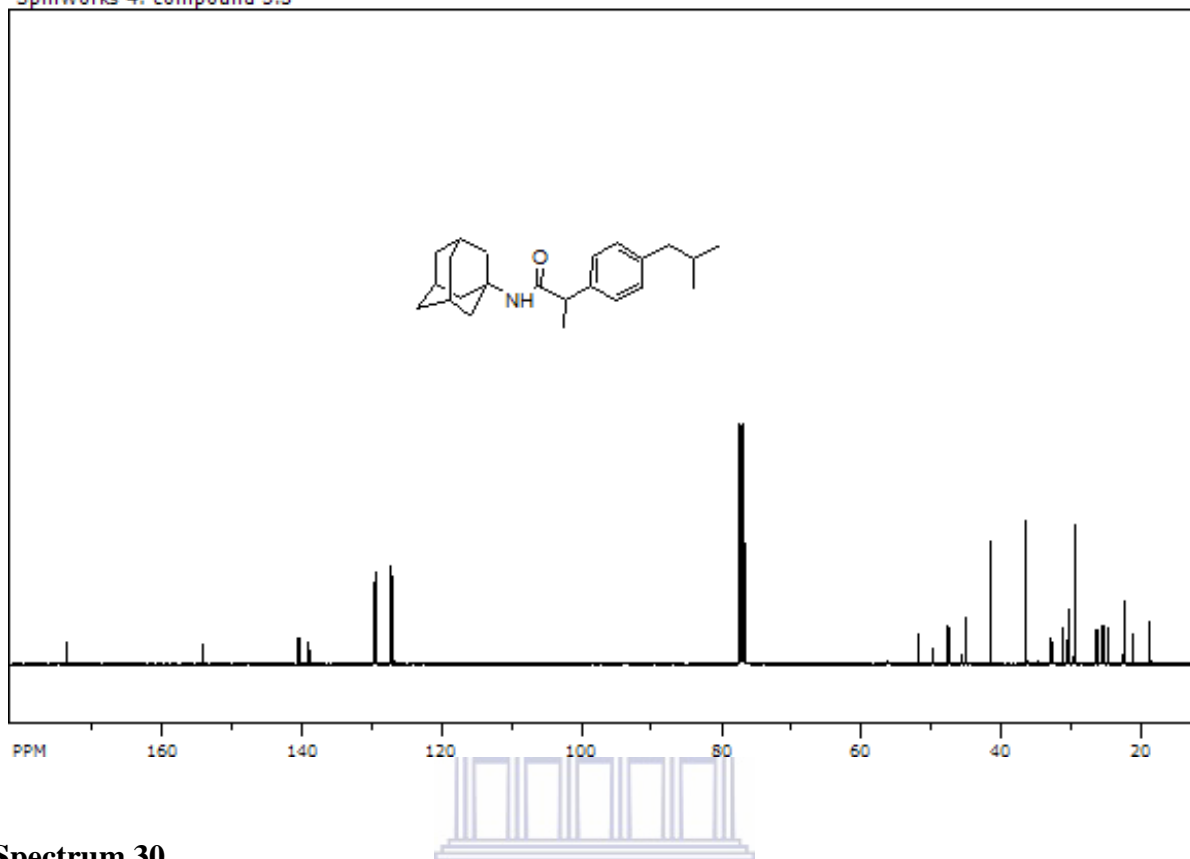
WESTERN CAPE

SpinWorks 4: 5.3

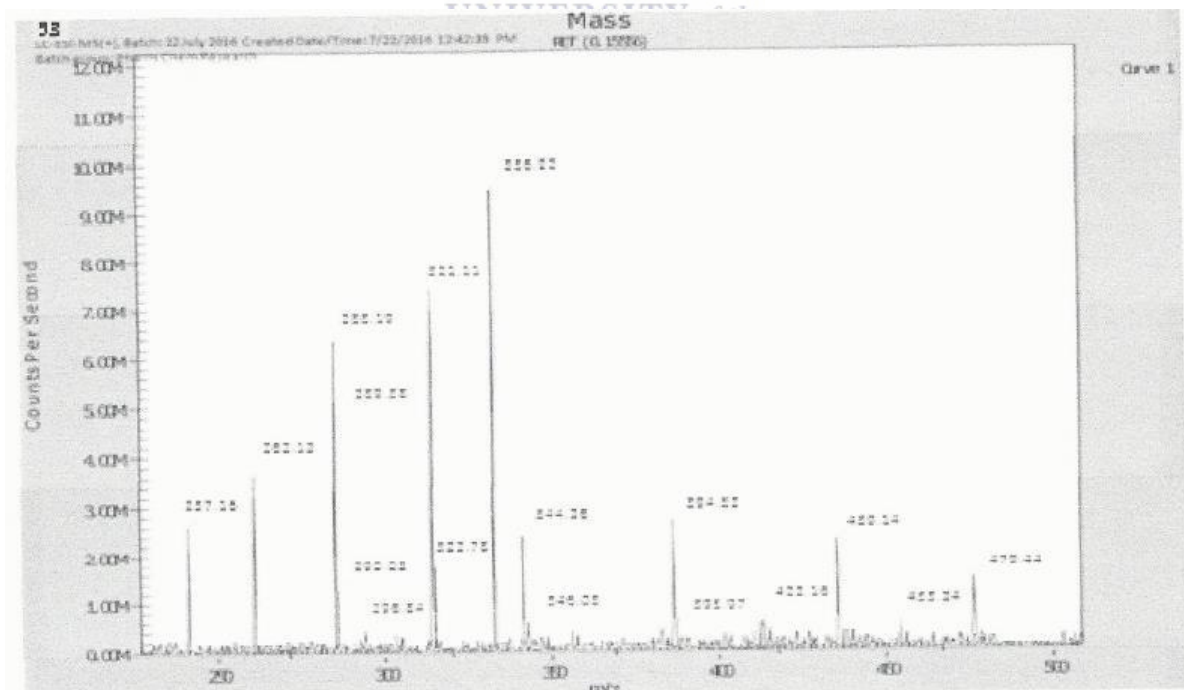


Spectrum 29

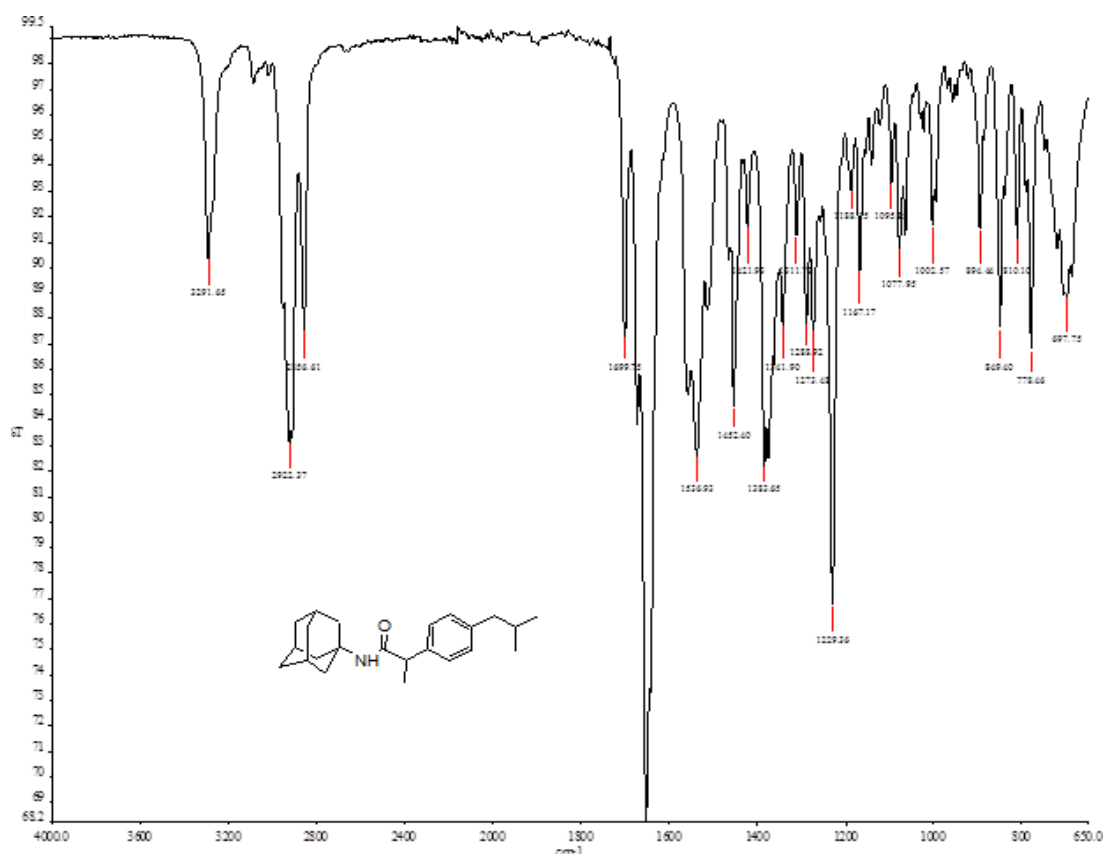
SpinWorks 4: compound 5.3



Spectrum 30

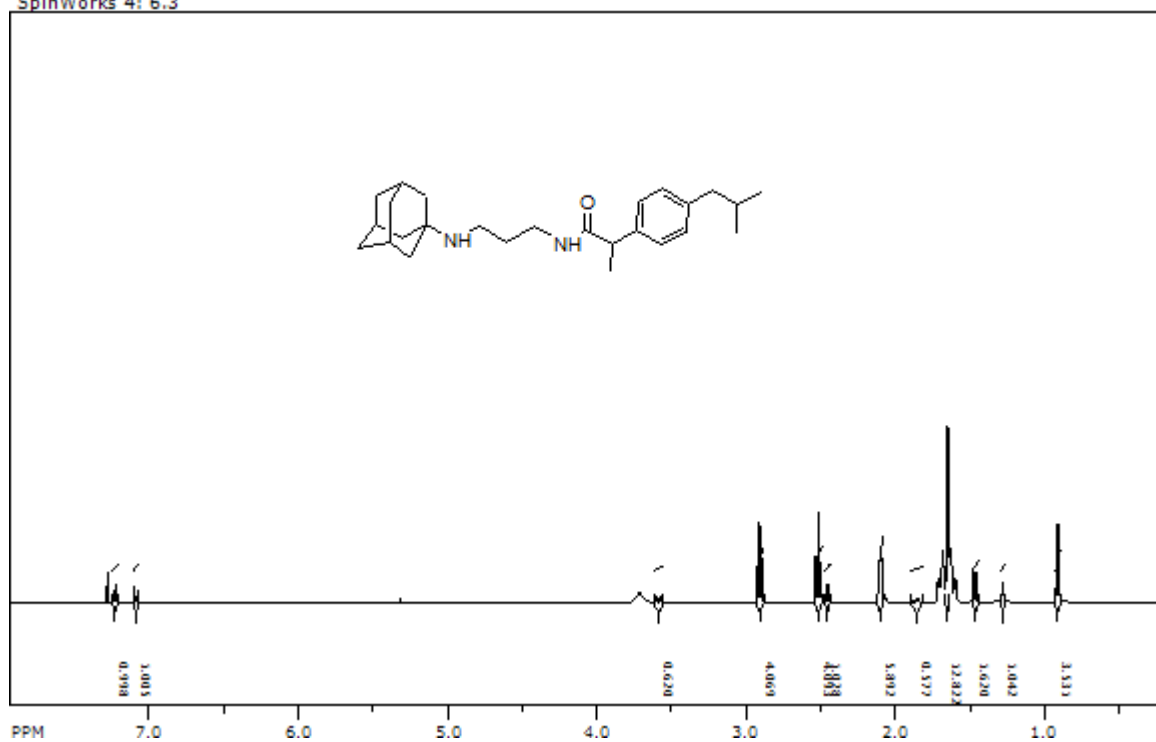


Spectrum 31



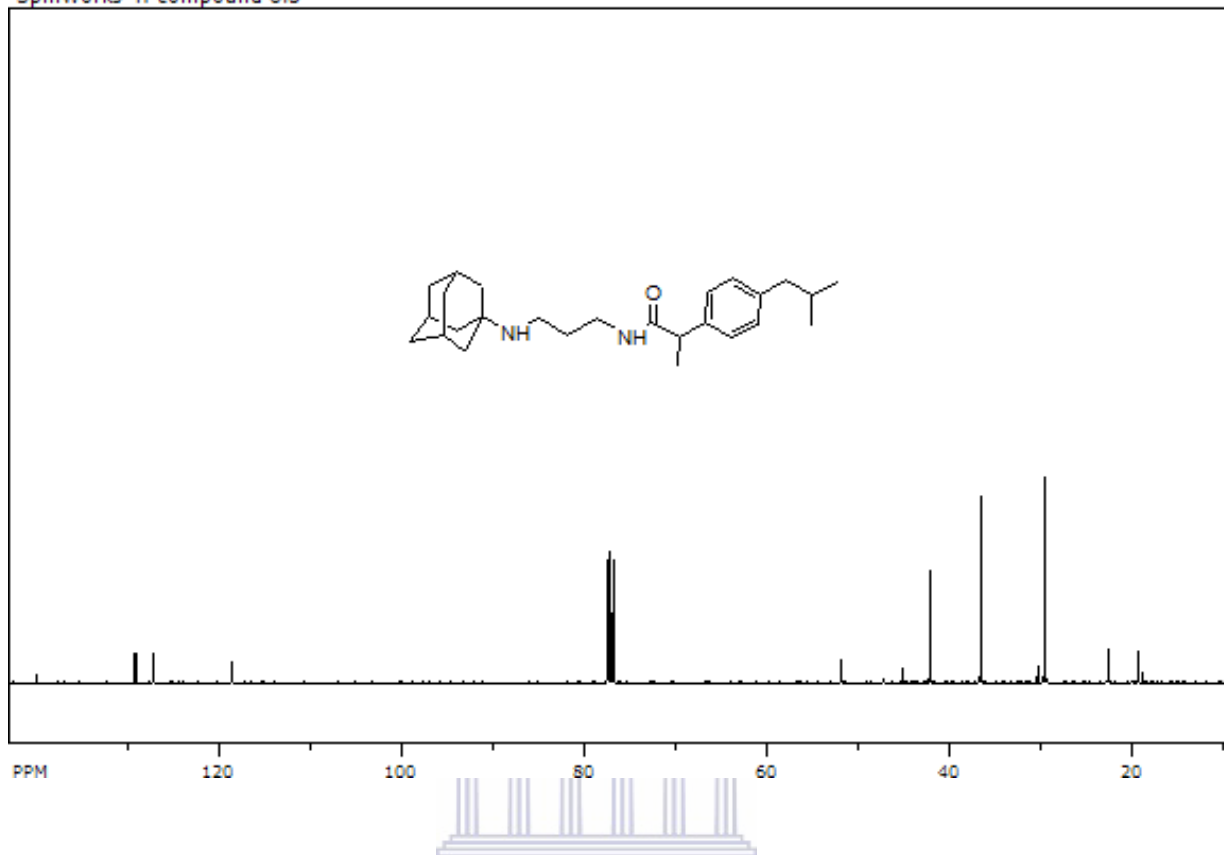
Spectrum 32

SpinWorks 4: 6.3

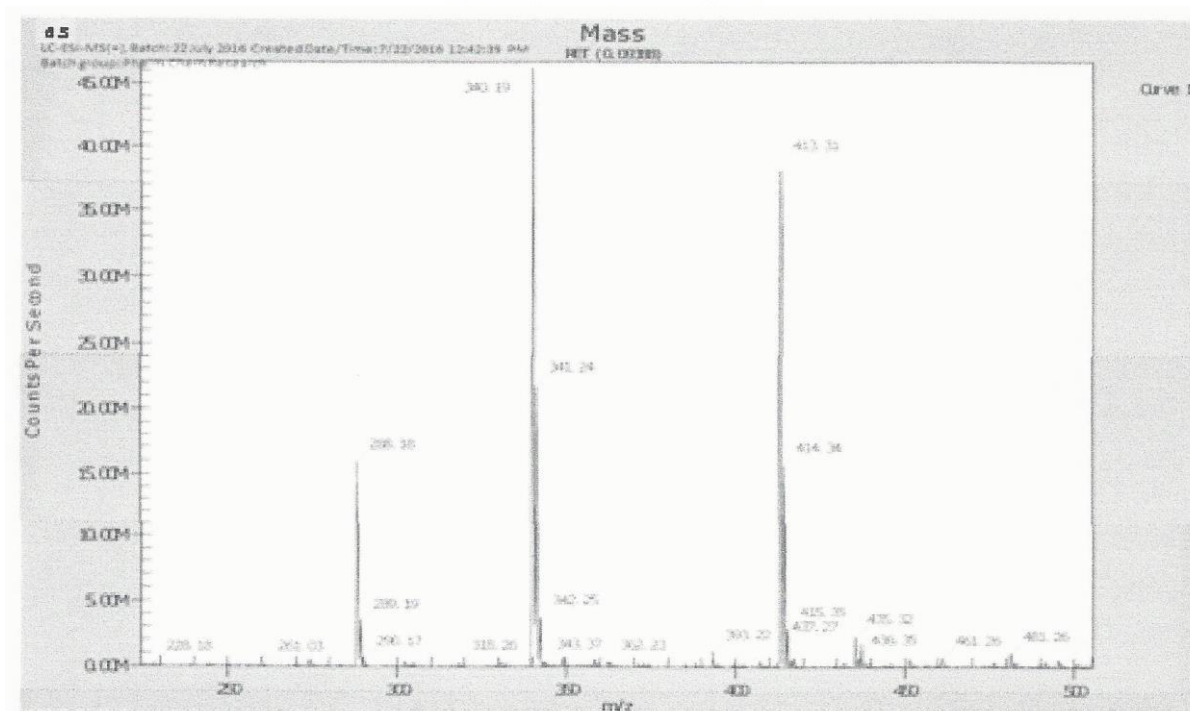


Spectrum 33

SpinWorks 4: compound 6.3

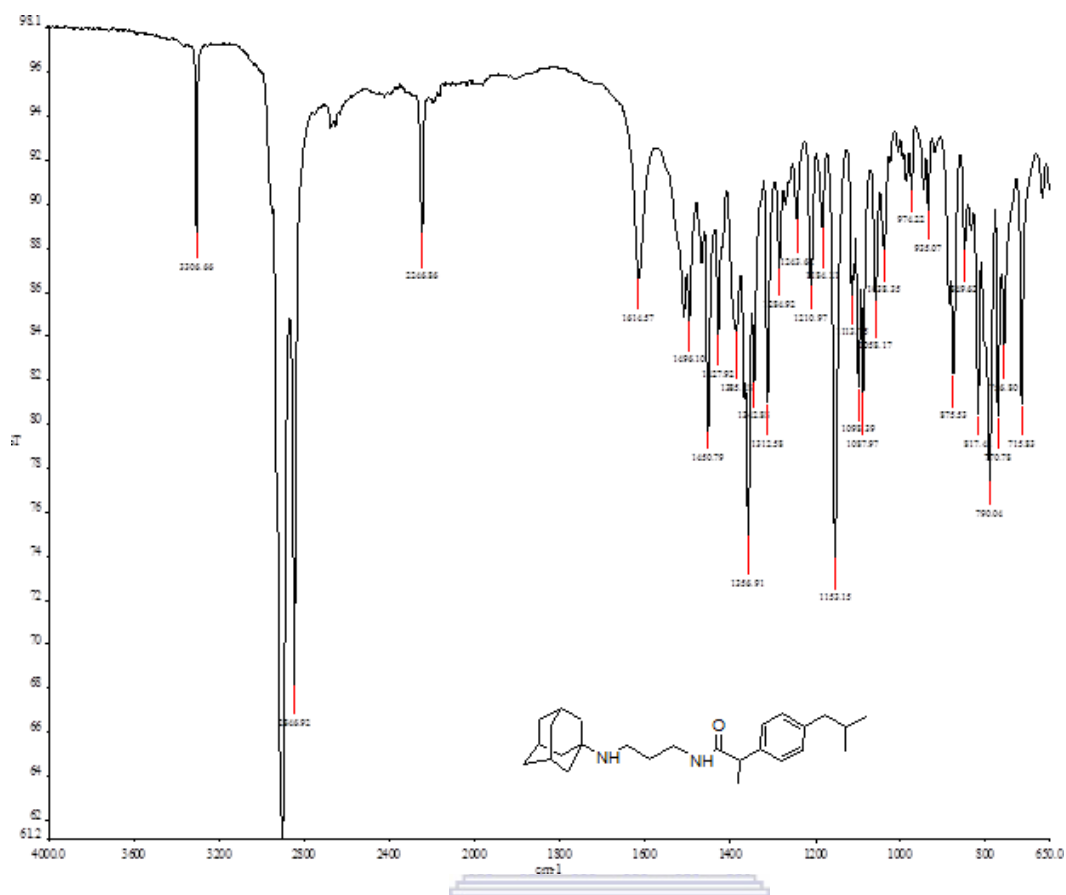


Spectrum 34



124

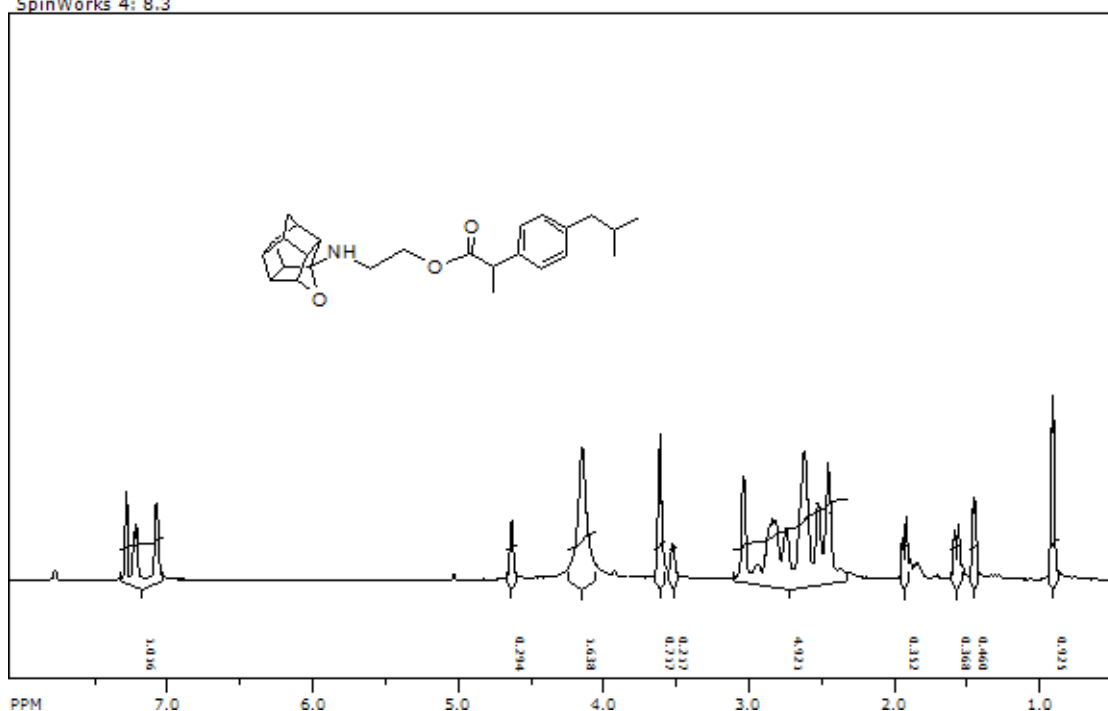
Spectrum 35



UNIVERSITY of the
WESTERN CAPE

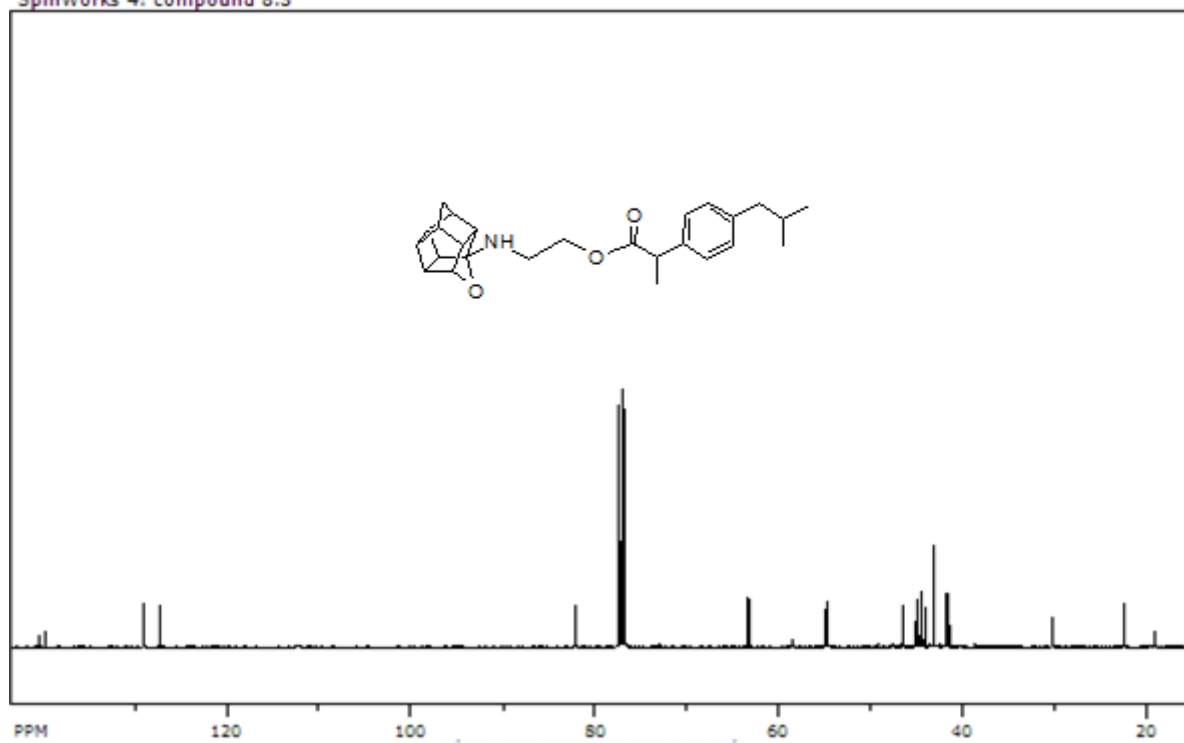
Spectrum 36

SpinWorks 4: 8.3

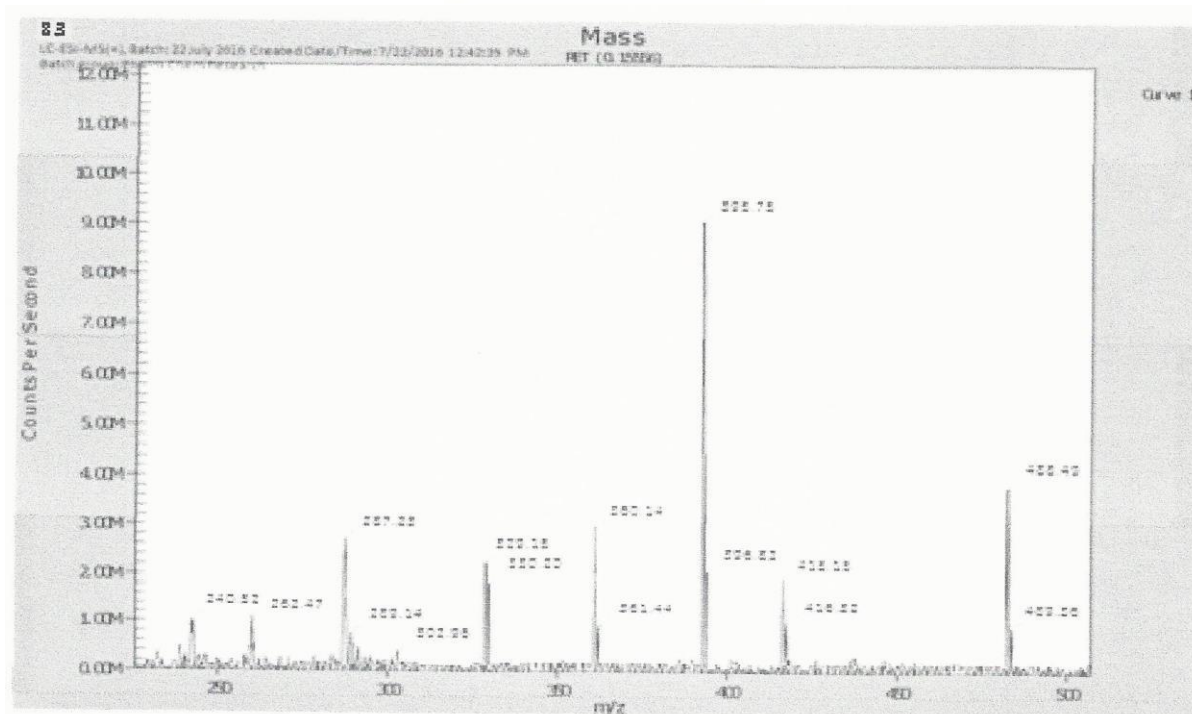


Spectrum 37

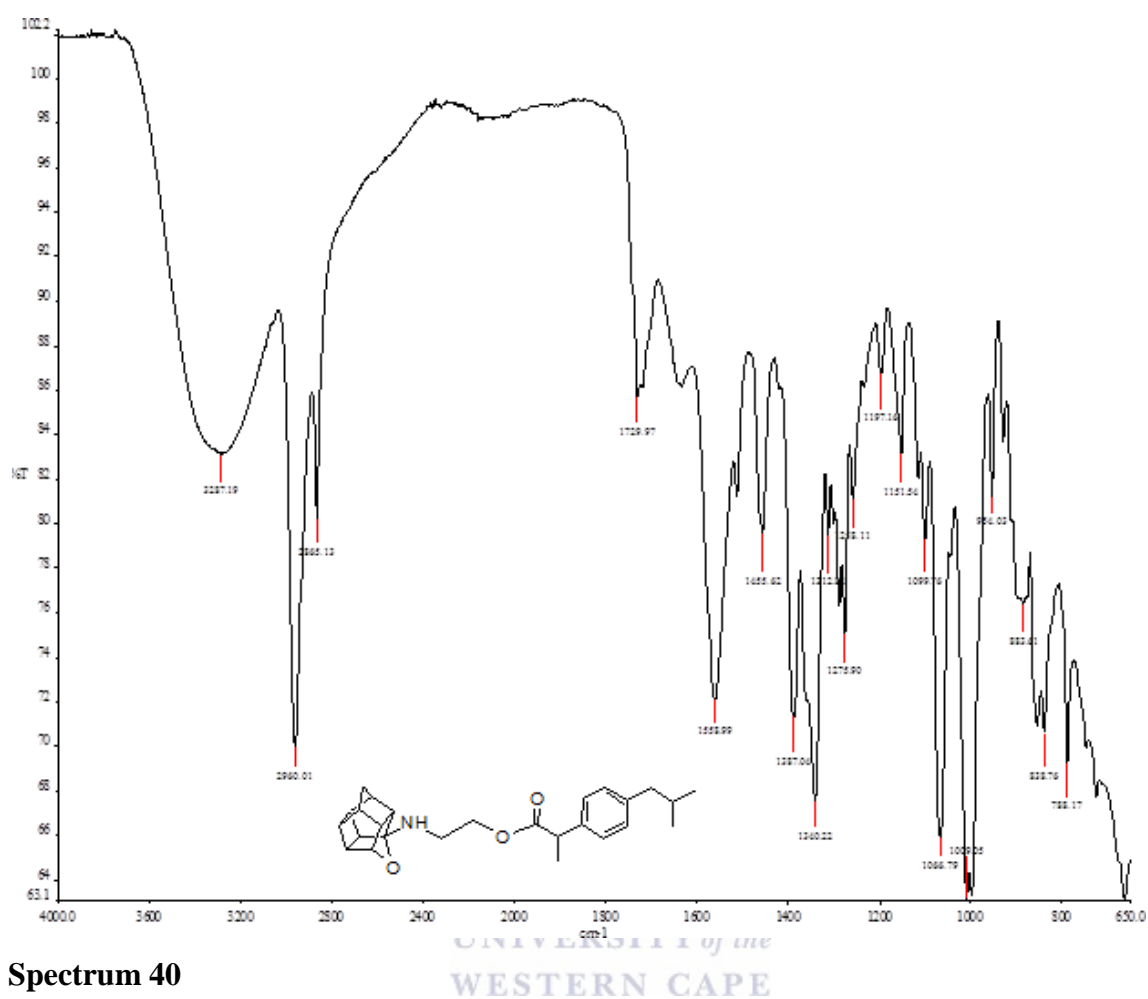
SpinWorks 4: compound 8.3



Spectrum 38

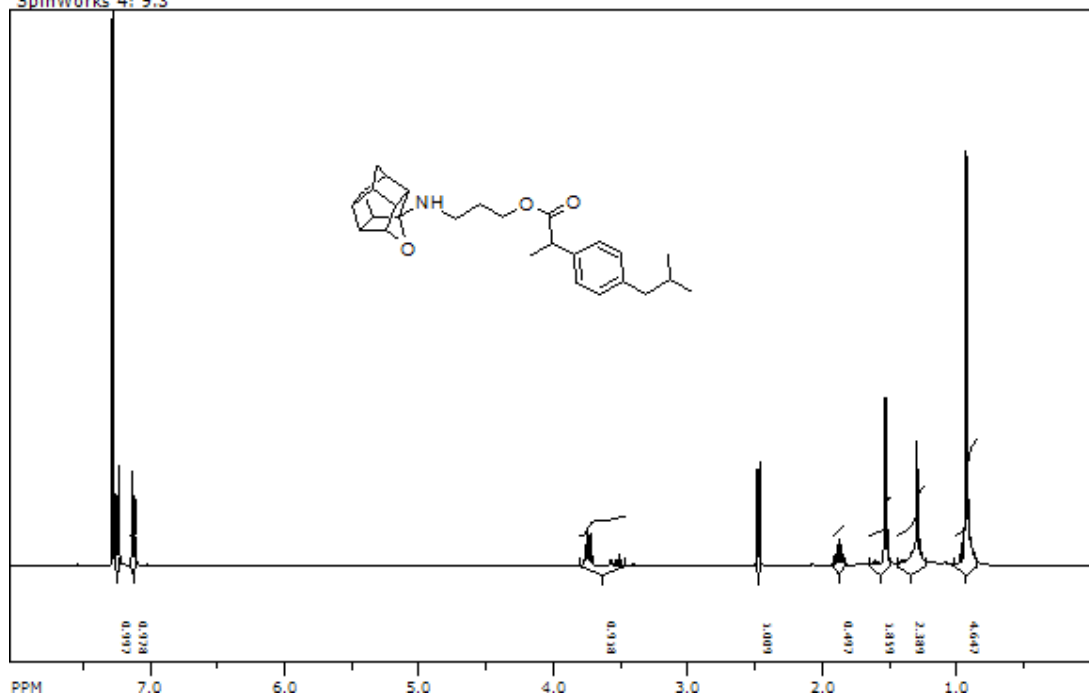


Spectrum 39



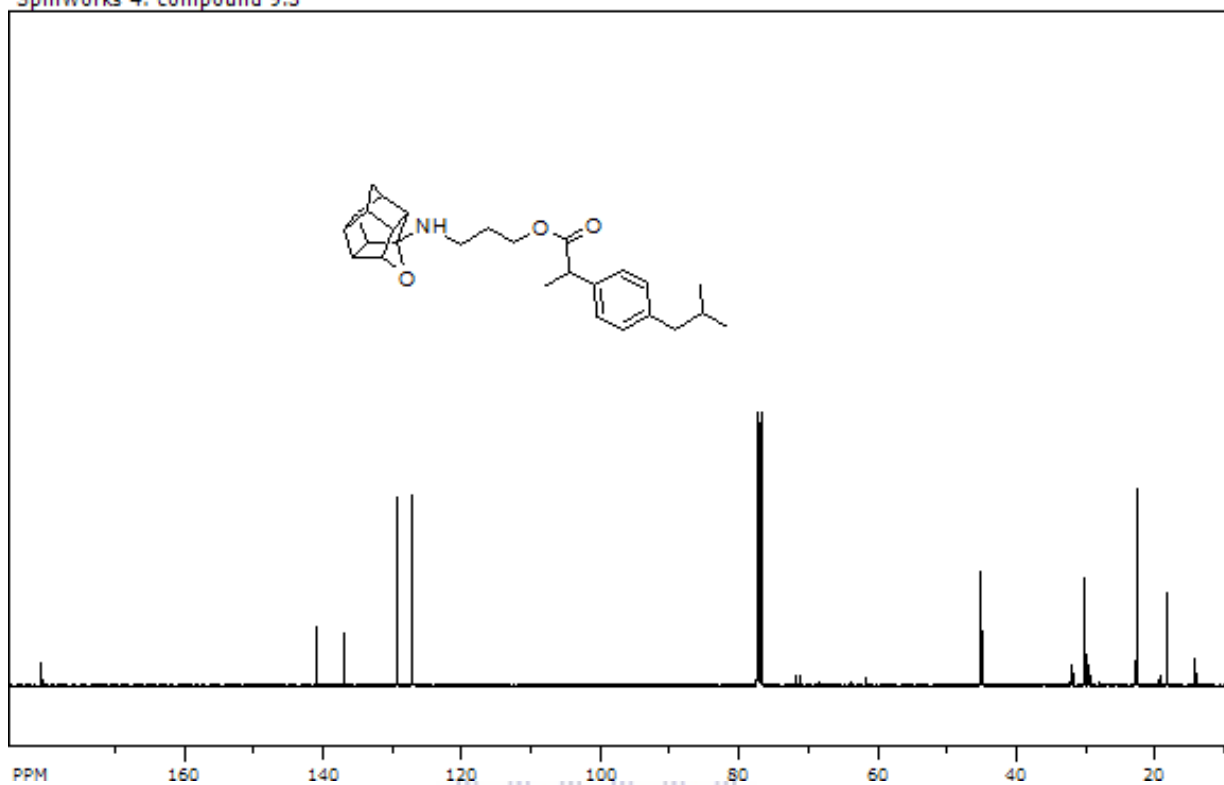
Spectrum 40

SpinWorks 4: 9.3

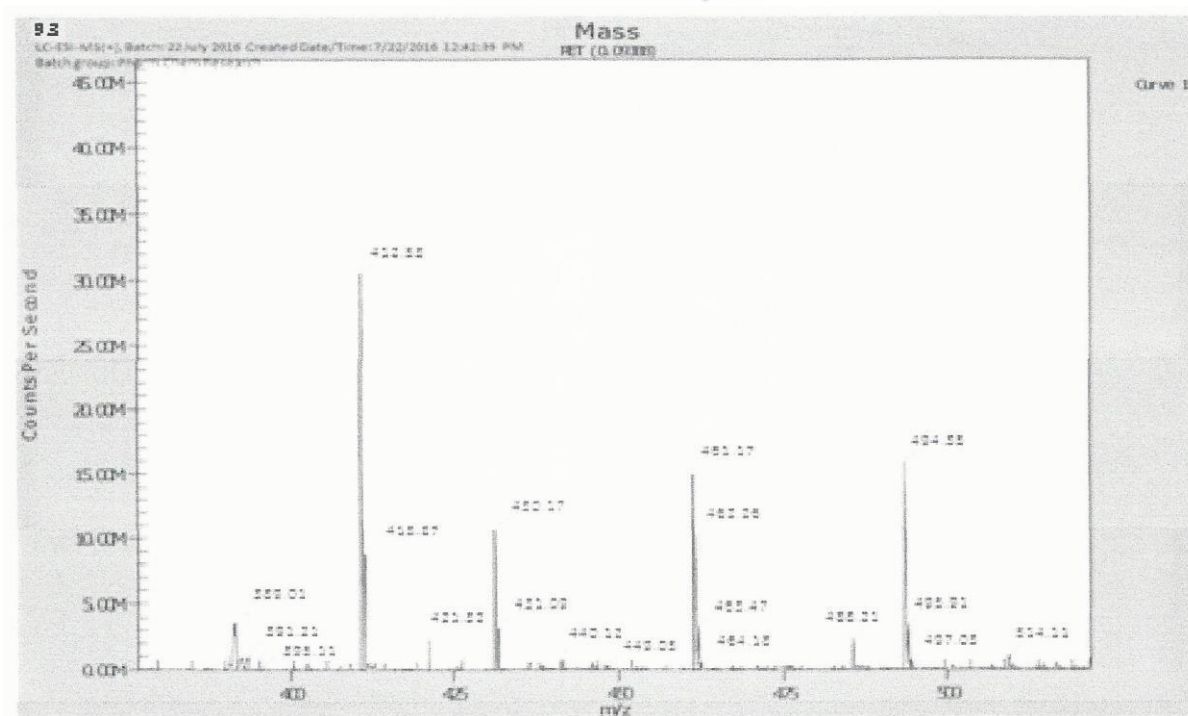


Spectrum 41

SpinWorks 4: compound 9.3

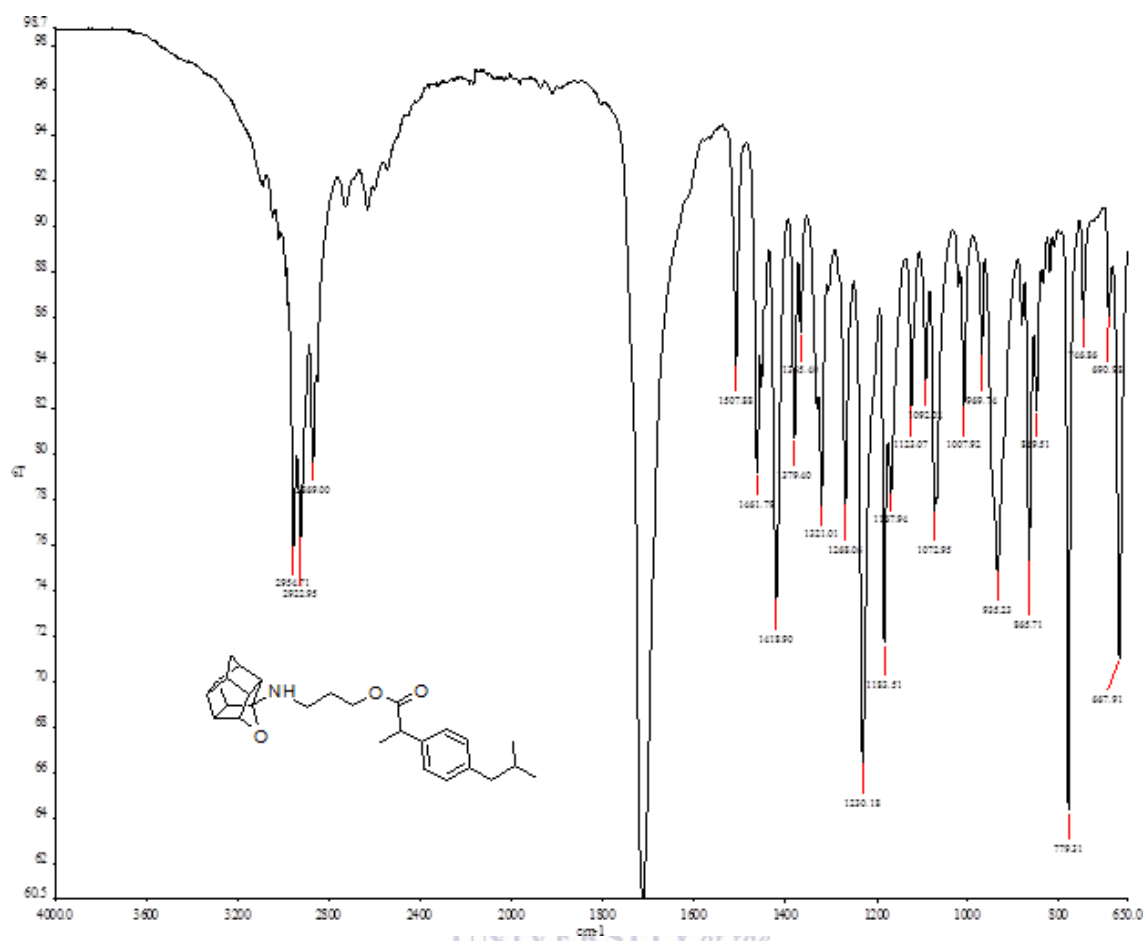


Spectrum 42



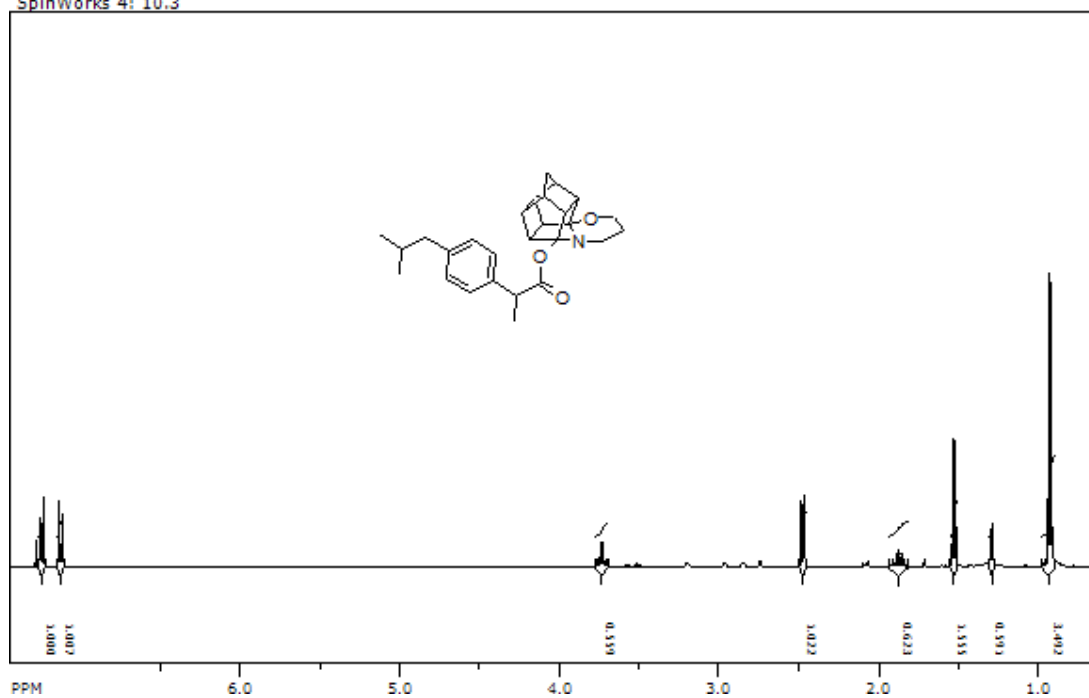
128

Spectrum 43



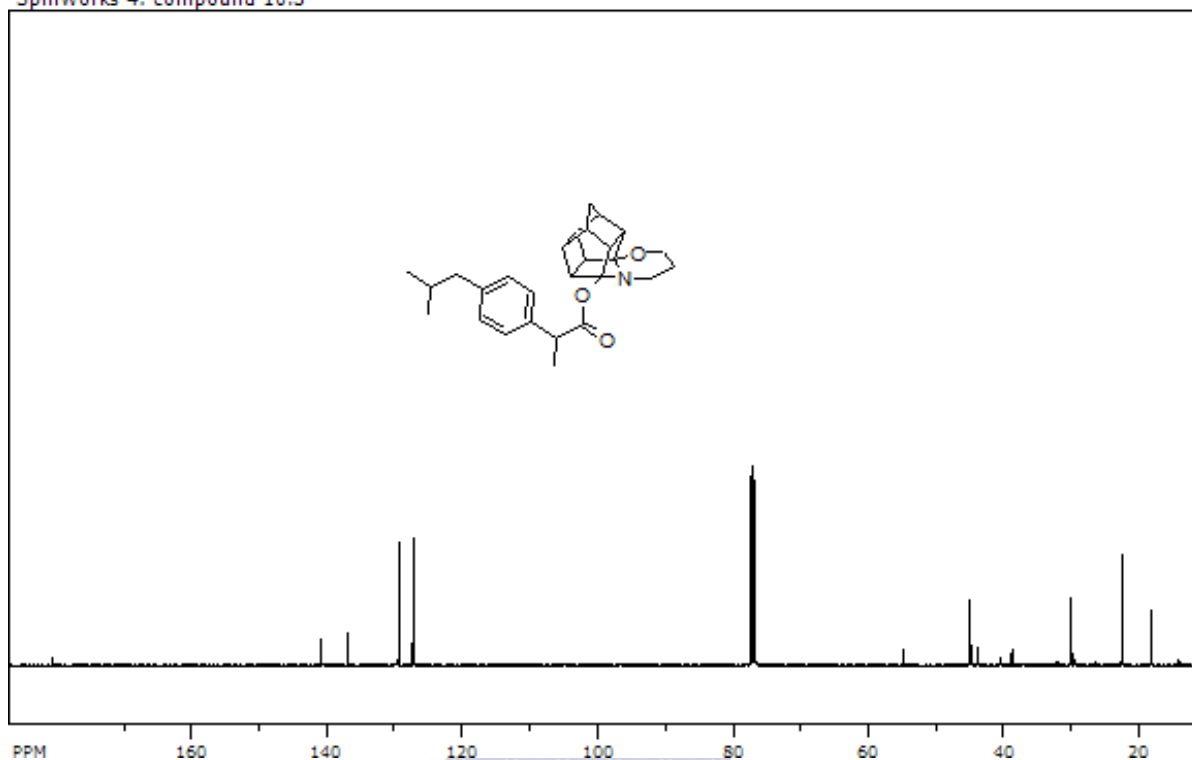
Spectrum 44

SpinWorks 4: 10.3

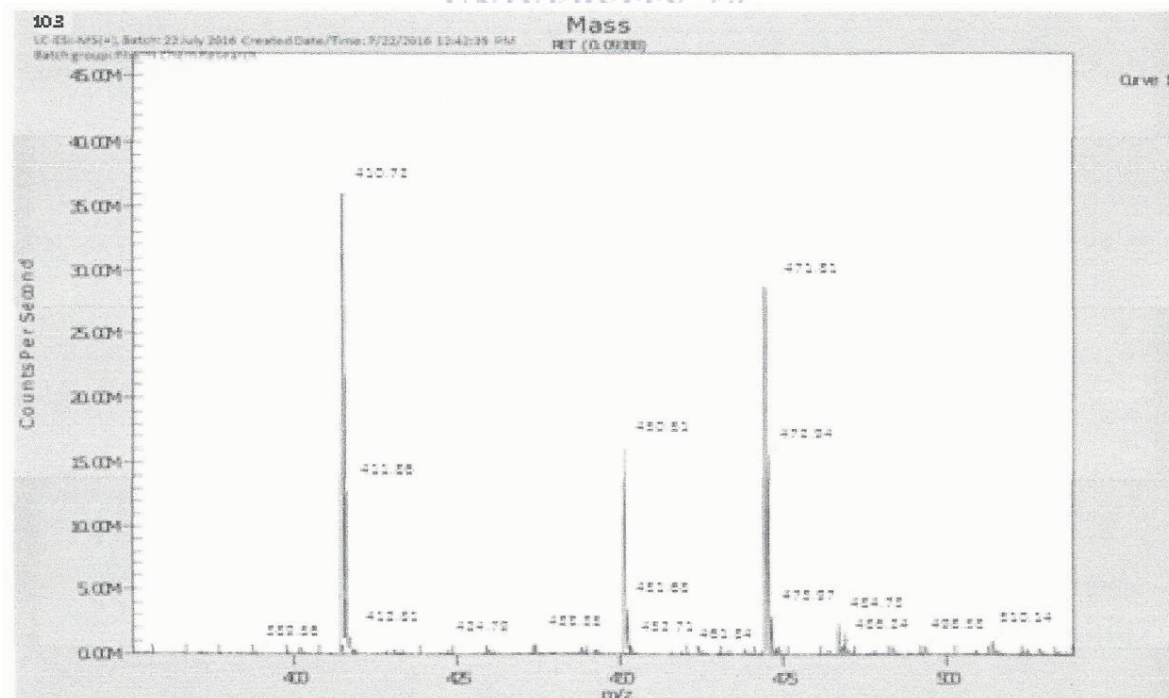


Spectrum 45

SpinWorks 4: compound 10.3



Spectrum 46



Spectrum 47

